Measurement of methane emissions from confined sources using the inverse dispersion method

Inaugural dissertation
of the Faculty of Science,
University of Bern

presented by

Marcel Bühler

from Erlenbach im Simmental (BE)

Supervisor of the doctoral thesis:
Prof. Dr. Stefan Brönnimann
Institute of Geography, University of Bern

Co-supervisor of the doctoral thesis:
Dr. Christof Ammann
Climate and Agriculture Group, Agroscope

Measurement of methane emissions from confined sources using the inverse dispersion method

Inaugural dissertation
of the Faculty of Science,
University of Bern

presented by

Marcel Bühler

from Erlenbach im Simmental (BE)

Supervisor of the doctoral thesis:
Prof. Dr. Stefan Brönnimann
Institute of Geography, University of Bern

Co-supervisor of the doctoral thesis:
Dr. Christof Ammann
Climate and Agriculture Group, Agroscope

Accepted by the Faculty of Science.

Bern, 22.02.2022

The Dean
Prof. Dr. Zoltan Balogh

Thesis summary

Greenhouse gas (GHG) emissions are reported in annual national inventories. Globally, the main anthropogenic sources of methane (CH_4) are fossil fuel burning, agriculture, landfills, and waste management. The main source of CH_4 from agriculture is enteric fermentation in the digestive tract of ruminants and a minor source are emissions from manure management. In 2019, the Swiss Federal council decided that Switzerland must reduce its GHG emission to net-zero until 2050. To reach this goal, the agricultural sector is obliged to contribute to the emission reduction. However, emissions from the agriculture and waste sector imply large uncertainties as, among other reasons, the availability of data based on real-world studies is limited. Several investigations showed that measurements from laboratory- or pilot-scale experiments do often not comply with real-world conditions. For studies under real-world conditions, different measurement approaches are available. One of the most promising methods is the inverse dispersion method (IDM) that was applied in this thesis to measure CH_4 emissions from livestock production and the waste management sector in order to evaluate the method for complex source configurations and to specify emission factors of these sources.

For the IDM, a backward Lagrangian stochastic (bLS) model in combination with concentration measurements up- and downwind of the source using open-path tunable diode laser spectrometers (GasFinders) were employed. GasFinders are simple to use, flexible in their application, and relatively cost-effective measuring devices. However, several challenges were faced and overcome throughout the thesis. The precision of the employed GasFinder model was about 10 times lower than the manufacturer stated, which necessitated adaptation in the measurement setup. Additionally, an intercomparison before or after each measurement campaign was necessary to correct the offset and span between the employed GasFinders.

In the first two studies presented in this thesis, experiments were conducted to evaluate the IDM. In a third study, experiments were conducted to assess the handling of complex source configurations with the IDM. The emissions determined in the third study were used as a basis for emission factors of Swiss biogas plants (BGPs) and wastewater treatment plants (WWTPs).

In the first study, a known and predefined amount of CH_4 was released by an artificial source in a barn that mimics a dairy housing. For concentration measurements, GasFinders with a path length

of 110 m were placed in downwind direction of the barn at a distance of 50 m, 100 m, 150 m, and 200 m. At the first three distances, an ultrasonic anemometer was placed in the middle of the GasFinder path length for executing turbulence measurements. Upwind of the barn, an additional GasFinder and an ultrasonic anemometer were installed. The main objective was to test the ideal measurement fetch for the IDM. The results of this experiment are included in the method section, where the conditions and the setup of an IDM measurement campaign are outlined. A release rate of 140 norm litres min^{-1} was chosen to achieve sufficient concentration enhancement at the GasFinder locations. The mean recovery rates of the experiment were between 0.55 – 0.76.

In the second study, CH_4 emission measurements from a naturally ventilated dairy housing were conducted in two measurement campaigns. During part of the campaign duration, emissions were also measured inside the housing with the inhouse tracer ratio method (iTRM). This allowed comparing the IDM with the iTRM, which was considered as a reference method for naturally ventilated livestock housings. For simultaneous emission intervals, the average IDM emissions were lower by 1 % and 8 % compared to the iTRM measurements, which was within the uncertainty of either of the two methods. Additionally, an uncertainty analysis for the IDM showed that measurement campaigns of at least 10 consecutive days are necessary to acquire reliable emission data.

The third study addressed the handling of complex source configurations with the IDM. Emissions from four agricultural BGPs and two WWTPs in Switzerland were measured. The average BGP CH_4 emission varied between 0.39 kg h^{-1} and 2.22 kg h^{-1}, which was less than 5 % of the plant's CH_4 production. The average CH_4 emissions for the two WWTPs were 166 g population-equivalent^{-1} y^{-1} and 381 g population-equivalent^{-1} y^{-1}, respectively. The BGPs often had livestock housings nearby that needed to be discriminated from the plant emission. It was demonstrated how the plant emission can be corrected for the nearby CH_4 sources, which confounded the GasFinder measurements. Further, it was demonstrated how to combine multiple GasFinder measurements to a single line concentration for the bLS modelling. WWTPs are complex sources as they consist of multiple sub-sources with different emission strengths spread over a large area. Three different calculation approaches with different degree of details are presented for the combination of the individual sources in the bLS modelling: (i) A polygon over the entire WWTP area as a single source. (ii) All potential sources within the WWTP have a uniform emission density. (iii) Based on literature data, relative weighting of the individual sources is carried out. The maximum difference in emission between the most complex approach (iii) and the simplest approach (i) was 42 %. It could be shown that for large source areas ($>$ 10,000 m^2), approach (iii) is the preferred option, whereas for the measured BGPs the simple polygon approach (i) was sufficient.

The recovery rate of the IDM from the release experiment (study 1) was below 1 and somewhat lower than previous studies with a similar experimental setting have shown. I was not able to conclusively identify the reasons for this result, which contrasts with the outcome of study 2 at the naturally ventilated dairy housing with a high consistency between the IDM and the iTRM used as a reference. Therefore, I suggest repeating the release experiment with an adapted setting and additionally roughly mapping the emission plume by a drone or a high-precision handheld sensor to monitor the dispersion of the plume. The field measurements at the WWTPs and the BGPs based on

the chosen approach of source combination yielded data that are in the expected range according to current state of knowledge.

The presented PhD thesis supports the aptitude of the IDM to measure emissions from complex sources like farms, BGPs, or WWTPs. Such measurements contribute to increasing the accuracy of national GHG inventories. Nevertheless, I suggest further investigations to better assess the accuracy of the IDM under complex conditions.

Contents

Symbols and abbreviations

θ	Potential temperature
ψ	Stability correction function
$\bar{}$	Mean (overbar)
‘	Fluctuating part (prime)
$\sigma_{u,v,w}$	The standard deviation of the wind components
$\hat{\sigma}_{\bar{D}_{bLS}}$	Standard error of the bLS dispersion factor
A	Source area [m^2]
ABL	Atmospheric boundary layer
BGP	Biogas plant
bLS	Backward Lagrangian Stochastic
C	Concentration [mg m^{-3}]
C_0	Kolmogorov constant of the Lagrangian structure function
CFD	Computational fluid dynamics
CH_4	Methane
CHP	Combined heat and power unit
CO_2	Carbon dioxide
D	Dispersion factor [m s^{-1}]
D_{bLS}	Dispersion factor of the bLS model [m s^{-1}]
E	Emission [kg m^{-2} s^{-1}]
eTRM	External tracer ratio method

g	Gravitational acceleration [m s^{-1}]
GF	GasFinder
GHG	Greenhouse gases
GPS	Global Positioning System
IC	Intercomparison campaign of the GasFinder
IDM	Inverse dispersion method
iTRM	Inhouse Tracer ratio method
k	Von Kármán constant (0.4)
L	Obukhov length [m]
MC	Measurement campaign
MFC	Mass flow controller
MOST	Monin–Obukhov similarity theory
N	Number
PEN	Polyethylene naphthalate
Q	Emission [kg s^{-1}]
R	Programming language
S	Source strength of the source layer [mg m^{-3} s m^3]
sim	simulated/modelled
sonic	3-dimensional ultrasonic anemometer
TD	Touchdown
TRM	Tracer ratio method
u_*	Friction velocity
u	Wind velocity of the along wind [m s^{-1}]
UTC	Coordinated Universal Time
v	Wind velocity of the across wind [m s^{-1}]
w	Wind velocity of the vertical wind [m s^{-1}]
WWTP	Wastewater treatment plant
z_0	Roughness length [m]

Chapter 1

Introduction

1.1 Methane emissions from anaerobic processes in the livestock sector and in waste management

Methane (CH_4) is the second most important greenhouse gas (GHG) after carbon dioxide (CO_2) (Stocker et al., 2013). CH_4 is emitted by thermogenic, biogenic, or pyrogenic processes and can be of anthropogenic or natural origin. Thermogenic CH_4 is produced by heat and pressure on geological timescales and emitted through marine and land geological gas seeps. CH_4 emitted by biogenic processes is due to the decomposition of organic matter by methanogenic Archaea in anaerobic environments. Potential sources are wetlands, wastewater treatment plants, landfills, or animal digestive systems. Pyrogenic CH_4 is produced by incomplete combustion of organic material such as biomass burning (Saunois et al., 2020). In the last decade, atmospheric CH_4 concentrations were dominated by emissions from fossil fuels, agriculture, landfills, and the waste management sector (Stocker et al., 2013).

Under the United Nations Framework Convention on Climate Change and under the Kyoto Protocol countries are obliged to report their annual GHG emissions. In Switzerland, GHG from the agriculture sector contributed 12.7 % of the total Swiss GHG emissions in 2019 (FOEN, 2021b). Within the livestock sector at a global scale, CH_4 mainly originates from enteric fermentation in the digestive tract of ruminants and to a minor extent from emissions from manure management. Emissions from manure management occur in the livestock building, during storage, and field application of manure (Gerber, 2013). In Switzerland, enteric fermentation and manure management are responsible for 55 % and 18 % of all agricultural GHG emissions, respectively (FOEN, 2021b). The national inventories are often based on emission factors (average emission per unit and time) from emission measurements with various measurement methods. The uncertainty of some of these emission factors is large, as there are only a limited amount of studies available that measured emissions under real-world conditions (Kupper et al., 2020). Kupper et al. (2020) published an extended review on ammonia and GHG emissions from slurry stores and concluded that pilot-scale or laboratory-scale studies poorly fit with real-world conditions and thus, further research is needed (see Annex). The same adjustment is

needed for emissions from livestock housings and, emissions from the wastewater treatment and anaerobic digestions at biogas facilities.

In Switzerland, CH_4 is also the most important GHG in the waste sector. CH_4 emissions from the waste sector are responsible for about 11 % of the total Swiss CH_4 emissions. Next to managed waste disposal sites, the emissions from wastewater treatment are the second major source in the waste sector. In the national inventories, some of the emissions from wastewater treatment and anaerobic digestions at biogas facilities are reported in the energy sector (FOEN, 2021b).

1.1.1 Livestock housings

In livestock housings, CH_4 is either produced due to fermentation in the digestive tract of the animals or by organic matter included in excretions and bedding material. Compared to non-ruminant livestock (e.g., pigs), ruminant livestock (e.g., cattle) are a major source of CH_4 (IPCC, 2006). In the following, the most common housing systems for dairy cows and fattening pigs are explained. In Switzerland, about 50 % (with increasing shares) of the dairy cows are kept in loose housing systems where the animals are free to walk around in the housing, and the other half in tied housing systems (Kupper et al., 2015). The most common loose housing system is a cubicle house, which is divided into walking areas and individual cubicles where the animals lay when they rest. Bedding material (straw, wood shavings or sawdust) is placed in each cubicle. The walking alley and feeding aisle are equipped with a slatted or a solid floor. The latter is cleaned with scrapers (mostly automated scrapers, tractor, or farm loader scrapers) that periodically remove the dung to a slurry pit. Below slatted areas, the excrements are collected as slurry in a pit or channel (Pain and Menzi, 2011; Sommer et al., 2013). The slurry from the channel is pumped to a slurry store adjacent or in the close vicinity to the housing. In a meta-study, no effect of the floor type on CH_4 emissions was found (Poteko et al., 2019).

Fattening pigs are kept solely in loose housing systems. In contrast to cattle housings where natural ventilation prevails, fattening pig housings often have a mechanical ventilation (Sommer et al., 2013).

1.1.2 Wastewater treatment plants

In 2019, wastewater treatment and discharge were responsible for 38 % of the CH_4 emissions from the waste sector (FOEN, 2021b). In Switzerland, wastewater is treated by 750 wastewater treatment plants (WWTPs) with more than 500 population equivalents each (Abegglen and Siegrist, 2012). A WWTP consists of a water line, sludge line and energy line as explained below (Figure 1).

1.1.2.1 Water line

A frequent type of WWTP comprises a water line with a conventional activated sludge system with the following parts: at the inlet, the coarse solids are removed by a screen and fine heavier particles in a sand trap (Figure 1). In the primary clarifier, the remaining solids settle at the bottom of the basin, are transported towards a funnel with an automated scraper and are removed there. This solid fraction is denoted as primary sludge. Those steps correspond to primary treatment. Afterwards, the wastewater flows to the activated sludge tanks where precipitants (e.g., FeCl, $FeClSO_4$) are added for phosphorus removal. To promote the growth of bacteria that degrade the organics in the wastewater, the tanks are aerated. This concomitantly leads to nitrification of ammonium (main form of nitrogen)

and to further denitrification. The biological removal of carbon as well as nitrification and denitrification are part of the secondary treatment, and phosphorus removal is the tertiary treatment. The biomass settles in the secondary clarifier. To promote growth of the bacteria, part of the settled biomass is redirected to the head of the activated sludge tank as return sludge. The residence time of the sewage in the activated sludge tank is in the order of several hours. A part of the sludge removed from the secondary clarifier is redirected back to the plant influent where in the primary clarifier, it is fed together with the primary sludge into the sludge line. The clarified water is then directed into the receiving water (Gujer, 2007).

The primary and secondary treatment are performed at all Swiss WWTPs, whereas the tertiary treatment depends on discharge requirements (FOEN, 2021a). With the new water protection law in Switzerland of 2016, the removal of micropollutants in the wastewater (quaternary treatment) is mandatory to be established until 2035 for about 100 of the 750 WWTPs (FOEN, 2015).

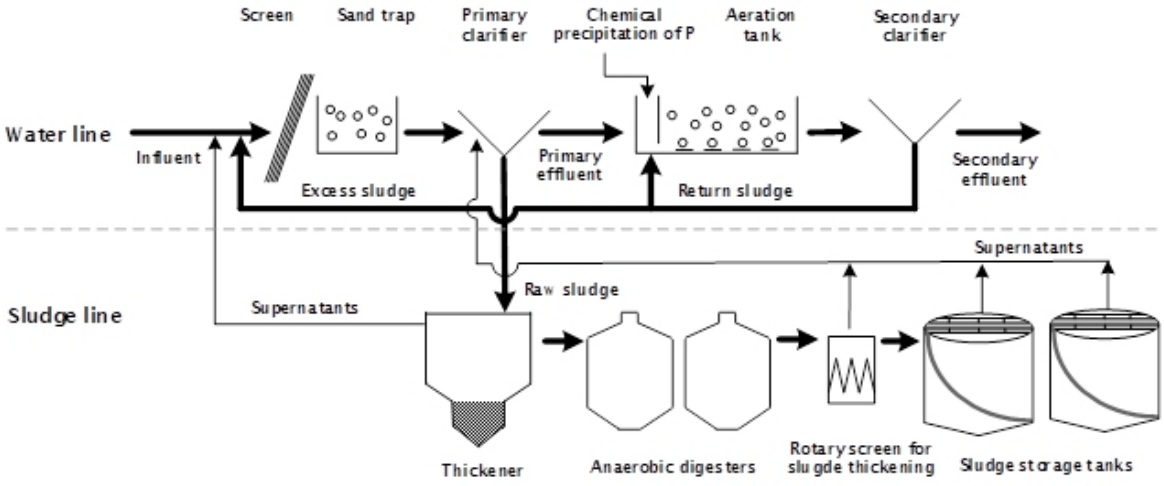

Figure 1: Flow scheme of a wastewater treatment plant with a conventional activated sludge system. Figure is adapted and republished from Kupper et al. (2006) with permission from Elsevier.

The second most common system in Switzerland after the conventional activated sludge system is the sequencing batch reactor system. It is mostly used in small WWTPs (population equivalent $< 1{,}000$) but has frequently been implemented at larger WWTPs (population equivalent $> 50{,}000$) as well (FOEN, 2021a). Compared to the conventional activated sludge system, in the sequencing batch reactor system the biological treatment (activated sludge tanks) and sedimentation (secondary clarifier) occur incrementally in the same reactor. This allows to adapt the duration and intensity of a single process to changing conditions in the pollution of the wastewater (Dutta and Sarkar, 2015).

1.1.2.2 Sludge and energy line

The primary goal of the sludge line is to sanitise and stabilise the sludge and reduce its volume for the final disposal. In the thickener, part of the supernatant water is removed from the sludge and redirected to the head of the water line (Figure 1). In the digester, the sludge undergoes anaerobic degradation where biogas is produced that is combusted in a combined heat and power unit (CHP). The biogas storage and the CHP are denoted as energy line. After the digester, the sludge can be

further dewatered. For temporarily storage before incineration or transportation to a larger WWTP (e.g., for further dewatering and incineration), the sludge is pumped to sludge storage tanks. The combined residence time of sludge in the thickener and digester is around 15 - 30 days. Depending on the storage time, the residence time of sludge in the sludge line can be more than 100 days (Gujer, 2007). Anaerobic sludge treatment and subsequent production of biogas is not a priori necessary. However, only mostly small WWTPs do not have a digester (FOEN, 2021a). The electrical power and heat usage produced by the WWTPs depends on their location. Usually, part of the heat from the CHP is used for heating the digester and the power is fed to the local power grid (Gujer, 2007).

1.1.2.3 Emissions

CH_4 is formed in the sewer system and enters the treatment plant in dissolved form with the wastewater (Fries et al., 2018; Mannina et al., 2018). It can be released into the atmosphere during the treatment process due to aeration of the basins. Therefore, a part of the CH_4 emitted at WWTPs does not originate from wastewater treatment, but from processes associated with the sewer system. CH_4 is produced in those parts of the WWTP where organic carbon is present under anaerobic conditions. This predominantly applies to the sludge line, e.g., in the thickener, during anaerobic digestion, i.e., through leakages or flaring, and during storage of the anaerobically digested sludge in the storage tanks (Daelman et al., 2012). CH_4 is also emitted from the CHP due to incomplete combustion of the biogas (Liebetrau et al., 2013). Production of CH_4 in the water line has rarely been reported in the literature.

1.1.3 Biogas plants

In biogas plants (BGPs), organic substrates are digested, and biogas is produced. This is comparable to the sludge and energy line in WWTPs. In Swiss agricultural BGPs, at least 80 % of the substrate must be livestock manure. The remaining 20 % are often co-substrates with a high biogas potential (FOEN, 2016). The substrate is filled via a dosage, where it is chopped, into the digester. The anaerobic digestion mostly occurs under mesophilic conditions (Liebetrau et al., 2013). After an average residence time of 25 days, the digestate is directed into a store (vTI, 2009). Some BGPs have a secondary digester to obtain additional biogas out of the remaining organic substance. The digesters are covered with a gastight membrane (Liebetrau et al., 2013). At some BGPs, the slurry store is also covered gastight to capture residual biogas. The liquid digestate is then applied as fertiliser to agricultural land (FOEN, 2016). The biogas is combusted in a CHP at the plant itself. Usually, part of the heat is used to heat the digester. The remaining heat can for example be fed into a district heating network or used by nearby industry. The produced electrical power is supplied into the power grid if not used onsite. The benefit of BGPs is that organic substance can be used to produce heat and power to replace fossil fuels. However, if CH_4 emissions exceed a certain limit the savings in fossil fuels are compensated taking into account the high global warming potential of CH_4 compared to CO_2 (Scheutz and Fredenslund, 2019). In this case the net effect of the BGP would contribute to global warming.

Emissions of CH_4 occur due to biogas production and combustion, from stored substrate and non-gastight covered digestate stores. Potentially high CH_4 emissions may occur due to flaring, incomplete combustion of the biogas or leakages in membranes and gas pipes (Liebetrau et al., 2013).

1.2 Overview of potential measurement methods

For emission measurements of agricultural sources, there are multiple methods available. They are roughly subdivided into intrusive and non-intrusive methods. Non-intrusive methods have the advantage of not altering the environmental and meteorological conditions, which are controlling the gas exchange between the atmosphere and the surface over the study area. Some of the most frequently applied methods for measuring emissions from the livestock sector and anaerobic processes in waste management are briefly described below.

1.2.1 Inverse dispersion method

The inverse dispersion method (IDM) belongs to the non-intrusive methods. The IDM is a micrometeorological method that combines concentration measurements up- and downwind of the source with an atmospheric dispersion model. The advantage of the IDM is that the concentration measurements are conducted outside of the building a few meters above ground and thus, do not influence any emitting surfaces or animal behaviour which might indirectly influence the emissions. A common used dispersion model for agriculture sources is the backward Lagrangian stochastic (bLS) model based on Flesch et al. (2004), that is implemented in this thesis. The employed bLS model uses the Monin-Obukhov Similarity Theory (MOST) (Monin and Obukhov, 1954) scaling. It targets diffusive ground sources in horizontal homogeneous and flat terrains. Nevertheless, the IDM has recently been used for non-ground sources, such as barns or whole farms. Often, with the IDM, a differentiation of emission sources within a small area (e.g., livestock housing and adjacent slurry store or sources within a WWTP) is difficult to achieve.

The IDM with the bLS model based on Flesch et al. (2004) was used to estimate emissions from slurry stores (Flesch et al., 2013), animal production buildings (Harper et al., 2010), and feedlots (Bai et al., 2017; McGinn et al., 2016) but also more complex sources such as whole farms (Flesch et al., 2009; VanderZaag et al., 2014) or biogas plants (Flesch et al., 2011; Reinelt et al., 2017). The reliability of the IDM was shown in ground release experiments conducted in open field conditions (Flesch et al., 2004; Häni et al., 2018).

1.2.2 Tracer ratio measurements

With the tracer ratio method (TRM), a known amount of the tracer gas is released at approximately the same locations as where the target gas is emitted. Either within the building (inhouse tracer gas ratio method, iTRM) or several 100 meters downwind (external tracer gas ratio method, eTRM) the concentration of the tracer gas and the target gas are measured (Ogink et al., 2013). By relating the background corrected target and tracer gas concentration and the mass flow of the tracer gas, the mass flow of the target gas and henceforth, the emission can be calculated (Mohn et al., 2018). The

tracer gas should exhibit the same atmospheric dispersion and transport properties as the target gas and can be either of natural (e.g., CO_2) or anthropogenic origin. The method bears the advantages that it is non-intrusive and precise measurement devices are applicable (Ogink et al., 2013). The TRM is the most likely candidate for a reliable reference method for emission measurements of naturally ventilated livestock housings according to Ogink et al. (2013). However, it remains a labour and cost intensive method and might be limited in the duration of application given the required volume of tracer gas.

The TRM has been used for a variety of sources including livestock housings (Poteko et al., 2020; Schrade, 2009; Mendes et al., 2015) and BGPs and WWTPs (Delre et al., 2017; Samuelsson et al., 2018; Scheutz and Fredenslund, 2019).

1.2.3 Chamber measurements

Chamber measurements are a simple and easy to use method to measure the surface-atmosphere gas exchange. Chambers are placed on soil or liquid surfaces such as slurry tanks. The chamber method can be subdivided into static and dynamic chambers. In static chambers, the flux is calculated by measuring the concentration increase over a given time. Dynamic chambers are flushed, and the flux is calculated from the concentration difference between the inlet and the outlet (Pumpanen et al., 2004). Chamber measurements allow measurements of individual sources within a source complex (e.g., WWTP). However, chamber measurements are intrusive and might change the environmental and meteorological conditions that are controlling the gas exchange over the study area (Pumpanen et al., 2004).

Chamber measurements were widely applied for slurry stores (Minato et al., 2013), BGPs (Liebetrau et al., 2013), and WWTPs (Ren et al., 2013; Daelman et al., 2012). For emission measurements of livestock (Poteko et al., 2020), there are respiration chambers that usually can house 1 - 2 cows. This allows for precise measurements of the enteric fermentation of the animals. However, cows are herd animals and behave differently if isolated (Huhtanen et al., 2015) and the artificial environment might affect their feeding behaviour (Storm et al., 2012).

1.3 Framework and objectives of the PhD thesis

The main objective of this PhD thesis was to evaluate the applicability of the IDM for various stationary sources under real-world conditions regarding surrounding topography and weather as occurring in Switzerland. The IDM was assessed with an artificial CH_4 release experiment inside a barn and emission measurements from a dairy housing. For these sources, the emission levels were known due to the CH_4 release or emission data obtained from a reference method. The IDM was further employed at BGPs and WWTPs where the emissions were not known. For the unknow sources the goal was to assess the handling of complex source configurations and providing emission data that can be used as a basis for country specific emission factors for the Swiss GHG inventory. Regarding the micrometeorological conditions, it was attempted to find a combination of filter criteria that reduces the data loss without including implausible emission values that were obtained under atmospheric conditions, which deviated largely from the MOST assumptions. For the surrounding

topography, the main objective was to find an optimal measurement setup design. All the measurements were related to one of four projects that are described in the following. Each project had slightly different goals regarding the assessment of the IDM.

Within the project "farms and stationary sources" an experiment with CH_4 release inside a barn was performed. In particular, it was evaluated whether there can be situations that lead to systematic under- or overestimation of emissions by means of bLS modelling. Such situations cannot be excluded a priori, since emission measurements from farms are related to sources of the target gas located in or around buildings, and the bLS model has, so far, mostly been validated for ground area sources without obstacles. The focus of the work was on the positioning of the concentration and turbulence measuring devices and the optimisation of the filtering of measurement data based on micrometeorological criteria and model parameters. Due to logistical constraints, only the lateral distance between the source and the sensors was assessed and the height above ground was not varied. This project was financed by the Swiss Federal Office for Environment (Contract 00.5082.PZ/BECDD68E6) and included further measurements that were out of the scope of this thesis. The results of this subproject are incorporated in the methods chapter (Section 2.7).

Within the project "livestock housing" CH_4 emission measurements by IDM were compared with the iTRM to quantify the emissions of a dairy housing. Taking the iTRM as a reference method, it was possible to assess the performance and suitability of the IDM for measuring housing emissions. This project was financed by the Swiss Federal Office for the Environment (Contract 00.5082.P2I R254-0652). The results of this project are described in Chapter 3.

Within the EvEmBi project (Evaluation and reduction of methane emissions from different European biogas plant concepts), CH_4 emission measurements from four different agricultural BGPs in a total of seven campaigns were conducted (Chapter 4). The goal of this project was to determine emission factors for the national GHG inventory and potential mitigation effects of measures implemented at the plants. For the thesis, the focus was to measure emissions with the IDM under difficult conditions. The challenges included nearby sources not belonging to the BGPs that confounded the emission measurements or non-horizontal, non-homogeneous, and non-flat terrain. This project was funded by the Swiss Federal Office for the Environment (Contract 17.0083.PJ/R035-0703) and the Swiss Federal Office for Energy (Contract SI/501679-01). Within the EvEmBi project, Ökostrom Schweiz had the lead for Switzerland, and the Bern University of Applied Sciences were subcontractors responsible for the emission measurements.

Within the WWTP project, the goal was to measure CH_4 emission from WWTPs and to determine emission factors for the national GHG inventory (Chapter 4). Compared to livestock housings, BGPs, or whole farms in Switzerland, WWTPs are of larger size and exhibit more individual sources with different emission strengths. Therefore, this project allowed to test the IDM for complex source configurations and for large source areas. This project was funded by the Swiss Federal Office for the Environment (Contract 06.0091.PZ/R281-0748).

Overall, in my thesis I investigated four different aspects of the applicability of the IDM to quantify emissions from the livestock sector and anaerobic digestion in waste management. For this purpose, I conducted CH_4 emissions measurements with the IDM from a release experiment inside a barn, a livestock housing, two WWTPs, and four agricultural BGPs.

1.4 References

Abegglen, C. and Siegrist, H.: Mikroverunreinigungen aus kommunalem Abwasser: Verfahren zur weitergehenden Elimination auf Kläranlagen, Federal Office for the Environment FOEN, Bern, Umwelt-Wissen Nr., 1214, 210p, 2012: https://www.bafu.admin.ch/bafu/de/home/themen/wasser/publikationen-studien/publikationen-wasser/mikroverunreinigungen-aus-kommunalem-abwasser.html, last access: 21 December 2021.

Bai, M., Sun, J., Denmead, O. T., and Chen, D.: Comparing emissions from a cattle pen as measured by two micrometeorological techniques, Environmental Pollution, 230, 584–588, doi:10.1016/j.envpol.2017.07.012, 2017.

Daelman, M. R. J., van Voorthuizen, E. M., van Dongen, U. G. J. M., Volcke, E. I. P., and van Loosdrecht, M. C. M.: Methane emission during municipal wastewater treatment, Water Research, 46, 3657–3670, doi:10.1016/j.watres.2012.04.024, 2012.

Delre, A., Mønster, J., and Scheutz, C.: Greenhouse gas emission quantification from wastewater treatment plants, using a tracer gas dispersion method, Science of the Total Environment, 605-606, 258–268, doi:10.1016/j.scitotenv.2017.06.177, 2017.

Dutta, A. and Sarkar, S.: Sequencing Batch Reactor for Wastewater Treatment: Recent Advances, Current Pollution Reports, 1, 177–190, doi:10.1007/s40726-015-0016-y, 2015.

Flesch, T. K., Desjardins, R. L., and Worth, D.: Fugitive methane emissions from an agricultural biodigester, Biomass and Bioenergy, 35, 3927–3935, doi:10.1016/j.biombioe.2011.06.009, 2011.

Flesch, T. K., Harper, L. A., Powell, J. M., and Wilson, J. D.: Inverse-dispersion calculation of ammonia emissions from Wisconsin dairy farms, Transactions of the Asabe, 52, 253–265, doi:10.13031/2013.25946, 2009.

Flesch, T. K., Vergé, X. P. C., Desjardins, R. L., and Worth, D.: Methane emissions from a swine manure tank in western Canada, Canadian Journal of Animal Science, 93, 159–169, doi:10.4141/cjas2012-072, 2013.

Flesch, T. K., Wilson, J. D., Harper, L. A., Crenna, B. P., and Sharpe, R. R.: Deducing ground-to-air emissions from observed trace gas concentrations: A field trial, Journal of Applied Meteorology, 43, 487–502, doi:10.1175/1520-0450(2004)043<0487:DGEFOT>2.0.CO;2, 2004.

Flesch, T. K., Wilson, J. D., and Yee, E.: Backward-time Lagrangian stochastic dispersion models and their application to estimate gaseous Emissions, Journal of Applied Meteorology, 34, 1320–1332, doi:10.1175/1520-0450(1995)034<1320:BTLSDM>2.0.CO;2, 1995.

FOEN: Gewässerqualität: Revision der Gewässerschutzverordnung, Federal Office for the Environment FOEN, Bern, 2015: https://www.bafu.admin.ch/bafu/de/home/themen/bildung/medienmitteilungen.msg-id-59323.html, last access: 13 December 2021.

FOEN: Biogasanlagen in der Landwirtschaft: Ein Modul der Vollzugshilfe Umweltschutz in der Landwirtschaft, Teilrevidierte Ausgabe 2021, Federal Office for the Environment FOEN, Bern, Umwelt-Vollzug Nr., 1626, 73 pp., 2016: https://www.bafu.admin.ch/bafu/de/home/themen/

wasser/publikationen-studien/publikationen-wasser/biogasanlagen-in-der-landwirtschaft.html, last access: 24 December 2021.

FOEN: Nicht validierte ARA Kennzahlen 2020 (preliminary data), Federal Office for the Environment FOEN, unpublished, 2021a.

FOEN: Switzerland's Greenhouse Gas Inventory 1990-2019, National Inventory Report: Including reporting elements under the Kyoto Protocol, Submission of April 2021 under the United Nations Framework Convention on Climate Change and under the Kyoto Protocol, Federal Office for the Environment FOEN, Bern, 2021b: https://www.bafu.admin.ch/dam/bafu/en/dokumente/klima/klima-climatereporting/National_Inventory_Report_CHE.pdf.download.pdf/National_Inventory_Report_CHE_2021.pdf, last access: 5 August 2021.

Fries, A. E., Schifman, L. A., Shuster, W. D., and Townsend-Small, A.: Street-level emissions of methane and nitrous oxide from the wastewater collection system in Cincinnati, Ohio, Environmental Pollution, 236, 247–256, doi:10.1016/j.envpol.2018.01.076, 2018.

Gerber, P. J.: Tackling climate change through livestock: A global assessment of emissions and mitigation opportunities, Food and Agriculture Organization of the United Nations FAO, Rome, 2013.

Gujer, W.: Siedlungswasserwirtschaft, 3. bearbeitete Auflage, Springer-Verlag Berlin Heidelberg, XV, 431 S, 2007.

Häni, C., Flechard, C., Neftel, A., Sintermann, J., and Kupper, T.: Accounting for field-scale dry deposition in backward Lagrangian stochastic dispersion modelling of NH3 emissions, Atmosphere, 9, 146, doi:10.3390/atmos9040146, 2018.

Harper, L. A., Flesch, T. K., and Wilson, J. D.: Ammonia emissions from broiler production in the San Joaquin Valley, Poultry Science, 89, 1802–1814, doi:10.3382/ps.2010-00718, 2010.

Huhtanen, P., Cabezas-Garcia, E. H., Utsumi, S., and Zimmerman, S.: Comparison of methods to determine methane emissions from dairy cows in farm conditions, Journal of Dairy Science, 98, 3394–3409, doi:10.3168/jds.2014-9118, 2015.

IPCC: 2006 IPCC Guidelines for National Greenhouse Gas Inventories: Volume 4, Agriculture, Forestry and Other Land Use, 2006.

Kupper, T., Bonjour, C., and Menzi, H.: Evolution of farm and manure management and their influence on ammonia emissions from agriculture in Switzerland between 1990 and 2010, Atmospheric Environment, 103, 215–221, doi:10.1016/j.atmosenv.2014.12.024, 2015.

Kupper, T., Häni, C., Neftel, A., Kincaid, C., Bühler, M., Amon, B., and VanderZaag, A.: Ammonia and greenhouse gas emissions from slurry storage - A review, Agriculture, Ecosystems & Environment, 300, 106963, doi:10.1016/j.agee.2020.106963, 2020.

Kupper, T., Plagellat, C., Brändli, R. C., Alencastro, L. F. de, Grandjean, D., and Tarradellas, J.: Fate and removal of polycyclic musks, UV filters and biocides during wastewater treatment, Water Research, 40, 2603–2612, doi:10.1016/j.watres.2006.04.012, 2006.

Liebetrau, J., Reinelt, T., Clemens, J., Hafermann, C., Friehe, J., and Weiland, P.: Analysis of greenhouse gas emissions from 10 biogas plants within the agricultural sector, Water Science and Technology, 67, 1370–1379, doi:10.2166/wst.2013.005, 2013.

Mannina, G., Butler, D., Benedetti, L., Deletic, A., Fowdar, H., Fu, G., Kleidorfer, M., McCarthy, D., Steen Mikkelsen, P., Rauch, W., Sweetapple, C., Vezzaro, L., Yuan, Z., and Willems, P.: Greenhouse gas emissions from integrated urban drainage systems: Where do we stand?, Journal of Hydrology, 559, 307–314, doi:10.1016/j.jhydrol.2018.02.058, 2018.

McGinn, S. M., Janzen, H. H., Coates, T. W., Beauchemin, K. A., and Flesch, T. K.: Ammonia emission from a beef cattle feedlot and its local dry deposition and re-emission, Journal of Environment Quality, 45, 1178–1185, doi:10.2134/jeq2016.01.0009, 2016.

Mendes, L. B., Edouard, N., Ogink, N. W., van Dooren, H. J. C., Tinôco, I. d. F. F., and Mosquera, J.: Spatial variability of mixing ratios of ammonia and tracer gases in a naturally ventilated dairy cow barn, Biosystems Engineering, 129, 360–369, doi:10.1016/j.biosystemseng.2014.11.011, 2015.

Minato, K., Kouda, Y., Yamakawa, M., Hara, S., Tamura, T., and Osada, T.: Determination of GHG and ammonia emissions from stored dairy cattle slurry by using a floating dynamic chamber, Animal Science Journal, 84, 165–177, doi:10.1111/j.1740-0929.2012.01053.x, 2013.

Mohn, J., Zeyer, K., Keck, M., Keller, M., Zähner, M., Poteko, J., Emmenegger, L., and Schrade, S.: A dual tracer ratio method for comparative emission measurements in an experimental dairy housing, Atmospheric Environment, 179, 12–22, doi:10.1016/j.atmosenv.2018.01.057, 2018.

Monin, A. S. and Obukhov, A. M.: Basic laws of turbulent mixing in the surface layer of the atmosphere, Doklady Akademii Nauk SSSR Institute of Theoretical Geophysics, 151, e187, 1954.

Ogink, N., Mosquera, J., Calvet, S., and Zhang, G.: Methods for measuring gas emissions from naturally ventilated livestock buildings: Developments over the last decade and perspectives for improvement, Biosystems Engineering, 116, 297–308, doi:10.1016/j.biosystemseng.2012.10.005, 2013.

Pain, B. F. and Menzi, H.: Glossary of terms on livestock manure management 2011, Second Edition, Recycling Agricultural, Municipal and Industrial Residues in Agriculture Network, 2011.

Poteko, J., Schrade, S., Zeyer, K., Mohn, J., Zaehner, M., Zeitz, J. O., Kreuzer, M., and Schwarm, A.: Methane emissions and milk fatty acid profiles in dairy cows fed linseed, measured at the group level in a naturally ventilated housing and individually in respiration chambers, Animals, 10, doi:10.3390/ani10061091, 2020.

Poteko, J., Zähner, M., and Schrade, S.: Effects of housing system, floor type and temperature on ammonia and methane emissions from dairy farming: A meta-analysis, Biosystems Engineering, 182, 16–28, doi:10.1016/j.biosystemseng.2019.03.012, 2019.

Pumpanen, J., Kolari, P., Ilvesniemi, H., Minkkinen, K., Vesala, T., Niinistö, S., Lohila, A., Larmola, T., Morero, M., Pihlatie, M., Janssens, I., Yuste, J. C., Grünzweig, J. M., Reth, S., Subke, J.-A., Savage, K., Kutsch, W., Østreng, G., Ziegler, W., Anthoni, P., Lindroth, A., and Hari, P.:

Comparison of different chamber techniques for measuring soil CO2 efflux, Agricultural and Forest Meteorology, 123, 159–176, doi:10.1016/j.agrformet.2003.12.001, 2004.

Reinelt, T., Delre, A., Westerkamp, T., Holmgren, M. A., Liebetrau, J., and Scheutz, C.: Comparative use of different emission measurement approaches to determine methane emissions from a biogas plant, Waste Management, 68, 173–185, doi:10.1016/j.wasman.2017.05.053, 2017.

Ren, Y. G., Wang, J. H., Li, H. F., Zhang, J., Qi, P. Y., and Hu, Z.: Nitrous oxide and methane emissions from different treatment processes in full-scale municipal wastewater treatment plants, Environmental Technology, 34, 2917–2927, doi:10.1080/09593330.2012.696717, 2013.

Samuelsson, J., Delre, A., Tumlin, S., Hadi, S., Offerle, B., and Scheutz, C.: Optical technologies applied alongside on-site and remote approaches for climate gas emission quantification at a wastewater treatment plant, Water Research, 131, 299–309, doi:10.1016/j.watres.2017.12.018, 2018.

Saunois, M., Stavert, A. R., Poulter, B., Bousquet, P., Canadell, J. G., Jackson, R. B., Raymond, P. A., Dlugokencky, E. J., Houweling, S., Patra, P. K., Ciais, P., Arora, V. K., Bastviken, D., Bergamaschi, P., Blake, D. R., Brailsford, G., Bruhwiler, L., Carlson, K. M., Carrol, M., Castaldi, S., Chandra, N., Crevoisier, C., Crill, P. M., Covey, K., Curry, C. L., Etiope, G., Frankenberg, C., Gedney, N., Hegglin, M. I., Höglund-Isaksson, L., Hugelius, G., Ishizawa, M., Ito, A., Janssens-Maenhout, G., Jensen, K. M., Joos, F., Kleinen, T., Krummel, P. B., Langenfelds, R. L., Laruelle, G. G., Liu, L., Machida, T., Maksyutov, S., McDonald, K. C., McNorton, J., Miller, P. A., Melton, J. R., Morino, I., Müller, J., Murguia-Flores, F., Naik, V., Niwa, Y., Noce, S., O'Doherty, S., Parker, R. J., Peng, C., Peng, S., Peters, G. P., Prigent, C., Prinn, R., Ramonet, M., Regnier, P., Riley, W. J., Rosentreter, J. A., Segers, A., Simpson, I. J., Shi, H., Smith, S. J., Steele, L. P., Thornton, B. F., Tian, H., Tohjima, Y., Tubiello, F. N., Tsuruta, A., Viovy, N., Voulgarakis, A., Weber, T. S., van Weele, M., van der Werf, G. R., Weiss, R. F., Worthy, D., Wunch, D., Yin, Y., Yoshida, Y., Zhang, W., Zhang, Z., Zhao, Y., Zheng, B., Zhu, Q., Zhu, Q., and Zhuang, Q.: The Global Methane Budget 2000–2017, Earth System Science Data, 12, 1561–1623, doi:10.5194/essd-12-1561-2020, 2020.

Scheutz, C. and Fredenslund, A. M.: Total methane emission rates and losses from 23 biogas plants, Waste Management, 97, 38–46, doi:10.1016/j.wasman.2019.07.029, 2019.

Schrade, S.: Ammoniak- und PM10-Emissionen im Laufstall für Milchvieh mit freier Lüftung und Laufhof anhand einer Tracer-Ratio-Methode, Christian-Albrechts-Universität, Kiel, Germany, 131 pp., 2009.

Sommer, S. G., Christensen, M. L., Schmidt, T., and Jensen, L. S.: Animal Manure Recycling, John Wiley & Sons, Ltd, Chichester, UK, 2013.

Stocker, T. F., Qin, D., Plattner, G.-K., Alexander, L. V., Allen, S. K., Bindoff, N., Bréon F.-M., Church, J. A., Cubasch, U., Emori, S., Forster, P., Friedlingstein P., Gillett, N., Gregory, J. M., Hartmann, D. L., Jansen, E., Kirtman, B., Knutti, R., Krishna Kumar, K., Lemke, P., Marotzke, J., Masson-Delmotte, V., Meehl, G. A., Mokhov, I. I., Piao, S., Ramaswamy, V., Randall, D., Rhein, M., Rojas, M., Sabine, C., Shindell, D., Talley, L. D., Vaughan, D. G., and Xie, S.-P.:

Technical Summary: In: Climate Change 2013: The Physical Science Basis. Contribution of Working Group I to the Fifth Assessment Report of the Intergovernmental Panel on Climate Change, Cambridge, United Kingdom and New York, NY, USA., 2013.

Storm, I. M. L. D., Hellwing, A. L. F., Nielsen, N. I., and Madsen, J.: Methods for measuring and estimating methane emission from ruminants, Animals, 2, 160–183, doi:10.3390/ani2020160, 2012.

VanderZaag, A. C., Flesch, T. K., Desjardins, R. L., Baldé, H., and Wright, T.: Measuring methane emissions from two dairy farms: Seasonal and manure-management effects, Agricultural and Forest Meteorology, 194, 259–267, doi:10.1016/j.agrformet.2014.02.003, 2014.

vTI: Biogas-Messprogramm II: 61 Biogasanlagen im Vergleich, Johan Heinrich von Thünen-Institut (vTI), Braunschweig, 2009: https://www.infothek-biomasse.ch/images/178_2009_FNR_Biogasanlagen_im_Vergleich.pdf, last access: 11 May 2020.

Chapter 2

Methods

2.1 Boundary layer meteorology

The atmospheric boundary layer (ABL) is the lowest part of the atmosphere. Its extension varies between 50 to 4000 m depending on the geographical position and the prevailing meteorological conditions. A detailed description of the ABL can be found in Kaimal and Finnigan (1994), Stull (1988) and Stull (2000).

Close to earth's ground there are strong gradients in the mean wind speed due to surface friction and large temperature gradients, which are related to the atmospheric radiation and its interaction with the surface. Owing to the strong vertical gradients in the ABL, there is an effective exchange of momentum, sensible heat, latent heat, and pollutants interactively emitting and absorbing from the surface. Thus, the ABL is influenced by the presence of diurnal cycles of temperature, wind, humidity, and pollution and prone to turbulence. Turbulent transport is caused by eddies that can be understood as superimposed swirls of motions on the mean wind. Eddies or turbulent flow can transport momentum, energy, and mass without a mean velocity component in the respective coordinate direction (Stull, 1988, 2000).

Whereas surface friction is always a source of turbulence, solar radiation can increase or dampen turbulence. During the day the surface usually heats up and an air parcel is displaced vertically away from the ground as it is warmer than its surroundings. This is an unstable stratification of the ABL with enhanced turbulence that can further be increased by surface friction. The extend of the unstable, strongly turbulent ABL is between one and four kilometres. If the surface is cooler than the air with prevailing light winds, the ABL is stable. Such a situation often occurs during the night or when warm air blows over a cold surface. In the stable ABL, the turbulence is weak adjacent to the ground and the ABL extent is between 50 to 500 m. In between the unstable and stable stratification there are neutral conditions. Neutral conditions are associated with rather strong winds and little cooling or heating from the surface. A neutral stratification often occurs during overcast conditions (Stull, 1988; Kaimal and Finnigan, 1994).

To determine the turbulence within a certain area, the spatial structure of the turbulence is of interest. However, it is beyond possibility to measure the three wind velocity components (u, v, w) at every location over a large area. Instead, turbulence measurements are conducted over a long time period at a single point in space (Figure 2). With Taylor's Hypothesis of 'frozen' turbulence, this temporal information can be converted into a spatial information (Taylor, 1938; Stull, 1988). The Taylor Hypothesis requires stationarity and homogeneity regarding the turbulence characteristics, i.e., turbulence production and dissipation remain constant in time and equal in space.

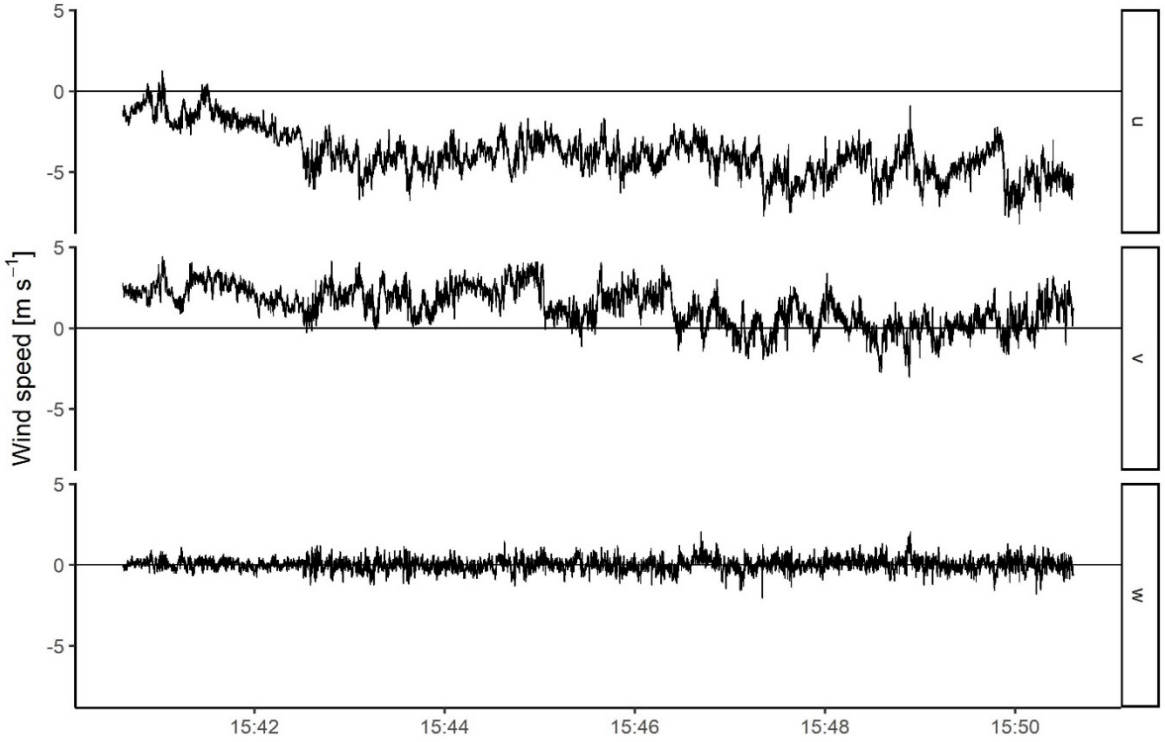

Figure 2: Snapshot of a high frequency (20 Hz) time series (UTC+1) measurements of an ultrasonic anemometer for all three wind velocity components (u, v, w).

When examining the spectral energy distribution in the turbulent atmosphere, a local minimum between 10 - 120 min is visible that is called spectral gap. It separates the lower frequencies of the energy spectrum, due to daily cycle and long-term developments like changing weather, from the higher frequencies that can be identified as turbulence.

In the surface layer, which corresponds to the bottom 5 to 10 % of the ABL, the air flow is considered to be always turbulent. While the flow can theoretically be described by the Navier-Stokes equations, due to the deterministic chaotic nature of turbulence, analytical results are limited to computational power und thus only feasible for micro scale domains (Stull, 1988). According to the Reynolds Decomposition of turbulent flow, every variable a is a superposition of a mean $\bar{a}$ and a turbulent part a',

$$a = \bar{a} + a' \qquad \text{Eq. 1}$$

where the averaging time of $\bar{a}$ should be chosen within the spectral gap (Stull, 1988). With the help of the Reynolds Decomposition, the turbulent flow can be described by means of turbulence statistics (averages, covariances, etc).

The most widely used approach to address the turbulent flow in the surface layer is the Monin-Obukhov similarity theory (MOST, Monin and Obukhov, 1954), where any scaled mean variable can be expressed as a function of the surface flux of momentum $\overline{u'w'_0}$, the surface flux of sensible heat $\overline{w'\theta'_0}$, the buoyancy parameter $g/\bar{\theta}$ and the height z (Stull, 1988). However, Monin and Obukhov (1954) used the friction velocity u_*

$$u_* \equiv \left[\overline{(u'w'_0)^2 + (v'w'_0)^2}\right]^{1/4} \quad \text{Eq. 2}$$

instead of $\overline{u'w'_0}$, and a characteristic temperature scale θ_*

$$\theta_* \equiv \frac{-\overline{w'\theta'_0}}{u_*} \quad \text{Eq. 3}$$

For practical reasons, u_* and θ_* are evaluated at a convenient measurement height, as their fluxes are assumed constant within the surface layer. Further, Monin and Obukhov (1954) used the Obukhov length L (Obukhov, 1946) as a characteristic length scale.

$$L \equiv \frac{1}{k}\frac{{u_*}^2}{\theta_*}\left(\frac{g}{\bar{\theta}}\right)^{-1} = -\frac{1}{k}\frac{{u_*}^3}{\overline{w'\theta'_0}}\left(\frac{g}{\bar{\theta}}\right)^{-1} \quad \text{Eq. 4}$$

whereby k is the von Kármán constant, $k \approx 0.4$. L can be interpreted as the height at which in the stable surface layer the turbulence produced by buoyancy exceeds the turbulence produced by wind shear (Stull, 2000). For unstable conditions, the heat flux is positive and therefore $L < 0$ and for stable conditions, the heat flux is negative thus $L > 0$. When approaching neutral conditions ($\overline{w'\theta'_0} \to 0$), $L \to \infty$. If the coordinate system is rotated into the mean flow direction and the assumption of horizontally homogeneous conditions are fulfilled, Eq. 2 can be reduced to

$$u_* = \sqrt{\overline{(u'w'_0)}} \quad \text{Eq. 5}$$

With MOST the logarithmic wind profile in the surface layer is expressed as

$$\frac{\partial \bar{u}}{\partial z}\frac{kz}{u_*} = \psi_m\left(\frac{z}{L}\right) \quad \text{Eq. 6}$$

and the thermal stratification and the variability in the vertical wind w can be expressed as

$$\frac{\partial \bar{\theta}}{\partial z}\frac{kz}{\theta_*} = \psi_h\left(\frac{z}{L}\right) \quad \text{Eq. 7}$$

$$\frac{\sigma_w}{u_*} = \psi_w\left(\frac{z}{L}\right) \quad \text{Eq. 8}$$

where σ_w is the standard deviation of w (Kaimal and Finnigan, 1994).

In neutral conditions $z/L \to 0$ and thus $\psi_m = 1$. From multiple field experiments, ψ_m was empirically defined for unstable and stable conditions:

unstable $\psi_m = (1 - \gamma\frac{z}{L})^{\beta} \quad for\ \frac{z}{L} < 0$ Eq. 9

stable $\psi_m = 1 + \alpha\frac{z}{L} \quad for\ \frac{z}{L} > 0$ Eq. 10

neutral $\psi_m = 1 \quad for\ \frac{z}{L} = 0$ Eq. 11

where, often $\alpha \approx 6$, $\beta \approx -1/4$ and $\gamma \approx 16$ (Högström, 1988).

In fact, the surface layer can be subdivided into a roughness sublayer and an inertial sublayer, whereas MOST is only applicable for the latter. The inertial sublayer begins at the roughness height z_0, where the wind speed of the logarithmic wind profile is assumed to be zero. Thus, an integration of Eq. 6 from $z = z_0$ where $\bar{u}(z_0) = 0$ to any height z in the surface layer, yields

$$\bar{u}(z) = \frac{u_*}{k}\left(\ln(\frac{z}{z_0}) - \Psi_m\left(\frac{z}{L}\right) + \Psi_m\left(\frac{z_0}{L}\right)\right) \quad \text{Eq. 12}$$

where Ψ_m is the integrated form of the non-dimensional wind shear (Eq. 10 - Eq. 9) (Kaimal and Finnigan, 1994).

2.2 Inverse dispersion method concept

The IDM combines concentration measurements with an atmospheric dispersion model to calculate emissions from sources of atmospheric trace gases. The IDM requires a spatially limited source area of known extension e.g., a livestock housing. The source is emitting an unknown amount of gas (e.g., CH_4) that is dispersed due to atmospheric turbulence as schematically shown in Figure 3. Downwind of the source, the concentration of the emitted gas is measured with either a point or an open-path sensor. To separate the contribution of the source from the incoming (background) concentration at the downwind measurement location, the concentration upwind of the source is equally measured. In the vicinity of the downwind concentration measurements, also the turbulence characteristics are determined by using a 3-dimensional ultrasonic anemometer. There are a variety of dispersion models available e.g., a simple Gaussian plume model or a more complex Lagrangian model (Harper et al., 2011). All the models have in common that they simulate, for a given state of the atmosphere, a concentration-emission relationship at the downwind concentration sensor location (Clauss et al., 2019). This simulated (sim) concentration (C) – emission (E) relation is called dispersion factor D [s m^{-1}]:

$$D = \left(\frac{C}{E}\right)_{sim} \quad \text{Eq. 13}$$

The dispersion factor is independent of the source's real emission. It is solely dependent on the wind field and the turbulence. With the background corrected concentration data (ΔC)

$$\Delta C = C_{downwind} - C_{upwind} \quad \text{Eq. 14}$$

and the dispersion factor D, emissions E of the source can be calculated:

$$E = \frac{\Delta C}{D} \quad \text{Eq. 15}$$

By rearranging Eq. 15, it is also possible to calculate an expected concentration at a certain location if the emission of the source is known.

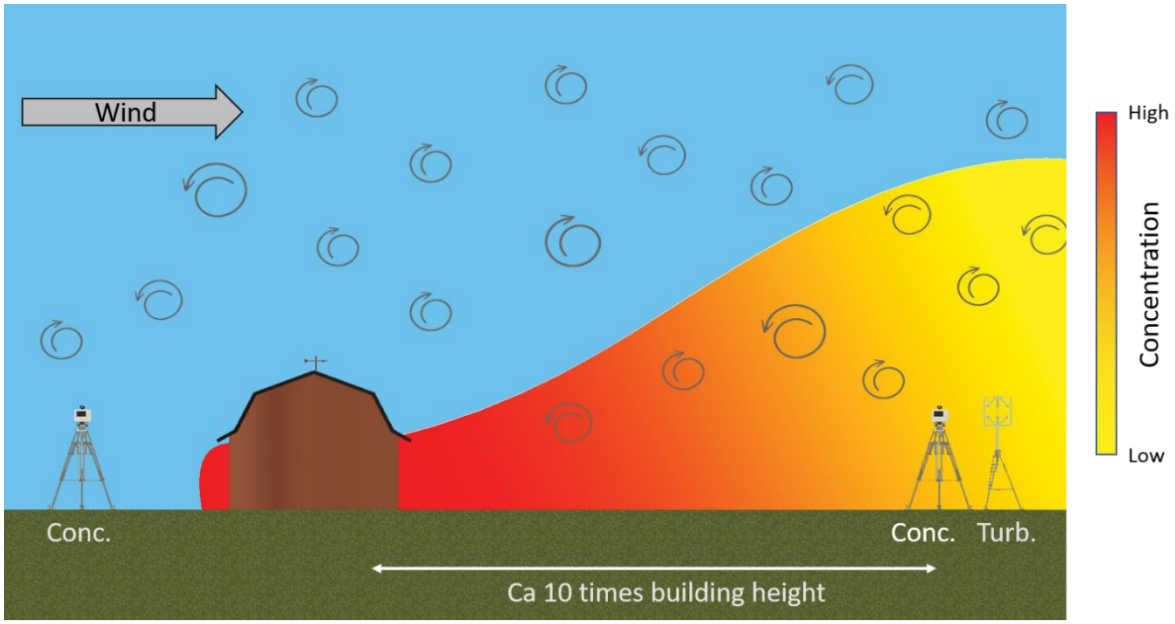

Figure 3: Concept of the inverse dispersion method for emission measurements of a livestock housing. There are up- and downwind concentration measurements (Conc.). Additionally, the turbulence parameters are measured (Turb.) with a 3-dimensional ultrasonic anemometer.

The advantage of the IDM is that no measurements are conducted within the source area. Thus, it does not alter the environmental properties of the source (e.g., if emissions from soils are measured) or influence the behaviour of animals (Ogink et al., 2013). The drawback of the method is that the wind field is strongly simplified and thus idealised. The dispersion in the entire study area is represented by turbulence measurements conducted at a single point in space. Depending on the topography, this could lead to substantial differences between the modelled and the real turbulence conditions. Additionally, obstacles like buildings lead to disturbances, which are not reflected in the modelled wind field. With increasing distance (downwind) to the obstacles, the impact of disturbances decreases (Häni, 2019). Therefore, it is advised to conduct concentration and turbulence measurements at least 10 times the building height downwind of the source and in horizontal, homogeneous, and flat terrains (Harper et al., 2011).

Due to the large distance between the source and the concentration measurement location, especially if open-path sensors are used, it is not possible with the IDM to differentiate between sources that are close to each other (Ogink et al., 2013). Therefore, only an emission integrated over a certain area remains determinable. Nevertheless, such results are of high interest, if the average emission of a whole farm (housing, outside yard, slurry store), or a WWTP are to be quantified.

2.3 bLS model

In this thesis, the backward Lagrangian stochastic (bLS) model based on Flesch et al. (2004) was implemented according to Häni et al. (2018). It is assumed that a concentration measurement C at point M is conducted (Figure 4).

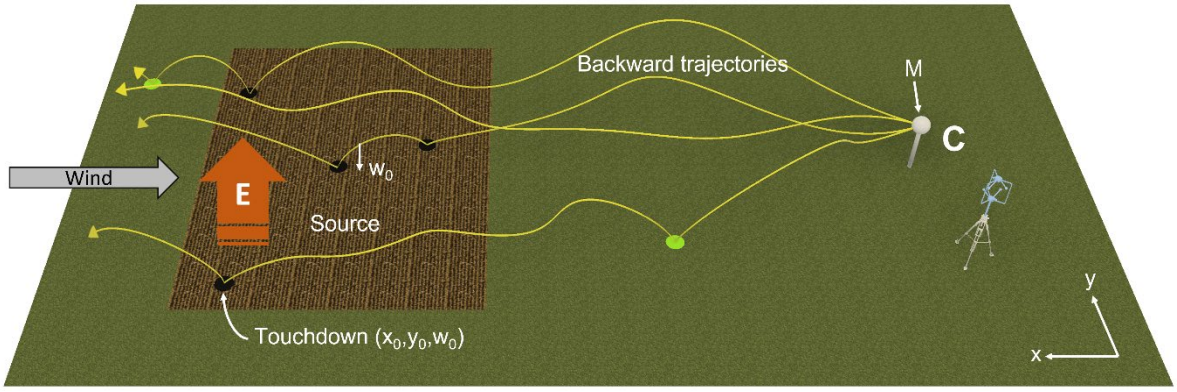

Figure 4: Illustration of the bLS model for estimating gaseous emission rate E. Average concentration C is measured at point M downwind of the source. The ratio $(C/E)_{sim}$ is calculated from backward trajectory touchdowns inside the source (w_0 is the vertical velocity at touchdown). Figure and figure caption are adapted from Flesch et al. (2004).

From point M, at random a trajectory out of a Gaussian distribution is calculated backward in time. If the air parcel hits the ground the instantaneous wind components are inverted so that the covariances $(\overline{u'w'}, \overline{v'w'})$ remain constant. The bLS considers the source area as a ground with indefinitely small extension z. The residence time $t_{residence}$ of the air parcel within this layer is defined as

$$t_{residence} = \frac{z}{w_{TD}} * 2 \qquad \text{Eq. 16}$$

whereas w_{TD} is the vertical velocity of the air parcel at the touchdown (TD) location. The source layer is emitting and has a source strength S in unit concentration per time and volume. It can be understood as concentration charging layer, thus with $t_{residence}$ the concentration C can be calculated.

$$C = S * t_{residence} \qquad \text{Eq. 17}$$

Inserting Eq. 16 in Eq. 17 results in

$$\frac{C}{E} = \frac{2}{w_{TD}} \qquad \text{Eq. 18}$$

with E being an emission with the unit mass per area per time. As there might be multiple touchdowns within the source, for each trajectory Eq. 18 is summed up. To get the unbiased best estimate a number of N trajectories from the given distribution are calculated backward in time and then the average of them is taken. This leads to the equation

$$(C/E)_{sim} = \frac{1}{N} \sum_{TD} \frac{2}{w_{TD}} \qquad \text{Eq. 19}$$

In this thesis, for N a number between 250,000 and 1,000,000 was used. With increasing number of touchdowns within the source area the uncertainty of the modelled ratio will decrease.

In this thesis E is defined as an emission density with the unit mass per area per time and Q as the emission with unit mass per time.

$$(C/Q)_{sim} = \frac{(C/E)_{sim}}{A_{source}} \qquad \text{Eq. 20}$$

With the simulated concentration-emission ratio, sometimes denoted as dispersion factor D_{bLS}, and a measured concentration difference between the downwind concentration $C_{downwind}$ and the upwind concentration C_{upwind}, an emission can be calculated

$$E = \frac{C_{downwind} - C_{upwind}}{(C/E)_{sim}} \quad \text{Eq. 21}$$

In this thesis, the implementation of the bLS model in the R software (R Core Team, 2020) package bLSmodelR (Häni et al., 2018), available at https://github.com/ChHaeni/bLSmodelR, was used. As input parameters the bLSmodelR requires source-sensor geometry and the turbulence parameters u_*, L, σ_u, σ_v, σ_w, z_0 together with the wind direction (Häni et al., 2018). The advantage of the bLSmodelR is that all data handling from raw data to final emissions can be done in the R software and no external software is needed. Components of the bLS model are parallelised and the model can be executed on a computer cluster. This substantially reduces the computational time, and the personal computer may be simultaneously switched off or used for different tasks.

2.4 Requirements for the measurement sites

As described in section 2.1, MOST needs stationarity and homogeneity regarding the turbulence conditions. Therefore, ideally horizontal homogeneous and flat areas extending over several kilometres are preferred as measurement sites. To avoid adaptation of the measurement setup every few hours or days, one or two main wind directions are necessary. If emissions from buildings are measured, the distance between the source and the downwind measurement locations should be not less than about 10 times the source height so that the turbulence fulfils the assumptions of homogeneity and stationarity (Gao et al., 2010; Harper et al., 2011). Therefore, enough space upwind and downwind of the source should be available to set up the measurement devices. With open-path measurements with path lengths up to 300 m, a wide-open space is required. The measurement height should be at least three times the canopy height. Additionally, there should not be any source of the measured gas species upwind or between the concentration measurement location that could confound the concentration measurements. Thus, an extended assessment of the preselected location is needed to test its viability as a measurement site.

2.5 Performance of open-path GasFinder3 devices for CH_4 concentration measurements close to ambient levels*

Christoph Häni[1], Marcel Bühler[1,2,3], Albrecht Neftel[4], Christof Ammann[5], Thomas Kupper[1]

[1]*School of Agricultural, Forest and Food Sciences HAFL, Bern University of Applied Sciences, Switzerland*

[2]*Oeschger Centre for Climate Change Research, University of Bern, Switzerland*

[3]*Institute of Geography, University of Bern, Switzerland*

[4]*Neftel Research Expertise, Switzerland*

[5]*Climate and Agriculture Group, Agroscope, Switzerland*

Atmospheric Measurement Techniques, Vol. 14, 1733-1741, 2021

Abstract. Open-path measurements of methane (CH_4) with the use of GasFinder systems (Boreal Laser Inc, Edmonton Canada) have been frequently used for emission estimation with the inverse dispersion method (IDM), particularly from agricultural sources. It is common to many IDM applications that the concentration enhancement related to CH_4 sources is small, typically between 0.05 and 0.5 ppm, and accurate measurements of CH_4 concentrations are needed at concentrations close to ambient levels. The GasFinder3-OP (GF3) device for open-path CH_4 measurements is the latest version of the commercial GasFinder systems by Boreal Laser Inc. We investigated the uncertainty of six GF3 devices from side-by-side intercomparison measurements and comparisons to a closed-path quantum cascade laser device. The comparisons were made at near-ambient levels of CH_4 (85 % of measurements below 2.5 ppm) with occasional phases of elevated concentrations (max. 8.3 ppm). Relative biases as high as 8.3 % were found, and a precision for half-hourly data between 2.1 and 10.6 ppm-m (half width of the 95 %confidence interval) was estimated. These results deviate from the respective manufacturer specifications of 2 % and 0.5 ppm-m. Intercalibration of the GF3 devices by linear regression to remove measurement bias was shown to be of limited value due to drifts and step changes in the recorded GF3 concentrations.

*For this co-author publication, I was responsible for all GasFinder measurements from 2018 onwards and provided feedback regarding the GasFinder handling and faced issues. Further, I advised proofreading the manuscript and gave minor inputs regarding its implementation.

Atmos. Meas. Tech., 14, 1733–1741, 2021
https://doi.org/10.5194/amt-14-1733-2021

Atmospheric Measurement Techniques
Open Access
EGU

Performance of open-path GasFinder3 devices for CH_4 concentration measurements close to ambient levels

Christoph Häni[1], **Marcel Bühler**[1,2,3], **Albrecht Neftel**[4], **Christof Ammann**[5], **and Thomas Kupper**[1]

[1]School of Agricultural, Forest and Food Sciences HAFL, Bern University of Applied Sciences, Zollikofen, 3052, Switzerland
[2]Oeschger Centre for Climate Change Research, University of Bern, Bern, 3012, Switzerland
[3]Institute of Geography, University of Bern, Bern, 3012, Switzerland
[4]Neftel Research Expertise, Wohlen b. Bern, 3033, Switzerland
[5]Climate and Agriculture Group, Agroscope, Zürich, 8046, Switzerland

Correspondence: Christoph Häni (christoph.haeni@bfh.ch)

Received: 12 August 2020 – Discussion started: 7 October 2020
Revised: 30 December 2020 – Accepted: 12 January 2021 – Published: 3 March 2021

Abstract. Open-path measurements of methane (CH_4) with the use of GasFinder systems (Boreal Laser Inc, Edmonton Canada) have been frequently used for emission estimation with the inverse dispersion method (IDM), particularly from agricultural sources. It is common to many IDM applications that the concentration enhancement related to CH_4 sources is small, typically between 0.05 and 0.5 ppm, and accurate measurements of CH_4 concentrations are needed at concentrations close to ambient levels. The GasFinder3-OP (GF3) device for open-path CH_4 measurements is the latest version of the commercial GasFinder systems by Boreal Laser Inc. We investigated the uncertainty of six GF3 devices from side-by-side intercomparison measurements and comparisons to a closed-path quantum cascade laser device. The comparisons were made at near-ambient levels of CH_4 (85 % of measurements below 2.5 ppm) with occasional phases of elevated concentrations (max. 8.3 ppm). Relative biases as high as 8.3 % were found, and a precision for half-hourly data between 2.1 and 10.6 ppm-m (half width of the 95 % confidence interval) was estimated. These results deviate from the respective manufacturer specifications of 2 % and 0.5 ppm-m. Intercalibration of the GF3 devices by linear regression to remove measurement bias was shown to be of limited value due to drifts and step changes in the recorded GF3 concentrations.

1 Introduction

The experimental determination of methane (CH_4) emission rates from agricultural sources is a key element for emission inventories and for the development of mitigation strategies. A large diversity of approaches to derive emission rates from measurements is available. Focusing on micrometeorological methods, they can broadly be divided into flux-based and concentration-based approaches. The latter combine measurements of the concentration enhancement downwind or above the source with the modeling of the dispersion of the concentration released by the source. One frequently applied concentration-based approach is the inverse dispersion method (IDM; Flesch et al., 2005) where, generally, two concentration measurements are used in parallel, placed up- and downwind of the source under investigation. It is common to many IDM applications that the concentration enhancement related to CH_4 sources is small, typically between 0.05 and 0.5 ppm.

In recent years, optical open-path instruments have become commercially available that determine the path-integrated CH_4 concentration over measurement path lengths of up to several hundred meters. Regarding the IDM, path-integrated concentration measurements are preferable over point measurements, since they capture a larger fraction of the emission-related plume and, therefore, are less sensitive to variation and uncertainty in the measured wind direction.

On the other hand, it is more difficult to assess and control the quality of measurements by open-path gas analyzers in comparison to closed-path instruments. The latter can

be checked or recalibrated periodically during a field campaign using common cylinder standards (also for multiple spatially separated instruments). This is usually not possible for open-path devices with longer measurement paths. The use of cylinder standard gases is feasible for very short path lengths (few meters), but the corresponding calibration may not be representative for other setups with longer path lengths (DeBruyn et al., 2020). Therefore, the quality of open-path measurements in the field with path lengths of 10 to 100 m (or longer) needs to be tested in other ways using instrument internal quality indicators, plausibility checks and intercomparisons of two or more instruments.

In this paper, we focus on the GasFinder3-OP (GF3) system for CH_4 measurements (Boreal Laser Inc, Edmonton Canada; "Lo-Range" methane variant, i.e., detection range between 2 and 8500 ppm-m). This open-path system has a very user-friendly design and is in the lower cost range of available instruments. It is an improved version of the GasFinder2 system, which has been frequently used to measure emission rates with the IDM (e.g., Flesch et al., 2007; Harper et al., 2010; McGinn et al., 2019; VanderZaag et al., 2014). The aim of this study is to characterize the stability and accuracy of the GF3 instruments for CH_4 measurements close to ambient levels. We present an overview of several field campaigns including (i) intercomparisons between GF3 devices and a fast-response quantum cascade laser spectrometer (QCL) considered to be a state-of-the-art reference and (ii) direct intercomparisons between various GF3 instruments. They served to generate a basis to correct the measurement data of individual GF3 instruments placed up- and downwind of emitting sources, which induced a low concentration enhancement where instrument stability and accuracy are particularly important. This article is written from the point of view of a GF3 instrument's end user.

2 Materials and methods

2.1 GasFinder3-OP instrument

The GF3 instrument from Boreal Laser Inc. is an open-path instrument with a tunable laser diode emitting in the infrared centered around 1654 nm where CH_4 shows a distinct absorption line. The measurement output of the GF3 is provided as path-integrated concentration C_{PI} in units of parts per million meter (denoted ppm-m) that reflects the concentration integrated over the one-way path length (distance between laser source and reflector). The output data in units of ppm-m were converted to the path-averaged concentration C in units of parts per million (i.e., divided by the one-way path length) and corrected with temperature and pressure correction functions provided by the manufacturer. Six different open-path GF3 devices were used in this study (Table 1). The two devices OP-Ext and OP-1, as well as OP-3 and OP-5, had identical pressure and temperature correction functions.

The "Lo-Range" version of the GF3 for CH_4 measures in the range of 2 to 8500 ppm-m with a sensitivity (precision) of 0.5 ppm-m at a sample rate of 1 to 1/3 Hz as stated by the manufacturer (Boreal Laser Inc., 2020). The accuracy of the GF3 system is specified as 2 % of the reading (Boreal Laser Inc., 2018a) with a lower value for the "typical accuracy" of 0.5 % of the reading (Boreal Laser Inc., 2018b). Details on the instrument are given in DeBruyn et al. (2020).

Together with the concentration measurement, the supporting parameters "received power" (of the reflected incoming beam) and "R2" (the goodness of fit between the sample and the calibration waveform) are provided as standard outputs of the GF3 instruments. According to the manufacturer, a valid concentration measurement can be expected if the following constraints are met: received power is in the range of 50 to 3000 µW and R2 is above 0.85 (Boreal Laser Inc., 2018b). We decided to be stricter and kept data for further analysis only if the received power was in the range of 100 to 2500 µW (as suggested in Boreal Laser Inc., 2016) and R2 was equal to or greater than 0.98. The quality-assessed data were aggregated to 1 and 30 min average concentrations. Only averages resulting from a data coverage of 90 % or more of the respective time interval were retained for further evaluation.

2.2 Intercomparison campaigns

In total, eight intercomparison campaigns were conducted at different sites in Switzerland with varying ranges of near-ambient concentrations of CH_4 (Table 2). Two campaigns, P16 and P17, with a focus on the comparison between GF3 devices and a QCL (QC-TILDAS, Aerodyne Research Inc.) as a reference system, were conducted in Posieux (46°46′4.22″ N, 7°6′27.65″ E) close to an animal housing facility (approx. 100 m north). The QCL is a closed-path instrument with a 20 m inlet tube flushed by a vacuum pump at 13 sL min^{-1}. The sample air is analyzed in a multi-pass cell (0.5 L) with a fixed optical path length of 76 m. The cell is kept at constant temperature (294 K) and pressure (31 Torr). Due to the stabilized operation, the instrument exhibits a high precision (1 s) around 0.004 ppm or 0.2 % (Nelson et al., 2004; Wang et al., 2020).

Seven intercomparison campaigns including various GF3 instruments placed side by side were carried out at the following locations: A18 in Aadorf (47°29′19.03″ N, 8°55′8.83″ E) next to a dairy housing facility; K19 in Kaufdorf (46°50′34.60″ N, 7°30′12.23″ E); H19-1, H19-2 and H19-3 in Hindelbank (46°59′11.86″ N, 7°28′22.01″ E) close to a wastewater treatment plant; I19 in Ittigen (46°59′13.04″ N, 7°28′20.38″ E) in the vicinity of a biogas plant; and P17 where both the intercomparison of the GF3 and the comparison to the QCL were assessed. Different types of reflectors for the open-path instruments were in us-

Table 1. GasFinder3-OP devices and their deployment in the different intercomparison campaigns. Details on the intercomparison campaigns are given in Table 2.

Name used in this study	Unit number	Year of manufacture	Intercomparison campaign							
			P16	P17	A18	K19	I19	H19-1	H19-2	H19-3
OP-Ext*	CH4OP-30015	2016	•							
OP-1	CH4OP-30017	2016		•	•	•	•	•	•	•
OP-2	CH4OP-30016	2016		•	•	•	•			•
OP-3	CH4OP-30018	2016		•	•	•	•			•
OP-4	CH4OP-30025	2019					•		•	•
OP-5	CH4OP-30026	2019				•	•	•		•

* On loan from Boreal Laser Inc.

Table 2. Characteristics of the intercomparison campaigns (Cmp.). Dur.: duration of the campaign. Conc.: measured average (minimum and maximum) concentration. Air temperature: average (and minimum, maximum) values. Air press.: average air pressure.

Cmp.	Location	Date	Dur. (days)	Instruments	Conc. (ppm)	Air temperature (°C)	Air press. (hPa)
P16	Posieux	12 Oct–1 Nov 2016	19.7	QCL, 1 × GF3	2.5 (1.9 to 7.2)	7.5 (−0.1 to 16.8)	946
P17	Posieux	19 Jul–15 Aug 2017	26.8	QCL, 3 × GF3	2.3 (1.6 to 5.8)	18.3 (7.3 to 32.2)	943
A18	Aadorf	23 Oct–21 Nov 2018	28.6	3 × GF3	2.2 (1.6 to 3.8)	6.3 (−2.4 to 17.9)	952
K19	Kaufdorf	25 Apr–30 Apr 2019	4.7	4 × GF3	1.8 (1.7 to 2.2)	7.7 (2.3 to 21.7)	955
I19	Ittigen	19 Jul–29 Jul 2019	10.2	5 × GF3	2.3 (1.6 to 8.3)	22.6 (13.6 to 35.4)	951
H19-1	Hindelbank	23 Sep–7 Oct 2019	12.7	2 × GF3	1.9 (1.6 to 2.7)	13.9 (3.6 to 24.7)	956
H19-2	Hindelbank	7 Oct–14 Oct 2019	5.1	2 × GF3	2.0 (1.6 to 2.7)	12.7 (5.1 to 22.4)	959
H19-3	Hindelbank	25 Oct–6 Nov 2019	12.3	5 × GF3	2.0 (1.6 to 3.4)	9.7 (4.2 to 17.7)	953

age[1]. In the campaigns P16, P17 and A18, the seven-corner cube array type was used; in H19-1, H19-2, H19-3 and I19, the 12-corner cube array type was used; and in K19 both types were used.

During side-by-side intercomparisons, the laser beams of the GF3 devices were always aligned in parallel with small lateral distances of 1 to 2 m. Instrument and laser beam heights were between 1.3 and 1.7 m above ground. For the comparison to the QCL measurements, the QCL inlet was located approx. 4 to 12 m from the center of the laser beams 1.9 m above ground.

For the temperature and pressure correction of the GF3 instruments (Sect. 2.1) during the field campaigns, the temperature and pressure data from a close-by weather station were used. In A18, the weather station was situated 1.2 km away with a negligible difference in the elevation of approx. 6 m. At all other sites, the weather station was within 100 m of the devices. All measurements were conducted continuously, i.e., during day and night, in regions characterized by agricultural activities related to livestock production.

[1]In 2016, when the first devices of GF3 (OP-1 to OP-3) were ordered, Boreal Laser Inc. recommended seven-corner cube array reflectors for path lengths up to 200 m. Meshes of different grid sizes could be installed in front of the corner cubes for path lengths that are shorter than the specified range. Prior to the second order in 2019 (devices OP-4 and OP-5), the recommendation was adapted to use the 12-corner cube array reflectors for path lengths up to 200 m.

2.3 Data evaluation

For a valid concentration comparison between the parallel instruments, the internal clocks of the individual devices were adjusted such that all concentration data were synchronous. This time synchronization was done by maximizing the covariance of the high-frequency concentration data in parts per million between the individual instruments. For each day, the data were broken down to 1 s data (i.e., inserting repetition values where necessary), and the time shift with the highest covariance was assessed. From these daily estimates of time shifts, a constant time lag was estimated and corrected for each device and each campaign individually. Time lags around 2 to 5 s d^{-1} between the devices have been observed and corrected for.

In two intercomparison campaigns (P16 and P17) four different GF3 devices (OP-Ext, OP-1, OP-2 and OP-3) were compared to the closed-path point measurements by the QCL instrument based on the 30 min averaged concentrations.

In seven intercomparisons (P17, A18, K19, I19, H19-1, H19-2 and H19-3), the GF3 devices OP-1, OP-2, OP-3, OP-4 and OP-5 were compared by parallel measurements. The analysis of these intercomparisons is based on both 1 and

30 min averaged concentration data. The device OP-1 was running during all side-by-side campaigns and, thus, was selected as the (relative) reference instrument; i.e., any comparison was done with reference to OP-1.

Based on the synchronized time series, the concentration difference ΔC between the parallel instruments was calculated for each averaging interval. The ΔC data partly showed significant deviations (asymmetry, outliers) from an ideal Gaussian distribution. Thus, for analyzing the difference between devices, the median ΔC and the "median absolute deviation" (MAD) of ΔC over each campaign were determined for each pair of devices. The two quantities are robust estimates of the mean and variability of ΔC that are insensitive to outliers and do not rely on prescribed data distributions. For the ideal case of a Gaussian distribution, the MAD can be related to twice the standard deviation (comprising 95 % of the data) by multiplication with a factor of 2.9. The resulting value represents an estimate for the (random) precision of ΔC, whereas the median ΔC represents the (systematic) bias between the two instruments. The estimates of bias and precision of ΔC can be partitioned equally to the concentrations of both intercompared devices by dividing by the square root of 2 (according to Gaussian error propagation). Thus, the relative bias and the precision of an individual GF3 device for a campaign period were estimated as

$$\text{Rel. bias} = \frac{\text{median}(\Delta C)}{C_{\text{avg}}\sqrt{2}}, \quad (1)$$

$$\text{Precision} = \frac{2.9 \times \text{MAD}(\Delta C)}{l_{\text{path}}\sqrt{2}}, \quad (2)$$

where the relative bias was expressed relative to the concentration average of the two devices C_{avg}, and the precision was converted back to path-integrated concentrations C_{PI} using the one-way path length l_{path} of the GF3 device (in the case of the intercomparison of two GF3 devices the path lengths were averaged).

In addition to the concentration differences, the parallel measurements were also analyzed concerning their linear relationship using the Deming regression that considers measurement errors from both instruments. The GF3 devices were analyzed with reference to OP-1. Coefficients from the linear regression and the predicted ΔC at OP-1 concentration levels of 2 and 4 ppm were reported for each device (OP-2, OP-3, OP-4 and OP-5) and campaign, if the number of observations exceeded 20 and the concentration range was large enough (difference between 0.025 and 0.975 quantiles greater than 0.4 ppm).

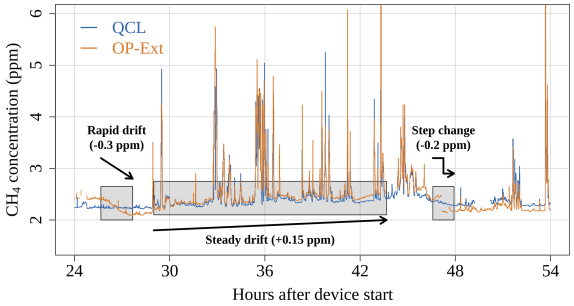

Figure 1. Time series of the average CH_4 concentration (1 min averages) measured with the QCL and the GF3 device OP-Ext during the intercomparison campaign P16. The figure shows a 30 h window at the beginning of the campaign (1 to 2.5 d after instrument start). Three sub-periods with specific features are marked by grey shading.

3 Results and discussion

3.1 Intercomparison between GF3 and QCL

During the two intercomparison campaigns P16 and P17, the magnitude and temporal course of the GF3 concentrations measured by the devices OP-Ext, OP-1, OP-2 and OP-3 compared well to the concentration measured by the QCL, specifically for high-frequency structures. Figure 1 shows 1.5 d of parallel QCL and OP-Ext measurement in campaign P16. However, when focusing on the lower end "baseline" concentrations near 2.2 ppm, the OP-Ext signal shows drifts and steps relative to the more stable QCL signal on the order of 0.2 ppm (shaded phases in Fig. 1). This corresponds to instrument-related changes in the path-integrated concentration of about 7.4 ppm-m (path length of 37 m).

At the 26 h timestamp, a drift occurred dropping the concentration of OP-Ext from roughly 0.2 ppm above to roughly 0.1 ppm below the QCL concentration. There is no indication of a deterioration of the measurement quality of the GF3 values during this period. The received laser beam power was always above 100 µW, and the R2 value for the waveform fit was greater than 0.98 (Sect. 2.1). Further, there was no correlation of the drift with the local weather data (air temperature, wind direction, wind speed, relative humidity, etc.; data not shown). The same applies to step changes and drifts of GF3 devices, typically over several hours, during other phases of the intercomparison campaigns. In some selected cases, step changes in the concentration could occur when there was activity related to device handling during operation (such as downloading data, checking the reference cell state, etc.), as observed at hour 46 in Fig. 1. However, such device handling should not affect the measurements, and it remains unclear what exactly causes the signal changes. Since these drifts and step changes cannot be distinguished from real changes in the ambient concentration without the information from a further

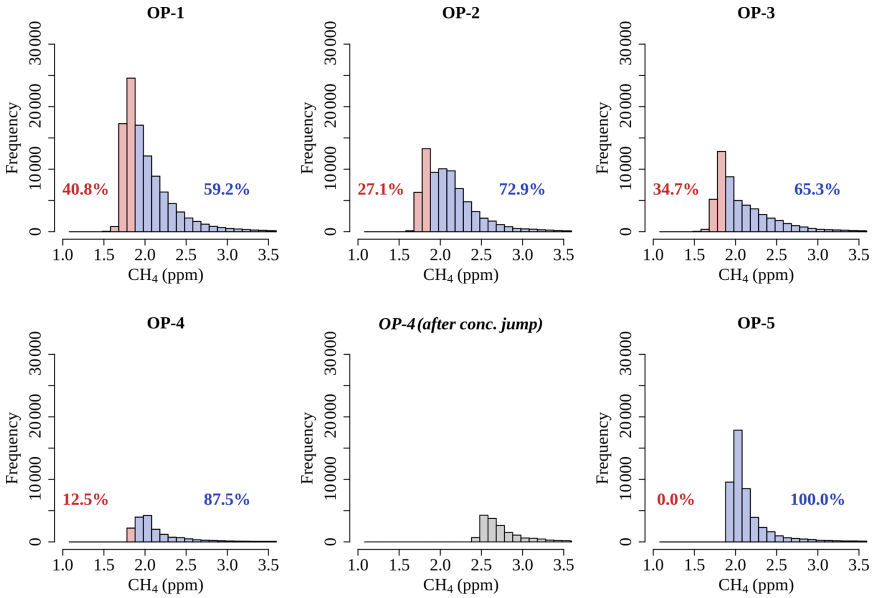

Figure 2. Histograms of recorded 1 min average concentrations of GF3 devices OP-1, OP-2, OP-3, OP-4 and OP-5. A few values greater than 3.5 ppm are not shown. Blue: values > 1.88 ppm; red: values ≤ 1.88 ppm. Grey: data from device OP-4 during the campaign H19-3 that passed the quality check but have been omitted in the analysis due to an obvious jump in the concentration (Fig. 3).

parallel measurement, they affect the uncertainty in the GF3 measurements.

Bias and precision of the GF3 devices (Sect. 2.3) were estimated and compared to the accuracy (2 % of reading) and sensitivity (0.5 ppm-m) specified in the GF3 operation manual. The magnitude of the relative bias of the GF3 is higher than the stated 2 %, with values ranging from −2.7 % to −8.3 % (Table 3). The C_{PI} precision for the GF3 devices was determined to 2.1 up to 10.6 ppm-m, which is between 4 and 21 times higher than the specified sensitivity of 0.5 ppm-m.

3.2 GF3 side-by-side intercomparisons

A cumulated dataset of 60 d in total with GF3 side-by-side measurements that passed the enhanced quality checks was produced within the seven intercomparison campaigns P17, A18, K19, I19, H19-1, H19-2 and H19-3. It contains the periods during which at least two devices were running in parallel, i.e., the reference device OP-1 and at least one further instrument (OP-2, OP-3, OP-4 or OP-5). Data from device OP-4 measured during the campaign H19-3 passed the quality check but have been omitted in the further analysis due to an obvious jump in concentration (Figs. 2 and 3). The overall average CH_4 concentration was 2.1 ppm. The 1 min averages ranged between 1.3 and 40.3 ppm, with most of the data centered around 2.0 ppm.

Extended periods of CH_4 concentrations constantly below 1.88 ppm, the minimum of the monthly average background

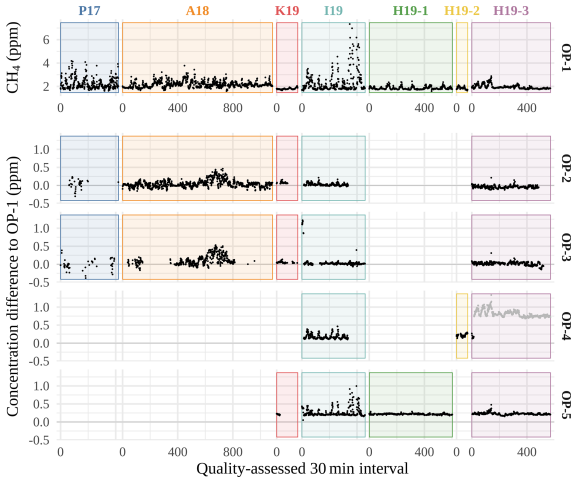

Figure 3. CH_4 concentrations recorded by OP-1 (30 min averages) and the corresponding differences to OP-2, OP-3, OP-4 and OP-5. Grey dots: data from device OP-4 during the campaign H19-3 that passed the quality check but have been omitted in the analysis due to an obvious jump in the concentration.

concentration in Switzerland since 2016 (BAFU, 2019), could be observed with devices OP-1, OP-2 and OP-3. Overall, shares of measured CH_4 concentration (1 min averages) below 1.88 ppm ranged from 0 % (OP-5) and 13 % (OP-4) to

Table 3. Direct comparison of GF3 to QCL (30 min averages) during campaigns P16 and P17. *N*: number of 30 min intervals. Path: path length of GF3 device. Median *C*: median concentration of the GF3 device. Rel. bias: estimate of the GF3 relative bias. Precision: estimate of the GF3 precision.

Campaign	Device	*N*	Path (m)	Median *C* (ppm)	Rel. bias (%)	Precision (ppm-m)
P16	OP-Ext	505	37	2.27	−2.7	10.6
P17	OP-1	405	12	2.04	−5.1	2.8
P17	OP-2	105	12	2.14	−3.2	2.1
P17	OP-3	66	12	1.97	−8.3	2.6

27 % (OP-2), 35 % (OP-3) and 41 % (OP-1), whereas values above 3.5 ppm rarely occurred: 1 % (OP-2), 2 % (OP-1) and 3 % (OP-3, OP-4 and OP-5). This agrees with the systematically lower concentrations measured with the GF3 devices compared to the measurement by the QCL device in the previous section.

Figure 3 shows the 30 min averages of the recorded OP-1 concentration with the corresponding differences between the measured concentration by the individual devices and the OP-1 concentration. The differences are generally small, but larger deviations, as during the A18 campaign, occur.

Table 4 provides statistics on the differences between the GF3 devices OP-2 to OP-5 and the reference device OP-1 regarding directly comparable 30 min concentration averages. The differences were determined in units of parts per million and transformed to ppm-m related to the path length of the GF3 device that has been compared to OP-1. The relative bias ranged from −1.7 % to 8.0 % and the precision of C_{PI} between 2.6 and 8.8 ppm-m, which lies within the range of the precision estimates in Sect. 3.1. A large offset in the concentration, reflected by the relative bias, could be observed for OP-4 and OP-5 compared to concentration measurements from OP-1 (on average > 0.15 ppm higher). Devices OP-4 and OP-5 were acquired 2 years later than instruments OP-1 to OP-3, and this offset may be due to a difference in the internal calibration by the manufacturer between the instruments acquired in 2017 and the instruments acquired in 2019.

The devices OP-1 and OP-3 episodically showed dents in the concentration output that are in line with step decreases in the received power. Figure 4 shows an example of such a dent recorded by OP-1 with OP-3 measuring in parallel as a reference. The rapid loss of receiving power at 27.1 h after device start seems to have triggered a gradual loss of up to 0.15 ppm in the concentration of OP-1. A few minutes later a step change in the concentration by almost 0.2 ppm occurred, while the received power was still low. We assign these concentration variations to the wrong concentration determination of OP-1, as the OP-3 concentration remained constant at the ambient background value slightly above 1.8 ppm. This indicates that a constant threshold for the received power (50 or 100 µW) may not be sufficient for quality filtering. We noticed that the "optimal" threshold varied between individual

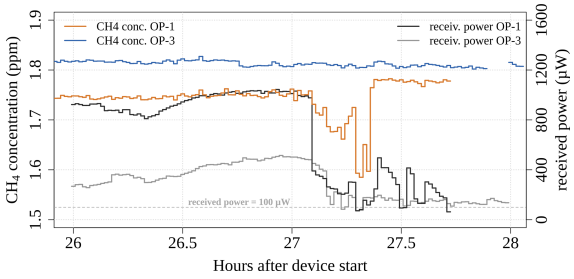

Figure 4. Example of a concentration dent followed by a step change related to losses in the received power of device OP-1. The data were recorded during the intercomparison campaign K19 on 26 April 2019 between 02:00 and 04:00 CET. From hour 27 onwards, the data exhibit R2 values above 0.98.

instruments and campaigns, with threshold values ranging up to 400 µW.

Frequently, linear regression is used to correct for differences between instruments. There are two problems, however, that can occur with this correction method for GF3 devices in the case of CH_4 concentration measurements close to ambient level. One problem arises if the dataset contains drifts and steps as shown in Figs. 1 and 4. Inspecting the A18 intercomparison between OP-1 and OP-2 closer (intercept: −0.04, slope: 1.04), a period of approximately 5.4 continuous days is apparent (around intervals 550 to 750 in Fig. 3) where OP-2 (and OP-3) recorded systematically higher concentrations than OP-1. If we separate this "offset" period from the remaining part of the campaign (Fig. 5), we see that the regression results are systematically different. The offset period shows an intercept of 0.04 and a slope of 1.05, whereas we get an almost perfect 1 : 1 relationship for the residual time (intercept: 0.01, slope: 1.00). Using the overall regression results for the entire period (Table 5) instead of two separate periods thus introduces a bias in the evaluation.

The second problem is the observed rather large variation in the intercalibration from one campaign to another (Table 5). Such a variation between different campaigns was also observed with GF3 devices for ammonia measurements by Baldé et al. (2019). Concentration response of the instru-

Table 4. Direct comparison of GF3 devices OP-2 to OP-5 to the reference device OP-1 (30 min averages). N: number of 30 min intervals. Path OP-1/OP-x: path length of GF3 devices. Median C: median concentration of OP-x. Rel. bias: estimate of the GF3 relative bias. Precision: estimate of the GF3 precision.

Campaign	Device (OP-x)	N	Path OP-1 (m)	Path OP-x (m)	Median C (ppm)	Rel. bias (%)	Precision (ppm-m)
P17	OP-2	35	12	12	2.30	2.0	2.6
	OP-3	48	12	12	2.10	−0.8	3.0
A18	OP-2	1081	37	37	2.15	0.9	5.5
	OP-3	465	37	37	2.24	2.6	8.8
K19	OP-2	53	170	118	1.83	2.7	3.6
	OP-3	82	170	176	1.82	1.8	6.1
	OP-5	25	170	118	1.98	8.0	2.7
I19	OP-2	322	110	110	1.89	0.6	5.3
	OP-3	404	110	110	1.96	0.6	3.4
	OP-4	317	110	110	2.03	5.4	4.9
	OP-5	456	110	110	2.10	7.3	5.3
H19-1	OP-5	542	112	111	2.01	7.9	4.0
H19-2	OP-4	66	65	65	2.04	7.5	5.9
H19-3	OP-2	483	110	50	1.86	−1.7	5.2
	OP-3	485	110	51	1.93	0.9	6.7
	OP-5	559	110	109	2.11	7.7	5.5

Table 5. Coefficients from the Deming regression between OP-1 and OP-2 to OP-5 with 30 min averaged data. Standard errors of the estimates are given in parentheses. Only campaigns were analyzed, where $N > 20$ and the concentration range was large enough (difference between 0.025 and 0.975 quantiles greater than 0.4 ppm). Dev.: GF3 device used as regressand. Cmp.: intercomparison campaign. N: number of 30 min intervals. σ_{resid}: standard deviation of the model residuals. $\Delta C_{y\,\text{ppm}}$: predicted difference between the OP-x concentration and the OP-1 concentration at a level of y ppm (2 or 4 ppm). Lower and upper bounds of the 95 % confidence interval are given in parentheses. For each device and concentration level, intercomparison campaigns not sharing a superscript letter exhibit significantly different ΔC.

Dev.	Cmp.	N	Intercept (ppm)	Slope (–)	σ_{resid} (ppm)	$\Delta C_{2\,\text{ppm}}$ (ppm)	$\Delta C_{4\,\text{ppm}}$ (ppm)
OP-2	P17	35	0.15 (0.11)	0.96 (0.05)	0.09	0.06^{ab} (−0.13, 0.24)	-0.03^{ab} (−0.28, 0.22)
	A18	1081	−0.04 (0.03)	1.04 (0.01)	0.07	0.04^{ab} (−0.10, 0.17)	0.11^{ab} (−0.04, 0.25)
	I19	322	−0.10 (0.01)	1.06 (0.00)	0.02	0.02^{a} (−0.01, 0.05)	0.14^{a} (0.10, 0.17)
	H19-3	483	−0.12 (0.03)	1.04 (0.02)	0.02	-0.04^{b} (−0.09, 0.01)	0.04^{b} (−0.05, 0.12)
OP-3	P17	48	−0.01 (0.11)	1.00 (0.05)	0.11	-0.01^{a} (−0.23, 0.21)	-0.02^{a} (−0.32, 0.29)
	A18	465	−0.09 (0.06)	1.10 (0.03)	0.09	0.10^{a} (−0.09, 0.28)	0.29^{a} (0.07, 0.50)
	I19	404	0.03 (0.01)	1.01 (0.01)	0.11	0.04^{a} (−0.19, 0.27)	0.05^{a} (−0.18, 0.28)
	H19-3	485	−0.14 (0.04)	1.08 (0.02)	0.03	0.02^{a} (−0.04, 0.08)	0.18^{a} (0.09, 0.28)
OP-4	I19	317	−0.12 (0.01)	1.14 (0.00)	0.01	0.16 (0.14, 0.19)	0.44 (0.41, 0.47)
OP-5	I19	456	−0.03 (0.01)	1.13 (0.00)	0.03	0.22^{a} (0.16, 0.28)	0.47^{a} (0.41, 0.53)
	H19-1	542	0.14 (0.01)	1.04 (0.01)	0.01	0.22^{a} (0.20, 0.24)	0.31^{b} (0.27, 0.35)
	H19-3	559	0.03 (0.02)	1.10 (0.01)	0.02	0.23^{a} (0.20, 0.26)	0.43^{a} (0.37, 0.49)

ment does change between different campaigns as seen by the regressions and can thus not be generalized. A significant difference in the predicted concentration between different campaigns can be seen for devices OP-2 and OP-5; e.g., within the same year 2019 (campaigns I19 and H19-3), intercalibrating OP-2 with OP-1 would provide significantly different 30 min concentration estimates at concentration levels of 2 and 4 ppm. Even though, in theory, an intercalibration of the devices after an IDM measurement campaign could solve the issue of differences in the measurements, the nec-

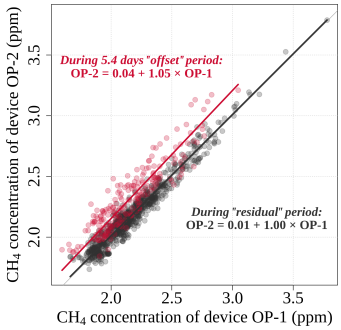

Figure 5. Scatter plot of 30 min data from OP-1 and OP-2 recorded during campaign A18. Deming regression lines and corresponding regression equations are shown for the offset period and the remaining ("residual") period.

essary change in the setup to perform such an intercalibration could lead to a change in the response of the devices, and the intercalibration would then be useless.

4 Conclusion

We found that the uncertainty in the measurements of several GasFinder3-OP instruments is higher than given in the specification provided by the manufacturer when measuring concentrations close to ambient levels. From on-site intercomparisons at various field sites (side-by-side intercomparisons and comparisons to a reference QCL instrument), we estimate a bias up to 8.3 % of the reading and a precision between 2.1 and 10.6 ppm-m for our devices. This is 4 to 21 times higher than the sensitivity specified by the manufacturer. A large part of the inferior precision is attributed to low-frequency drifts, whereas high-frequency changes in the concentration are often well captured, as the similarity of the small features between hours 25 and 27 in Fig. 1 demonstrates. Drifts and step changes in the concentration occur up to 0.3 ppm (Fig. 1). Most critical are changes in the concentration that can hardly be distinguished from fluctuations of the atmospheric concentrations. Some of the step changes are caused by activity related to the handling of the GF3 device (e.g., downloading data, checking time, checking reference cell quality). It remains unclear though what activity causes these step changes, since none of the activities consistently cause such step changes. The internal calibrations of the GF3 seem to differ between devices. Devices OP-1, OP-2 and OP-3 show systematically lower concentration measurements than the devices OP-4 and OP-5. Application with paired devices needs an intercalibration of the devices. However, it remains unclear to what extent a side-by-side intercalibration can be transferred to the actual measurement setup, since relocation of the devices might cause systematic changes, as indicated by the different regression coefficients for different intercomparison campaigns.

Code and data availability. Code and data are available at https://doi.org/10.5281/zenodo.4569847 (Häni, 2021.).

Author contributions. TK designed and coordinated the field campaigns. MB performed the GasFinder3 measurements. CA provided the QCL measurements. CH evaluated the data and prepared the manuscript with contributions from MB and AN. TK, AN and CA reviewed and corrected the draft manuscript.

Competing interests. The authors declare that they have no conflict of interest.

Acknowledgements. Funding by the Swiss Federal Office for the Environment is gratefully acknowledged. We thank the operators of the wastewater treatment plants (WWTPs) and of the biogas plant, the three farmers in the surroundings of the WWTPs, and the Agroscope stations Tänikon and Posieux for providing the sites for the measurements.

Financial support. This research has been supported by the Swiss Federal Office for the Environment (grant nos. 00.5082.PZ/R254-0652, 06.0091.PZ/R281-0748 and 10.0021.PJ/N253-1914).

Review statement. This paper was edited by Glenn Wolfe and reviewed by two anonymous referees.

References

BAFU: Luftqualität 2018: Messresultate des Nationalen Beobachtungsnetzes für Luftfremdstoffe (NABEL), Bundesamt für Umwelt BAFU, Ittigen, Switzerland, Umwelt-Zustand, UZ-1916-D, 2019.

Baldé, H., VanderZaag, A., Smith, W., and Desjardins, R. L.: Ammonia emissions measured using two different GasFinder open-path lasers, Atmosphere, 10, 261, https://doi.org/10.3390/atmos10050261, 2019.

Boreal Laser Inc.: GasFinder3-OP Operation Manual, Part No. NDC-200029-D, Edmonton, Canada, 2016.

Boreal Laser Inc.: GasFinder3-OP + ACCESSORIES, available at: https://boreal-laser.com/wp-content/uploads/2016/02/GasFinder3-OP-Info-Package.pdf (last access: 12 May 2020), 2018a.

Boreal Laser Inc.: GasFinder3-OP Operation Manual, Part No. NDC-200036, Edmonton, Canada, 2018b.

Boreal Laser Inc.: "Lo-Range" Methane (CH_4) Monitoring, available at: https://boreal-laser.com/gases/methane/, last access: 12 May 2020.

DeBruyn, Z. J., Wagner-Riddle, C., and VanderZaag, A.: Assessment of open-path spectrometer accuracy at low path-integrated methane concentrations, Atmosphere, 11, 184, https://doi.org/10.3390/atmos11020184, 2020.

Flesch, T. K., Wilson, J. D., Harper, L. A., and Crenna, B. P.: Estimating gas emissions from a farm with an inverse-dispersion technique, Atmos. Environ., 39, 4863–4874, https://doi.org/10.1016/j.atmosenv.2005.04.032, 2005.

Flesch, T. K., Wilson, J. D., Harper, L. A., Todd, R. W., and Cole, N. A.: Determining ammonia emissions from a cattle feedlot with an inverse dispersion technique, Agr. Forest Meteorol., 144, 139–155, https://doi.org/10.1016/j.agrformet.2007.02.006, 2007.

Häni, C.: Data and code from the publication "Performance of open-path GasFinder3 devices for CH_4 concentration measurements close to ambient levels" [Data set], Zenodo, https://doi.org/10.5281/zenodo.4569847, 2021.

Harper, L. A., Flesch, T. K., Weaver, K. H., and Wilson, J. D.: The effect of biofuel production on swine farm methane and ammonia emissions, J. Environ. Qual., 39, 1984–1992, https://doi.org/10.2134/jeq2010.0172, 2010.

McGinn, S. M., Flesch, T. K., Beauchemin, K. A., Shreck, A., and Kindermann, M.: Micrometeorological Methods for Measuring Methane Emission Reduction at Beef Cattle Feedlots: Evaluation of 3-Nitrooxypropanol Feed Additive, J. Environ. Qual., 48, 1454–1461, https://doi.org/10.2134/jeq2018.11.0412, 2019.

Nelson, D. D., McManus, B., Urbanski, S., Herndon, S., and Zahniser, M. S.: High precision measurements of atmospheric nitrous oxide and methane using thermoelectrically cooled mid-infrared quantum cascade lasers and detectors, Spectrochim. Acta A, 60, 3325–3335, https://doi.org/10.1016/j.saa.2004.01.033, 2004.

VanderZaag, A. C., Flesch, T. K., Desjardins, R. L., Baldé, H., and Wright, T.: Measuring methane emissions from two dairy farms: Seasonal and manure-management effects, Agr. Forest Meteorol., 194, 259–267, https://doi.org/10.1016/j.agrformet.2014.02.003, 2014.

Wang, D., Wang, K., Zheng, X., Butterbach-Bahl, K., Díaz-Pinés, E., and Chen, H.: Applicability of a gas analyzer with dual quantum cascade lasers for simultaneous measurements of N_2O, CH_4 and CO_2 fluxes from cropland using the eddy covariance technique, Science Total Environment, 729, 138784, https://doi.org/10.1016/j.scitotenv.2020.138784, 2020.

2.6 From raw data to emissions

The following section explains how an IDM measurement campaign was typically conducted. For a campaign, the used equipment comprised at least a weather station, a 3-dimensional ultrasonic anemometer, and multiple GasFinders. A schematic overview of the steps involved is displayed in Figure 5. A series of R software scripts were established to complete the following steps (R Core Team, 2020).

Even though Figure 5 is plotted as a flow chart, it was often necessary to iterate in order to optimise some of the steps as the result still contained erroneous emissions estimates. In most cases, this was the processing of the concentration data (Section 2.6.5) or the appropriate combination of quality filter criteria (Section 2.6.7).

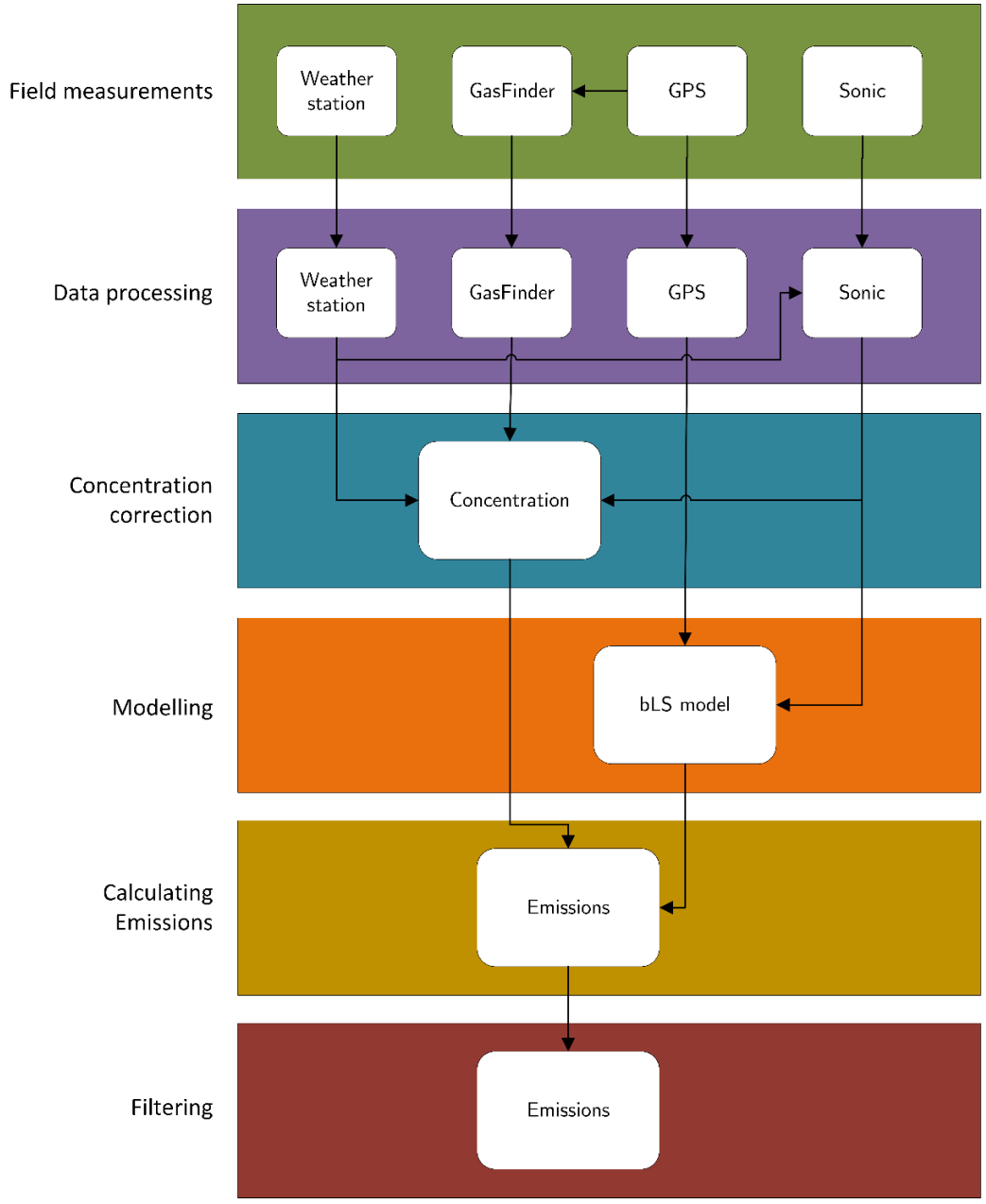

Figure 5: Flowchart of an IDM campaign to determine CH_4 emission from raw data.

2.6.1 GPS data

A Global Positioning System (GPS, Trimble Pro 6T, Trimble Navigation Limited, Sunnyvale, USA) was used to record the exact position of the measurement devices and the sources with a precision of ± 0.1 m. The GPS coordinates were recorded twice or three times to minimise potential errors in the GPS. Logging the coordinates of buildings was difficult due to accessibility or reduced satellite connections, therefore the location points of buildings were added manually afterwards in an editing software (e.g., ArcGIS (Esri, Redlands, US)). The GPS data were then saved and imported in R software, where the data were processed for use in the bLS model.

2.6.2 Weather station

Atmospheric pressure and air temperature were needed for the GasFinder evaluation, ultrasonic wind direction validation, and interpretation of the emission data. From November 2018 onwards, data from a weather station (Lufft WS700-UMB Smart Weather Sensor, G. Lufft Mess- und Regeltechnik GmbH Fellbach, Germany) placed at the study site were used. The Lufft weather station recorded air temperature [°C], wind speed (avg) [m s^{-1}], wind speed (vect) [m s^{-1}] and wind direction (vect) [°] in 1 min resolution; dew point [°C], relative humidity [%], absolute humidity [g m^{-3}], absolute air pressure [hPa], air density [kg m^{-3}], precipitation amount absolute [mm], precipitation amount difference [mm], precipitation intensity [mm h^{-1}], precipitation type [] and solar radiation [W m^{-2}] in 5 min resolution; Compass [°] in daily resolution. The accuracy of the wind direction was $< 3°$ RMSE for wind speeds of > 1.0 m s^{-1}.

The weather station was placed horizontally to avoid any errors in the wind direction measurement. As the weather station was usually not aligned with geographic north, the data from the magnetic compass were used to rotate the vectorial wind direction. As a few degrees of deviation in the wind direction might lead to substantially different results, the deviation between geographic north and magnetic north should be corrected for. At least at the beginning and at the end of the measurement campaign, the time difference between a reference time (UTC+1) was logged and the weather station data shifted accordingly. This guaranteed a synchronisation between the different measurement devices. An experiment showed, that due to internal buffering the 1-minute wind data needed to be shifted by 5 minutes. The script for reading the weather station data into R software can be found on GitHub (https://github.com/ChHaeni/gel-scripts/blob/main/weatherstation-functions.r).

Bevor November 2018 as no weather station was available that could be placed directly at the experimental site, data from nearby weather stations of a meteorological measurement network were used. Depending on the distance from the measurement site to the weather station, the temperature correction of the GasFinders might have been slightly biased.

2.6.3 Ultrasonic anemometer

For the wind profile measurements at least one 3-dimensional ultrasonic anemometers (Windmaster, Gill Instruments Limited, Lymington, UK) was installed. Before January 2020, only small tripods for the ultrasonic anemometers (sonics) were available that allowed measurements at a maximum height of 1.40 m above ground. Later, heavy duty tripods (Dönges telescopic tripods) that theoretically allowed measurements up to 5 m above ground, were available.

In the sonic evaluation (https://github.com/ChHaeni/gel-scripts/blob/main/sonic-turbulence.r) the model parameters u_*, L, z_0, σ_u/u_*, σ_v/u_*, σ_w/u_* were calculated from the (co-)variances of the rotated sonic data (u, v, w, T). A two-axes rotation was applied. As input parameters for the sonic evaluation, the averaging time, the sonic height, and the canopy height of the landscape were needed. As averaging time (Section 2.1), 30 min were applied for the measurements at the livestock housing, the BGPs and the WWTPs and 10 min for the release experiment to increase the number of available data points.

Additional inputs were the deviation towards geographic north and a time offset to a reference time (UTC+1). The deviation was needed to transform the wind field from the internal Cartesian coordinate systems into the geographical coordinate system. The deviation towards north of the sonics was measured with a handheld compass. However, it was often difficult to measure the deviation. Thus, the wind direction data from the sonics were compared to the corrected wind direction data from the weather station and the deviations towards geographic north of the sonics were determined. For this calculation, only wind sectors were used, for which the sonic and the weather station were uninfluenced by any objects, otherwise a bias is introduced (Figure 12).

If there were multiple sonics placed onsite, the obtained data from all sonics were compared for validation. Plotting a wind rose (https://github.com/ChHaeni/gel-scripts/blob/main/windrose.r) allowed a first validation of the setup. It enabled a crosscheck regarding the correct placement of the GasFinders. To avoid misplacement of GasFinders and to capture a maximum amount of the downwind plume from the source, sonic measurements at the site beforehand were conducted. If the recommended sonic measurements before a campaign were not feasible, the wind directions were assessed with data from nearby weather stations of a meteorological measurement network. In general, it is advised that the wind direction is thoroughly evaluated during the campaign and if necessary, the setup adjusted accordingly.

2.6.4 GasFinder data

A detailed description of the GasFinder is given in Section 2.5. In the field, the tripods of the GasFinder sensors and retroreflectors were fixed with a base screw and a clamping set to the ground to avoid misalignments of the laser beam which often occurred with wetting or drying soil and preferably with longer path lengths. At least at the beginning and the end of a campaign, the time offset to the reference time was recorded. It is advised to do that more often as the time offset to the reference time, does not change linearly. The data were downloaded via a USB drive. With temperatures around or below the freezing point, it could happen that the USB drive was not recognised by the GasFinder, and data could not be downloaded. Once this occurred, also warmer temperatures did not help. To overcome this problem, the GasFinder was switched off and turned back on. However, this solution might induce a different state of the GasFinder as pointed out by Häni et al. (2021).

A script for reading and processing GasFinder data in R software is provided on GitHub (https://github.com/ChHaeni/gel-scripts/blob/main/gasfinder-functions.r). For the GasFinder evaluation, the path lengths from the GPS data and the air temperature and atmospheric pressure

from the weather station were processed. The air temperature and atmospheric pressure were needed to correct the concentration data according to a function provided by the manufacturer.

2.6.5 Concentration correction

In a next step, the CH_4 concentration data from the GasFinder were analysed. For each GasFinder sensor a threshold for the received power and the goodness of the fit (R^2) were defined (Häni et al., 2021). A fixed fitting value of > 0.98 was used for every measurement conducted in this thesis. For the received power, the threshold differed from device to device, from campaign to campaign and even within a campaign. These thresholds were needed to eliminate unreasonable concentration levels e.g., drops in the concentrations. Additionally, it was observed that in the first few hours after starting a GasFinder or after a longer period without any light that was reflected to the sensor, recorded data needed to be excluded. Once all implausible concentration data were removed, the 0.3 - 1 Hz data were pooled to the desired averaging period/interval length. For the pooling, a minimum coverage of 75 % of data within an interval was needed. Otherwise, the value of this interval was not taken into account.

Individual GasFinders differed in measured concentration levels. Thus, the offset and span between the employed GasFinders needed to be corrected. This correction was done with a simple linear regression (deming) between two GasFinders. The offset and span correction were usually based on data from an intercomparison conducted before or after the actual measurement campaign. If these data were not available, wind sectors, for which the GasFinders were expected to capture the same background concentration, were used. For the concentration correction, usually data were only used if recorded during a minimum wind speed of about 0.8 m s^{-1}. Due to the described behaviours of the GasFinder in Häni et al. (2021), the offset and span correction remained a challenging task.

2.6.6 bLS model and emission calculation

With the coordinates of the source and sensors (GPS data) and the sonic data, the bLS model could be executed. For this, the R software package bLSmodelR was used (Häni et al., 2018). The package and a documentation of the bLSmodelR is provided on GitHub (https://github.com/ChHaeni/bLSmodelR). Once the model run was finished, the bLS output and the concentration data were combined to calculate emissions according to Eq. 21. Before the processed data could be analysed, a quality filter needed to be applied.

2.6.7 Quality filtering

As described in Section 2.3, the bLS model uses MOST scaling. Thus, the emission data required compatibility with MOST assumptions and consequently a screening of the data with the goal to exclude situations that substantially deviated from MOST conditions. Identifying such conditions and removing them from the data set is called quality filtering. The goal of this screening or quality filtering was retaining as much data as possible without including too many erroneous data. Such filters can be applied to the sonic data or on parameters generated by the bLS model. In the literature, filter criteria for the friction velocity u_*, the Obukhov length L, the roughness length z_0 and the fraction of the source covered by touchdowns can be found (e.g., Flesch et al., 2005; Gao et al., 2011;

Flesch et al., 2014). As described in Flesch et al. (2014), applying a filter of $u_* > 0.15$ m s^{-1}, leads to substantial data loss. This would be especially the case for the measuring sites in this thesis where low wind speeds usually occurred. Flesch et al. (2014) reduced the filter threshold for u_* to $u_* > 0.05$ m s^{-1} by introducing a filter for the measured vertical temperature gradient. To filter for the same low u_* or even completely omit filtering for u_*, filters for the wind direction, L, z_0, and additionally other filter criteria that to my knowledge have not been used in combination with the bLS model were used. For the sonic data, these were the standard deviation of the u wind velocity (along wind) scaled by the friction velocity σ_u/u_*, and the standard deviation of the v wind velocity (across wind) scaled by the friction velocity σ_v/u_*. For the bLS model parameters, filters for the dispersion factor D_{bLS}, the standard error of the dispersion factor divided by the dispersion factor $\hat{\sigma}_{\bar{D}_{bLS}}/D_{bLS}$, the Kolmogorov constant of the Lagrangian structure function C_0, the number of touchdowns within the source area and, a minimum concentration difference between the up- and downwind GasFinder measurements were used as filter criteria. The fraction of the source covered by touchdowns criterion was not used in this thesis as its implementation in the bLSmodelR deviates from that in WindTrax.

The values of the individual filter criteria were defined empirically separately for each measurement site, as the influence of local topographical factors differed. The most often used criteria besides L and z_0 were σ_u/u_* and σ_v/u_* that were regarded as criteria for stationary conditions. For C_0, values for quality filtering have not yet been provided in the literature. Single values are available between 1.6 and 7.6 (Du et al., 1995; Degrazia et al., 2008; Rizza et al., 2010), but not necessarily in combination with a bLS model. The thresholds of this criterion were set to $2 < C_0 < 10$.

The combination of filter criteria that were used in this thesis differed from campaign to campaign. Emissions that did not fulfil all the applied filer criteria were excluded. As some of the criteria are interrelated, one criterion might not have induced any data removal at the end as invalid data were excluded by other criteria previously. In the following, the wind direction filter is explained in detail as it was not directly related to the above discussed turbulence criteria.

As only a limited number of GasFinder instruments were available, wind direction filters were necessary to avoid intervals for which the emission plume was on the edge or even outside of the GasFinder path. During this PhD thesis, three slightly different wind direction filter approaches were applied (Figure 6). Only data between two predefined wind directions were analysed. The directions were defined by drawing a line from each end of the GasFinder path through a defined point in space.

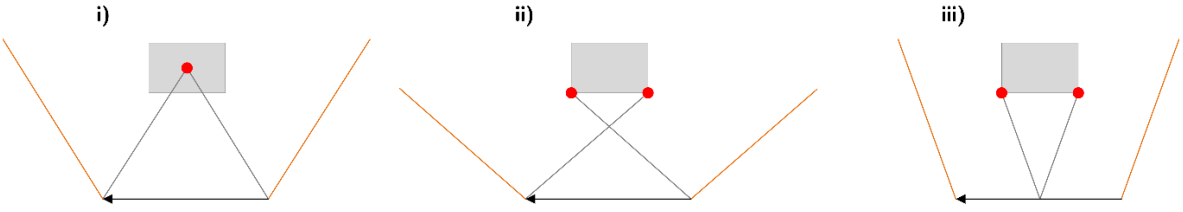

Figure 6: Three approaches for wind direction filtering. The grey square is the emission source, the black arrow the GasFinder path with sensor and retroreflector, the grey solid lines define the wind direction filtering that were drawn through specific points (red dots). Emissions recorded outside the wind sector defined by the orange lines (shifted grey lines) were excluded.

For approach (i), from each end of the GasFinder path, a line through the centre of the source was drawn. The lines for approach (ii) were defined by connecting the ends of the GasFinder path with

the most outer edge of the source closest to the GasFinder path. For each end, the edge situated further away was chosen. (iii) Instead of drawing lines from the end of the GasFinder path like in approach (ii) the lines were drawn from the middle of the path. Depending on the source-sensor geometry, one of those approaches was used. Approach (iii) was not meaningful, if the source was of small extension (e.g., the barn of the release experiment). This approach was only used for the WWTPs where the lateral extension of the source was of similar length than the distance between the source and the GasFinders. For the measurements at the livestock housings approach (ii) was used and for the BGPs approach (i) was applied.

The viability of filtering was tested by plotting the emissions against the wind direction and by subsequently drawing the potential wind direction thresholds. Often, the wind direction sector had to be narrowed down by a few degrees as emission started to vary if the plume was on the edge of the measurement path. At the edge of a GasFinder path, deviations between the modelled emission plume and real plume have a significant impact on the emission calculation.

2.7 Methane release experiment

In the following, some steps of an IDM campaign are explained in more detail on the example of the CH_4 release experiment inside a barn. The goal of this experiment was to validate the IDM for emission measurements from an agricultural building e.g., a dairy housing. McGinn et al. (2006) conducted a release experiment of a barn with the three release positions on top of the roof and three positions outside the walls of the barn. Gao et al. (2010) released the CH_4 via four side vents of a barn. The barn in study of Gao et al. (2010) is comparable to a mechanical ventilated building that is common for fattening pigs or poultry. However, dairy cows are housing to a larger extent in naturally ventilated buildings. Thus, in this study, the CH_4 was released inside a building without mechanical ventilation to optimise the quality of the measurement results and minimise the uncertainty range of the IDM. Compared to Gao et al. (2010), in this experiment, multiple sonics were available. Thus, the focus of this experiment was on the positioning of the GasFinders and the sonics in different distances to the source and the optimisation of the filtering of measurement data based on micrometeorological criteria and model parameters.

2.7.1 Measurement site and periods

Finding an empty dairy housing in Switzerland for the CH_4 release experiment in a location that is suitable for IDM measurements is difficult. Thus, a barn was chosen instead that allowed a setup which mimics a naturally ventilated housing. The barn is located in the Grand Marais (47.04307 N, 7.22691 E) that is a flat region in the Seeland region in Switzerland. About 350 m northeast of the barn is a river with dams on each side that are 4 m higher than the agricultural land surrounding the barn. The canopy height directly around the barn was 20 cm or lower and remained constant over the course of the measurements. The barn is 25 m long, 17 m wide and 8 m high. The interior of the barn serves for storing agricultural equipment. During the release experiment, there were four agricultural machines located inside the barn. About 1/6 of the barn's surface was occupied by storage boxes reaching almost up to the ceiling. Despite the goods inside, about 1/3 of the south end of the

barn was empty. The barn had on each side a 5 m wide and 4 m high gate. Whereas the gate on the south side was fully open, the gate on the northeast side was opened 1.2 m during the CH_4 releases. The north facing wall of the barn was windproof, however the south wall exhibited small holes and cracks all over the wall allowing air exchange. The lateral sides of the barn were not airtight as well. Especially below the roof, there was a gap of about 0.6 m that was covered by cracked plastic sheets. About 20 m southwest of the barn is a tree (Figure 7).

Figure 7: Barn used for the CH_4 release experiment. The photo was taken from the southwest side of the barn. In the foreground, there is an ultrasonic anemometer.

The barn is not connected to the power grid. Thus, during all times a petrol-powered Honda EU 20i generator connected to a 30 L fuel tank was used that allowed continuous measurements over several days. The generator was located outside in a shelter at the southeast side.

The whole experiment took place over several months and was divided into different periods. In December 2020, measurements to determine the prevailing wind direction were conducted. In January 2021, a first intercomparison (IC1) of the GasFinder and additional sonic measurements were performed. These GasFinder data were not further used. In a second intercomparison of the GasFinder (IC2), measurements were conducted from 05 March to 10 March 2021. Then the setup was changed to the actual experiment denoted as measurement campaign (MC) that took place from 18 March 2021 11:00 to 21 March 2021 13:00 UTC+1. The third GasFinder intercomparison (IC3) was from 18 March 2021 15:00 to 26 March 2021 10:00 UTC+1 (Figure 8). High-purity CH_4 was released inside the barn during MC and IC3.

2.7.2 Experimental setup

For all measurements, the five GasFinders (sensor modules and retroreflectors) were placed 1.6 m above ground with a path length of 110 m. For the IC2, the GasFinders were placed about 100 m southwest of the barn. For the MC, four GasFinders were placed southwest of the barn and one northeast of the barn. The distances between the barn and the middle of the GasFinder path on the southwest side, ranged from 50 m to 200 m (Figure 8, Table 1). For IC3, the average distance to the middle of the GasFinder paths was 50 m. During the MC, the three sonics were placed downwind in the middle of the GasFinder paths and one upwind of the barn (Figure 8, Table 1). The measuring

height of all sonics in the MC was 2.16 m. For IC3, the sonics were placed about 55 m southwest from the barn at heights between 0.85 m and 3 m. The sonic measurements of IC3 are beyond the scope of this thesis and only the data of SonicD (2 m above ground) were used. All the setups were intendent for a wind direction of 45°.

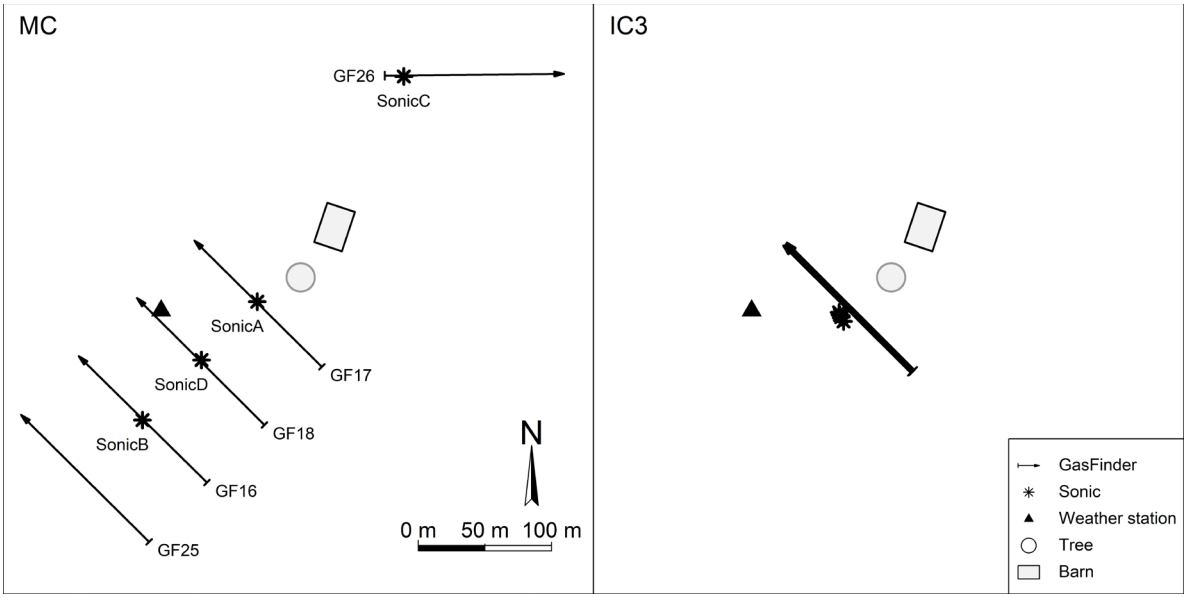

Figure 8: Schematic overview of the measurement setup during the measurement campaign (MC) and the third intercomparison (IC3). For the IC3 the GasFinders and the sonics were all placed next to each other.

Table 1: Position of the GasFinders and ultrasonic anemometers during the measurement campaign.

Location	GasFinder	Ultrasonic anemometer
50 m downwind	GF17	SonicA
100 m downwind	GF18	SonicD
150 m downwind	GF16	SonicB
200 m downwind	GF25	-
upwind	GF26	SonicC

2.7.3 Methane source

During the pre-sounding measurements and in IC3, two gas cylinders with 50 L at 200 bars with high-purity (> 99.5 % mol) CH_4 were used. During the MC and half of IC3, a gas bundle of 12 cylinders with 50 L at 200 bar each were used. Attached to the bundle was a pressure regulator (Figure 9). The pressure on the high-pressure side was measured with a digital pressure sensor (LEX1-Ei / 200bar / 81770.5, Keller AG, Winterthur, Switzerland). The low-pressure side was set to 3 bar. The pressure regulator and the mass flow controller (MFC, EL-FLOW Select F-202AV-M20-AGD-22-V, Bronkhorst High-Tech B.V., Ruurlo, The Netherlands) were connected by a polyethylene naphthalate (PEN) tubing (FESTO, PEN-16X2,5-BL-100 551449) with an inner diameter of 10.8 mm. After the MFC, there was 8 m long PNE tube with an inner diameter of 10.8 mm to a gas distribution block made of aluminium with three outlets (ITV, 124 A24 G1/2”). Each outlet had an L-fitting (FESTO, QSL-G1/2-16 186126) and a 1.5 m of the same tubing connected to another gas distribution block with eight outlets with a reduction of the tubing to 2.7 mm (FESTO, FR-8-1/4 2078). To each of these outlets a L-fitting (FESTO, QSLL-1/4-4 190662) and a 20 m long with an inner diameter of 2.7 mm PEN tubing (FESTO, PPEN-4X0,75-BL-500 551444) was attached that released the gas

(Figure 9). At the end of these tubes, no pressure reduction was added. The total pressure drop of the system was expected to be around 0.4 bar.

The Keller pressure sensor and the MFC were connected to a computer. The pressure and the temperature recorded with the Keller pressure sensor were logged with 10 Hz. From the MFC, the setpoint (L_n min^{-1}), the flow rate (L_n min^{-1}) and the temperature were logged with 0.1 Hz resolution. The setpoint of the MFC was controlled via computer. The MFC had a maximum flow of 160 L_n min^{-1} and was calibrated for CH_4 at 15 °C. During the MC, the MFC was set to 140 L_n min^{-1} and remained unchanged. During the IC3, the setpoint was varied. The high flow rate was chosen to achieve sufficient concentration enhancement at the GasFinders location and thus an adequate signal to noise ratio. The 140 L_n min^{-1} or 6.02 kg h^{-1} correspond to the emission of about 360 dairy cows. The cumulative flow through the MFC whilst the gas bundle was connected, was within 1 % of the CH_4 volume inside the gas bundle.

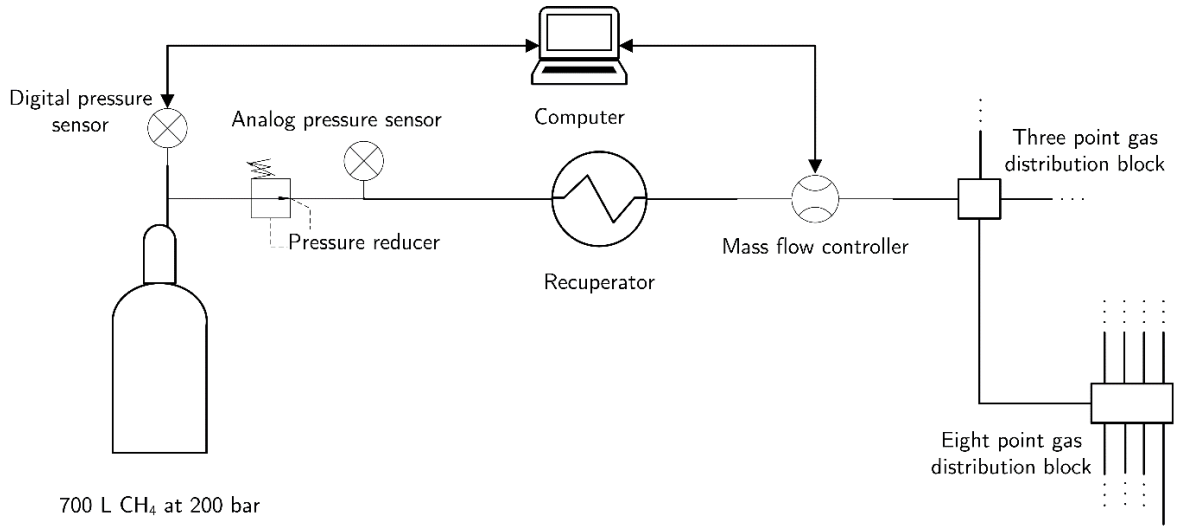

Figure 9: Schematic of the CH_4 source for the artificial release experiment.

The gas bundle and the MFC were placed outside the barn on the north side. The release points inside the barn were at 1.5 m above ground. The 24 release points were equally distributed in the southern half of the barn. This setup was chosen to mimic CH_4 release due to enteric fermentation of a dairy cow herd inside a housing.

Due to the high flow rate in combination with the large pressure differences (Joule-Thomson effect), gas temperatures below -70 °C were expected. Thus, the Keller pressure sensor was connected over a 50 cm stainless steel tube with an inner diameter of 4 mm to the pressure regulator to avoid freezing of the sensor, as the minimal operation temperature was -10 °C. Further, two steel metal blocks were mounted to the pressure regulator and heated with a heating cartridge, to keep the regulator temperature above -30 °C. The minimal operation temperature of the MFC was -10 °C and thus a water-air recuperator was added in between the pressure regulator and the MFC (Figure 9). The recuperator consisted of a 120 L barrel that was filled with about 90 L of water with an initial temperature of around 45 °C. During the gas release in the MC, the water was replaced before the second release. Inside the barrel, about 10 m of the PEN tubing was placed. This setup kept the gas temperature at the MFC besides the last 30 mins always above 0 °C (Figure 10).

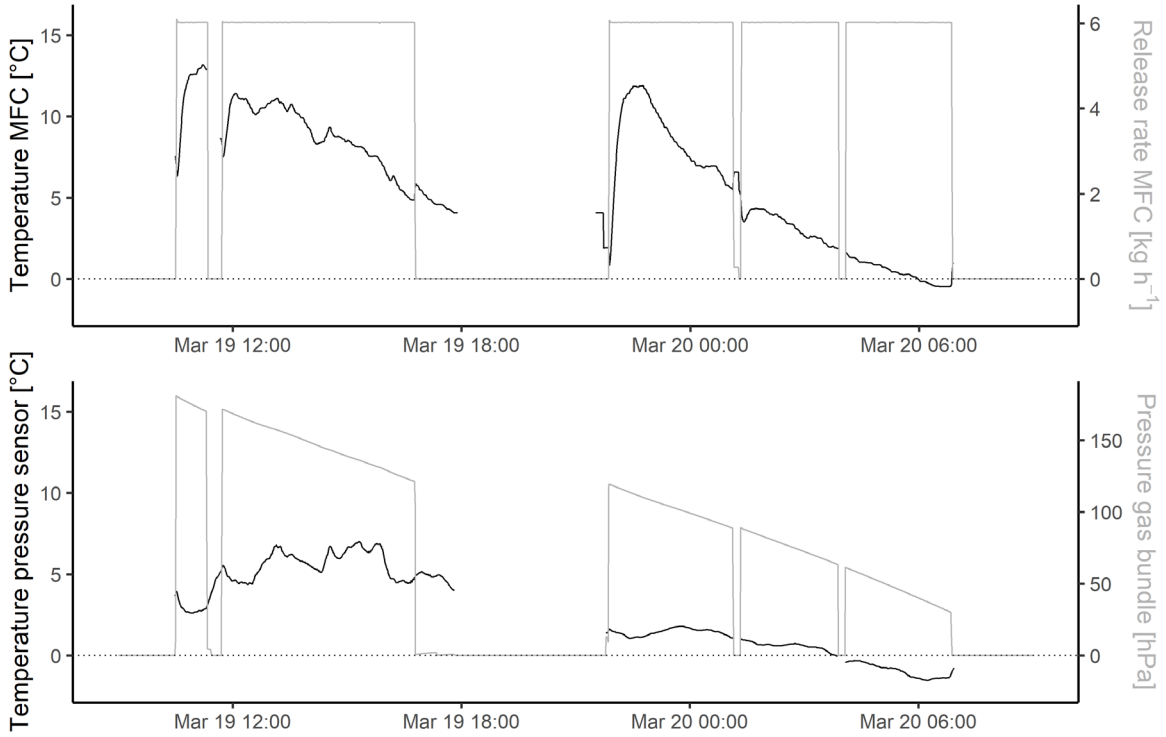

Figure 10: Upper panel: Temperature (black) and flow rate (grey) recorded by the mass flow controller (MFC). Lower panel: Temperature (black) and pressure logged (grey) by the sensor at the high-pressure side during the measurement campaign. The time is in UTC+1. The location of the devices within the source setup are given in Figure 9.

At the beginning of the first release in the MC, an overheating of a heating cartridge occurred that led to a short circuit and shut down of the power generator. After about 30 min, the problem was fixed, and the measurements were continued. Around 1:00 UTC+1, the computer was needed to check data from a sonic and thus, the gas release was stopped for a few minutes. Around 4:00 UTC+1, the computer switched to the sleeping mode and therefore, no data was logged (Figure 10). However, during these about 10 min, CH_4 was still being released and thus, the flow rate of the MFC was interpolated for the emission plots (Figure 16, Figure 17, Figure 20).

2.7.4 Filtering

For the release experiment, filters were applied for the wind direction, z_0, L, σ_u/u_*, σ_v/u_*, and C_0.The thresholds for these filters were $z_0 < 0.07$ m, $|1/L| < 0.5$ m, $\sigma_u/u_* < 4$, $\sigma_v/u_* < 4$ and, $C_0 \leq 10$. For the wind direction filter, approach (ii) was applied (Section 2.6.7). For the release experiment, no u_* filter, any other filter related to the bLS model, or a minimum concentration difference between the up- and downwind measurements were applied, as they did not improve the result.

2.7.5 Results

2.7.5.1 Weather station data

The declination at the barn was 2.8°east (swisstopo, 2021). With an eastward declination, the difference must be added to the magnetic direction to get the geographical direction. During the CH_4

in the MC and IC3, the ambient air temperatures were between -1.3 °C and 6.1 °C and wind speeds ranged between 2.1 and 6.5 m s^{-1} (Figure 11). There were only northeasterly winds during the MC.

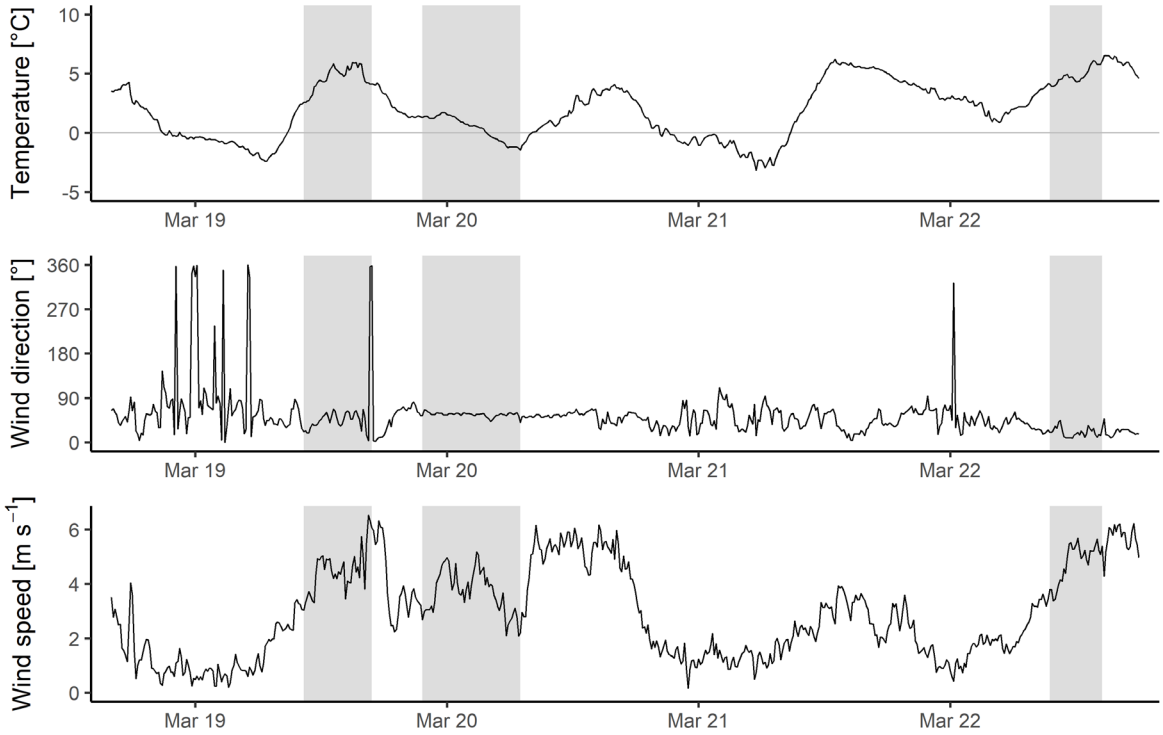

Figure 11: Meteorological data measured by the Lufft weather station at 47.04259 N, 7.225523 E coordinate during the measurement campaign and part of the third intercomparison. The shaded areas represent the time whilst CH_4 was being released. The time series is in UTC+1.

2.7.5.2 Ultrasonic anemometer data

The closer the sonic was placed to the barn in the present study, the further the wind direction deviates from the weather station data. The upwind sonic (SonicC) accounted for the smallest deviation. All sonics recorded a similar positive deviation between 60° and 75°, whilst the weather station measurement was influenced by the proximity of the barn. The applied wind direction correction was successful as outside the influenced sector the average difference was zero. The problem of the present study was that there were only limited times where the sonics and the weather station were not influenced by any objects, as there were no southwesterly winds during the times the sonics were in the MC setting (Figure 8).

The mean wind direction of the downwind sonics deviated with decreasing distance to the barn. The closer the sonic was placed to the barn the more a wind direction from north was measured. The variation in the wind direction was larger for the downwind sonics than for the upwind sonic. Considering the upwind sonic, the measurement setup was not ideal (Figure 13).

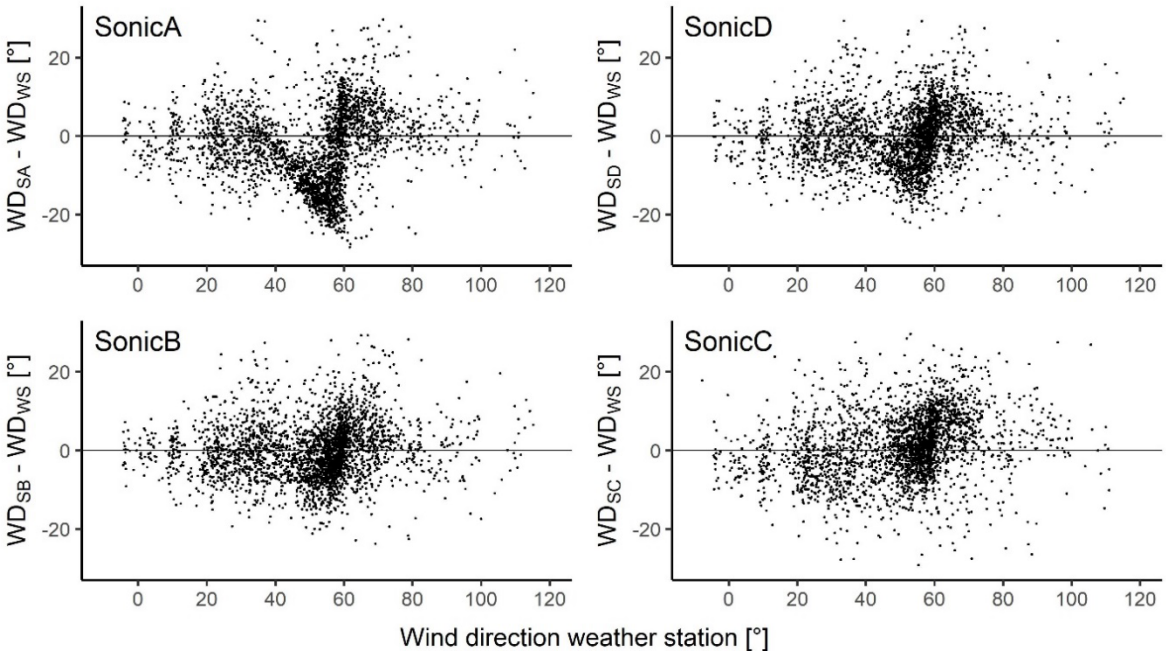

Figure 12: Absolute difference in the wind direction between the sonics and the weather station recorded during the measurement campaign, for the corrected wind data. SonicA = 50 m, SonicD = 100 m, SonicB = 150 m, SonicC = background. The exact locations of the sonics are given in Figure 9.

Table 2: Mean wind direction and wind speed recorded during the measurement campaign setup of the four sonics.

	Mean wind direction [°]	Mean wind speed [m s^{-1}]
SonicA	46	2.9
SonicD	51	2.7
SonicB	51	2.9
SonicC	52	2.6

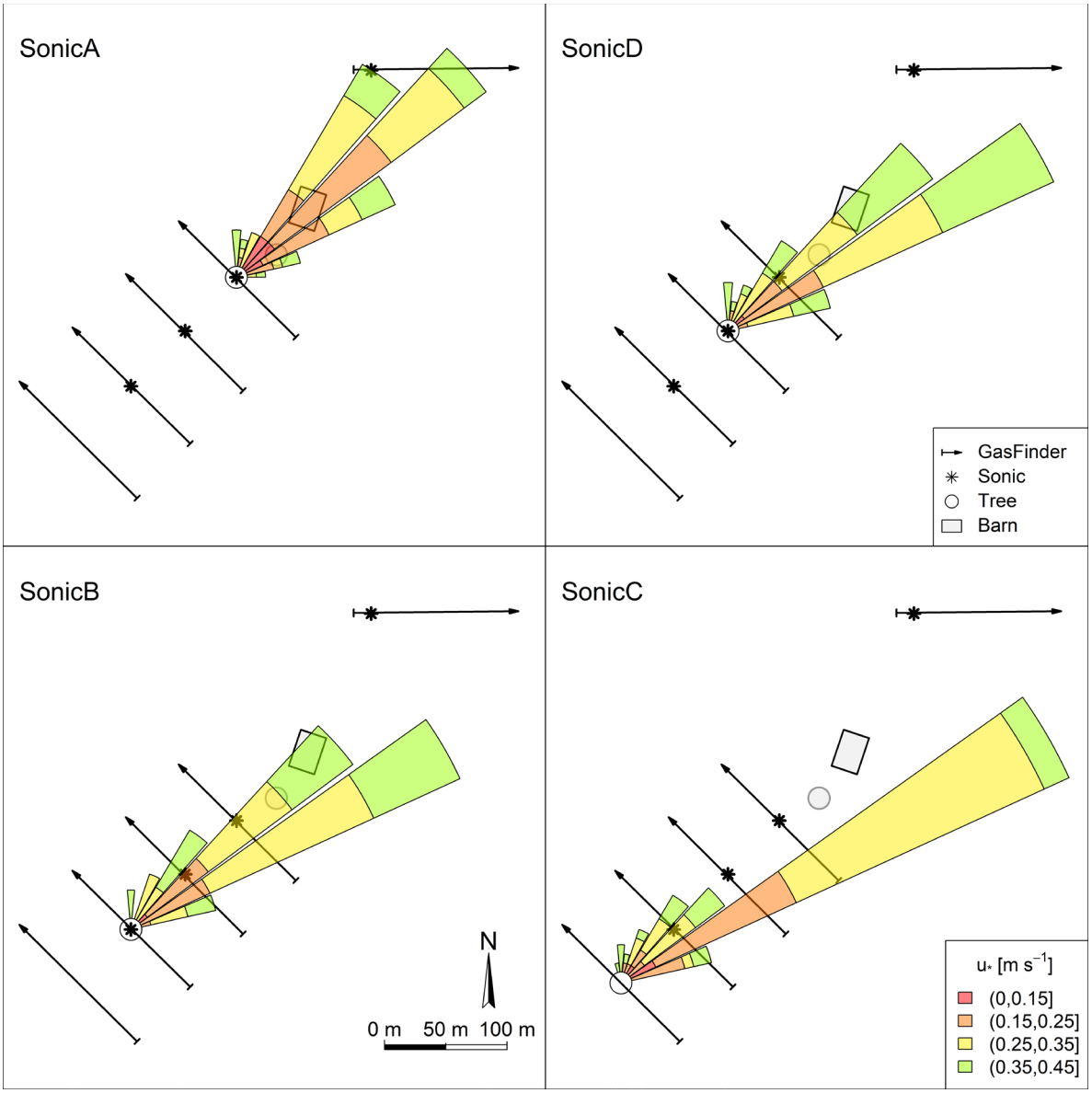

Figure 13: Schematic overview and wind rose of the four sonics for the measurement campaign whilst CH_4 was being released. The wind rose indicates the frequency of occurrence of wind directions and the friction velocity u_* in each wind direction sector. For display purposes the wind rose of the upwind sonic (SonicC) is plotted at the 200 m location. The names for the GasFinders are given in Figure 8.

2.7.5.3 Concentration analysis

The threshold for the received power of the used GasFinders are given in Table 3. For the concentration correction of the release experiment, data from IC2 and IC3 were used and only data that were recorded during times with a minimum wind speed of 0.5 m s^{-1} were taken into account. The intricate task of the offset and span correction is described in the following.

The two newer GasFinders (GF25, GF26, built in 2019) showed higher concentrations than the three older ones (GF16, GF17, GF18, built in 2016) (Figure 14, top panel). In the following analysis, GF26 was used as a reference device for comparing the measurements of all other GasFinders. The smoothed concentration differences between GF26 and the remaining GasFinders (Figure 14, bottom panel) seem to have a similar pattern. For the smoothing, a nonparametric local regression (loess) was used (Jacoby, 2000). The differences to GF26 tended to get less negative at the beginning of IC2

but increased again after 07 March 2021 and reached a maximum around 08 March 2021. Towards 10 March 2021, the differences were less negative (GF16, GF17, GF18) respectively more positive (GF25) again. If GF18 is compared to the other GasFinders instead, no general pattern in the concentration differences in IC2 was found (data not shown). This indicates that the pattern in IC2 (Figure 14, bottom panel) was due to some variation in GF26 that was not measured in any other device. However, without an external reference device, it remains unclear if GF26 measured precisely - not necessarily accurately - or all other devices did not measure precisely.

Table 3: Threshold values for the received power for the different GasFinders for the first intercomparison (IC1), the second intercomparison (IC2), the measurement campaign (MC), and the third intercomparison (IC3).

GasFinder	IC1	IC2	MC	IC3
GF16	70	70	70	70
GF17	600	600	400	100
GF18	120	120	120	120
GF25	50	50	50	50
GF26	200	200	200	200

During the MC whilst no CH_4 was being released, the most prominent feature is the lower concentration difference between GF26 and GF17. As the other concentration differences were similar to those by the end of IC2, the concentration measurement of GF17 was around 0.04 mg m^{-3} higher than before. Additionally, the differences to GF26 from GF16, GF18 and GF25 in the MC changed from the beginning until the end by about 0.04 mg m^{-3}. Although during this time, the GasFinders were in the MC setup (Figure 8), they should still have measured the same concentration as no CH_4 was being released during this time and the next known upwind CH_4 source was about 2 km away. Thus, it is more likely that GF17 had a concentration step change and GF26 a drift similar as described in Häni et al. (2021).

The record obtained by IC3 underscores the difficulty of interpreting the recorded data. At this time, all the GasFinders were placed next to each other and there were only a few hours in between the end of the MC and the beginning of IC3. However, the concentration difference from GF26 to GF25 changed by about 0.05 mg m^{-3}. Towards the end of IC3, there seems to be an increase in GF26 concentrations and a simultaneous decrease in GF25 as the decrease was strongest for GF25 compared to the other GasFinders (Figure 14). It appears that over the course of this thesis, the unstable behaviours of the GasFinder became more frequent. Therefore, they were sent to the manufacturer for revision.

A challenge faced was to choose the correct time ranges for the offset and span correction that were most representative for the concentrations in the MC whilst CH_4 was being released. However, with the chosen emission rate of the artificial source concentration enhancements between 0.2 and 2.0 mg m^{-3} were expected, thus roughly 10 times higher as the biases between the individual GasFinders.

A first offset and span correction were based on the data of IC2 and IC3. In IC3, also CH_4 was released to have higher variations in the concentrations for a more accurate span correction. As reference device GF25 was used as its measured concentrations were closest matching to real atmospheric concentrations. First, GF18 was corrected to GF25. Afterwards, GF16, GF17 and GF26

were corrected to GF18. For the correction of GF18 to GF25 and GF26 to GF18 the periods from 21 March 18:30 to 22 March 2021 01:50 UTC+1 and 23 March to 27 March 2021 were excluded as these might contain drifts or step changes. For the corrections of GF16 and GF17 to GF18, the period from 21 March 18:30 to 22 March 2021 01:50 UTC+1 was excluded for the same reason.

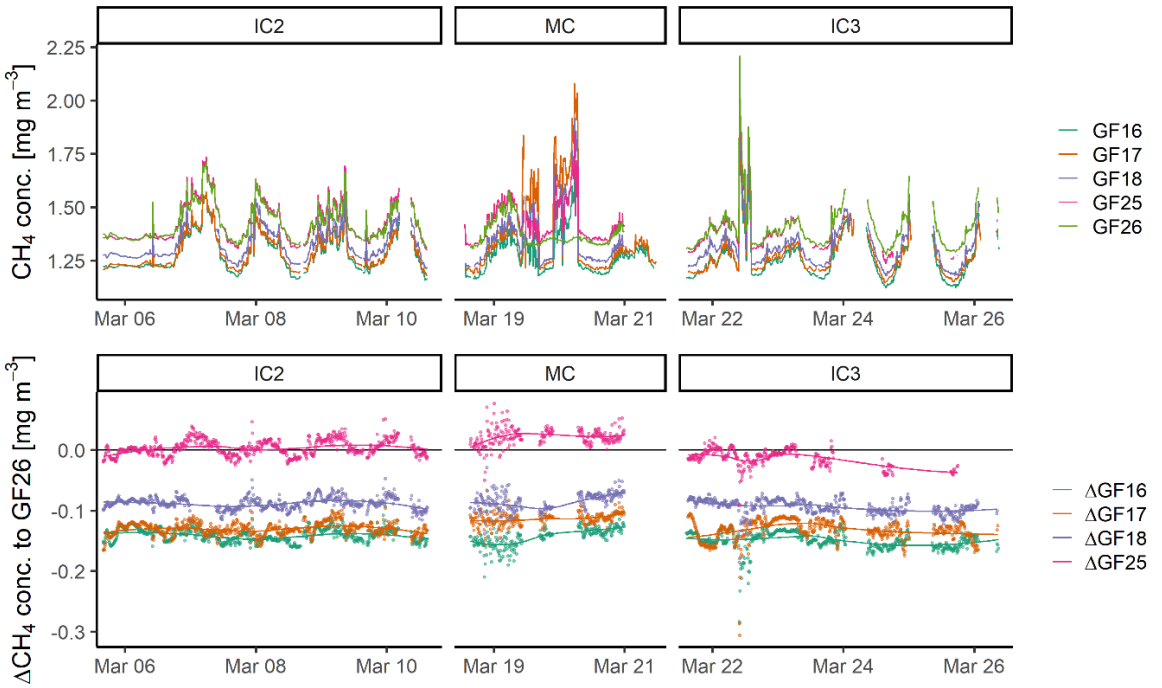

Figure 14: Upper panel: Uncorrected concentration (conc.) data recorded by the five GasFinders during the second intercomparison (IC2), the measurement campaign (MC), and the third intercomparison (IC3). Lower panel: Concentration differences to GF26 of the uncorrected GasFinder data, without the times during the MC whilst CH_4 was being released. The solid coloured lines are a graphical smoothing based on a nonparametric local regression (loess) (Jacoby, 2000). The time series is in UTC+1.

After these offset and span corrections, the corrected concentration data still showed an offset between the GasFinders in the MC (Figure 15, upper panel). Therefore, the offset to GF26 (background) in the MC was once again corrected (Figure 15, lower panel). For this, data from 19 March 17:10 to 19 March 2021 21:30 UTC+1 and 20 March 07:30 to 20 March 2021 11:50 UTC+1 were used. This was the time between the two releases in the MC and right after the second release in the MC.

As written above, during IC3, also CH_4 was released. To calculate emissions from these intervals a background concentration was needed. Therefore, the corrected concentration of all five GasFinders in IC3 when no CH_4 was being released were averaged. From the beginning to the end of the CH_4 release in IC3, the averaged concentration was linearly interpolated and used as background concentration. This was feasible as the concentrations during this time period on the day before and the three days after the release, exhibited only small variations (data not shown). The corrected GasFinder concentrations were then used to calculate CH_4 emissions.

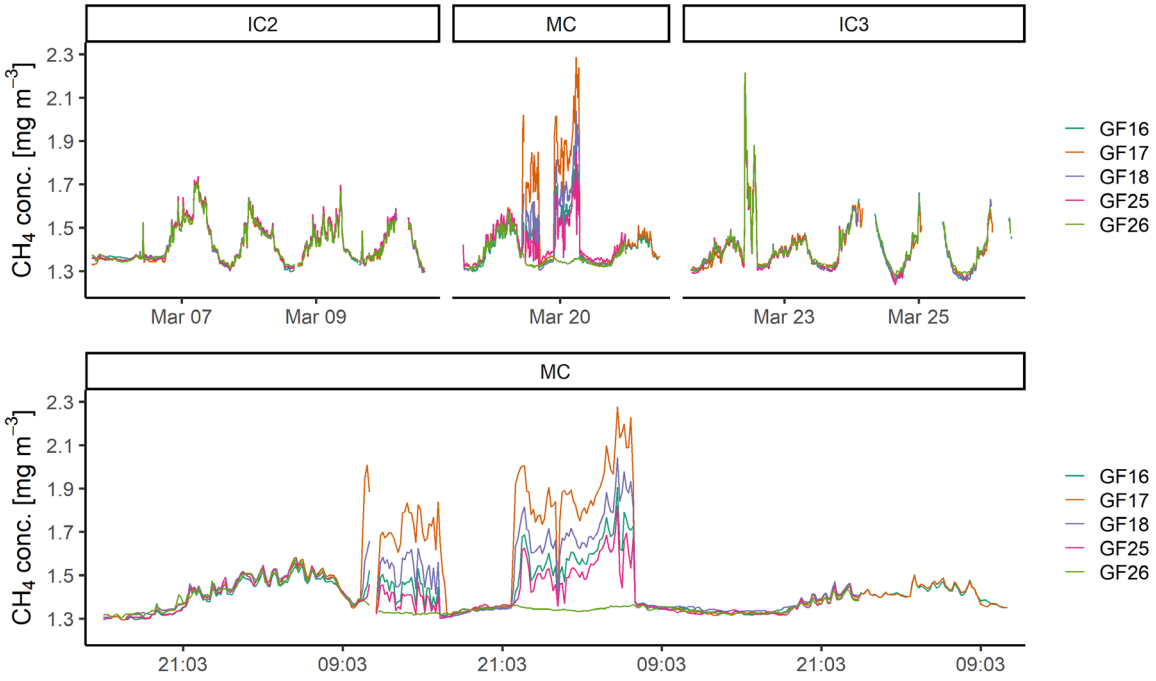

Figure 15: Upper panel: CH_4 concentration (conc.) data recorded by the five GasFinders during the second intercomparison (IC2), the measurement campaign (MC), and the third intercomparison (IC3) after a span and offset correction, based data from IC2 and IC3. Lower panel: CH_4 concentration after a second offset correction for the measurement campaign.

2.7.5.4 Emissions

The emissions determined from the different sonic and GasFinder combinations did not substantially differ during the MC (Figure 16, Figure 17). The determined emissions seem to increase with increasing distance of the GasFinders from the barn (Figure 17). The data loss during the MC whilst CH_4 was being released is highest with the combination SonicA and GF25 (81 %) and lowest with SonicB and GF17 (7 %) after quality filtering. On average, the closer the sonic was placed to the barn the larger the data loss (Table 4). For IC3, the emissions from all GasFinder were almost identical (Figure 18).

Table 4 Percentage of data loss of the different sonics and GasFinder combination after quality filtering.

	SonicA	SonicD	SonicB	SonicC
GF17	64 %	08 %	07 %	10 %
GF18	66 %	12 %	11 %	14 %
GF16	76 %	26 %	21 %	27 %
GF25	81 %	34 %	30 %	34 %
average	72 %	20 %	17 %	21 %

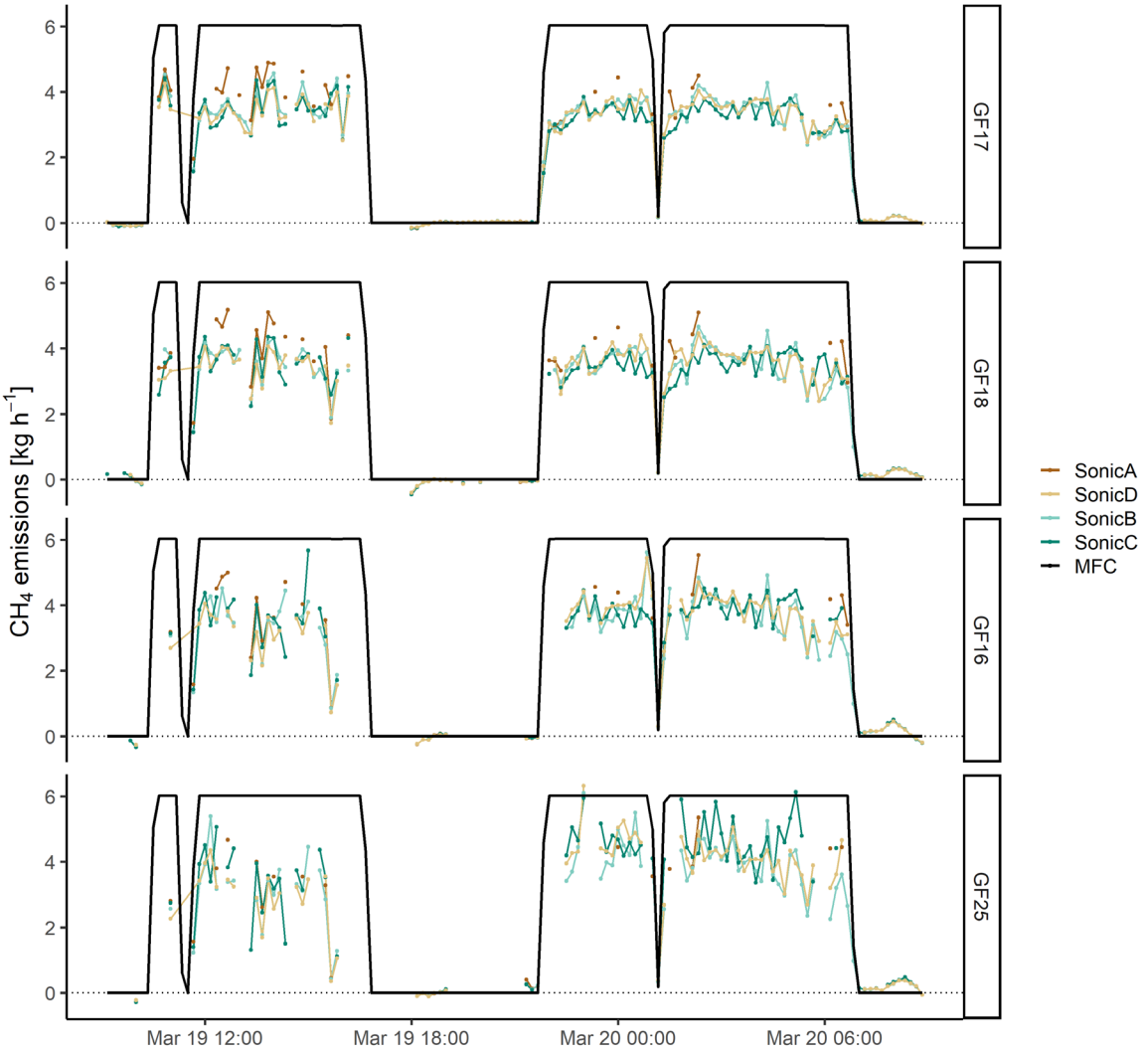

Figure 16: CH_4 emissions calculated for the measurement campaign with the concentrations of the GasFinders and the bLS output from the different sonics. Each panel represents a GasFinder (location) and the colours indicates the sonics used to calculate the emissions. The black solid line is the expected emission based on the flow rate of the mass flow controller (MFC). The positions of the GasFinders and sonics are given in Figure 8. The time series is in UTC+1.

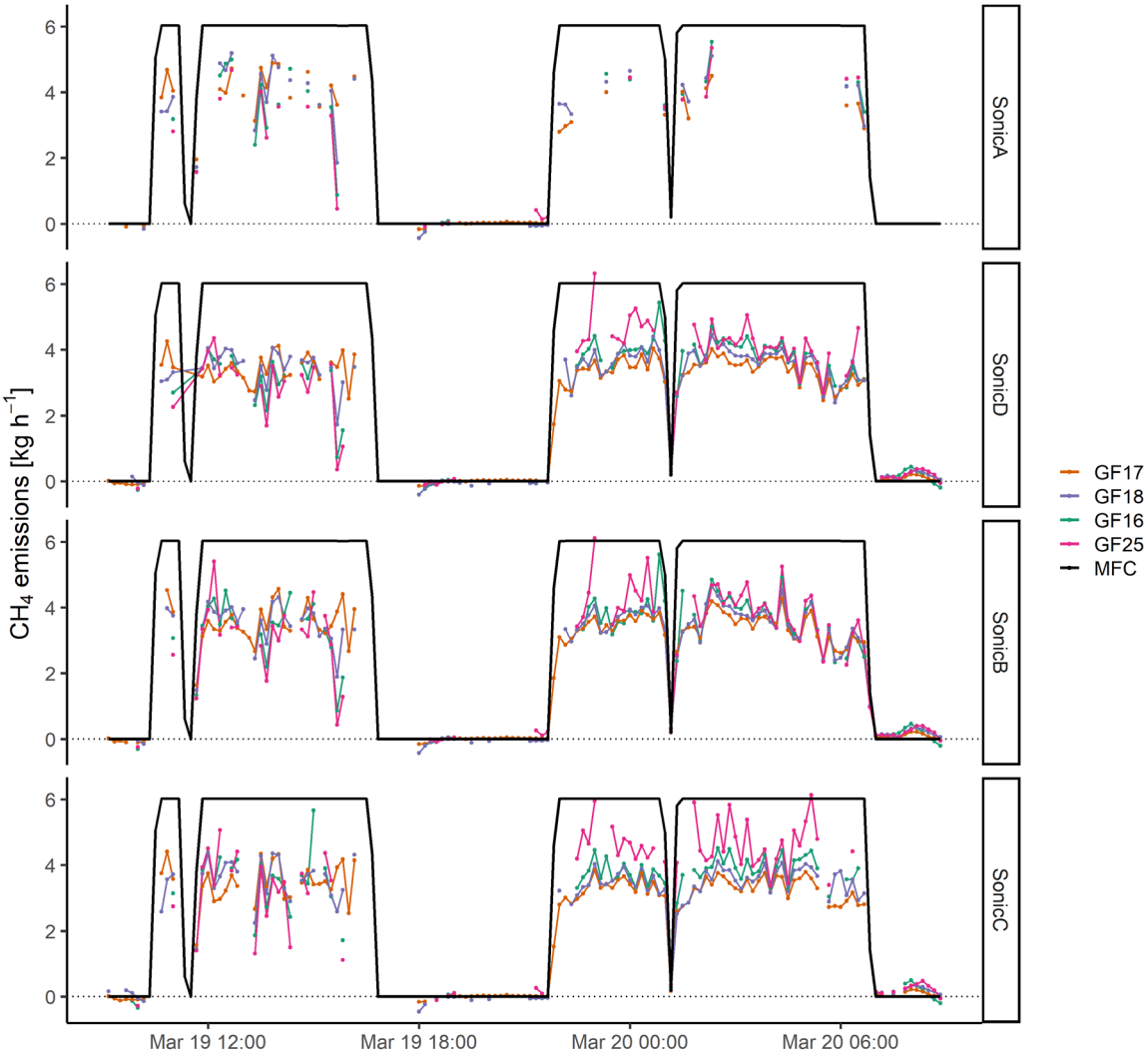

Figure 17: CH_4 emissions calculated for the measurement campaign with the concentrations of the GasFinders and the bLS output from the different sonics. Each panel represents a sonic and the colours indicates the GasFinder used to calculate the emissions. The black solid line is the expected emission based on the flow rate of the mass flow controller (MFC). The positions of the GasFinders and sonics are given in Figure 8. The time series is in UTC+1.

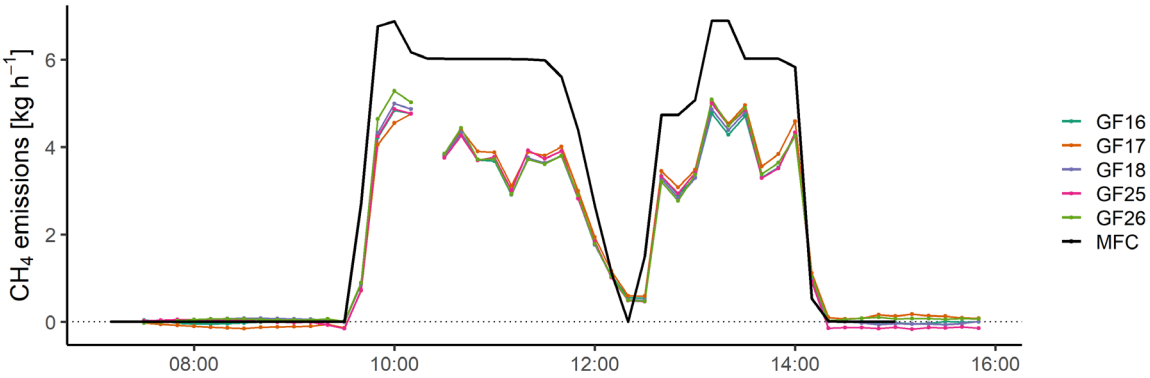

Figure 18: CH_4 emission data from the third intercomparison calculated with all five GasFinders and the data from SonicD. The black solid line is the expected emission based on the flow rate of the mass flow controller (MFC). The time series is in UTC+1.

The recovery rates (determined emission divided by expected emission) calculated from the CH_4 releases were always below 1 (Table 5). The mean recovery rates ranged between 0.56 - 0.72 for the MC and 0.55 - 0.76 for IC3.

Table 5: Recovery rates (mean, median) for all possible GasFinder-sonic combinations for the measurement campaign and the third intercomparison.

	SonicA	SonicD	SonicB	SonicC
Measurement campaign				
GF17	0.65, 0.66	0.57, 0.58	0.58, 0.57	0.56, 0.56
GF18	0.67, 0.69	0.60, 0.61	0.60, 0.60	0.59, 0.59
GF16	0.64, 0.70	0.63, 0.63	0.61, 0.61	0.64, 0.63
GF25	0.60, 0.63	0.67, 0.67	0.63, 0.61	0.72, 0.71
Third intercomparison				
GF26	-	0.69, 0.66	-	-
GF17	-	0.76, 0.66	-	-
GF18	-	0.66, 0.64	-	-
GF16	-	0.67, 0.63	-	-
GF25	-	0.55, 0.65	-	-

2.7.6 Discussion

Recovery rates between 0.55 and 0.76 have been determined. This deviates from the findings of Gao et al. (2010) that conducted a similar experiment and achieved a recovery rate between 0.93 and 1.03 for a fetch of 10 - 25 times the building height. For a fetch of 5 times the building height the recovery rate in Gao et al. (2010) was 0.66. For a similar fetch in this study (GasFinders at 50 m), the recovery rates for the MC were 0.56 - 0.65 and for IC3 55 – 0.76, thus comparable. However, for larger fetches the recovery rate in this study did generally not increase.

The setup was intended for an average wind direction of 45°. The average wind direction during the MC measured by the upwind sonic deviated by 6° toward the east compared to the setup chosen according to the predicted wind direction (Figure 5). About 3° were due the erroneously omission of declination correction in the test measurements conducted prior to the campaign. The slightly inaccurately placed setup was the reason that most of the emission plume was rather close to the edge of the GasFinder path (Figure 19). A deviation between the modelled plume and the emission plume leads to large differences in the determined emission, if most of the plume is not inside the GasFinder path. In the following, possible reasons for the lower recovery rate are discussed.

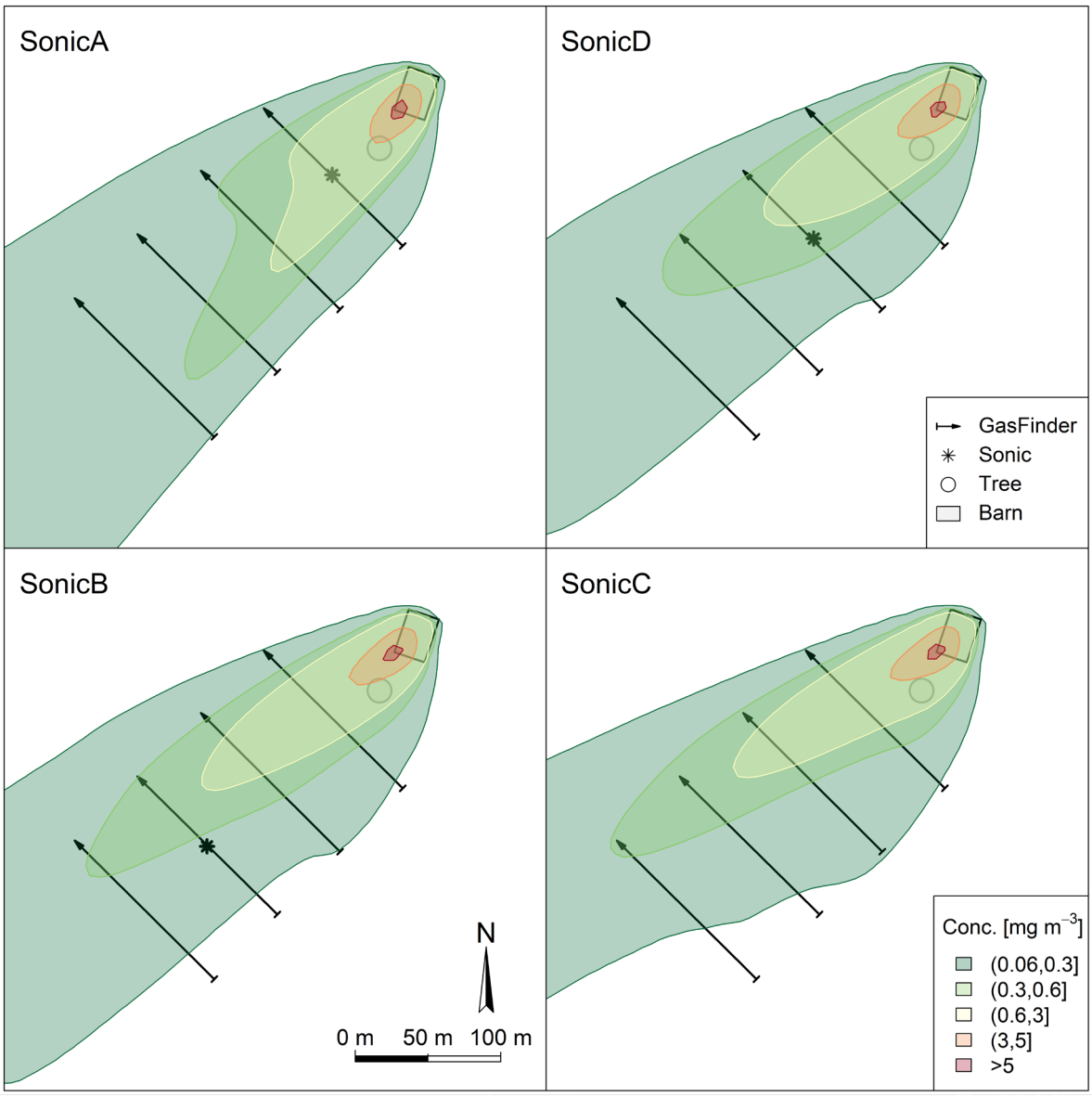

Figure 19: Contours of the modelled emission plume given as concentration enhancements for the xy-plane at a height of 1.6 m above ground for the bLS runs based on the four sonics. The name of the GasFinders and the position of SonicC are given in Figure 8.

2.7.6.1 Deviation of the plume in the xy-plane

A deviation in the xy-plane between the modelled plume and the real emission plume could be potentially the cause for the lower recovery rate. This can be either due to wrong wind direction data or a lateral deflection of the plume.

Wrong wind direction data could be due to a bias in the magnetic compass of the weather station which would cause an error in the sonic wind field transformation into the geographical coordinate system. Additionally, the wind direction correction of the sonics with the weather station could off by a few degrees. Especially due to the lack of southwesterly winds, there were only a few undisturbed wind directions for the comparison available (Figure 12). In the worst case, the measured wind direction could deviate by about 6° from the real wind direction. Thus, the implications on the emission data if the wind field was rotated by 15° clock- and anticlockwise in 1° steps was tested (Figure 20).

The general pattern of the wind field rotation was similar for all sonics (only data for SonicB are shown). The GasFinder closest to the barn was almost unaffected by any change in wind direction (Figure 20). The more the GasFinders were placed away from the barn, the larger were the changes in emissions due to the wind field rotation. Generally, a clockwise shift of the wind field led to higher emissions and an anticlockwise shift led to lower or unchanged emission estimates, whereas the changes were more pronounced with a clockwise rotation. This indicates that the emission plume was on the edge of the GasFinder paths. Thus, shifting the wind field clockwise turned the plume further out of the GasFinder paths and therefore decreased the modelled dispersion factors. Smaller dispersion factors with the unchanged measured concentrations led to higher emissions (Eq. 21). On the other hand, shifting the wind field anticlockwise shifted the plume more towards the middle of the GasFinder paths and thus increased the dispersion factors or remained unchanged as already the whole plume was inside the GasFinder paths. Hence, an anticlockwise shift decreased the emission or left it unchanged. That is a reason why it is important to cover a large distance with the GasFinder paths. A clockwise shift of 6° would have led to mean recovery rates between 0.54 and 0.80 with an average at 0.68. Nevertheless, it seems unlikely that the wind direction was off by so many degrees.

There could be other reasons for the discrepancies between the modelled plume in the bLS model and the real plume. The CH_4 could have left the barn in a way that would lead to a large deviation from the modelled plume. Before the CH_4 release, the wind speed inside the barn was about 0.9 m s^{-1} (only 10 min of data available). During the CH_4 release, no data are available as there were no electronic devices placed inside the barn for safety reasons. Nevertheless, it is likely that most of the CH_4 left the barn through the gate or gaps in the south wall. As described in Section 2.3, the bLS model assumes a homogeneous diffusive ground source. One could argue that due to the wind inside the barn, the source in the bLS model should be only the most southern part of the barn. By considering this kind of source definition as being less biased to natural conditions, it would decrease the recovery rate further as the dispersion factors of the GasFinders increase, since the average source area is now closer to the GasFinders. To overcome the problem of heterogeneous emissions within the source area, the GasFinders were placed 50 – 200 m downwind.

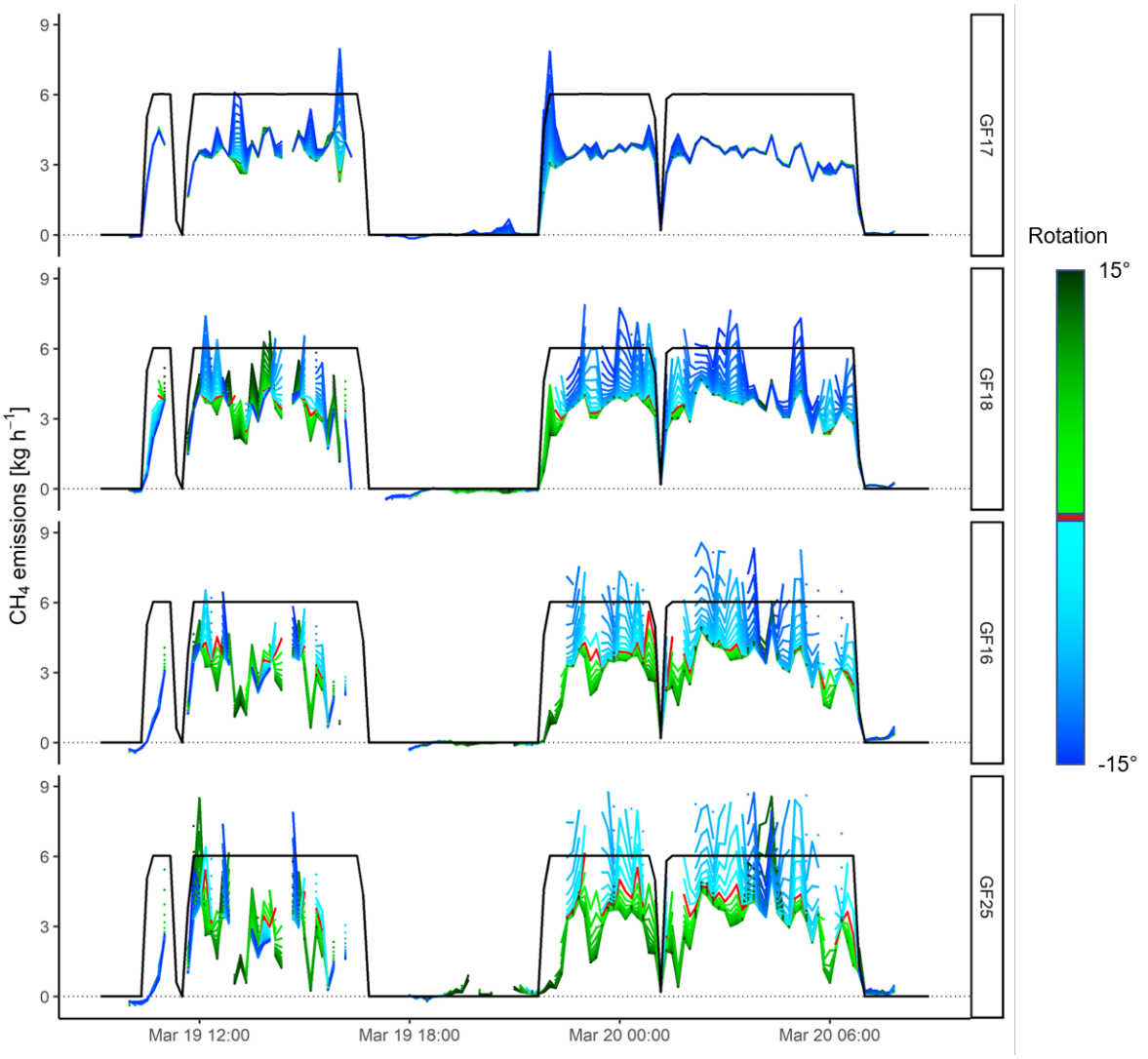

Figure 20: Effects of the wind field rotation on emission data calculated with SonicB and the four downwind GasFinders. Each colour represents a rotation by 1°. Green: anticlockwise rotation of the wind field. Blue: clockwise rotation of the wind field. Red: original line. The black solid line is the expected emission based on the flow rate of the mass flow controller. The time series is in UTC+1. Note that due to wind direction filtering (for every run the same) not every run has the same number of data points. Emissions over 9 kg h^{-1} are not displayed.

Another possibility is that the CH_4 left the barn almost jet like that was increased by the disturbance of the wind field due to the barn. That jet could have further been deflected by the tree southwest of the barn displacing the plume westwards. After several meters, the CH_4 would have reached the open field and dispersed according to the bLS model. In this case, the difference between the real and modelled plume (regarding the xy-plan only) would have been largest for the GasFinder closest to the barn and decreasing with rising distance to the barn. However, due to the long GasFinder paths this difference should not have affected the emissions calculated with the GasFinder closest to the barn as the real and the modelled plume were still inside the measurement path. The differences between the modelled and the real plume rather affected the emissions calculated with the GasFinders further downwind as can be seen in the wind direction variation (Figure 20). In combination with the setup that was not ideal, this could have shifted the plume outside the GasFinder paths the more distant the devices were placed away from the source. A hypothetical illustration of such a deflected plume is given in Figure 21.

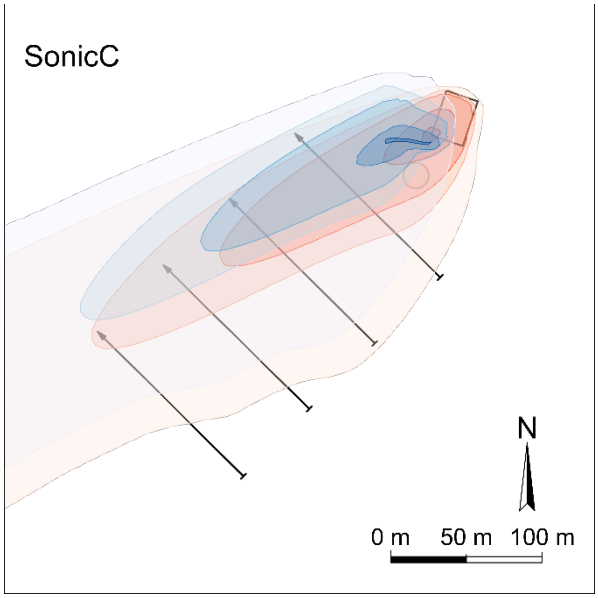

Figure 21: Illustration of a hypothetical deflected plume (blue) in contrast to the originally modelled plume (red).

2.7.6.2 Deviation of the plume in the xz-plane

Besides the deviations in the xy-plane, the modelled plume could also have differed from the real plume in the xz-plane. For a qualitative analysis a forward model with WindTrax was executed to investigate the effect of different release heights. As micrometeorological conditions provided by WindTrax, the stability classes neutral, slightly stable, and slightly unstable were used. A wind speed of 3 m s^{-1} and a wind direction of 51° were employed. As release heights, 0.05 m, 1 m, 2 m, 3 m, 4 m, and 5 m were selected. The 0.05 m were chosen as it is not possible to use ground emissions in the forward mode of WindTrax. The forward model run showed that with increasing release height the expected concentration at the GasFinders locations compared to a ground release decreases (Figure 22). This effect decreases with increasing distance of the GasFinder from the source. For a measurement height of 3 m instead of 1.6 m the effects are less pronounced. For all stability classes, the effects are similar.

As the concentration is proportional to the emission rate, this could explain the low recovery rate of the GasFinder closest to the barn and the findings of Gao et al. (2010) for a fetch 5 times the building height, as most of the CH_4 flew over the laser path. This is another reason for placing the concentration measurements with a fetch of 10 times the building height downwind of the source. However, it seems unlikely that the CH_4 exclusively left the barn at 4 m above ground level or higher. Additionally, only small differences in the emissions between the different GasFinder positions were recorded (Figure 17), and thus, according to results of the forward mode, the release rate must have been rather near ground.

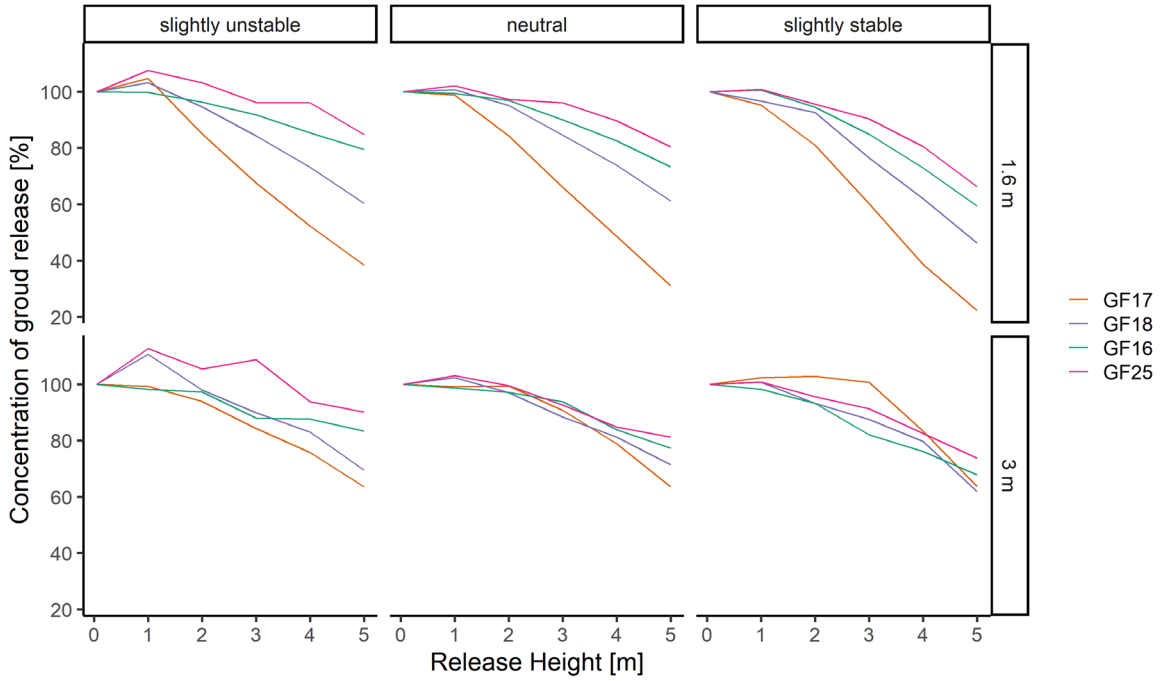

Figure 22: Percentage of the concentration found at the different GasFinder location with different release heights compared to a ground release calculated with the forward mode of WindTrax. The upper row shows the original GasFinder height (1.6 m above ground) and the lower panel the ratios resulting from GasFinder positions at 3 m above ground. Slightly unstable conditions: L = -30.37 m, $u_* = 0.2355$ m s^{-1}. Neutral conditions: L = 10^5 m, $u_* = 0.2265$ m s^{-1}. Slightly stable conditions: L = 30.37 m, $u_* = 0.2138$ m s^{-1}, For all conditions a wind speed of 3 m s^{-1} and a wind direction of 51° was used.

2.7.6.3 Other reasons for the low recovery rate

An erroneous offset correction between the downwind and the background concentration is unlikely as between the two releases during the measurement campaign all the GasFinders measured a similar concentration (Figure 15). Another possibility is an inadequate span correction by a factor of about 1.6. The same span correction for the MC was also applied to IC3. In the IC3, all GasFinders, inclusively GF26, which was used as background in the MC, had almost identical emissions (Figure 18). Thus, an error in the span that could explain the low recovery rate did not occur. Emissions were also calculated for times without any CH_4 release. On average these emissions were -0.01 kg h^{-1} with a standard deviation of 0.18 kg h^{-1} and thus support the statement that the concentration correction was correct. The somewhat higher emissions of GF25 during the measurement campaign (Figure 17) might also be due to errors in the concentration of the GasFinder (drift, step changes) that could not be corrected with the intercomparisons data. For the third intercomparison, GF25 did not seem to have any issues and the emission of all GasFinders (background was interpolated) was identical (Figure 18).

The cumulative flow through the MFC was within 1 % of the volume inside the gas cylinders. It is possible that there were compensation errors in the source but the bias of the CH_4 source is not higher than 5 %. It is also unlikely that the released CH_4 concentrated up inside the barn and leaked out in small doses over a several hours after the release. A concentration change was measured almost instantaneously after CH_4 was being released or the release was stopped. Additionally, the missing amount of CH_4 was just too much. In the first release during the MC, about 14 kg of CH_4 were missing. Directly after the release, all the gates and doors were fully opened to flush all remaining

CH_4 out and thus, one would have expected a concentration increase for at least the GasFinder closest to the barn (GF17), which did not occur. If despite venting the barn the missing CH_4 remained inside, the maximum leaking in the following time could not have been more than about 0.1 kg h^{-1}, considering a detection limit of the GasFinder of 0.027 mg m^{-3} (Häni et al., 2021). With a rate of 0.1 kg h^{-1}, it would have taken over a week until all the missing gas has left the barn.

2.7.7 Conclusions

The recovery rates of the release experiment were 0.56 - 0.76 and thus, smaller than 1, which cannot be conclusively explained. It is likely a combination of a deflected lateral plume and an uplift due to the wake of the barn or the tree. Additionally, a smaller part of the deviation could be due the uncertainty in the GasFinder concentrations and their correction. However, reliable information regarding the outflow of the gas from the barn, its interaction with the tree and the shape of the plume is not available. To test the impact of these three factors, a simulation of the air flows at this barn using a CFD model would be necessary.

To examine if there was a limitation of the IDM and to be able to better assess the measured emission, I suggest repeating the experiment. For a repetition of the experiment at the same location, several improvements can be suggested. First, low-cost CH_4 sensors should be installed at several places inside the barn for monitoring the dispersion of the CH_4 and safety reasons, as CH_4 is explosive in high concentrations. Second, the gate on the north side should be closed completely to reduce the wind flow through the barn. Third, turbulence measurements or wind measurements inside the barn would be desirable. These three suggestions were all well planned, but the concentration sensors were not ready at the time the experiment was conducted and the experiment could not be further delayed. Thus, for safety reasons the north gate was opened more than intended and no electronic device (a second weather station) was placed inside the barn. Fourth, longer path length of the GasFinders (140 – 200 m) should be employed in a corrected setup to be even less dependent on wind direction and lateral differences of the bLS model plume and the emission plume. However, longer path lengths will decrease the measured concentration differences between the up- and downwind GasFinders. For distances between 50 m and 150 m from the barn and the given release rate of the CH_4, the enhancement should however, not be a problem. Considering the uncertainty in the GasFinder measurements, there might be an issue with the measurement 200 m downwind, though. Fifth, if possible, also conditions with wind directions from southwest should be measured in the measurement setup to crosscheck the sonics wind direction and the GasFinder concentrations. Independent of the experimental site, an analysis of the plume shape via a drone or a mobile, high resolution measurement device (e.g., GasScouter™ G4301 Mobile Gas Concentration Analyzer, Picarro Inc, Santa Clara, USA) and an inlet attached to a telescope bar are advisable. Even though such measurements can only be conducted over a short period and the concentrations are expected to vary inside a plume, such measurements could give a general impression of the shape of the plume. This might be enough to see at which height the gas is released from the building and if the plume got deflected. This would allow a better interpretation of the IDM emission data.

2.8 References

Clauss, T., Reinelt, T., Liebetrau, J., Vesenmaier, A., Reiser, M., Flandorfer, C., Stenzel, S., Piringer, M., Fredenslund, A. M., Scheutz, C., Hrad, M., Ottner, R., Huber-Humer, M., Innocenti, F., Holmgren, M., and Yngvesson, J.: Recommendations for reliable methane emission rate quantification at biogas plants, Leipzig, DBFZ-Report, 33, 2019.

Degrazia, G. A., Welter, G. S., Wittwer, A. R., da Costa Carvalho, J., Roberti, D. R., Acevedo, O. C., Moraes, O. L., and Campos Velho, H. F. de: Estimation of the Lagrangian Kolmogorov constant from Eulerian measurements for distinct Reynolds number with application to pollution dispersion model, Atmospheric Environment, 42, 2415–2423, doi:10.1016/j.atmosenv.2007.12.018, 2008.

Du, S., Sawford, B. L., Wilson, J. D., and Wilson, D. J.: Estimation of the Kolmogorov constant (C0) for the Lagrangian structure function, using a second-order Lagrangian model of grid turbulence, Physics of Fluids, 7, 3083–3090, doi:10.1063/1.868618, 1995.

Flesch, T. K., McGinn, S. M., Chen, D., Wilson, J. D., and Desjardins, R. L.: Data filtering for inverse dispersion emission calculations, Agricultural and Forest Meteorology, 198-199, 1–6, doi:10.1016/j.agrformet.2014.07.010, 2014.

Flesch, T. K., Wilson, J. D., Harper, L. A., and Crenna, B. P.: Estimating gas emissions from a farm with an inverse-dispersion technique, Atmospheric Environment, 39, 4863–4874, doi:10.1016/j.atmosenv.2005.04.032, 2005.

Flesch, T. K., Wilson, J. D., Harper, L. A., Crenna, B. P., and Sharpe, R. R.: Deducing ground-to-air emissions from observed trace gas concentrations: A field trial, Journal of Applied Meteorology, 43, 487–502, doi:10.1175/1520-0450(2004)043<0487:DGEFOT>2.0.CO;2, 2004.

Gao, Z., Desjardins, R. L., and Flesch, T. K.: Assessment of the uncertainty of using an inverse-dispersion technique to measure methane emissions from animals in a barn and in a small pen, Atmospheric Environment, 44, 3128–3134, doi:10.1016/j.atmosenv.2010.05.032, 2010.

Gao, Z., Yuan, H., Ma, W., Liu, X., and Desjardins, R. L.: Methane emissions from a dairy feedlot during the fall and winter seasons in Northern China, Environmental Pollution, 159, 1183–1189, doi:10.1016/j.envpol.2011.02.003, 2011.

Häni, C.: Computational fluid dynamics modelling of a dairy housing using OpenFOAM, Bern University of Applied Sciences School of Agricultural, Forest and Food Sciences HAFL, unpublished, 2019.

Häni, C., Bühler, M., Neftel, A., Ammann, C., and Kupper, T.: Performance of open-path GasFinder3 devices for CH4 concentration measurements close to ambient levels, Atmospheric Measurement Techniques, 14, 1733–1741, doi:10.5194/amt-14-1733-2021, 2021.

Häni, C., Flechard, C., Neftel, A., Sintermann, J., and Kupper, T.: Accounting for field-scale dry deposition in backward Lagrangian stochastic dispersion modelling of NH3 emissions, Atmosphere, 9, 146, doi:10.3390/atmos9040146, 2018.

Harper, L. A., Denmead, O. T., and Flesch, T. K.: Micrometeorological techniques for measurement of enteric greenhouse gas emissions, Animal Feed Science and Technology, 166-167, 227–239, doi:10.1016/j.anifeedsci.2011.04.013, 2011.

Högström, U.: Non-dimensional wind and temperature profiles in the atmospheric surface layer: A re-evaluation, Boundary-Layer Meteorology, 42, 55–78, doi:10.1007/BF00119875, 1988.

Jacoby, W. G.: Loess, Electoral Studies, 19, 577–613, doi:10.1016/S0261-3794(99)00028-1, 2000.

Kaimal, J. C. and Finnigan, J. J.: Atmospheric boundary layer flows: Their structure and measurement, Oxford University Press, New York etc., 1994.

Kupper, T., Bonjour, C., and Menzi, H.: Evolution of farm and manure management and their influence on ammonia emissions from agriculture in Switzerland between 1990 and 2010, Atmospheric Environment, 103, 215–221, doi:10.1016/j.atmosenv.2014.12.024, 2015.

McGinn, S. M., Flesch, T. K., Harper, L. A., and Beauchemin, K. A.: An approach for measuring methane emissions from whole farms, Journal of Environmental Quality, 35, 14–20, doi:10.2134/jeq2005.0250, 2006.

Monin, A. S. and Obukhov, A. M.: Basic laws of turbulent mixing in the surface layer of the atmosphere, Doklady Akademii Nauk SSSR Institute of Theoretical Geophysics, 151, e187, 1954.

Obukhov, A. M.: Turbulence in an atmosphere with a non-uniform temperature, Doklady Akademii Nauk SSSR Institute of Theoretical Geophysics, No 1, doi:10.1007/BF00718085, 1946.

Ogink, N., Mosquera, J., Calvet, S., and Zhang, G.: Methods for measuring gas emissions from naturally ventilated livestock buildings: Developments over the last decade and perspectives for improvement, Biosystems Engineering, 116, 297–308, doi:10.1016/j.biosystemseng.2012.10.005, 2013.

R Core Team: R: A Language and Environment for Statistical Computing, R Foundation for Statistical Computing, Vienna, Austria, 2020.

Rizza, U., Degrazia, G. A., Mangia, C., and Filho, E. P. M.: Estimation of the Kolmogorov constant for the Lagrangian velocity spectrum and structure function under different PBL stability regimes generated by LES, Physica A, 389, 4009–4017, doi:10.1016/j.physa.2010.05.059, 2010.

Stull, R. B.: An Introduction to Boundary Layer Meteorology, 1st ed., Atmospheric Sciences Library, 13, Springer, Dordrecht, 670 pp., 1988.

Stull, R. B.: Meteorology for Scientists and Engineers, A Technical Companion Book with Ahrens' Meteorology Today, 2nd, Brooks/Cole, 2000.

swisstopo: Magnetic declination, Swiss Federal Office of Topography swisstopo, 2021: https://www.swisstopo.admin.ch/en/maps-data-online/calculation-services/deklination.html, last access: 13 December 2021.

Taylor, G. I.: The Spectrum of Turbulence, Royal Society of London. Series A. Mathematical and Physical Sciences, 164, 476–490, doi:10.1098/rspa.1938.0032, 1938.

Chapter 3

Assessment of the inverse dispersion method for the determination of methane emissions from a dairy housing

Marcel Bühler[1,2,3], Christoph Häni[1], Christof Ammann[4], Joachim Mohn[5], Albrecht Neftel[6], Sabine Schrade[7], Michael Zähner[7], Kerstin Zeyer[5], Stefan Brönnimann[2,3], Thomas Kupper[1]

[1]School of Agricultural, Forest and Food Sciences HAFL, Bern University of Applied Sciences, Switzerland

[2]Oeschger Centre for Climate Change Research, University of Bern, Switzerland

[3]Institute of Geography, University of Bern, Switzerland

[4]Climate and Agriculture Group, Agroscope, Switzerland

[5]Laboratory for Air Pollution/Environmental Technology, Empa, Switzerland

[6]Neftel Research Expertise, Switzerland

[7]Ruminants Research Unit, Agroscope, Switzerland

Agricultural and Forest Meteorology Vol 307, 108501, 2021

Abstract. Methane (CH_4) emissions from dairy housings, mainly originating from enteric fermentation of ruminating animals, are a significant source of greenhouse gases. The quantification of emissions from naturally ventilated dairy housings is challenging due to the spatial distribution of sources (animals, housing areas) and variable air exchange. The inverse dispersion method (IDM) is a promising option, which is increasingly used to determine gaseous emissions from stationary sources, as it offers high flexibility in the application at reasonable costs. We used a backward Lagrangian stochastic model combined with concentration measurements by open-path tunable diode laser spectrometers placed up- and downwind of a naturally ventilated housing with 40 dairy cows to determine the CH_4 emissions. The average emissions per livestock unit (LU) were 317 (±44) g LU^{-1} d^{-1}

and 267 (±43) g LU^{-1} d^{-1} for the first and second campaign, in September - October and November - December, respectively. For each campaign, inhouse tracer ratio measurements (iTRM) were conducted in parallel during two subperiods. For simultaneous measurements, IDM showed average emissions which were lower by 8 % and 1 % than that of iTRM, respectively, for the two campaigns. The differences are within the uncertainty range of any of the two methods. The IDM CH_4 emissions were further analysed by wind direction and atmospheric stability and no differences in emissions were found. Overall, IDM showed its aptitude to accurately determine CH_4 emissions from dairy housings or other stationary sources if the site allows adequate placement of sensors up- and downwind in the prevailing wind direction. To acquire reliable emission data, depending on the data loss during measurements due to quality filtering or instrument failure, a measuring time of at least 10 days is required.

Agricultural and Forest Meteorology 307 (2021) 108501

Contents lists available at ScienceDirect

Agricultural and Forest Meteorology

journal homepage: www.elsevier.com/locate/agrformet

Assessment of the inverse dispersion method for the determination of methane emissions from a dairy housing

Marcel Bühler [a,b,c,*], Christoph Häni [a], Christof Ammann [d], Joachim Mohn [e], Albrecht Neftel [f], Sabine Schrade [g], Michael Zähner [g], Kerstin Zeyer [e], Stefan Brönnimann [b,c], Thomas Kupper [a]

[a] School of Agricultural, Forest and Food Sciences HAFL, Bern University of Applied Sciences, Länggasse 85, 3052 Zollikofen, Switzerland
[b] Oeschger Centre for Climate Change Research, University of Bern, Hochschulstrasse 4, 3012 Bern, Switzerland
[c] Institute of Geography, University of Bern, Hallerstrasse 12, 3012 Bern, Switzerland
[d] Climate and Agriculture Group, Agroscope, Reckenholzstrasse 191, 8046 Zürich, Switzerland
[e] Laboratory for Air Pollution/Environmental Technology, Empa, Überlandstrasse 129, 8600 Dübendorf, Switzerland
[f] Neftel Research Expertise, 3033, Wohlen bei Bern, Switzerland
[g] Ruminants Research Unit, Agroscope, Tänikon 1, 8356 Ettenhausen, Switzerland

ARTICLE INFO

Keywords:
GasFinder3
Open-path tunable diode laser
Backward Lagrangian stochastic
Inhouse tracer ratio method
Uncertainty analysis
Enteric fermentation

ABSTRACT

Methane (CH_4) emissions from dairy housings, mainly originating from enteric fermentation of ruminating animals, are a significant source of greenhouse gases. The quantification of emissions from naturally ventilated dairy housings is challenging due to the spatial distribution of sources (animals, housing areas) and variable air exchange. The inverse dispersion method (IDM) is a promising option, which is increasingly used to determine gaseous emissions from stationary sources, as it offers high flexibility in the application at reasonable costs. We used a backward Lagrangian stochastic model combined with concentration measurements by open-path tunable diode laser spectrometers placed up- and downwind of a naturally ventilated housing with 40 dairy cows to determine the CH_4 emissions. The average emissions per livestock unit (LU) were 317 (±44) g LU^{-1} d^{-1} and 267 (±43) g LU^{-1} d^{-1} for the first and second campaign, in September – October and November – December, respectively. For each campaign, inhouse tracer ratio measurements (iTRM) were conducted in parallel during two subperiods. For simultaneous measurements, IDM showed average emissions which were lower by 8% and 1% than that of iTRM, respectively, for the two campaigns. The differences are within the uncertainty range of any of the two methods. The IDM CH_4 emissions were further analysed by wind direction and atmospheric stability and no differences in emissions were found. Overall, IDM showed its aptitude to accurately determine CH_4 emissions from dairy housings or other stationary sources if the site allows adequate placement of sensors up- and downwind in the prevailing wind direction. To acquire reliable emission data, depending on the data loss during measurements due to quality filtering or instrument failure, a measuring time of at least 10 days is required.

1. Introduction

Global emissions of greenhouse gases from the livestock sector are estimated at 7100 Tg CO_2-eq per year, which corresponds to 14.5% of the anthropogenic GHG emissions (Gerber, 2013). Approximately 3100 Tg CO_2-eq or 44% of livestock emissions are due to the release of methane (CH_4) with the main share provided by cattle (2000 Tg CO_2-eq per year) (Gerber, 2013). CH_4 in the livestock sector is mainly produced through enteric fermentation in the digestive tract of livestock animals (Niu et al., 2018) and to a smaller extent during manure management, which in temperate regions accounts for about 15-20% of CH_4 emissions (Petersen, 2018), and includes the livestock building, manure processing and storage (Gerber 2013). For the period 2008-2017, Saunois et al. (2020) estimated total emissions for enteric fermentation and manure management at 111 Tg CH_4 yr^{-1} or 2775 Tg CO_2-eq which corresponds to one third of the global anthropogenic CH_4 emissions (366 Tg CH_4 yr^{-1}).

Loose housing systems in a naturally ventilated building are becoming the most common housing type for cattle in Switzerland (Kupper et al., 2015). CH_4 emissions from this system for dairy cows

* Corresponding author.
E-mail address: marcel.buehler@bfh.ch (M. Bühler).

https://doi.org/10.1016/j.agrformet.2021.108501
Received 1 December 2020; Received in revised form 29 April 2021; Accepted 29 May 2021
Available online 15 June 2021

were found to vary over a large range (Poteko et al., 2019). The quantification of gaseous emissions from naturally ventilated livestock buildings is challenging due to the spatial distribution of sources (animals, housing areas) and variable air exchange rates.

The inverse dispersion method (IDM) is a promising option for emission determination from stationary sources such as livestock housings, without the need to access the buildings. It combines concentration measurements up- and downwind of the source with turbulence measurements and a dispersion model to quantify the emission strength. Backward Langrangian stochastic (bLS) models are most commonly used in the IDM approach, but simple Gaussian plume models or complex fluid dynamics models are also possible (Harper et al., 2011; Sonderfeld et al., 2017). The IDM has been successfully applied to estimate emissions e.g. from whole farms (including stationary sources such as animal housings and manure stores) (Flesch et al., 2005; Flesch et al., 2009; McGinn et al., 2006; VanderZaag et al., 2008), animal production buildings (Harper et al., 2010), feedlots (Bai et al., 2017; Flesch et al., 2007; McGinn et al., 2007; McGinn et al., 2016), grazing cattle (Laubach et al., 2013; Laubach et al., 2014) and manure stores (Flesch et al., 2013). In an experiment with controlled CH_4 release in an animal housing, a recovery rate between 0.93 and 1.03 was achieved for IDM at a fetch between 10 and 25 times the housing height (Gao et al., 2010). These studies have highlighted the flexibility in the application of IDM for farm scale measurements.

In contrast to the current published studies with IDM application, livestock farms in Switzerland are often located in hilly terrain with substantial topographical variation in nearby surroundings. The prevailing micrometeorological conditions are often associated with low wind speed and unsteady wind directions. Furthermore, the average Swiss dairy farm is relatively small, housing only 22 dairy cows on average (Federal Statistical Office, 2020) and there are often neighbouring farms with potentially confounding CH_4 emissions in the vicinity of the target source. This leads to a small CH_4 concentration gradient up- and downwind of the source. All these factors make a successful application of the IDM challenging.

In this study, we investigate the applicability and performance of the IDM for a naturally ventilated dairy housing in eastern Switzerland as a relatively weak CH_4 source where variable and unsteady wind conditions prevail. The dependence of the IDM results on micrometeorological conditions and the housing dimensions, influencing the turbulence at the positions of the measuring devices, are analysed. This is necessary, as the bLS model assumes a flat topography with emissions released at ground level. The average CH_4 emission obtained by the IDM are compared to independent simultaneous measurements by an in-house tracer ratio method (iTRM).

2. Material and methodology

2.1. Experimental site and periods

2.1.1. Geographical location

Measurements were conducted at a naturally ventilated dairy housing in Aadorf, Switzerland (47.489175° N, 8.919663° E) which is an experimental facility of Agroscope (Mohn et al., 2018). The housing is built on a small plain that extends > 1 km in southwest direction and 220 m in northeast direction (main two wind directions). In the northeast, the plain terrain is followed by a descending slope of about 9%. Next to the dairy housing towards the northwest, outside the main wind directions, there is a building and some trees, which exceed 10 m height (Fig. 1). 200 m westward, a small forest is situated. Apart from the associated slurry pit at the southwest side of the housing (Fig. 1), no other potential CH_4 sources were present in close vicinity of the building. However, within a radius of 600 m of the dairy housing there are three other livestock housings (280 m south, 370 m east, 570 m west) and temporary grazing cattle and sheep (200 m northwest, 380 m east, 100-500 m north).

2.1.2. Experimental dairy housing and livestock

The dairy housing is 50 m long, 25 m wide and 5 m and 8.5 m high in the southwest and northeast side, respectively. It has a mono-pitched roof with the slope towards southwest. The main building axis is oriented perpendicular to the prevailing wind direction (Fig. 1). The housing consists of two experimental compartments for 20 cows each with cubicles equipped with straw mattresses and solid floors with a common rubber mat. The layout of the functional areas is further described in Poteko et al. (2018). In the centre section between the two compartments, the milking parlour and waiting area as well as technical installations, office and analytics are placed. The feeding aisles and cubicle access areas were equipped with stationary scrapers, which removed the dung 12 times per day to cross channels. These cross channels were emptied in around 8 to 12 days intervals into the two separated below-ground slurry pits at the southwest side situated outside of the building. The slurry pits are covered with a concrete ceiling that contains eight openings (each around 0.8 m^2). The total volume and slurry surface of the slurry pits are 252.2 m^3 and 127 m^2, respectively.

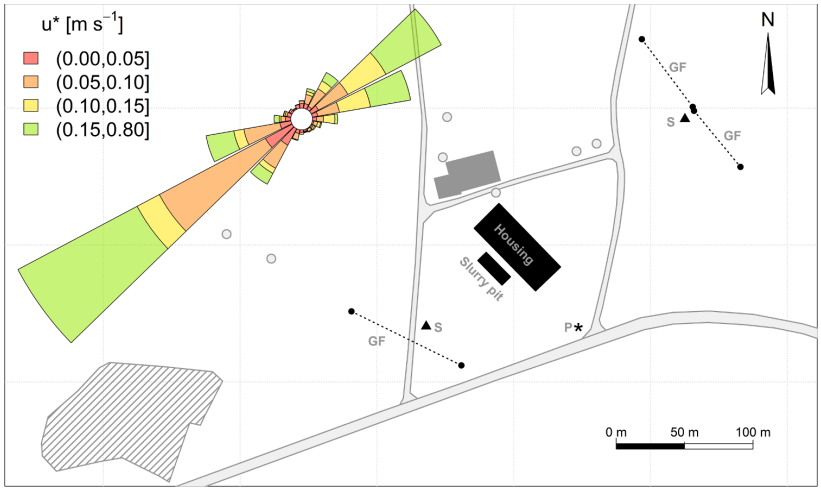

Fig. 1. Schematic overview of the measuring location with a wind rose. The wind rose indicates the frequency of occurrence of wind directions and the friction velocity u* in each wind direction sector. The large black rectangle is the dairy cattle housing with the underground slurry pit on the southwest side. Filled black circles indicate positions of GasFinder (GF) sensors and retroreflectors with the dashed line representing the measuring path. The black triangles mark the position of the sonic anemometers (S). The inlet for the iTRM background measurements (P) is denoted as asterisk. Further, trees (grey circles), forest area (hatched polygon), a building (dark grey polygon) and the streets (light grey) are drawn.

The experimental compartments are naturally ventilated without thermal insulation and with flexible curtains as facades. Management routines such as milking (05:30 and 16:30) and dung removal with stationary scrapers were the same in both measuring campaigns. Due to nutrition trials, which were carried out in parallel using the two groups of 20 dairy cows each, the diets during the iTRM measurements phases consisted of (i) hay, maize pellets and pellets of a mixture of maize and beans, or (ii) grass silage, maize silage and hay in compartment one and two, respectively. In addition, concentrates rich in energy and protein were allocated according to milk yield and body condition by an automatic feeder individually. Between the two iTRM measurements in each campaign, the rations (i) and (ii) were interchanged between the groups in the two compartments with prior phases allowing the cows to gradually adapt to the new diet. The silage-free diet (i) was provided twice per day (05:00 and 15:30) and the silage diet (ii) once per day (15:30). The cows had access to the fresh feed after each milking. The feed was automatically moved towards the cows 18 times a day.

During both measuring periods 40 lactating cows of Brown Swiss and Swiss Fleckvieh breeds were housed in the dairy housing for emission measurements (Table 1). The cows had no access to pasture or to the outdoor exercise areas during the measurements.

2.1.3. Measurement campaigns

Measurements were conducted during two campaigns in 2018. The first campaign lasted for 36 days from 17 September to 23 October with iTRM measurements conducted for two subperiods of eight days from 24 September to 02 October and 15 October to 23 October. The second campaign comprised 23 days of measurements from 24 November to 17 December with iTRM measurements divided into two subperiods of four days conducted from 26 November to 30 November and 11 December to 15 December.

The two campaigns were planned as two individual campaigns to reflect varying meteorological conditions which turned out to be substantially different in the first and second campaign (Section 3). Additionally, the herd composition was not identical (Table 1). Therefore, in the following we differentiate between the two campaigns.

2.2. Inverse dispersion method

2.2.1. Concept

IDM is a micrometeorological method to determine gaseous emissions from a spatially limited source of known area. The difference between measured concentrations upwind (C_{UW}, background concentration) and downwind (C_{DW}) of the source is proportional to the total emission rate Q between upwind and downwind concentration measurement (Eq. 1).

$$C_{DW} - C_{UW} = D * Q \quad (1)$$

The dispersion factor D is determined from measured turbulence characteristics by a dispersion model. Here, the bLS model described in Flesch et al. (2004) was used. With the modelled D_{bLS} [s m^{-3}] values and the measured concentrations C_{DW} and C_{UW} [mg m^{-3}] the emission flux Q [mg s^{-1}] can be calculated (Eq. 2).

Table 1
Herd composition in the first and second campaign (means ± standard deviation).

		Campaign 1	Campaign 2
No of animals per breed	Brown Swiss	27	30
	Swiss Fleckvieh	13	10
No of animals	primiparous	7	11
	multiparous	33	29
Body weight ± 1 SD [kg]		701 ± 82	685 ± 77
Milk yield per day ± 1 SD [kg]		23.2 ± 8.8	25.7 ± 11.0

$$Q = \frac{C_{DW} - C_{UW}}{D_{bLS}} \quad (2)$$

The line-integrating concentration measurements (Section 2.2.2) were approximated by a series of point sensors with a 1 m spacing along the path length. For each sensor and emission interval, 250,000 backward trajectories were calculated and analysed for touchdowns within the source area. The simulations were done with the R package bLSmodelR (Häni et al., 2018), available at https://github.com/ChHaeni/bLSmodelR.

2.2.2. Methane concentration measurements

For the concentration measurements, open-path tunable diode laser spectrometers (GasFinder3-OP, Boreal Laser Inc., Edmonton, Canada) and retroreflectors with seven corner cubes were utilised. The GasFinders measure at a frequency range of 0.3 - 1 Hz. The sensors and heated retroreflectors were connected to the power grid. The CH_4 concentration measurements were corrected for temperature and pressure influences using device specific relationships determined by Boreal Laser after construction (Boreal Laser Inc., 2018).

Concentration data was used only if the 'received power' of the reflected incoming laser beam was in the range of 200 to 2500 μW for two of the GasFinders. Due to erroneous concentration measurements when 'received power' was low, a more restrictive threshold of 400 to 2500 μW was used for the third GasFinder. For all three GasFinders the threshold for the goodness of fit between the sample and the calibration waveform quantified as R2 was 98%. The 0.3 - 1 Hz data were then averaged to 30 min intervals and periods with a data coverage of less than 75% (22.5 min) were removed. The three GasFinders were intercalibrated between the two campaigns and further, to relate measurements to international scales (WMO X2004A), the data was corrected to match independent background measurements from a cavity ring-down spectrometer (CRDS, model G2301, Picarro Inc., Santa Clara, USA) with an inlet 30 m southeast of the housing (Fig. 1). The interquartile range of the background concentration was 2.04 – 2.45 ppm. The interquartile range of the concentration difference (downwind – background) was 0.09 – 0.38 ppm. The median precision of GasFinder devices used in this study for 30 min averaged concentration measurements is 0.04 ppm (Häni et al., 2021).

2.2.3. Experimental setup

Based on experimental findings, Harper et al. (2011) advised placing concentration and turbulence measurements at the downwind side of the housing at a distance of at least 10 times the maximum building height so that the devices are outside the disturbed turbulence field. For the present site this corresponds to a distance of 85 m. From previous wind measurements at the site, two distinct main wind sectors, northeast and southwest had been identified (Fig. 1). Towards northeast, GasFinders and the sonic anemometer (Gill Windmaster, Gill Instrument Ltd., Lymington, UK) were placed at a distance of at least 120 m. Towards southwest, however, the instruments had to be placed at a shorter distance of at least 60 m (Fig. 1) due to a main road passing on this side of the housing.

On the northeast side two GasFinders with a path length of 50 m and 42 m were placed next to each other. The average heights of the measuring paths for the two GasFinders were 1.41 m and 1.35 m above ground. These two GasFinders were combined to a single sensor in the bLS simulations to cover a larger fraction of the emission plume and to be less prone to erroneous measurements (Supporting information 1). For the intervals where only one of the devices passed the quality checks (Section 2.2.2), the emission estimate was based on the measurement of this single sensor only. On the southwest side a single GasFinder was placed with a path length of 75 m with an average height of 1.54 m above ground. At both sides of the dairy housing a 3D sonic anemometer was installed at 1.35 and 1.40 m height (Fig. 1) to derive the turbulence characteristics that are needed as input for the bLS model. Two sonics

were used because it was expected to have two dominant wind directions, therefore necessitating two downwind sonics. Sonic measurements were recorded as 10 Hz data in daily files.

The coordinates of the housing and the main GasFinder modules and retroreflectors that were needed to run the bLS model were logged with a handheld global positioning system (Trimble Pro 6T, Trimble Navigation Limited, Sunnyvale, USA). For both campaigns, the GasFinders and sonics were placed at the same location.

2.2.4. Data processing and filtering

The 10 Hz sonic data were corrected for a Gill software bug affecting the magnitude of the vertical wind component (Gill Instruments, 2016). After wind vector rotation (two-axis coordinate rotation), averaged wind and turbulence characteristics for 30 min intervals were calculated. For the evaluation, only the data from the downwind sonic were used. This is more representative as the location coincides with the concentration measurement of the emission plume.

The bLS model is suspected to provide erroneous results given extreme micrometeorological conditions (e.g. very low wind speed, highly unstable or stable conditions). To avoid unrealistic and error-prone emission results, the data were quality filtered (e.g Flesch et al., 2005; Flesch et al., 2018). Filters were applied for the friction velocity (u^*), the Obukohv length (L) and the roughness length (z_0). In addition, to exclude periods with instationary wind directions filters for the standard deviation of the along wind divided by u^* (σ_u/u^*), the standard deviation of the crosswind divided by u^* (σ_v/u^*) and the estimated Kolmogorov constant of the Lagrangian structure function ($C0$) were applied. Emission values with either $u^* < 0.05$ m s^{-1}, $|L| < 2$ m, $z_0 > 0.1$ m, $\sigma_u/u^* > 4.5$, $\sigma_v/u^* > 4.5$, $C0 > 10$ were removed. Additionally, the data were filtered for wind direction. Wind direction filtering is done to make sure that most of the plume from the source is caught by the line-integrating concentration measurements. More information on wind direction filtering is given in the Supporting information 3. Data from measurement intervals which coincided with processes of the slurry pit (e.g. emptying cross channels, slurry agitation) were discarded.

2.2.5. Uncertainty analysis

We estimated the uncertainty ε of the mean IDM emission rate $Q(\Delta t)$ over a certain measurement integration time Δt from the standard deviation SD of consecutive measurement periods of length Δt:

$$\varepsilon_Q(\Delta t) = 2 \cdot \mathrm{SD}\left\{\overline{Q}_i(\Delta t)\right\} \tag{3}$$

ε_Q was analysed for time periods Δt of increasing length (effective measurement time without data gaps). This was done with the data set of the first campaign as it is longer and has less gaps than the second campaign. For practical reasons, the data set was truncated to 360 h and Eq. 3 was evaluated for $\overline{Q}_i$ averaged over time periods between 1 h and 45 h. ε_Q corresponds to a 95% confidence interval of the respective mean under the ideal assumption of a constant Q with time. Since the calculated SD may also include true variations of Q, ε_Q is considered as an upper boundary estimate for the uncertainty of the mean emission.

To estimate the IDM measurement time length, which is necessary to determine the mean emission rate $\overline{Q}$ with a given precision, the results were fitted with a power function of Δt. By extrapolating this function to the total cumulative measurement length of the measurement campaigns, the uncertainty of the mean campaign emissions was estimated.

2.3. Inhouse tracer ratio method

Emissions were measured using a dual tracer ratio method (Schrade et al., 2012) as described in detail by Mohn et al. (2018). The goal of this setup and this housing is to measure two variants in two experimental compartments simultaneously, for comparison as conducted previously by Poteko et al. (2020). The method involves dosing of two different tracer gases, sulphur hexafluoride (SF_6) and trifluoromethyl sulphur pentafluoride (SF_5CF_3), one per compartment, to quantify emissions for each experimental compartment independently and detect potential cross-contamination. Both tracer gases were dosed constantly at floor level using mass flow controllers (Contrec AG, Dietikon, Switzerland) to regulate the total flow and critical steel orifices to achieve homogenous spatial distribution. Representative air sampling in each compartment was accomplished with critical glass orifices (250 µm in diameter 2.5 m above the ground; Thermo-Instruments, Dortmund, Germany, and Louwers, Hapert, The Netherlands). Concentrations of the tracer gases and CH_4 were analysed in real time by gas chromatography with electron capture detection (GC-ECD, model 7890A, Agilent Technologies AG, Basel, Switzerland) and by cavity ring-down spectrometer (CRDS, model G2301, Picarro Inc., Santa Clara, USA).

The quantification of emissions with the tracer ratio method is based on the assumption that the tracer gas (SF_6, SF_5CF_3) behaves in the same way as the target gas and thus mimics the emitting source (Demmers et al., 2001). The mass flow of the target gas ($\dot{m}_{target}$) is calculated from the ratio of the background corrected target (c_{target}) and tracer gas concentration (c_{tracer}) and the mass flow of the tracer gas ($\dot{m}_{tracer}$) as given in Eq. 4:

$$\dot{m}_{target} = \frac{\dot{m}_{tracer} * C_{target}}{C_{tracer}} \tag{4}$$

Background concentration was sampled at a point situated at 30 m southeast of the building (Fig. 1). More details on the implemented analytical technique and its performance with respect to suitability for point/areal sources, sensitivity, and uncertainty have been described in Mohn et al. (2018). In the study of Mohn et al. (2018), with constant CH_4 dosing through critical orifices, the absolute uncertainty of the iTRM was reported to be better than 10% for daily averages.

The applied measurement sequence provided emission data with a temporal resolution of 10 min per compartment. To make the iTRM data comparable to the IDM data, 30 min averages for each experimental compartment were calculated and afterwards both compartments summed up. Milking times were excluded from the iTRM analysis, as no animals or only parts of the herd were present in the experimental compartments during these periods.

2.4. Comparison with iTRM emissions

The iTRM measurements were running only during certain times of the IDM campaigns (Section 2.1.3). To make a valid comparison, only 30 min measurement intervals where both methods provided valid data were considered. Based on those data pairs, the average CH_4 emissions of IDM and iTRM were calculated separately for campaign 1 and campaign 2. For this purpose, the data were not weighted e.g. in relation to hour of the day or micrometeorological conditions.

The experimental site comprises two CH_4 sources, the dairy housing and the adjacent slurry pit (Fig. 1), with the second expected to have a much lower emission strength (Petersen, 2018). It can be assumed that measurements of the iTRM do not capture emissions from the slurry pit. Thus, for comparison of CH_4 emissions by IDM and iTRM, the emissions from the slurry pit were subtracted from the total IDM emissions. This correction and the assumptions used to estimate emissions from slurry storage are described in detail in the Supporting information 2. If not otherwise noted, CH_4 emissions are given without the slurry pit.

3. Results

3.1. Meteorological conditions

The average temperature during campaign 1 and campaign 2 was 12.3 °C and 3.4 °C, respectively. The predominant wind directions were southwest (around 233°) and northeast (around 60°) during both

campaigns. Wind speeds were mostly below 2 m s^{-1}, with occasional periods with higher wind speeds (Fig. 2).

The diurnal pattern observed for the wind direction resembles a mountain-valley wind system. This means that there is wind during the day from one direction and during the night from the opposite direction. For this site, there was predominantly northeasterly wind and unstable atmospheric conditions at day and southwesterly wind and stable conditions at night. The diurnal pattern is more distinct in the first than in the second campaign. During the second campaign, periods prevailed over several days with wind from one direction and the mountain-valley like wind system was only observed occasionally (Fig. 2).

3.2. Quality selected IDM emissions

Fig. 3 shows the percentage of data loss for both IDM campaigns as a function of time of day. In campaign 1, the data loss was largest in the morning and evening, while in campaign 2, the proportion of data loss was largest during the night. In total, there are 745 and 448 valid half-hourly IDM emission intervals for the first and second measurement campaign, respectively. This corresponds to a data loss of 57% and 64% (average 60%) due to quality filtering and failure of the GasFinders for the first and second campaign, respectively.

Fig. 4 displays the filtered IDM CH_4 emission data for campaign 1 and campaign 2. The subperiods, during which parallel measurements with the iTRM were conducted, are highlighted by orange shaded areas. Valid data were obtained throughout the entire duration of the measurement campaigns with larger data gaps (Fig. 4) due to mostly GasFinder measurement failure. The main reasons for the larger data loss in campaign 2 was displacement of the GasFinders due to unstable mounting on the wet soil or impacts of wind, resulting in a misalignment of the laser beam of the GasFinders. The data loss in the morning and evening hours of campaign 1 coincided with instationary time periods where the wind direction changed from southwest to northeast and vice versa. Data loss in the second campaign was largest during the night.

As the number of 30 min intervals with valid IDM CH_4 emission data varies over the course of the day, the data were first averaged within groups of equal 'hour of day' values before calculating the overall average. This resulted in daily-average CH_4 IDM emission estimates for the first campaign and second campaign of 0.74 (±0.10) kg h^{-1} and 0.61 (±0.10) kg h^{-1}, respectively. The uncertainty is given as 95% confidence interval derived according to Section 2.2.5. The relative uncertainty for the first and second campaign is 14% and 16%, respectively. For comparison with literature data, daily average emissions were scaled to LU (Livestock Unit with 500 kg live weight) with the live weight given in Table 1. For the first and second campaign, the resulting CH_4 emissions by IDM were 317 (±44) g LU^{-1} d^{-1} and 267 (±43) g LU^{-1} d^{-1}, respectively.

If the emissions from the slurry pits are included, the resulting CH_4 emissions by IDM for the first and second campaign were 342 (±48) g LU^{-1} d^{-1} and 269 (±43) g LU^{-1} d^{-1}, respectively.

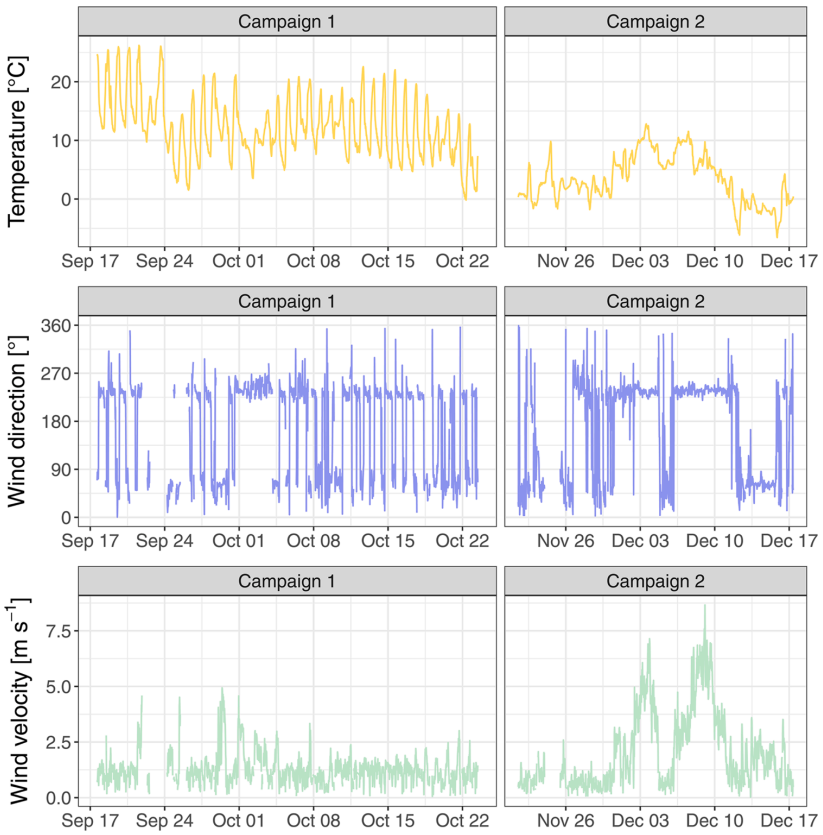

Fig. 2. Meteorological conditions during campaign 1 and campaign 2: temperature (upper panel), wind direction (mid panel) and wind velocity (lower panel). The temperature was recorded at the MeteoSwiss weather station in Tänikon. The wind direction and wind speed were taken from the upwind sonic anemometer at the measuring site.

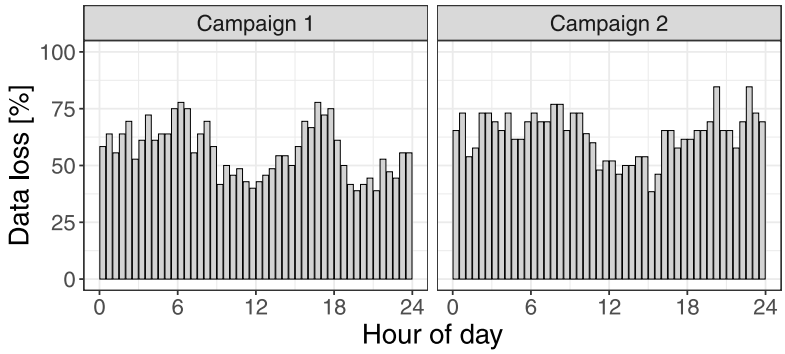

Fig. 3. Data loss of quality filtered IDM emission data as function of hour of day for the two campaigns. Lower values mean more valid data.

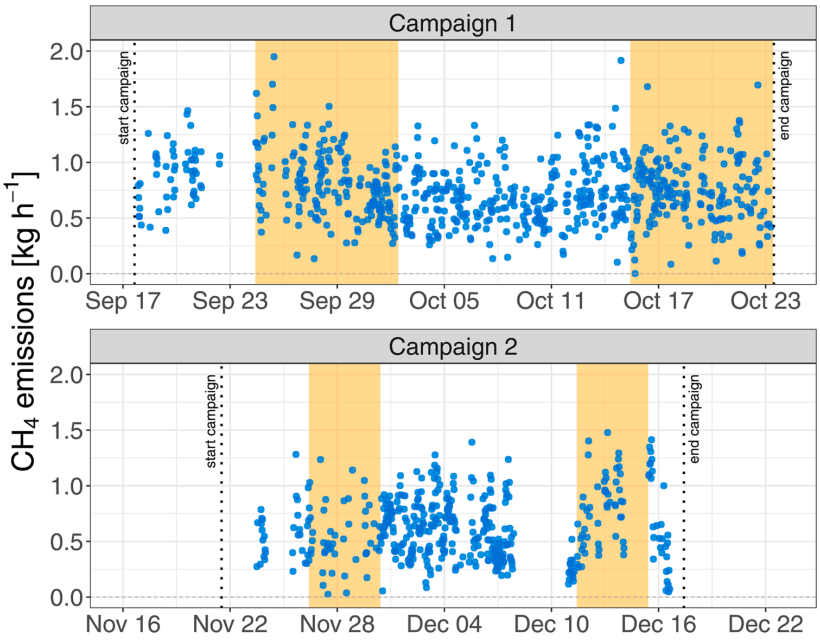

Fig. 4. Half-hourly CH_4 emissions of the dairy housing determined by IDM for campaign 1 (upper panel) and campaign 2 (lower panel). Displayed data are quality filtered. The subperiods with simultaneous iTRM measurements are marked as orange shaded areas.

3.3. Dependence on micrometeorological conditions and diurnal variation

In the first campaign during the day (07:30 – 16:30), there were mostly unstable conditions and northeast wind. During the night (16:30 – 07:30), stable conditions and southwest wind with on average slightly lower friction velocity than during the day prevailed. In campaign 1, the mean CH_4 emission, determined with the IDM, for northeast wind was 4% lower than for southwest wind. For stable conditions the CH_4 emission was 6% lower than with unstable conditions. A correlation between the atmospheric stability, represented by the Obukhov length L, and wind direction in the first campaign is discernable (Fig. 5). The algebraic sign of L is given by the sensible surface heat flux. For convective or unstable conditions (typically during the day) the surface heat flux is positive and hence $L < 0$. For stable conditions the surface heat flux is negative and hence $L > 0$. If $|L| \to \infty$ then $L^{-1} \to 0$ which are neutral conditions (Monin and Obukhov, 1954).

In the second campaign, the distribution of stability, wind direction and friction velocity are very similar during the day and night. In campaign 2 the mean CH_4 emission was 18% lower for southwest wind than for northeast. For stable conditions the CH_4 emission was 9% lower than with unstable conditions. The differences in CH_4 emission in either campaign for wind direction or atmospheric stability are within the standard deviation and the approximated uncertainty of the emissions.

The diurnal variations of CH_4 emission, housing temperature (average of the two compartments) which is proportional to ambient temperature and wind speed recorded at the downwind sonic, are plotted as hourly averaged boxplots (Fig. 6). Temperature and wind speed values are shown for corresponding intervals with a valid emission number. In campaign 1, highest emissions were observed between 8:30 and 13:30 and smallest emission are visible around 3:30 and 15:30. In campaign 2, emission minima occur around 5:00 and 17:00. From 6:00 to 16:00 and 18:00 to 20:00, the emissions are slightly higher than

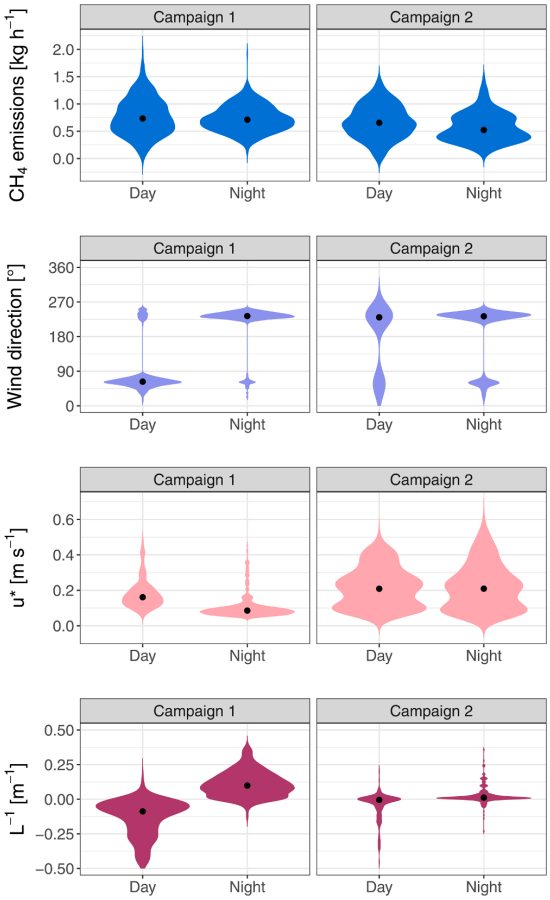

Fig. 5. Violine plots for CH_4 IDM emission (fist panel), wind direction (second panel), friction velocity u^* (third panel) and the inverse of the Obukhov length L (last panel) differentiated by day (07:30–16:30) and night (16:30–07:30) local time for both campaigns. The black dot indicates the median.

at other times. The temperature in the first campaign was lowest around 6:00 and highest at 14:30, whereas in the second campaign the temperature remained constant during the day. In the first campaign, wind speed was increasing from 10:00 onwards and decreases after 15:00 again. In the second campaign, highest wind speeds were recorded around 6:00 but the variation was high throughout the day.

3.4. Comparison with iTRM emission

Fig. 7 shows the scatterplot of CH_4 emission data, where simultaneous IDM and iTRM measurements were available. The variation in the IDM emission data is somewhat larger than that of the iTRM emissions and the correlation between the two methods is 0.02.

In campaign 1 and campaign 2, there are 324 and 90 data pairs derived from the IDM and the independent ITRM measurements, respectively, with valid simultaneous half-hourly data (Table 2). For this subset of data, the iTRM emissions exceeded the IDM results by 0.06 kg h^{-1} and 0.01 kg h^{-1} (or 8% and 1%), for the first and second campaign, respectively. The uncertainty for the average IDM emission (Section 2.2.5), in the first and second campaign is 0.14 and 0.17 kg h^{-1}, respectively. For iTRM the uncertainty is 0.09 and 0.07 kg h^{-1} for the first and second campaign, respectively (Section 2.4). The differences in average emission for the two methods are within the uncertainty of both methods.

4. Discussion

4.1. IDM emission estimates

The average emissions determined by IDM agree, within their uncertainty range of 18-24%, with the emissions simultaneously determined by the fully independent iTRM (Table 2). The iTRM that has been installed in the dairy housing earlier is considered a good candidate for a reference method (Ogink et al., 2013). In a previous validation study, with constant CH_4 dosing through critical orifices, the absolute uncertainty of the iTRM was reported to be below 10% (Mohn et al., 2018), which is lower than that of IDM. Therefore, the good agreement of both methods indicates that the IDM achieved a good accuracy for average CH_4 emissions in the present study.

The mean emissions per LU obtained in this study of 317 (±44) g LU^{-1} d^{-1} and 267 (±43) g LU^{-1} d^{-1} for the first and second campaign, respectively, lie within the range of other published studies. Poteko et al. (2020) reported an emission of 327 g LU^{-1} d^{-1} based on measured emissions from dairy cows in respiration chambers. Hempel et al. (2020) investigated two naturally ventilated dairy cattle buildings and obtained mean CH_4 emissions of 276 g LU^{-1} d^{-1} and 340 g LU^{-1} d^{-1}, respectively. Schmithausen et al. (2018) determined emissions between 225 and 307 g LU^{-1} d^{-1} for a naturally ventilated dairy cattle housing. Both studies investigated systems with loose housings and cubicles, solid or slatted floors and applied a CO_2 mass balance method. In summary, we conclude that the average IDM CH_4 emissions agree well with both, the independent iTRM measurements and the literature.

4.2. Factors influencing IDM emissions

At the measurement site, the dairy housing causes a disturbance of the wind field. The induced disturbance conflicts with the requirements of the bLS model that assumes a horizontally homogeneous wind field. To keep errors small due to such a disturbance, the sonics and GasFinders should to be placed at a minimum distance of about ten times the maximal building height downwind of the source as suggested by Harper et al. (2011). On the northeast side the minimal distance of the measuring path to the dairy housing was 120 m. With a maximum building height of 8.5 m the distance between the GasFinders and the housing was thus sufficient. On the southwest side the minimal distance was only 60 m due to the nearby main road and thus rather close to the housing (Fig. 1). Average emissions for the two wind directions and two stabilities lie within the uncertainty range of the measurements. Thus, we conclude that the measurement fetch did not cause a detectable difference in the measured CH_4 emissions. Nevertheless, there is a distinction between the measurement with southwest and northeast wind which could be due to the difference in the distance to the building (Supporting information 4).

In the first campaign, there is a distinct diurnal cycle of the housing temperature that follows the ambient temperature. For wind speed, a small diurnal cycle with higher values during the day is discernable. For the CH_4 emissions however, no diurnal cycle was detected. There is a decrease in emissions from midnight towards early morning and then slightly higher emissions until the afternoon. However, the boxplots in Fig. 6 show a large variation. In the second campaign, there is almost no variation in wind speed and housing temperature, but the emissions are slightly higher during the day. No systematic dependency of the CH_4 emissions on temperature or wind speed was detected as they are either phase shifted (first campaign) or are constant at varying CH_4 emissions (second campaign). In contrast to our study, Hempel et al. (2020) found a minimum in the CH_4 emissions for temperatures at around 10 °C to 15 °C. Poteko et al. (2020) observed a diurnal cycle in the CH_4 emissions with a peak in the evening after the second milking. Felber et al. (2015)

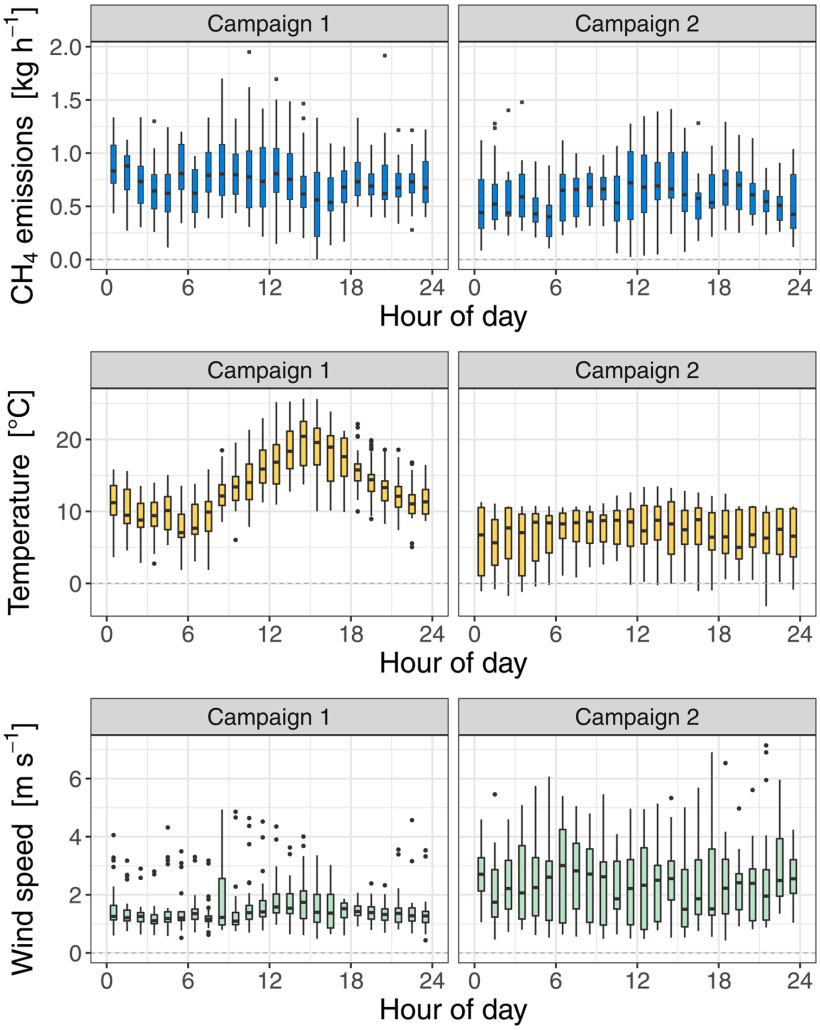

Fig. 6. Average diurnal variation of CH_4 emission (upper panel), average housing temperature of the two compartments (mid panel) and wind speed at the downwind sonic (lower panel) plotted as hourly boxplots.

observed a similar pattern where the maximum emission in the evening coincided with the most distinct grazing activity. The studies of Hammond et al. (2016) and Poteko et al. (2020) suggest that such high CH_4 emissions are associated with feeding. On the other hand, Laubach et al. (2014) and McGinn et al. (2011) observed higher emissions during day for grazing cattle. Overall, the studies provided diverse diurnal emission patterns.

Four our study, we cannot rule out that the observed variation in IDM CH_4 emission data may be mainly controlled by the temporal fluctuations (within precision levels) in the concentration measurements. The median (and respective interquartile range) of the measured concentration difference ΔC between the up- and downwind GasFinder was 0.18 ppm (0.09–0.40 ppm). For the GasFinders used in this study (all of them were also used in the study of Häni et al. (2021)), the median precision for one 30 min measurement is 0.04 ppm. This corresponds to a median uncertainty in the concentration measurements of 22%.

We conclude that the variation in the real CH_4 emission were smaller than the modulation of the IDM calculations through other influences (e.g. concentration measurements, deviations of bLS model from reality, diurnal cycle associated with feeding). This is supported by the lacking correlation between the half-hourly results of both measurement methods IDM and iTRM (Fig. 7) which could be due to uncertainty in either or both methods. For IDM, we assume the factor dominating temporal variability was the CH_4 analytics because concentrations measured downwind were close to ambient levels and thus more affected by the precision of the GasFinder analysers.

4.3. Uncertainty analysis

The uncertainty of the average IDM emissions (calculated according to Eq. 3) depends on the averaging period Δt. This relationship is plotted in Fig. 8. Instead of the absolute uncertainty, the relative uncertainty $(\varepsilon / \overline{Q})$ is used here.

The more measurement intervals are included for the calculation of the mean emission the smaller the relative uncertainty gets. We have an average data loss of 60% in this study, which is in the range of other

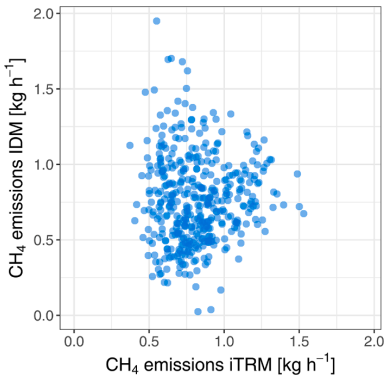

Fig. 7. Scatterplot of CH_4 30min emission data for both campaigns, where simultaneous and valid measurement data for both IDM and iTRM method are available.

Table 2
Number of valid data pairs and average CH_4 emissions and standard deviation (in parentheses) for time intervals with simultaneous IDM and iTRM measurements, specified for both campaigns.

	Campaign 1	Campaign 2
Number of valid data pairs	324	90
Average CH_4 emissions IDM [kg h^{-1}]	0.79 (0.28)	0.69 (0.31)
Average CH_4 emissions iTRM [kg h^{-1}]	0.85 (0.22)	0.70 (0.12)

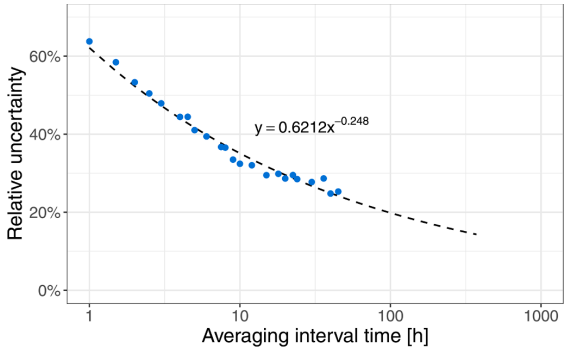

Fig. 8. Relative uncertainty of the mean emission given for different averaging intervals according to Eq. 3. The dotted line indicates the fitted power law. Note that the x-axis has a logarithmic scaling.

studies reporting between 50% and 90% periods of time with invalid data (Flesch et al., 2014; VanderZaag et al., 2014). More important, we obtained sufficient observations throughout 24 h of the day (Fig. 3). With the power function given in Fig. 8 and assuming a constant emission it is possible to calculate the minimum needed effective measuring time to reach a certain uncertainty. For e.g. 20% uncertainty this would be 96 h. Accounting for a data loss of about 60%, a measurement period of about 10 days is thus necessary. We recommend measuring beyond 10 consecutive days to obtain data under different micrometeorological conditions and to have a sufficient safety margin in case of larger data loss.

5. Conclusions

The CH_4 emissions from a small dairy housing with 40 lactating cows measured with IDM are in good agreement with the simultaneously determined iTRM emissions. The differences are within the uncertainty of either of the two methods. The emission factors per LU from this study agree well with the range of other studies. The findings suggest that the bLS model is not affected by external parameters like stability, friction velocity or temperature at this site with difficult micrometeorological conditions. Unlike other studies, no clear diurnal cycle in the CH_4 emissions was detected. However, it is possible that the different factors influencing the emission determination (wind direction, stability, feeding) cancel each other out which could induce the observed constant emissions patterns or temporal changes might be masked by the limited precision of the analysers. To disentangle these effects and identify shortcomings of any or both methods (IDM, iTRM), an optimised experimental design and extended measurements would be required. For IDM, we suggest an experiment with controlled artificial release of CH_4 well above ambient concentrations within an empty dairy housing and concentration measurements at several distances downwind of the source to determine the recovery rate at each distance under stable and unstable conditions and different u^* values.

Declaration of Competing Interest

The authors declare that they have no known competing financial interests or personal relationships that could have appeared to influence the work reported in this paper.

Acknowledgments

Funding by the Swiss Federal Office for the Environment (Contract 00.5082.P2I R254-0652) is gratefully acknowledged. We thank Markus Jocher (Climate and Agriculture Group, Agroscope, Zürich) for supporting the operation of the measurement devices and gratefully acknowledge the contribution of Michael Döring (Niels Bohr Institute, University of Copenhagen) to the manuscript. We are grateful to the support and assistance of the following persons involved in the experiment: M. Keller, M. Hatt, T. Kupferschmid (Agroscope Tänikon), S.A. Wyss (Empa Dübendorf) and the farmer of the land in the surrounding area of the experimental housing, W. Denzler.

Supplementary materials

Supplementary material associated with this article can be found, in the online version, at doi:10.1016/j.agrformet.2021.108501.

References

Bai, M., Sun, J., Denmead, O.T., Chen, D., 2017. Comparing emissions from a cattle pen as measured by two micrometeorological techniques. Environ. Pollut. 230, 584–588.
Boreal Laser Inc., 2018. GasFinder3-OP Operation Manual. Part No. NDC-200036.
Demmers, T., Phillips, V.R., Short, L.S., Burgess, L.R., Hoxey, R.P., Wathes, C.M., 2001. SE—Structure and environment: Validation of ventilation rate measurement methods and the ammonia emission from naturally ventilated dairy and beef buildings in the United Kingdom. J. Agric. Eng. Res. 79 (1), 107–116.
Federal Statistical Office, 2020. Agriculture and food: Pocket statistics 2020. Agriculture and forestry 07. Federal Statistical Office, Neuchâtel, Switzerland.
Felber, R., Münger, A., Neftel, A., Ammann, C., 2015. Eddy covariance methane flux measurements over a grazed pasture: effect of cows as moving point sources. Biogeosciences 12 (12), 3925–3940.
Flesch, T.K., Basarab, J.A., Baron, V.S., Wilson, J.D., Hu, N., Tomkins, N.W., Ohama, A.J., 2018. Methane emissions from cattle grazing under diverse conditions: an examination of field configurations appropriate for line-averaging sensors. Agric. For. Meteorol. 258, 8–17.
Flesch, T.K., Harper, L.A., Powell, J.M., Wilson, J.D., 2009. Inverse-dispersion calculation of ammonia emissions from Wisconsin dairy farms. Trans. ASABE 52 (1), 253–265.
Flesch, T.K., McGinn, S.M., Chen, D., Wilson, J.D., Desjardins, R.L., 2014. Data filtering for inverse dispersion emission calculations. Agric. For. Meteorol. 198-199, 1–6.
Flesch, T.K., Vergé, X.P.C., Desjardins, R.L., Worth, D., 2013. Methane emissions from a swine manure tank in western Canada. Can. J. Anim. Sci. 93 (1), 159–169.
Flesch, T.K., Wilson, J.D., Harper, L.A., Crenna, B.P., 2005. Estimating gas emissions from a farm with an inverse-dispersion technique. Atmos. Environ. 39 (27), 4863–4874.

Flesch, T.K., Wilson, J.D., Harper, L.A., Crenna, B.P., Sharpe, R.R., 2004. Deducing ground-to-air emissions from observed trace gas concentrations: a field trial. J. Appl. Meteorol. 43 (3), 487–502.
Flesch, T.K., Wilson, J.D., Harper, L.A., Todd, R.W., Cole, N.A., 2007. Determining ammonia emissions from a cattle feedlot with an inverse dispersion technique. Agric. For. Meteorol. 144 (1–2), 139–155.
Gao, Z., Desjardins, R.L., Flesch, T.K., 2010. Assessment of the uncertainty of using an inverse-dispersion technique to measure methane emissions from animals in a barn and in a small pen. Atmos. Environ. 44 (26), 3128–3134.
Gerber, P.J., 2013. Tackling climate change through livestock: A global assessment of emissions and mitigation opportunities. Food and Agriculture Organization of the United Nations FAO, Rome.
Gill Instruments, 2016. Technical key note: Software bug affecting 'w' wind component of the WindMaster family. Gill Instruments, Lymington, UK. http://gillinstruments.com/data/manuals/KN1509_WindMaster_WBug_info.pdf.
Hammond, K.J., Crompton, L.A., Bannink, A., Dijkstra, J., Yáñez-Ruiz, D.R., O'Kiely, P., Kebreab, E., Eugène, M.A., Yu, Z., Shingfield, K.J., Schwarm, A., Hristov, A.N., Reynolds, C.K., 2016. Review of current in vivo measurement techniques for quantifying enteric methane emission from ruminants. Anim. Feed Sci. Technol. 219, 13–30.
Häni, C., Bühler, M., Neftel, A., Ammann, C., Kupper, T., 2021. Performance of open-path GasFinder3 devices for CH_4 concentration measurements close to ambient levels. Atmos. Meas. Tech. 14 (2), 1733–1741.
Häni, C., Flechard, C., Neftel, A., Sintermann, J., Kupper, T., 2018. Accounting for field-scale dry deposition in backward Lagrangian stochastic dispersion modelling of NH_3 emissions. Atmosphere 9 (4), 146.
Harper, L.A., Denmead, O.T., Flesch, T.K., 2011. Micrometeorological techniques for measurement of enteric greenhouse gas emissions. Anim. Feed Sci. Technol. 166-167, 227–239.
Harper, L.A., Flesch, T.K., Wilson, J.D., 2010. Ammonia emissions from broiler production in the San Joaquin Valley. Poult. Sci. 89 (9), 1802–1814.
Hempel, S., Willink, D., Janke, D., Ammon, C., Amon, B., Amon, T., 2020. Methane emission characteristics of naturally ventilated cattle buildings. Sustainability 12 (10), 4314.
Kupper, T., Bonjour, C., Menzi, H., 2015. Evolution of farm and manure management and their influence on ammonia emissions from agriculture in Switzerland between 1990 and 2010. Atmos. Environ. 103, 215–221.
Laubach, J., Bai, M., Pinares-Patiño, C.S., Phillips, F.A., Naylor, T.A., Molano, G., Cárdenas Rocha, E.A., Griffith, D.W.T., 2013. Accuracy of micrometeorological techniques for detecting a change in methane emissions from a herd of cattle. Agric. For. Meteorol. 176, 50–63.
Laubach, J., Grover, S.P., Pinares-Patiño, C.S., Molano, G., 2014. A micrometeorological technique for detecting small differences in methane emissions from two groups of cattle. Atmos. Environ. 98, 599–606.
McGinn, S.M., Flesch, T.K., Crenna, B.P., Beauchemin, K.A., Coates, T., 2007. Quantifying ammonia emissions from a cattle feedlot using a dispersion model. J. Environ. Qual. 36 (6), 1585–1590.
McGinn, S.M., Flesch, T.K., Harper, L.A., Beauchemin, K.A., 2006. An approach for measuring methane emissions from whole farms. J. Environ. Qual. 35 (1), 14–20.
McGinn, S.M., Janzen, H.H., Coates, T.W., Beauchemin, K.A., Flesch, T.K., 2016. Ammonia emission from a beef cattle feedlot and its local dry deposition and re-emission. J. Environ. Qual. 45 (4), 1178–1185.
McGinn, S.M., Turner, D., Tomkins, N., Charmley, E., Bishop-Hurley, G., Chen, D., 2011. Methane emissions from grazing cattle using point-source dispersion. J. Environ. Qual. 40 (1), 22–27.
Mohn, J., Zeyer, K., Keck, M., Keller, M., Zähner, M., Poteko, J., Emmenegger, L., Schrade, S., 2018. A dual tracer ratio method for comparative emission measurements in an experimental dairy housing. Atmos. Environ. 179, 12–22.
Monin, A.S., Obukhov, A.M., 1954. Basic laws of turbulent mixing in the surface layer of the atmosphere. Contrib. Geophys. Inst. Acad. Sci. USSR 151 (163), e187.
Niu, M., Kebreab, E., Hristov, A.N., Oh, J., Arndt, C., Bannink, A., Bayat, A.R., Brito, A.F., Boland, T., Casper, D., Crompton, L.A., Dijkstra, J., Eugène, M.A., Garnsworthy, P.C., Haque, M.N., Hellwing, A.L.F., Huhtanen, P., Kreuzer, M., Kuhla, B., Lund, P., Madsen, J., Martin, C., McClelland, S.C., McGee, M., Moate, P.J., Muetzel, S., Muñoz, C., O'Kiely, P., Peiren, N., Reynolds, C.K., Schwarm, A., Shingfield, K.J., Storlien, T.M., Weisbjerg, M.R., Yáñez-Ruiz, D.R., Yu, Z., 2018. Prediction of enteric methane production, yield, and intensity in dairy cattle using an intercontinental database. Global Change Biol. 24 (8), 3368–3389.
Ogink, N., Mosquera, J., Calvet, S., Zhang, G., 2013. Methods for measuring gas emissions from naturally ventilated livestock buildings: Developments over the last decade and perspectives for improvement. Biosystems Eng. 116 (3), 297–308.
Petersen, S.O., 2018. Greenhouse gas emissions from liquid dairy manure: Prediction and mitigation. J. Dairy Sci. 101 (7), 6642–6654.
Poteko, J., Schrade, S., Zeyer, K., Mohn, J., Zaehner, M., Zeitz, J.O., Kreuzer, M., Schwarm, A., 2020. Methane emissions and milk fatty acid profiles in dairy cows fed linseed, measured at the group level in a naturally ventilated housing and individually in respiration chambers. Animals 10 (6).
Poteko, J., Zähner, M., Schrade, S., 2019. Effects of housing system, floor type and temperature on ammonia and methane emissions from dairy farming: a meta-analysis. Biosystems Eng. 182, 16–28.
Poteko, J., Zähner, M., Steiner, B., Schrade, S., 2018. Residual soiling mass after dung removal in dairy loose housings: Effect of scraping tool, floor type, dung removal frequency and season. Biosystems Eng. 170, 117–129.
Saunois, M., Stavert, A.R., Poulter, B., Bousquet, P., Canadell, J.G., Jackson, R.B., Raymond, P.A., Dlugokencky, E.J., Houweling, S., Patra, P.K., Ciais, P., Arora, V.K., Bastviken, D., Bergamaschi, P., Blake, D.R., Brailsford, G., Bruhwiler, L., Carlson, K. M., Carrol, M., Castaldi, S., Chandra, N., Crevoisier, C., Crill, P.M., Covey, K., Curry, C.L., Etiope, G., Frankenberg, C., Gedney, N., Hegglin, M.I., Höglund-Isaksson, L., Hugelius, G., Ishizawa, M., Ito, A., Janssens-Maenhout, G., Jensen, K.M., Joos, F., Kleinen, T., Krummel, P.B., Langenfelds, R.L., Laruelle, G.G., Liu, L., Machida, T., Maksyutov, S., McDonald, K.C., McNorton, J., Miller, P.A., Melton, J.R., Morino, I., Müller, J., Murguia-Flores, F., Naik, V., Niwa, Y., Noce, S., O'Doherty, S., Parker, R.J., Peng, C., Peng, S., Peters, G.P., Prigent, C., Prinn, R., Ramonet, M., Regnier, P., Riley, W.J., Rosentreter, J.A., Segers, A., Simpson, I.J., Shi, H., Smith, S. J., Steele, L.P., Thornton, B.F., Tian, H., Tohjima, Y., Tubiello, F.N., Tsuruta, A., Viovy, N., Voulgarakis, A., Weber, T.S., van Weele, M., van der Werf, G.R., Weiss, R. F., Worthy, D., Wunch, D., Yin, Y., Yoshida, Y., Zhang, W., Zhang, Z., Zhao, Y., Zheng, B., Zhu, Q., Zhu, Q., Zhuang, Q., 2020. The Global Methane Budget 2000–2017. Earth Syst. Sci. Data 12 (3), 1561–1623.
Schmithausen, A.J., Schiefler, I., Trimborn, M., Gerlach, K., Südekum, K.-H., Pries, M., Büscher, W., 2018. Quantification of methane and ammonia emissions in a naturally ventilated barn by using defined criteria to calculate emission rates. Animals 8 (5).
Schrade, S., Zeyer, K., Gygax, L., Emmenegger, L., Hartung, E., Keck, M., 2012. Ammonia emissions and emission factors of naturally ventilated dairy housing with solid floors and an outdoor exercise area in Switzerland. Atmos. Environ. 47, 183–194.
Sonderfeld, H., Bösch, H., Jeanjean, A.P.R., Riddick, S.N., Allen, G., Ars, S., Davies, S., Harris, N., Humpage, N., Leigh, R., Pitt, J., 2017. CH_4 emission estimates from an active landfill site inferred from a combined approach of CFD modelling and in situ FTIR measurements. Atmos. Meas. Tech. 10 (10), 3931–3946.
VanderZaag, A.C., Flesch, T.K., Desjardins, R.L., Baldé, H., Wright, T., 2014. Measuring methane emissions from two dairy farms: seasonal and manure-management effects. Agric. For. Meteorol. 194, 259–267.
VanderZaag, A.C., Gordon, R.J., Glass, V.M., Jamieson, R.C., 2008. Floating covers to reduce gas emissions from liquid manure storages: a review. Appl. Eng. Agric. 24 (5), 657–671.

Supporting information 1

Combining two sensors

The GasFinders on the northeast side were post-measurement combined to a single sensor to cover a larger fraction of the emission plume and to be less prone to erroneous measurements as fluctuations within one device are evened out. For each 30 min interval the weighted average according to the path length of the sensors over the concentration measurements and D_{bLS} values were taken (Eq. S1.1).

$$X_{comb} = \frac{X_{OP1} * P_{OP1} + X_{OP2} * P_{OP2}}{P_{OP1} + P_{OP2}} \quad \text{Eq. S1.1}$$

With *X* either concentration *C* or dispersion factor D_{bLS} for the corresponding device *OP*, *P* = path length, *OP1* = device 1, *OP2* = device 2 and *comb* = combined sensor.
For the intervals where only one of the devices passed the quality checks, the sensors were not combined, and the emission estimate was based on the measurement of the single sensor that passed the quality checks.

Supporting information 2

Source weighting

The dairy housing has a covered underground slurry pit which also emits CH_4. Because the emission from the slurry pit and the housing differ in their emission strength (g CH_4 m^{-2} h^{-1}) the two sources need to be weighted. This is done giving each area a prior emission based on Kupper et al. (2020) for the slurry pit and Poteko et al. (2020) for the housing (respiration chamber data).
For campaign 1, the pre assumed emissions for the housing and slurry pit are $E_{housing}$ = 0.6924 g m^{-2} h^{-1} and E_{slurry} = 0.4438 g m^{-2} h^{-1}, respectively. For the second campaign the assigned emissions are $E_{housing}$ = 0.5699 g m^{-2} h^{-1} and E_{slurry} = 0.0575 g m^{-2} h^{-1} for the housing and the slurry pit, respectively. For the slurry pit the baseline emissions for cattle from farm-scale for temperate and cold season were used with a reduction of 15% due to the solid cover (Kupper et al., 2020). With those values, the two sources were combined to a single source (Eq. S2.1) with an average *D* of:

$$D_{avg} = D_{housing} * w_{housing} + D_{slurry} * w_{slurry} \quad \text{Eq. S2.1}$$

Where the weights were calculated as

$$w_{housing} = \frac{A_{slurry} + A_{housing}}{\left(\frac{E_{slurry}}{E_{housing}} A_{slurry} + A_{housing}\right)} \quad \text{Eq. S2.2}$$

It is assumed that the iTRM method does not capture any emission from the slurry pit. Hence, to make IDM emissions comparable to iTRM, the slurry pit emissions need to be subtracted from the total IDM emissions. In a first step, it is assumed that the emission for every interval from the slurry pit varies proportional to the emission from the dairy housing. The average slurry pit emission (Q_{slurry}) for each campaign are therefore calculated by multiplying the average IDM emission (slurry pit + housing) (Q_{total}) with the share of the slurry pit (s_{slurry}) emission calculated with the individual emission strengths ($E_{housing}$ and E_{slurry}) and the area of each source ($A_{housing}$ = 1064 m^2, A_{slurry} = 140 m^2) (Eq. S2.3).

$$s_{slurry} = \frac{E_{slurry} * A_{slurry}}{E_{slurry} * A_{slurry} + E_{housing} * A_{housing}} \quad \text{Eq. S2.3}$$

The shares of the slurry pit are 7.8% and 1.3% for the first and second campaign, respectively. For the final results, we assumed a constant emission from the slurry pit. Therefore, Eq. 2 in the paper is expanded by the term ΔC_{slurry}, which is the theoretical concentration at the sensors that comes from in the first step calculated average slurry pit emission and the D_{bLS_slurry} value (Eq. S2.4).

$$\Delta C_{slurry} = D_{bLS\_slurry} * Q_{slurry} \quad \text{Eq. S2.4}$$

The emission from the dairy housing is then calculated as (Eq. S2.5):

$$Q_{housing} = \frac{C_{DW} - C_{UW} - \Delta C_{slurry}}{D_{bLS\_housing}} \quad \text{Eq. S2.5}$$

We assumed a constant emission rate for the slurry store which is not perfect as it is likely varying with temperature during the day (Kupper et al., 2020). The variation is expected to be small due to the coverage of the pits with a concrete ceiling. Overall, this simplification will not introduce a major error the emission calculation.

Supporting information 3

Wind direction filtering

Wind sectors were defined by drawing imaginary lines from one end of the sensor path to the nearer diagonal edge of the source (Figure S3.1)

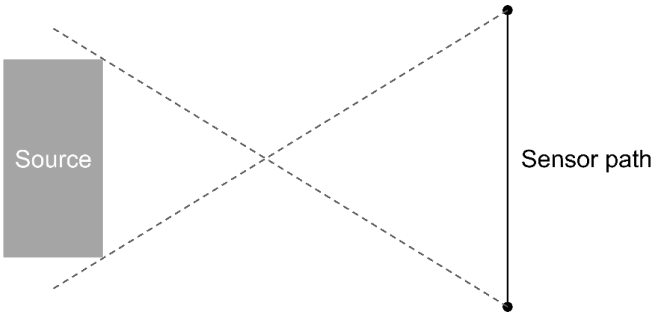

Figure S3.1 Defining wind sectors for filtering by drawing imaginary lines to the nearer diagonal edge of the source. Dots = GasFinder sensor and retroreflector, solid line = measuring path, dotted line = line for wind sector filter

Figure S3.2 shows the CH_4 emission data for the northeast and southwest side for both measuring campaigns with all filters applied as outlined in section 2.2.4 of the paper. The initial wind sectors for the northeast side had to be narrowed by 8° to eliminate the high variation of emission estimates at the edge of the chosen wind sectors. The higher emissions towards the edge of the wind sectors are most likely to the corresponding GasFinder capturing only a part of the plume. This can be a problem because the plume from the bLS model does not entirely coincide with the real emission plume. For the presented IDM emissions, the narrowed wind direction filter was used.

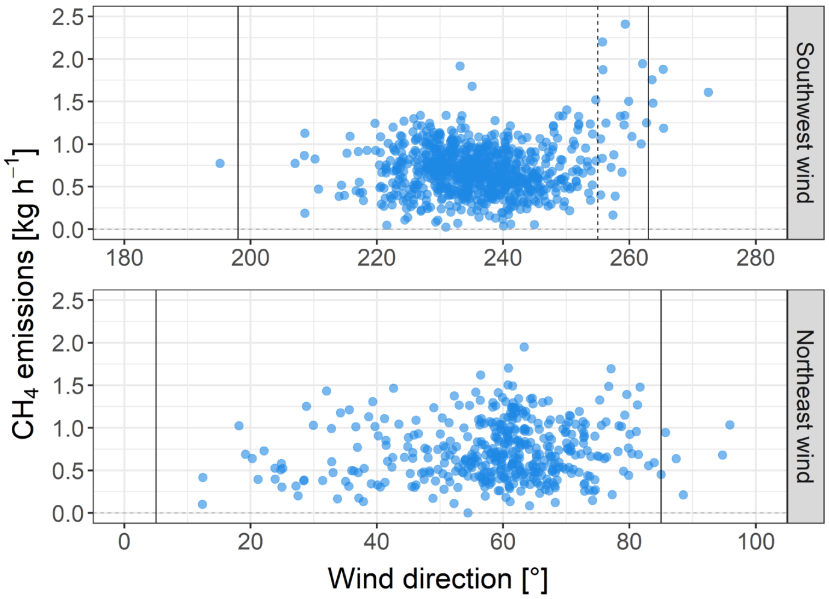

Figure S3.2 CH_4 emission flux (kg h^{-1}) plotted against wind directions. Vertical solid line indicates initial wind sector filtering. Dotted line indicates revised wind sector used for the further data processing.

Supporting information 4

A detailed overview on emission estimates differentiated by stability and wind direction is given in Table S4.1. As written in the paper, the differences are within the standard deviation and the uncertainty of the IDM.

	Campaign 1		**Campaign 2**	
	N	Emissions [kg h^{-1}]	N	Emissions [kg h^{-1}]
SW Wind	440	0.76 (0.24)	322	0.58 (0.27)
NE Wind	305	0.73 (0.34)	126	0.71 (0.31)
L > 0	438	0.73 (0.25)	301	0.6 (0.28)
L < 0	307	0.78 (0.33)	147	0.66 (0.31)

Table S4.1 Average CH_4 emission estimates in kg h-1 ±SD (in parentheses) for both campaigns separated by wind direction and stability conditions. *N* = number of valid half-hourly IDM emission intervals, *SW* = southwesterly, *NE* = northeasterly, *L* = Obukhov length, *L* > 0 = stable conditions, *L* < 0 = unstable conditions.

However, if the IDM retrieved CH_4 emissions are plotted against friction velocity (u^* values) and grouped by wind direction a small trend is discernable (Figure S4.1). For northeast wind, it seems that there is an increase in the CH_4 emissions with higher u^* values. For southwest wind no trend is discernable. One hypothesis could be that the GasFinders and the sonic on the southwest side of the housing were too close to the building and that their emission estimates show systematic (model) biases that vary with wind strength.

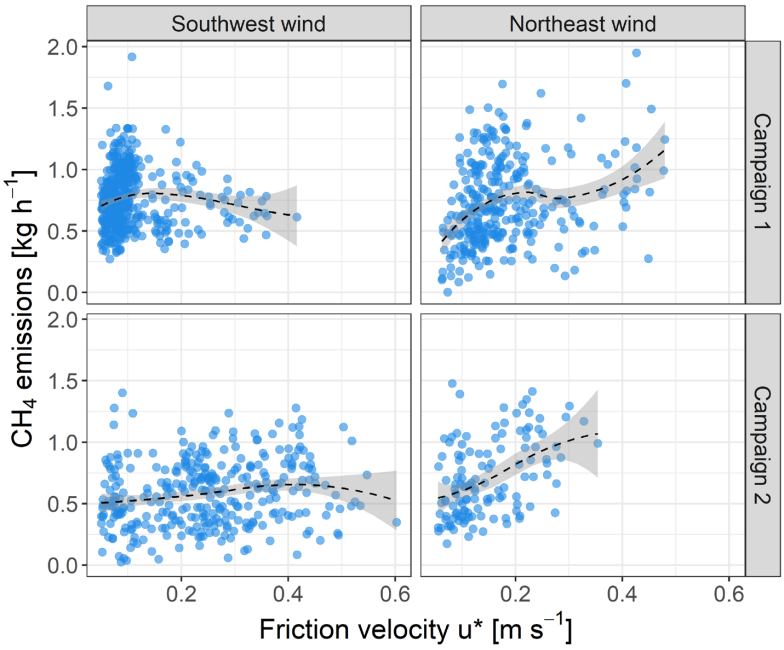

Figure S4.1 CH_4 emission estimates, determined with the IDM method, plotted against friction velocity (u*) values for different wind directions and campaigns. Left column: emissions with southwesterly wind. Right column: emissions with north easterly wind. Upper panel = Campaign 1, lower panel = campaign 2. Dashed line: local regression (loess) with standard error.

Supporting information 5

Measurement data

Measurement data of the study are provided in the additional excel file “Supporting information 5”.

References

Kupper, T., Häni, C., Neftel, A., Kincaid, C., Bühler, M., Amon, B., VanderZaag, A., 2020. Ammonia and greenhouse gas emissions from slurry storage - A review. Agriculture, Ecosystems & Environment 300, 106963.

Poteko, J., Schrade, S., Zeyer, K., Mohn, J., Zaehner, M., Zeitz, J.O., Kreuzer, M., Schwarm, A., 2020. Methane emissions and milk fatty acid profiles in dairy cows fed linseed, measured at the group level in a naturally ventilated housing and individually in respiration chambers. Animals 10 (6).

Chapter 4

Determination of methane emissions from complex source configurations with the inverse dispersion method

Marcel Bühler[1,2,3], Christoph Häni[1], Christof Ammann[4], Stefan Brönnimann[2,3], Thomas Kupper[1]

[1]School of Agricultural, Forest and Food Sciences HAFL, Bern University of Applied Sciences, Switzerland

[2]Oeschger Centre for Climate Change Research, University of Bern, Switzerland

[3]Institute of Geography, University of Bern, Switzerland

[4]Climate and Agriculture Group, Agroscope, Switzerland

Atmospheric Environment X, in revision (minor revisions)

Abstract. Wastewater treatment plants (WWTPs) and biogas plants (BGPs) are significant sources of methane (CH4), with a combined share of around 40% within the waste sector of the Swiss national emission inventory. We conducted whole-plant CH_4 emission measurements at two WWTPs and four agricultural BGPs in Switzerland using the inverse dispersion method (IDM). It was based on line-integrated concentration measurements up- and downwind of the plant in combination with a backward Lagrangian stochastic (bLS) model. Average CH_4 emissions for WWTP-1 and WWTP-2 were 0.82 kg h^{-1} and 0.61 kg h^{-1} and scaled to population equivalents (PE) they were 166 and 381 g population $equivalent^{-1}$ y^{-1}, respectively. BGPs CH_4 emissions varied between 0.39 kg h^{-1} and 2.22 kg h^{-1} whereas highest numbers were due to measurements during other than normal operating conditions. The emissions of WWTPs and BGPs comply with literature values. WWTPs in particular consist of multiple CH_4 sources with different areas and emission strengths. For the combination of the individual emission sources in the bLS modelling, three different calculation approaches with different levels of detail were applied: (i) single source over enveloping polygon area, (ii) uniform

emission density for all individual source areas, (iii) specified relative weighting of individual sources based on literature data. The most complex approach with source weighting led to a difference of up to 42 % for the two WWTPs compared to the assumption of uniform emissions. Furthermore, we demonstrate how multiple line-integrated concentration measurements can be combined and how the measurements can be corrected for nearby external CH_4 sources not belonging to the investigated plants.

Determination of methane emissions from complex source configurations with the inverse dispersion method

Marcel Bühler[1,2,3,*], Christoph Häni[1], Christof Ammann[4], Stefan Brönnimann[2,3], Thomas Kupper[1]

[1] School of Agricultural, Forest and Food Sciences HAFL, Bern University of Applied Sciences, Länggasse 85, 3052 Zollikofen, Switzerland

[2] Oeschger Centre for Climate Change Research, University of Bern, Hochschulstrasse 4, 3012 Bern, Switzerland

[3] Institute of Geography, University of Bern, Hallerstrasse 12, 3012 Bern, Switzerland

[4] Climate and Agriculture Group, Agroscope, Reckenholzstrasse 191, 8046 Zürich, Switzerland

* Correspondence: marcel.buehler@bfh.ch; Tel.: +41-31-910-29-60

Abstract

Wastewater treatment plants (WWTPs) and biogas plants (BGPs) are significant sources of methane (CH_4), with a combined share of around 40% within the waste sector of the Swiss national emission inventory. We conducted whole-plant CH_4 emission measurements at two WWTPs and four agricultural BGPs in Switzerland using the inverse dispersion method (IDM). It was based on line-integrated concentration measurements up- and downwind of the plant in combination with a backward Lagrangian stochastic (bLS) model. Average CH_4 emissions for WWTP-1 and WWTP-2 were 0.82 kg h^{-1} and 0.61 kg h^{-1} and scaled to population equivalents (PE) they were 166 and 381 g PE^{-1} y^{-1}, respectively. BGPs CH_4 emissions varied between 0.39 kg h^{-1} and 2.22 kg h^{-1} whereas highest numbers were due to measurements during other than normal operating conditions. The emissions of WWTPs and BGPs comply with literature values. WWTPs in particular consist of multiple CH_4 sources with different areas and emission strengths. For the combination of the individual emission sources in the bLS modelling, three different calculation approaches with different levels of detail were applied: (i) single source over enveloping polygon area, (ii) uniform emission density for all individual source areas, (iii) specified relative weighting of individual sources based on literature

data. The most complex approach with source weighting led to a difference of up to 42% for the two WWTPs compared to the assumption of uniform emissions. Furthermore, we demonstrate how multiple line-integrated concentration measurements can be combined and how the measurements can be corrected for nearby external CH_4 sources not belonging to the investigated plants.

Keywords: *Wastewater treatment plant, Biogas plant, GasFinder, Open-path tunable diode laser, Source combination, Backward Lagrangian stochastic*

1. Introduction

Methane (CH_4) is a relevant greenhouse gas (GHG) with a global warming potential 28 times greater than that of carbon dioxide (CO_2). Anthropogenic CH_4 emissions of which agriculture (ruminants and rice paddies), fossil fuel extraction and the emissions from landfills and waste are the principal sources and account for 50% to 65% of total CH_4 emissions (Stocker et al. 2013). Within the framework of the revised CO_2 Act and the Kyoto Protocol, Switzerland is obliged to regularly report on the current status of the national emissions of GHGs including CH_4 with regard to the specified reduction targets (FOEN 2021a). After agriculture, the waste sector is the second most important source of CH_4 emissions in Switzerland. Wastewater treatment plants (WWTPs) and biogas plants (BGPs) are significant sources of CH_4 with a combined share of around 40% within the waste sector (as of 2019) (FOEN 2021b). WWTPs comprise a mechanical, biological and chemical stage for wastewater treatment (Gujer 2007) denoted as water line. Solids removed from the water line during treatment are directed to the sludge line where dewatering, anaerobic digestion and storage of the sludge occur. In WWTPs, CH_4 is mainly produced in the sludge line and in the energy line i.e. combustion of biogas in the combined heat and power (CHP) unit and biogas storage (Daelman et al. 2012; Delre et al. 2017). Besides WWTPs, the sewer system is also a significant source of CH_4 within urban water management (Eijo-Río et al. 2015; Mannina et al. 2018). Agricultural biogas plants (BGPs) process manure from livestock production, organic residues from food processing, landscape and garden maintenance and catering waste. As for WWTPs, the main sources of CH_4 from BGPs are anaerobic digestion, storage of feedstock material and digestates and the combustion of biogas. The organic waste is directly fed into an anaerobic digester and, in contrast to most WWTPs, there is often a post digester and often no balloon for biogas storage.

Measurements of CH_4 emissions from the whole WWTPs based on direct measurements at exhaust pipes or indirectly by means of the tracer gas dispersion method are available. However, the former is based on measuring the flow rates and the concentration of air from exhaust pipes from plants where the parts of a WWTP producing odours are covered, ventilated and the exhaust air undergoes a treatment. Still, not all parts of WWTPs are necessarily covered and thus some emissions of a WWTP are not included in the measurements (Daelman et al. 2012; STOWA 2010). For the investigations with the tracer gas dispersion method mobile analysers were used to obtain a cross-section of the downwind plume. The analysers were mounted to a car. This implies relatively short measurement periods, i.e. mostly ≤ 5 measurement campaigns over ca. 1 to ≤ 6 h (Yoshida et al.

2014; Delre et al. 2017; Samuelsson et al. 2018). Thus, whole WWTP emission measurements including all sources over a longer time period are lacking.

Measurements with the inverse dispersion method (IDM) have been successfully conducted to estimate emissions from stationary sources such as whole farms (Bühler et al. 2021; VanderZaag et al. 2014), manure stores (Flesch et al. 2013) and BGPs (Flesch et al. 2011; Reinelt et al. 2017). These studies have highlighted the flexibility in the application of IDM measurements of various sources. Thus, the IDM is a promising option to conduct whole plant emission measurements of WWTPs over a period of several weeks.

In this study, we conducted CH_4 emissions measurements with the IDM deploying line integrating CH_4 measurements and a bLS (backward Lagrangian Stochastic) model at two WWTPs and four agricultural BGPs in Switzerland. They all represent source configurations of greater complexity because they consist of multiple spatially distributed sources, and/or the measurements were complicated by the influence of other nearby CH_4 sources that needed to be corrected for. We investigated the effect of the complex source distribution and associated uncertainties on the quantification of the total CH_4 emission of the whole plant (WWTP or BGP). For this purpose, different approaches for combining individual sources were compared. It is hypothesised that with an optimised experimental setup, the effect of the distributed multiple sources within the plant is small and that neighbouring external sources can be separated from the emission of the investigated plant.

2. Material and Methodology

2.1 Experimental sites and periods

Measurements were conducted at the two WWTPs and at four agricultural BGPs in Switzerland.

2.1.1 Wastewater treatment plants

WWTP-1 (Table 1, Figure 1A) is located in a rather flat topography. The only major increase in elevation is a mound from the road crossing the train line and the motorway, situated about 110 m southwest of the WWTP-1. Between the WWTP-1 and the mound there were 11 heifers grazing. Along the river northeast of the WWTP-1, trees are growing. 300 m northeast of the WWTP-1 is a small settlement with several barns housing cattle (138 heads in total). Inside the WWTP-1 area, there is an open storage for road-sweepings covered by a roof. The WWTP-2 is located in a valley

with approximately south-north direction. In the prevailing wind directions at WWTP-2, there are no major obstacles or elevations outside the WWTP area that could potentially influence the turbulence. West of the WWTP-2 along the river are trees and 160 m north of the WWTP-2 is a small barn with 29 sheep (Figure 1B).

WWTP-1 consists of a conventional activated sludge treatment with complete nitrification and denitrification with open sludge storage tanks. The population equivalent (PE) of WWTP-1 during the measurements was 43,534. WWTP-2 consists of a sequencing batch reactor (SBR) system with complete nitrification and denitrification with open sludge storage tanks. The population equivalent of WWTP-2 during the campaigns was 14,071. For both WWTPs, the sludge is regularly evacuated and transported to a larger WWTP for further treatment and disposal. For both WWTPs the produced biogas in the digester is used in an onsite CHP unit and part of the heat is used to heat the digester. Further information on the WWTPs is given in Table 1 and the Supporting information 1, section 1. Measurements were conducted between 23 September 2019 and 14 October 2019 at WWTP-1 and between 6 May 2020 and 20 May 2020 at WWTP-2.

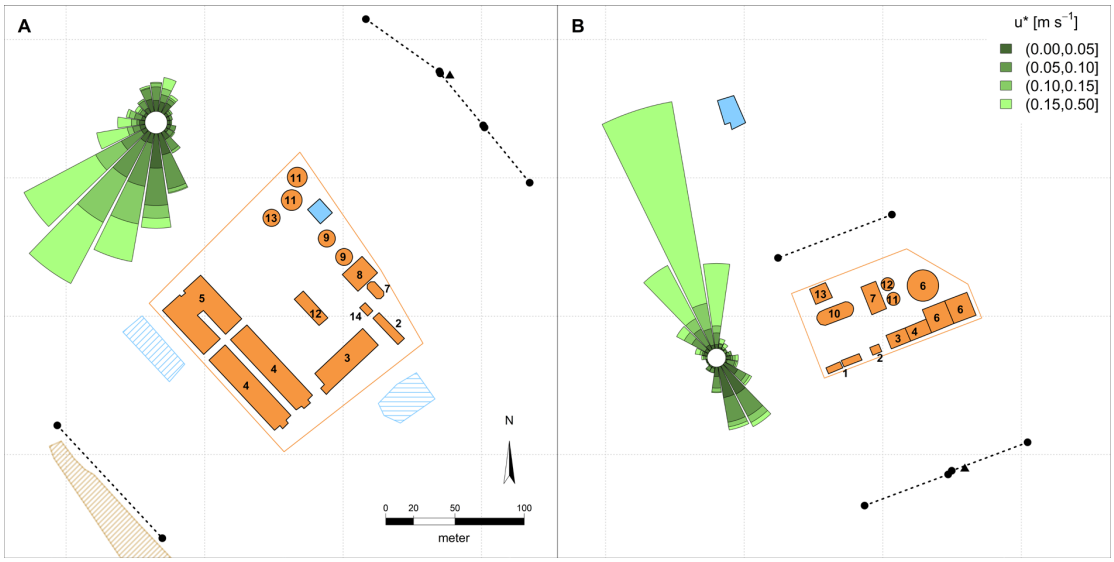

Figure 1 Schematic overview of the two WWTPs with a wind rose. A = WWTP-1, B = WWTP-2. The wind rose indicates the frequency of occurrence of wind directions and the friction velocity u* in each wind direction sector. Black solid circles mark positions of GasFinders with the dashed line representing the measuring path. Black triangles indicate the position of the sonic anemometers. Orange filled polygons are the sources within the WWTPs. The name for the numbers indicating the different sources are given in Table 4. The orange line surrounding the sources indicate the whole WWTP area. Blue are the external sources not belonging to the WWTP. Filled blue polygons are buildings, the diagonal blue hatched polygon indicates the resting place for the cattle and the horizontal blue hatched polygon is a pond. The brown hatched polygon is a mound with increasing height towards southeast.

		WWTP-1	WWTP-2
Name		Moossee-Urtenenbach	Gürbetal
Geographical coordinates		47.05572° N 7.53964° E	46.84409° N 7.50276° E
Total WWTP area [m^2]		21,803	7,354
Population equivalents		43,534	14,071
Connected inhabitants		33,126	14,365
Total digester volume [m^3]		2,200	1,400
Gas production during MC [$m^3\ d^{-1}$]		1,261	672
Sludge storage tanks (uncovered)	Total volume [m^3]	1,960	400
	Used volume during MC [m^3]	632	93
	Surface [m^2]	331	64

Table 1 Operating data and characteristics of the sludge line and energy line as major source of CH_4 for WWTP-1 and WWTP-2. MC: measuring campaign. The total WWTP area corresponds to the orange outlined polygon in Figure 1.

2.1.2 Biogas plants

Measurements were conducted at four different agricultural BGPs. A schematic overview of each BGP is given in Figure 2. The agricultural BGPs have at least 80% of dry matter input as manure and organic residues of agricultural origin. The remaining amount is organic waste from non-agricultural sources to increase gas production. BGP-1, BGP-3 and BGP-4 have a non-airtight digestate store, while the storage tank of BGP-2 is airtight (Table 2). At all BGPs, there were livestock animal housings in the close vicinity. At each BGP, the biogas is incinerated in an onsite CHP unit to produce electricity and heat. The heat is used to heat the digester and other purposes such as heating of houses or drying of agricultural goods. Biogas upgrading and injecting the biogas into a gas distribution grid did not occur at the four sites.

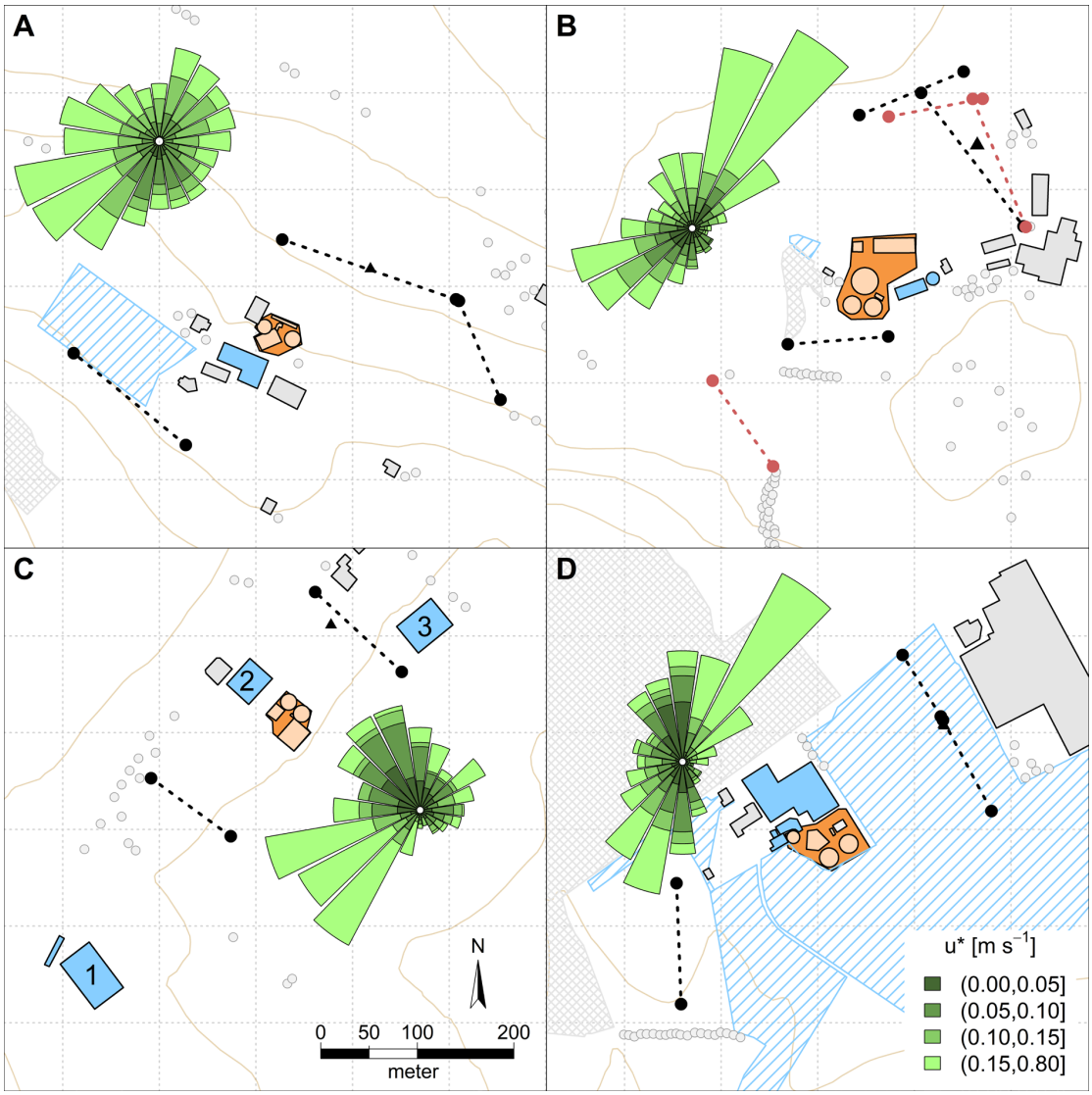

Figure 2 Schematic overview of BGPs with wind roses. A) BGP-1, B) BGP-2, C) BGP-3, D) BGP-4. The wind rose indicates the frequency of occurrence of wind directions and the friction velocity u* in each wind direction sector. For BGP-1 and BGP2 the wind data from both measuring campaigns are plotted. Black solid circled mark positions of GasFinders with the dashed line representing the measuring path. For BGP-2 the positions of the GasFinders for the second campaign which differed substantially from those of campaigns one, are plotted in red. Black triangles indicate the position of the sonic anemometers. The orange filled polygon is the area of the BGPs and used in the bLS model calculations. In blue, external sources not belonging to the BGPs are shown. Filled blue polygons are livestock buildings or slurry stores. Diagonal hatched polygons are pastures with grazing cattle or in case of BGP-2 the resting place of the cattle within the pasture area. 10 m contour lines are denoted as brown solid lines. Grey crosshatched polygons indicate forest areas. Grey circles are trees. Grey polygons with a black outline are buildings not emitting any CH_4.

BGP	Power size	Digestate storage	BGP area [m²]
BGP-1	small	covered	1,525
BGP-2	large	covered gastight	4,924
BGP-3	medium	covered	1,713
BGP-4	large	uncovered	3,211

Table 2 General characteristics of the BGP operating data. Power size according to energy production. Small: < 1000 MhW, medium: 1000 – 2000 MWh, large: > 2000 MWh. The BGP area corresponds to the filled orange polygon in Figure 2.

BGP-1 is located on a slope facing northeast. The average inclination of the slope is about 9%. Southwest of the farm on top of the hill is a small forest. BGP-1 belongs to a farm with dairy cows and heifers. At this site, CH_4 originating from ruminants can represent a source of CH_4 that is in a similar order of magnitude as that of the BGP. Next to the farm are residential buildings and farm buildings. During the second campaign (BGP-1.2) the dairy cows and heifers were occasionally grazing on the field northwest of the barn (Figure 2A). Measurements at BGP-1 were conducted from 21 February 2018 until 27 April 2018 (BGP-1.1) and from 30 May 2019 until 19 June 2019 (BGP-1.2). During the first period, 38 dairy cows and 17 heifers were present and during the second period 28 dairy cows and 16 heifers.

BGP-2 is located in a rather hilly area. However, the elevation differences in a radius of 250 m around the BGP are less than 10 m. Next to BGP-2 is a fattening pig barn and, adjacent to it, a circular slurry tank covered with a tent structure. Northwest of the BGP, there were non-lactating cows and heifers grazing. In Figure 2B, only the area within the pasture is denoted, where the animals were resting. Measurements were conducted from 7 June 2018 until 23 July 2018 (BGP-2.1) and 1 July 2019 until 19 July 2019 (BGP-2.2). During both campaign, there were 380 fattening pigs inside the barn. In the first campaign, 8 non-lactating dairy cows and 8 heifers were grazing and in the second campaign there were 5 non-lactating dairy cows grazing.

BGP-3 is in a valley on a southeast facing slope with an inclination of about 5%. Northwest of the BGP-3 was a fattening pig (480) farm (polygon 2 in Figure 2C), 300 m southwest was a farm with 59 dairy cows and 33 heifers (polygon 1) and 130 m northeast of the BGP-3 is a barn with 36 dairy cows, 6 non-lactating dairy cows and 3 heifers (polygon 3). Measurements were conducted between 2 December 2019 and 18 December 2019.

BGP-4 is located on a plain. But directly south of the BGP-4, there is a slope with an average inclination of about 7% facing southwest. Northeast of the BGP, a forest is situated. The farm

belonging to the BGP-4 has 91 dairy cows and 46 heifers that were either in the barn or grazing on the pastures around the BGP. Measurements were conducted from 10 August 2018 until 11 September 2018.

2.2 Measurement setup

2.2.1 Methane concentration measurements

CH_4 concentration measurements at all sites were conducted with GasFinder3-OP (Boreal Laser Inc., Edmonton, Canada), which are line-integrated tunable diode laser spectrometers. As retroreflectors either seven (BGP-1.1 BGP-2.1, BGP-4) or twelve (WWTP-1, WWTP-2, BGP-1.2, BGP-2.2, BGP-3) corner cubes were used. To reduce data loss due to misalignment of the laser beam with the retroreflectors, the tripods of the GasFinder sensors and retroreflectors were fixed to the ground by a clamping set and a base screw from 2019 onwards (Supporting information 1, section 3). The measured concentration was adjusted for local air temperature and pressure, using device specific relationships determined by factory calibration. The 0.3 - 1 Hz measured concentrations were averaged to 30 min periods, whereby periods with a data coverage lower than 75% (22.5 min) were excluded.

The GasFinders output concentrations have a bias, which needs to be corrected (Häni et al. 2021). Therefore, an offset and span correction of the individual concentration measurements must be done. This was either achieved with an intercomparison of the utilised GasFinders before or after the campaign by placing the GasFinders in parallel or/and by using wind sectors during the campaigns for which all GasFinders were exposed to the same background concentration (Supporting information 1, section 3). The uncertainty of the utilised GasFinder ranges from 2.1 to 10.6 ppm-m (Häni et al. 2021).

2.2.2 Positioning of GasFinders

Harper et al. (2011) recommend placing the GasFinder at least ten times the measuring height of the source. In our case this corresponds to a concentration fetch of 100 - 150 m. In Switzerland, southwest wind prevails during the day. During the night, there is mostly wind from northeast and often too low wind speeds for measurements (section 2.2.3). Thus, we generally planned the measurements for only southwesterly winds except for BGP-2.2, where we projected the measurements with two prevailing wind directions. The pathlengths of the downwind sensors and the minimal distance between the source and the closest downwind sensor are given in Table 3.

Site	Location of downwind sensor	Downwind path length [m]	minimal distance to source [m]
WWTP-1	Northeast side	65, 49, 52	106
WWTP-2	South side	64, 59	97
BGP-1.1*	Northeast side	145, 125	73
BGP-1.2	Northeast side	190, 111	73
BGP-2.1	Northeast side	125, 176	93
BGP-2.2	Northeast and southwest side	99, 143, 109**	107, 146**
BGP-3	Northeast side	122	93
BGP-4	Northeast side	75, 107	127

*The pathlength of the GasFinder in the north was extended towards west and the pathlength of the GasFinder in the east was reduced compared to BGP-1.1. In Figure 2A the setting of BGP-1.2 is shown.

**Sensor on the southwest side of BGP-2.2 measuring downwind concentration with northeasterly winds

Table 3 Path lengths and minimal distance between any source and the measuring path for all sites.

2.2.3 Turbulence measurements and data filtering

The turbulence characteristics were recorded with sonic anemometers (Gill Windmaster, Gill Instrument Ltd., Lymington, UK) and the data were corrected for a Gill software bug affecting the magnitude of the vertical wind component (Gill Instruments 2016). As wind vector rotation a two-axis coordinate rotation was used. The 10 Hz data were averaged to 30 min periods.

The measuring sites were located in landscapes with rather complex topography that does not fulfil the idealised assumptions (horizontal, homogeneous and flat terrain) of the Monin-Obukhov similarity theory (MOST). Therefore, the bLS model output was filtered to avoid unrealistic and error-prone emission results. For each site, an individual quality filtering was applied. Filters were used for friction velocity *(u*)*, the standard deviation of the along wind divided by *u* (σ_u/u*)*, the standard deviation of the crosswind divided by u* (σ_v/u*), the Kolmogorov constant of the Lagrangian structure function (*C0*), the Obukohv length (L), the roughness length z_0, the number of touchdowns within the source area, the dispersion factor *D* and a minimal concentration difference ΔC between the upwind (background) and the downwind concentration. The applied quality filtering for each site is given in the Supporting information 1, section 2.

2.3 bLS modelling and post-calculations

2.3.1 bLS model calculations

The inverse dispersion method (IDM) is a micrometeorological method that combines measurements of the turbulence parameters that are used in a dispersion model with gas concentration measurements up- and downwind of the spatially confined source.

$$Q = \frac{C_{DW} - C_{UW}}{D} \cdot A \qquad \text{Eq. 1}$$

Q is the emission of the source (standard SI units kg s^{-1}), C_{UW} and C_{DW} the upwind (background) and downwind concentration (kg m^{-3}) and D the dispersion factor (s m^{-1}) depending on the geometrical configuration of source and sensor as well as on the micrometeorological conditions. To gain emissions in kg s^{-1} the calculations have to be multiplied by the area A (units m^{-2}) of the source.

As dispersion model a backward Lagrangian stochastic model (bLS) described in Flesch et al. (2004) was used to simulate the dispersion factor D (Eq. 1) for each individual source and each line sensor based on the actual turbulence measurements and the source-sensor geometry. The line-integrating open-path concentration measurements were approximated by a series of point sensors with a 1 m spacing along the path length. For each of these point sensors and each emission interval, 50,000 – 250,000 backward trajectories were calculated and analysed for touchdowns within the source area. The simulations were done with the R package bLSmodelR (Häni et al. 2018), available at https://github.com/ChHaeni/bLSmodelR.

2.3.2 Combining multiple sensors

Often, there was more than one GasFinder used at the downwind side of the WWTPs and BGPs. If two or more GasFinders were used on one side, these GasFinders were post-measurement combined to a single sensor to cover a larger fraction of the emission plume and to be less prone to erroneous measurements as fluctuations within one device are evened out. For each 30 min interval, the weighted average according to the path length of the sensors over the concentration measurements and D values were taken (Eq. 2).

$$X_{comb} = \frac{\sum_i^N X_i * P_i}{\sum_i^N P_i} \qquad \text{Eq. 2}$$

With X either concentration C or dispersion factor D for the corresponding device, P = path length, *comb* = combined sensor. For the number of touchdowns within a source the numbers were

summed up. GasFinders that did not measure a valid CH_4 concentration were ignored and thus not combined with the remaining GasFinder(s).

2.3.3 Combining multiple sources

If the source (e.g. WWTP) consists of multiple sources different levels of detail on how to calculate the total emission are possible. In this study we used three approaches.

- ESP: Emissions with a single polygon. For this approach the WWTP is treated as a single polygon source that covers all individual sources.
- EHD: Emissions with homogeneous emission densities. For this approach, it is assumed that the individual source areas have equal emission densities (i.e. the same emission per area).
- EWS: Emissions with weighted sources. For this approach, the individual source areas have specified relative emissions.

The different approaches are explained with the example of WWTPs. ESP corresponds to the orange outlined polygon in Figure 1 and to calculate the emissions Eq. 1 is used. The approaches EHD and EWS are calculated as follow:

Each emission of an individual source Q_i within the WWTP contributes to the total emission Q_{tot} of the WWTP (Eq. 3):

$$Q_{tot} = \sum_{i=1}^{N} Q_i \qquad \text{Eq. 3}$$

We assume that the relative emission strengths w_i to a reference source Q_{ref}, which is a source within the WWTP, are known (Eq. 4):

$$Q_i = Q_{ref} \cdot w_i \qquad \text{Eq. 4}$$

With the values for w_i and for the areas A_i of the individual sources, the total emission of the WWTP can be calculated using Eq. 5:

$$Q_{tot} = \frac{\Delta C_{tot}}{\sum_{i=1}^{N} \left(\frac{w_i \cdot D_i}{A_i}\right)} \cdot \sum_{i=1}^{N} w_i \qquad \text{Eq. 5}$$

The full derivation of Q_{tot} is given in Annex A. Note, that the approaches EHD and EWS differ only in the determination of w_i. The w_i and A_i to calculate Q_{tot} with the EHD and EWS approaches are given in Table 4.

The ESP approach was used for the BGPs, because the components of the BGPs (storage, digester, CHP, etc) are positioned close to each other and the total extension of the plants is relatively small (Figure 2). This was not the case for the WWTPs where the total plant area and the distance between

the individual sources is larger. Within a WWTP, the individual sources differ in emission density, e.g. the emissions from the sludge storage tanks are expected to be substantially higher per area than those from the secondary settlers. Thus, the use of specified relative emissions is a more adequate solution. Therefore, for the WWTPs the EWS approach was used to calculate emissions. Nevertheless, emissions with the ESP and EHD approach were also calculated for the WWTPs and compared with the results based on the EWS approach.

To calculate the w_i for the EWS, literature data were used. Depending on the source, the emissions from the literature data were scaled to the corresponding WWTP with population equivalent (PE) or with the area. As reference source the sludge storage tanks were used. The used literature data for the specified emissions are given in the Supporting information 1, section 1.

No	Source	Area [m²]		w_i EHD		w_i EWS	
		WWTP-1	WWTP-2	WWTP-1	WWTP-2	WWTP-1	WWTP-2
1	Inlet	NA	123	NA	1.8	NA	0.0
2	Sand trap	163	41	0.5	0.6	0.5	0.8
3	Primary clarifier	808	156	2.4	2.2	0.3	0.3
4	Activated sludge tanks	2258	171	6.7	2.5	0.2	0.3
5	Secondary clarifier	1501	NA	4.5	NA	0.1	NA
6	SBR	NA	1017	NA	14.7	NA	0.2
7	Thickener for primary sludge	92	246	0.3	3.5	0.2	0.3
8	Overflow sludge	320	NA	1.0	NA	0.0	NA
9	Digester	236	NA	0.7	NA	0.1	NA
10	Digester + CHP unit	NA	274	NA	4.0	NA	3.1
11	**Sludge storage tanks**	**336**	**69**	**1.0**	**1.0**	**1.0**	**1.0**
12	Supernatants	226	69	0.7	1.0	0.1	0.5
13	Balloon for biogas storage	120	151	0.4	2.2	0.0	0.2
14	CHP unit	44	NA	0.1	NA	1.0	NA

Table 4 Data used for combining multiple sources with the approaches EHD and EWS for the two WWTPs. The number given in the first column indicates the location of the source in Figure 1. w_i= relative emission ratio in relation to sludge storage tanks used in Eq. 5. NA = This source does not exist on the corresponding WWTP.

For the WWTPs a simple sensitivity analysis of the EWS approach was done. For this purpose, the w_i of one individual source was multiplied or divided by a factor of 4, while the other w_i retained the original value. The resulting emission was then compared to the original WWTP emission. For the analysis, we used a factor of 4 because the specified emissions from the literature data are on

average about four times larger and four times smaller than the minimum and maximum value, respectively.

2.3.4 Treating external sources

At each site, CH_4 sources occurred in close vicinity not belonging to the WWTPs or BGPs. This is a problem if the influence of external source's CH_4 emissions on the up- and downwind concentration measurements differ. These emissions need to be corrected for in the emission calculation for the WWTPs and BGPs. The external sources were mostly emissions from livestock barns or grazing cattle. This issue is illustrated for the example of BGP-3 (Figure 2C). A few meters northwest of BGP-3, there is an animal housing with fattening pigs (polygon 2 in Figure 2C), 300 m southwest (1) and 130 m northeast (3) of the BGP are cattle housings. The emissions from the external sources (1, 2, 3) are confounding the concentration measurements and thus alter the determined emission of the BGP. The bLS model simulations included (besides the BGP source polygon) also calculations for all external sources. For each GasFinder measuring path (upwind and downwind), the dispersion factor $D_{external\_i}$ was available. Instead of calculating the BGP emission directly with the measured concentration difference (Eq. 1), the partial effect of the external sources ($Q_{external\_i}$) on the measured concentrations was simulated (Eq. 6).

$$\Delta C_{external\_i} = D_{external\_i} \cdot \frac{Q_{external\_i}}{A_{external\_i}} \qquad \text{Eq. 6}$$

The emission from the BGP was then calculated as (Eq. 7):

$$Q_{BGP} = \frac{\left(C_{DW} - \sum \Delta C_{DW\_external\_i}\right) - \left(C_{UW} - \sum \Delta C_{UW\_external\_i}\right)}{D} \cdot A_{BGP} \qquad \text{Eq. 7}$$

Frequently, it was not possible to measure the emissions of the external sources with IDM as they were too close to the target source or for other reason. In this case, the emissions of the external sources needed to be assigned based on literature values. Emissions from enteric fermentation of pigs are based on the national inventory values and for cattle on a model which considers age and energy corrected milk yield (FOEN 2021b). Emissions factors for manure stores are based on Kupper et al. (2020). These assigned emissions my differ from the gas release occurring in reality and thus induce an uncertainty in the emission in the source of interest. We assumed a general uncertainty of the of external CH_4 emissions, respectively their $\Delta C_{external}$ values of 20%.

For grazing cattle, we used two different approaches to define the source polygon in the bLS model. If the cattle had limited time access to the pasture, we used the entire pasture as source polygon (BGP-1.2 and BGP-4). However, if the animals were 24 h a day outside over a period of several days,

we used the area on which they usually rested as source polygon only. This is supported by Kilgour (2012) that found that cattle spends about one third of their activities with grazing if they are all day on the pasture and most of the remaining time with laying (resting and ruminating).

3. Results

3.1 Emissions from wastewater treatment plants

3.1.1 Overview on emissions

There were 398 and 280 valid half-hourly emission values for WWTP-1 and WWTP-2, respectively. This corresponds to an average data loss of 50% and 53% for WWTP-1 and WWTP-2, respectively, due to quality filtering or GasFinder failure. For both WWTPs, the data loss was two to three times larger during the night than during the day (Figure 3).

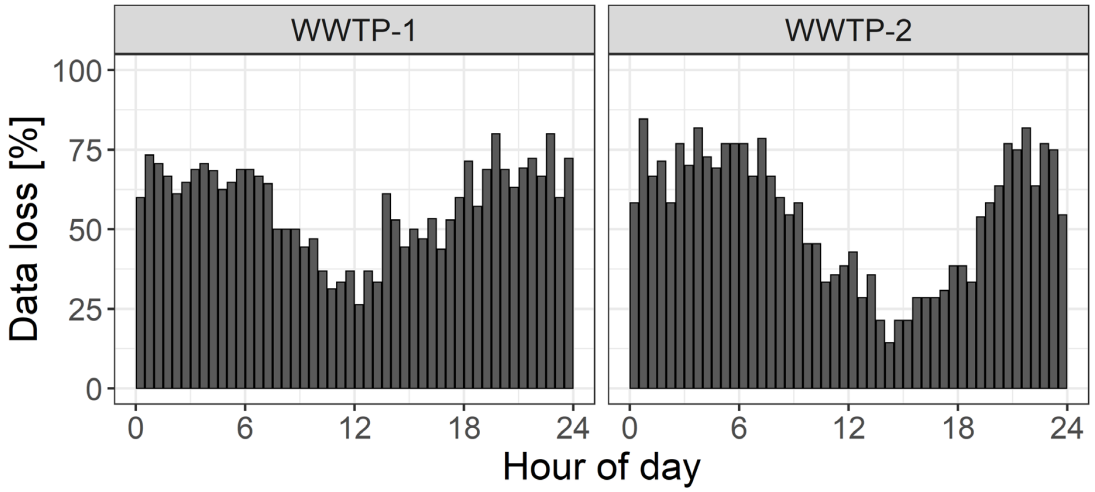

Figure 3 Proportion of data loss of IDM emission intervals after data filtering given as diurnal cycles for the two WWTPs. Higher bar means higher data loss.

As the number of valid data was not evenly spread over the course of the day and there might be a diurnal pattern in the emissions, daily averaged emissions were built (Figure 4). The daily averaged CH_4 emissions ± standard deviation (with the EWS approach) were 0.82 ± 0.15 kg h^{-1} and 0.61 ± 0.08 kg h^{-1}, for WWTP-1 and WWTP-2, respectively. The emissions scaled by population equivalent (PE) were 166 ± 31g PE^{-1} y^{-1} and 381 ± 17 g PE^{-1} y^{-1} for WWTP-1 and WWTP-2, respectively. The CH_4 emission scaled by chemical oxygen demand (COD) for WWTP-1 was 1.9 g m^{-3} of the inflow or 0.7% of COD. For WWTP-2, it was 4.0 g m^{-3} of the inflow or 1.5% of COD.

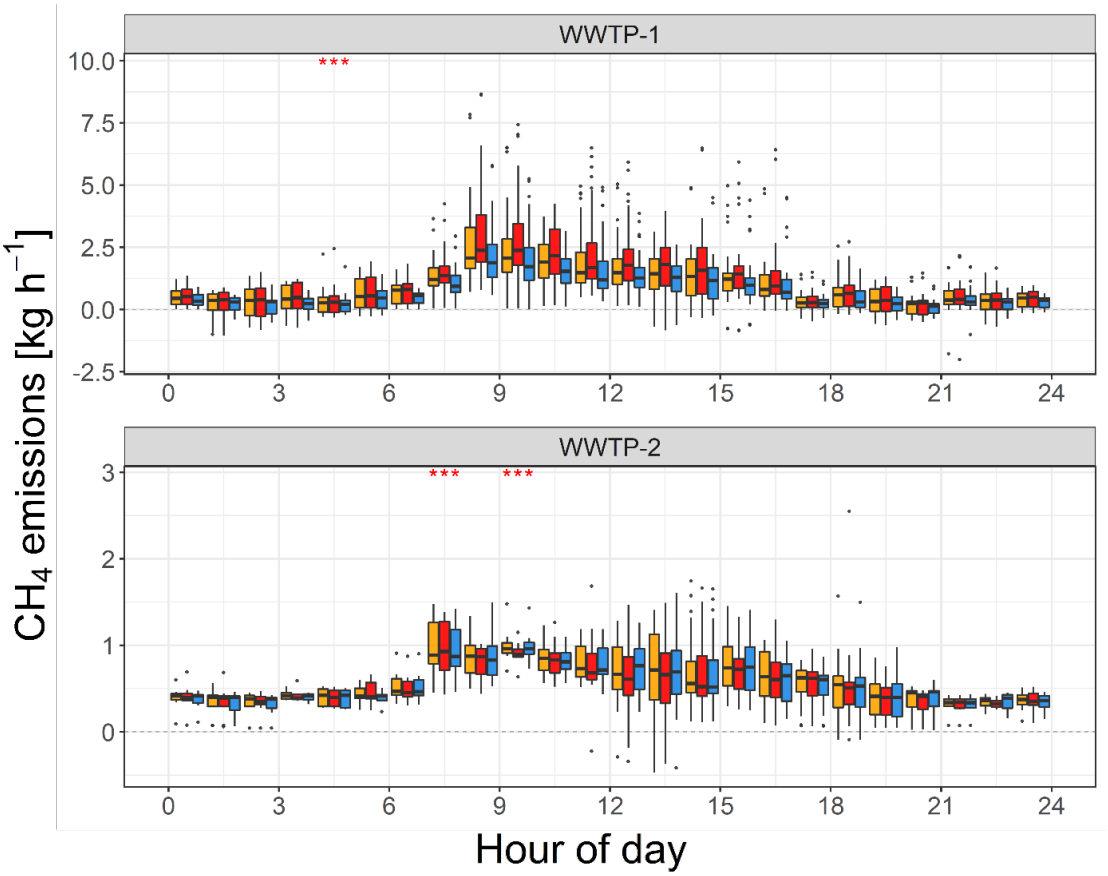

Figure 4 Diurnal cycle of CH_4 emissions calculated with three different approaches of the two WWTPs plotted as boxplot. ESP (orange), EHD (red) and EWS (blue). The red asterisks indicate outliers that are above 10 kg h^{-1} and 3 kg h^{-1} for WWTP-1 and WWTP-2, respectively. For WWTP-1 there are two outliers per asterisks. ESP (13.58 kg h^{-1} and 14.87 kg h^{-1}), EHD (14.48 kg h^{-1} and 16.24 kg h^{-1}), EWS (12.69 kg h^{-1} and 13.78 kg h^{-1}). For WWTP-2 there is one outlier per asterisks. In chronological order: ESP (6.63 kg h^{-1} and 5.32 kg h^{-1}), EHD (6.54 kg h^{-1} and 5.31 kg h^{-1}), EWS (6.35 kg h^{-1} and 5.04 kg h^{-1}).

Both WWTPs showed a similar emission pattern with lower emissions during the night, highest emission in the morning around 8:00 and then decreasing emission until late afternoon (Figure 4). Measurement data can be found in Supporting information 2.

3.1.2 Combining multiple sources

For both WWTPs the emissions with all three approaches according to section 2.3.3 were calculated. For the ESP approach, the daily averaged emissions for WWTP-1 and WWTP-2 would be 1.006 kg h^{-1} and 0.624 kg h^{-1}, respectively or 202 g PE^{-1} y^{-1} and 388 g PE^{-1} y^{-1}, respectively. For the EHD approach, the daily averaged emissions for WWTP-1 and WWTP-2 would be 1.173 kg h^{-1} and 0.602 kg h^{-1},

respectively or 236 g PE^{-1} y^{-1} and 375 g PE^{-1} y^{-1}, respectively. The diurnal cycles of the two methods are also given in Figure 4.

The simple sensitivity analysis showed that for WWTP-1 the sources that are most sensitive to the total WWTP emission are the sand trap and the sludge storage tanks. The activated sludge tanks and the primary clarifier have a smaller sensitivity on the total emission. All the other sources have low or no influence on the total emission. For WWTP-2 the source digester + CHP unit and the sand trap have the biggest sensitivity to the total plant emission. All other sources do only have small or negligible influence on the total emission of the WWTP according to the sensitivity analysis (Table 5).

Source	WWTP-1		WWTP-2	
	Increasing w_i by factor 4	Decreasing w_i by factor 4	Increasing w_i by factor 4	Decreasing w_i by factor 4
Inlet	NA	NA	0%	0%
Sand trap	+17%	-4%	-9%	+4%
Primary clarifier	+11%	-3%	-3%	+1%
Activated sludge tanks	+7%	-2%	-3%	+1%
Secondary clarifier	+2%	0%	NA	NA
SBR	NA	NA	0%	0%
Thickener for primary sludge	0%	0%	0%	0%
Overflow sludge	0%	0%	NA	NA
Digester	-4%	+1%	NA	NA
Digester + CHP unit	NA	NA	+9%	-6%
Sludge storage tanks	-14%	+26%	0%	0%
Supernatants	+1%	0%	+2%	0%
Balloon for biogas storage	-1%	0%	+2%	0%
CHP unit	+13%	-3%	NA	NA

Table 5 Results of the sensitivity analysis. Percent change in the total WWTP emission if the specified w_i of a single source is increased or decreased by a factor of 4. NA = This source does not exist on the corresponding WWTP.

3.2 Emissions from biogas plants

The number of valid half-hourly emission values for the measuring campaigns at BGPs ranged from 78 to 310 and the data loss from 77% to 91%, respectively (Table 6). The average CH_4 emissions varied between 0.44 kg h^{-1} and 2.95 kg h^{-1} and the median CH_4 emissions between 0.39 kg h^{-1} and

2.22 kg h^{-1}. The highest numbers are due to measurements during other than normal operating conditions (OTNOC). The emissions without treatment of external sources are substantially higher for BGP-1, but in a similar range for BGP-2 and lower for BGP-3 than the mean which includes the correction (Table 6). Figure 5 shows the large variation of hourly emissions of the BGPs.

For BGP-4, the calculation procedure gave predominantly physically implausible results, most likely because of the potentially strong but varying influence of the grazing cattle between the BGP and the concentration measurements. Therefore, no meaningful results can be shown. More information on this issue is provided in the section 4.3.1. Measurement data can be found in Supporting information 2.

	BGP-1.1	**BGP-1.2**	**BGP-2.1***	**BGP-2.2***	**BGP-3**
N of valid values	310	78	143	132	121
Data loss	77%	91%	91%	82%	81%
Median [kg h^{-1}] (with correction for external sources)	0.39	0.44	2.22	1.93	0.60
Mean [kg h^{-1}] (with correction for external sources)	0.44	0.49	2.95	2.61	0.57
SD [kg h^{-1}]	0.50	0.35	2.62	3.69	0.41
Mean without correction for external sources [kg h^{-1}]	0.94	0.82	3.23	2.83	0.37

*Measurements during other than normal operating conditions (OTNOC)

Table 6 Summary of CH_4 emissions of the BGP-1, BGP-2,and BGP-3 (data not shown for BGP-4; see section 4.3.1)

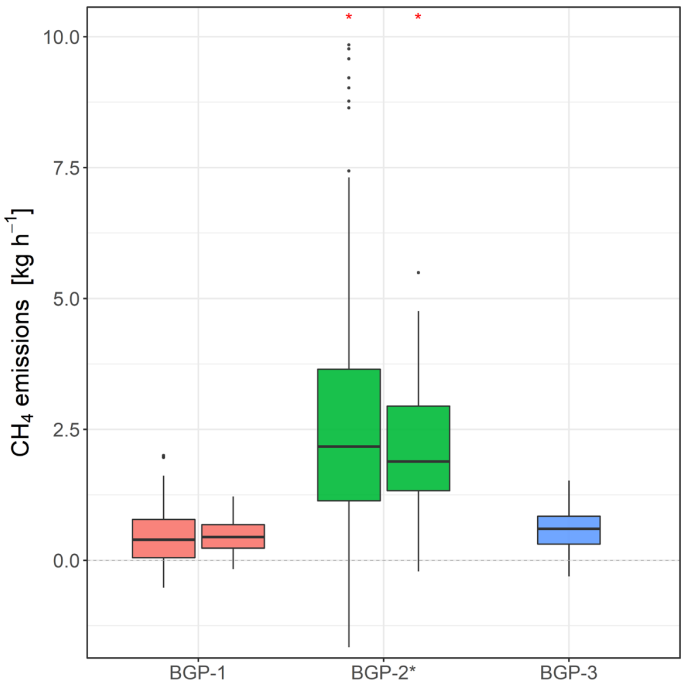

Figure 5 CH_4 emissions from three different BGPs. For BGP-1 and BGP-2 emissions from two campaigns. The red asterisks indicate outliers that are above 10 kg h^{-1}. There are three outliers for BGP-2.1 (10.77, 11.26, 11.93 kg h^{-1}) and BGP-2.2 (13.48, 21.65, 35.97 kg h^{-1}). BGP-2* measurements were conducted during other than normal operating conditions (OTNOC)

3.3 Uncertainty assessment

Bühler et al. (2021) conducted an uncertainty analysis of a measurement campaign with the IDM at an experimental dairy cow housing. They demonstrated that the uncertainty of the average emission decreases with increasing number of observations, i.e. valid emission intervals. As the sites in this study exhibit similar characteristics regarding topography and micrometeorological conditions as the location used by Bühler et al. (2021) and the same GasFinders were used, the function to determine the uncertainty from Bühler et al. (2021) was applied for the data of this study. The resulting random uncertainty ranged between 14 and 21%. However, the sites in this study exhibit additional (systematic) uncertainties due to external sources and the EWS approach. Assuming that the uncertainties introduced by the bLS model, external sources and the EWS approach are independent, the total uncertainty for each site was estimated. Using the corresponding values for each site, the total uncertainty in emission of WWTP-1 and WWTP-2 resulted in 36% and 27%, respectively. For the BGPs, the total uncertainties in emissions range

between 25% and 30%. Note that in section 3.1.1, the precisions of the daily averaged WWTPs emissions are given and not the uncertainty (or accuracy) calculated here.

4. Discussion

4.1 Wastewater treatment plants

4.1.1 Comparison with literature data

Daelman et al. (2012), Daelman et al. (2013), Delre et al. (2017), Samuelsson et al. (2018), Scheutz and Fredenslund (2019), STOWA (2010) and Yoshida et al. (2014) reported average CH_4 emissions from 16 European WWTPs in the range of 140 – 1339 g PE^{-1} y^{-1}. The average of these 16 WWTPs was 458 g PE^{-1} y^{-1} (median: 324 g PE^{-1} y^{-1}). Scaled to COD in the influent, the average emissions were 0.9% with a range of 0.3 - 1.7%. The 16 WWTPs have a size between 40,000 and 805,000 PE and the sewage was mostly of domestic origin. A detailed overview on the emission data of these plants is provided in the Supporting information 1, section 4.

The CH_4 emissions of 177 g PE^{-1} y^{-1} and 420 g PE^{-1} y^{-1} for WWTP-1 and WWTP-2, respectively, lay within the range of the reported literature data. Compared to the literature data, the emissions of WWTP-1 are at the lower end. In terms of COD in the influent, the emissions of 0.7% and 1.5% compare well with the literature. Overall, the measured emission observed in our study are in line with investigations conducted previously.

4.1.2 Combining multiple sources

The main problem of the source combination is that the ratios w_i of the specified emissions between the individual sources need to be known. As usually no direct measurement of an individual source is possible with the IDM, these ratios are estimated based on available literature data which are still sparse and might be uncertain. Additionally, the data need to be scaled to the site. For scaling, we used the PE if possible. This parameter may introduce an additional uncertainty as it depends on the accuracy of the measured WWTP inflow and the COD contents of the sewage. For the digester and the balloon for biogas storage, we made our own assumptions. Despite these challenges, the comparison in section 4.1.1 with the literature showed that the obtained results are reasonable.

For WWTP-2 the differences in total emissions between the ESP and EHD approach and the EWS approach were 2% and thus, of minor importance. But for WWTP-1, the differences were larger. The

total CH_4 emission of the ESP approach and the EHD approach were higher by 22% and 42%, respectively, than the EWS approach.

The higher differences between the different approaches in WWTP-1 compared to WWTP-2 are also reflected in the simple sensitivity analysis. For WWTP-1, a change by factor a of four in the w_i of the sludge storage tanks led to a maximum change of 26% in emission, whereas for WWTP-2 the maximum change caused by a single source was 9%. This shows that reliable literature data on the individual sources within a WWTP are important. For the sensitivity analysis, we expected that a change in the emission of the sources with the highest specified emission density would induce the largest change in the total WWTP emission. This was the case for both WWTPs. However, at WWTP-2, the total plant emission is not sensitive to a variation in the specified w_i of the sludge storage tank that had the second highest specified emission. The sensitivity analysis of the EWS approach done in this study suggests that a combination of the location of a source within the source complex, the distance between the emission source and the measurement path, the concentration measurements and the specified emission density, respectively the w_i, define the sensitivity. Sources that are rather at the edge of the source complex have a higher sensitivity than sources in its middle. Sources that are closer to the downwind measurement path tend to have a higher sensitivity than those situated further away. But if the w_i of these sources is low, they have a low sensitivity as well. The applicability of these findings to other sites needs to be investigated in further studies since other factors like the position of the GasFinders, the prevailing wind direction, or other micrometeorological parameters may also influence the resulting emission data.

Another reason for the differences between the three approaches for the two WTTPs could be the total WWTP area size. WWTP-1 (21,803 m^2) is about three times larger than WWTP-2 (7,354 m^2) and thus the distance between the different sources is larger. For WWTP-1, the EHD approach had the highest emission and the EWS approach the lowest. This can be explained by mechanism of the EWS approach: the sludge storage tanks (No 11 on Figure 1A) are located at the northern corner of the WWTP-1. Southwest of the sludge storage tanks, there is a larger empty area, that is included in the polygon for the ESP approach, thought. For this approach, this configuration allocates more “weight” to the northern part of the WWTP compared to the EHD approach, but less than for the EWS approach. Thus, the emissions with the ESP approach are between the other two approaches.

The question remains if for the source combination the specified relative emission densities are necessary or if one could use a simpler approach. Based on our two examples, we recommend the

EWS approach for sources like WWTPs. Additional emission data from individual sources within WWTPs will be available in the future which might improve the accuracy of the EWS approach.

4.1.3 Interrelations between emission rate and operations at WWTPs

The emission of individual measurement intervals varied over a large range (Figure 6). The variability can be due to fluctuations in the gas release from the WWTPs or/and due to varying micrometeorological conditions. Several studies reported CH_4 emission evolution characterised by a high incidental gas release from slurry storage (i.e. ebullition; Baldé et al. 2016; Kaharabata et al. 1998). They showed large variability in gas releases with or without operations at storage tanks. It seems likely that sludge storage tanks, which contribute a large proportion of emissions at the investigated WWTPs, show characteristics regarding emissions variability that are similar to those of slurry storage tanks at livestock farms. The temporal variability in CH_4 emission observed here is in the range as observed in previous studies e.g. conducted at farm sites (Flesch et al. 2005). Thus, we investigated interrelations between more than 100 parameters from the operational system and CH_4 emissions at WWTP-1. We selected those related to activities that potentially influence the gas release of CH_4. We identified several parameters associated to sludge treatment that coincided with emission peaks. Figure 6 shows a coincidence for periods with the agitation of sludge in either or both storage tanks and CH_4 emission peaks. Other parameters with interrelations are e.g. the filling level of the sludge storage tank or removal of sludge from the tank (not shown). Parameters related to the energy line (e.g. flaring, the volume of biogas storage balloon) did not coincide with CH_4 emission peaks.

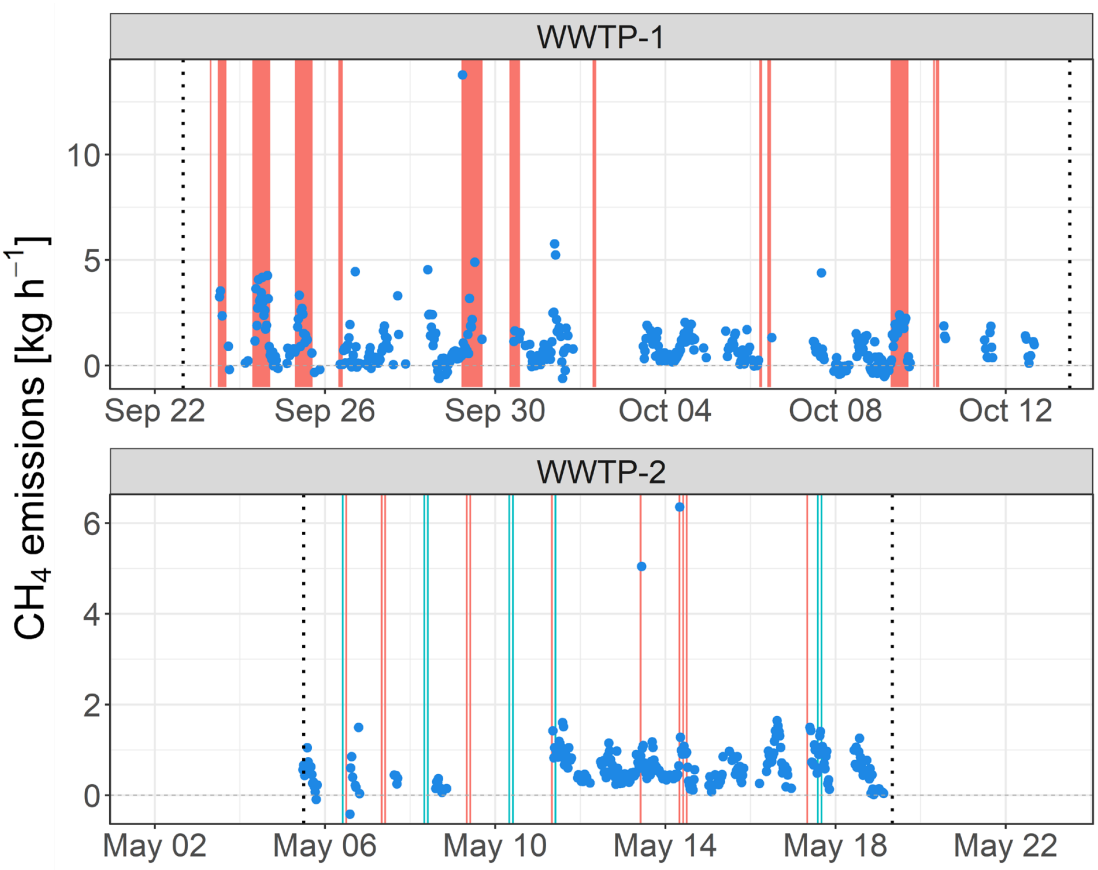

Figure 6 Interrelations between CH_4 emissions (EWS approach) and agitation of sludge storage tanks and flaring at WWTP-1 and WWTP-2. Red vertical bars indicate the operational time of the agitator of either or both storage tanks. Green vertical bars indicate the flaring periods. The CH_4 emissions are given as 30 min intervals. For WWTP-2, only the starting time of agitation is known and an operation time of 30 min was assumed. Grey dotted vertical lines indicate the start and the end of the measurement campaign.

For the WWTP-2, numerical data was not available, and we thus employed a visual analysis of images from agitation and flaring obtained from the operational system of the WWTP. Slurry store agitation mostly occurred over a period of less than 1h duration between 8:00 and 12:00 in the morning. Figure 6 shows a coincidence for periods with agitation of the sludge storage tank and flaring with emission peaks in some cases. The agitator was operated on average at a capacity of 70% and the gas torch of 10%, respectively, which suggests a relatively low effect on gas release.

Information on other potentially non-negligible emission sources such as leakages, e.g. bursts from pressure relief valves (Nisbet et al. 2020; Reinelt et al. 2017) could play a role in the total emissions at both of the investigated plants but could not be specifically obtained in the present study.

The CH_4 emissions at both WWTPs exhibited a diurnal cycle with a maximum at approximately 9:00 and a second, smaller peak in the mid-afternoon (Figure 4). As the pattern is not WWTP specific, we suggest coincidence with operating activities at the WWTPs and not with micrometeorological conditions. The peak in the morning is partly due to sludge storage tank agitation which did not occur every day, however. Another reason for the peak in the morning could be the CH_4 emissions from the sewer system. CH_4 builds up in the sediments and in the biofilm of the sewer system (Mannina et al. 2018) where the CH_4 production is higher with longer retention time of the wastewater in the sewer system (Guisasola et al. 2008). During the night, the influent into the WWTPs was small and thus CH_4 could have built up in the sewer system that was then released in the morning leading to an emission peak. There were no operation activities on the WWTP during the night and therefore the emissions were low.

The observed variability indicates that for a reliable emission estimate, measurement campaigns of sufficient duration are required. Based on our experience and to ensure data acquisition under different micrometeorological conditions, the distinct diurnal cycle and to compensate for an eventual data loss of more than 60%, we recommend measuring beyond 10 consecutive days (Bühler et al. 2021).

4.1.4 Source apportionment

With the bLS model it is not possible to distinguish between individual sources within a source complex. Therefore, we evaluated the feasibility of source apportionment based on literature data. Literature data were not available for CH_4 emissions from sludge storage tanks. Due to the similarity of human and pig excretions (both human and pigs are monogastric) data from pig slurry storage (Kupper et al. 2020) corrected for the lower methanisation potential when anaerobically digested (VanderZaag et al. 2018) were used as a proxy for emissions from stored sewage sludge. Based on these data, the estimated proportion of CH_4 emissions originating from sludge storage tanks was 48% and 13% of the total emissions for WWTP-1 and WWTP-2, respectively. The results of WWTP-1 coincide with the literature (Daelman et al. 2012; Delre et al. 2017; Samuelsson et al. 2018; STOWA 2010) that suggest the sludge line as main CH_4 source. WWTP-2 exhibits a substantially lower value. Given that a much higher emission share for the water line is implausible, we hypothesised that other sources occurred such as leakage from digestors, gas pipes or the CHP unit. Liebetrau et al. (2013) found emissions from the CHP unit ranging between 0.04% and 3.28% (average: 1.74%) of the utilised CH_4 at BGPs. Principally, the same technology is used for the CHP unit at WWTPs and it

can be assumed that CH_4 losses are similar at BGPs and WWTPs. We used the average value 1.74% from Liebetrau et al. (2013) of the gas production and the gas production data from Table 1. This yields CH_4 releases from the CHP unit of 3,493 kg CH_4 y^{-1} and 1,862 kg CH_4 y^{-1} for WWTP-1 and WWTP-2, respectively. This corresponds to a share relative to the total WWTP emissions of 48% and 35% for WWTP-1 and WWTP-2, respectively. The emissions from the sludge tanks and the CHP unit combined give 96% and 48% of the total plant emissions for WWTP-1 and WWTP-2, respectively, which is in the range of values for the sludge line found in the literature with WWTP-1 at the higher and WWTP-2 at the lower end. We thus assume that the emissions from the CHP unit at WWTP-1 are rather in the lower range of the reported values of Liebetrau et al. (2013) for the CHP unit and vice versa for the WWTP-2. A higher contribution of the CHP unit leakage for the latter is supported by the lower effect of the sludge storage tank agitation on CH_4 emission and the lower variability of the hourly emissions (Figure 6) which points at a continuous CH_4-flow which levels out emission peaks due to operations at the sludge and energy line. With the assumptions above regarding leakage from CHP unit, both plants would achieve a contribution of the sludge line to the total CH_4 WWTP emissions in the range of 60% to 80% which we assume as plausible.

4.1.5 Calculated emissions below zero

Emissions below zero occur, if after the treatment of potential external sources confounding any concentration measurement, the upwind concentration is higher than the downwind concentration. These negative emissions are solely due to calculations and must not be understood as deposition of CH_4. For WWTP-1 12% of the emissions were below zero (49 intervals). Most of the intervals (33) were in the time periods 29 September 2019 14:00 – 29 September 2019 23:00 and 8 October 2019 22:00 – 10 October 2019 08:00. The occurrence of an unknown external source emitting and confounding the upwind concentration over these time periods is rather unlikely. We also analysed all filtering parameters and could not find any reason allowing exclusion of these periods.

Due to low concentration differences between the up- and downwind measurements, negative emissions can occur due to statistical reasons according to Häni et al. (2021). They described an uncertainty range of the used GasFinders between 2.1 and 10.6 ppm-m. Häni et al. (2021) further reported drifts and jumps in the concentration measurements that could be indistinguishable from real concentration fluctuations without an external reference device. Such jumps or drifts could lead to systematic errors.

As we did not have a second GasFinder or another measuring device placed upwind, we were not able to verify if the upwind sensor was influenced by any external CH_4 source, or if a problem with the GasFinder occurred. Nevertheless, we decided to retain these two periods in the data set, because removing or excluding such calculated emissions below zero could unintentionally increase the emission of the measured source: without these two periods, the CH_4 emission of WWTP-1 would be higher by 14%.

4.2 Biogas plants

For all BGPs emission measurements were conducted for one wind direction sector only (Table 3). Except for BGP-2.2 where we placed the GasFinder on the southwest side further away compared to BGP-2.1 (Figure 2), measurements with two prevailing wind directions were possible. Reasons for only one general wind direction at the other BGPs were either the topography, the surrounding sources or lack of wind from more than one direction that would fulfil the filter criteria.

The relative fugitive CH_4 emissions of the BGPs in this study were lower than 5% of the plant's CH_4 production. This is in line with literature data based on measurements with IDM and GasFinder-2 from agricultural biogas plants that reported a range of 1.7 – 5.2% of fugitive emissions (Flesch et al. 2011; Groth et al. 2015; Hrad et al. 2015). A detailed literature review on BGPs emission (agricultural and non-agricultural) with different measuring techniques including IDM and tracer gas dispersion method, is given in Bakkaloglu et al. (2021).

The highest emissions were measured at BGP-2 with some very high emission intervals (Figure 5). First, this BGP has a large electrical power production and second, according to the operator of the plant, there were other than normal operating conditions during both measuring campaigns. Nevertheless, the relative fugitive emissions lie still within the range of literature data.

Other than for WWTPs, we used for the ESP approach for the BGPs in the bLS model calculations. This is reasonable as the dimension of the polygon of the BGPs are 1.5 – 4.8 times smaller than that of WWTP-2, which showed only small differences of <2% between the different approaches. Further, we believe that due to the open storage of substrate material in the BGPs and due to pipes running between the individual plant parts that could potentially have gas leakage, the assumption of a large polygon is warranted. For larger BGPs with more physical distance between individual parts, it might be preferable to use the EWS approach.

In contrast to WWTPs, BGPs did not exhibit a clear diurnal emission pattern and therefore, we did not use a diurnal cycle to calculate daily mean emissions. We suggest using the median value to

determine emission rates for BGPs to give outliers less weight (Figure 5). Emissions below zero are caused by small concentration differences between up- and downwind measurements in combination with the uncertainty of the GasFinders and the correction for external sources. However, excluding them would unintentionally increase the emissions as variations might also occur towards high emissions.

4.3 Coping with complex source configurations

4.3.1 Treatment of external sources

CH_4 sources outside of WWTPs or BGPs, which occurred at all sites confounding the concentration measurements, could be corrected for. The greater the distance between these sources and the GasFinder paths the more accurate results were obtained. The biggest problem were emissions from grazing cattle, especially if they were close to the measurement paths. This was one reason for unsuccessful measurements at BGP-4. At this site, there were about 90 grazing dairy cows and 25 heifers on the pastures around the BGP including the pasture where the GasFinders were placed. The assumption of homogeneous emissions from such a large area strongly differed from reality and thus produced obviously erroneous results with the bLS model calculations. The effect of external sources strongly depended on their position relative to the wind direction and to the measurement locations. For WWTP-1 and WWTP-2, the emissions without the correction for external source would be higher by 27% and lower by 4%, respectively. The average emissions of BGP-1.1 and BGP-1.2 without correction of external sources would be higher by 114% and 67%, respectively, and for BGP-2.1 and BGP-2.2, by 10% and 8%, respectively. For BGP-3, the emissions without treatment of external sources would be lower by 35%. For WWTP-1, BGP-1 and BGP-2, the external sources predominantly influenced the downwind concentration and thus, the emissions without treatment of external sources would be higher. At WWTP-2 the sheep stable at the northern side mostly influenced the upwind concentration and only to a smaller extent the downwind concentration. At BGP-3, the emission from the fattening pigs barn exclusively influenced the downwind concentration, however the dairy cow housing northeast of the BGP (Figure 2C) produced higher CH_4 emissions and therefore, the CH_4 upwind concentration was more confounded than the downwind concentration. Thus, for these two sites the emissions without treatment of external sources would be lower.

Correcting for external sources introduces an additional uncertainty of the WWTPs and BGPs emission. For the external sources, we assume a general uncertainty of the $\Delta C_{external\_i}$ (Eq. 6) of 20%.

The larger the share $\Delta C_{external}$ on the $\Delta C_{measured}$, the larger the uncertainty of the plant emission. A change in 20% in emission of the external sources would result in a change of the WWTP-1 and WWTP-2 emission of 6% and 1%, respectively. For BGP-1.1, BGP-1.2, BGP-2.1, BGP-2.2 and BGP-3, the changes in the average emission would be 19%, 14%, 2%, 2% and 7%, respectively.

The higher numbers for BGP-1 are because the external sources are close to the BGP and produce about the same amount of CH_4 as the BGP. Nevertheless, this study suggests that the treatment of external sources allows an accurate correction thereof as the resulting data are comparable with emissions obtained from other studies.

4.3.2 Placement of concentration sensors

At WWTP-1, due to the mound southwest of the WWTP measurements were only possible with southwestern wind. The background sensor was placed close to the mound as there were grazing heifers between the mound and the WWTP. At WTTP-2 we knew from previous turbulence measurements that data passing filtering would be unlikely with wind from south and thus we planned only measurements with northerly winds. At BGP-1, measurements with northeast wind were not possible due to the forest and the pasture. There was mostly northeast wind during the first campaign at BGP-2. Thus, we placed the GasFinder for the second campaign on the southwest side further away from the plant to enable measuring from the two prevailing wind directions. Also, the setup on the northeast side was optimised for the local wind directions. At BGP-3, measurements were planned with southwest wind only. For measurements with northeast wind, the cattle housing No 3 (Figure 2C) would have been too close.

Determining emissions from WWTPs and BGPs at sites with a mostly complex environment as prevailing in Switzerland is challenging. Placing GasFinder devices is often hampered due to several different factors that need to be considered. It depends on tract of land borders, canopy height of the different tract of land, traffic routes, topography (often non-flat), surrounding CH_4 sources and other obstacles like trees or buildings. An analysis of trade-offs between the different factors is necessary which often results in only one feasible wind direction for measurements: only in two out of seven campaigns it was possible to use data from two general wind directions. A prior determination of the prevailing wind direction is the most important factor. Before the campaign start, we used data from nearby weather stations to determine the wind direction. However, due to non-flat topography and forests, the available data were not always representative for the plant sites. In case of BGP-4, the latter factor was another reason for the unsuccessful results. At this site,

the wind direction was not parallel to the forest as previously expected. The wind direction was more towards 180° and therefore causing a wind edge rendering the turbulence measurements not representative for the entire area. Thus, the best case would be to make extended wind measurements directly at the experimental site prior to the campaign.

Another problem could be low concentration differences between the up- and downwind measurements. GasFinders-3 have a relatively large uncertainty (Häni et al. 2021) and therefore sufficient concentration differences are needed. With increasing wind speed and unstable conditions, concentration differences may decrease. This rises the uncertainty of the results and could also lead to calculated emissions below zero. At WWTP-2 we conducted a measuring campaign one year prior to the shown measurements that was not successful. We placed the GasFinder on the downwind side too far away from the WWTP with too long measuring paths and thus no concentration difference between the up- and downwind concentrations was detected. That is why the distance between the measuring path and the WWTP-1 shown in Table 3 is rather short.

5. Conclusions

In this study, CH_4 emission measurements from whole WWTPs and BGPs by IDM produced reasonable results that are in line with literature data. We could demonstrate that measurements under rather complex conditions are possible. This study thus provided several valuable insights on how to conduct successful CH_4 measurements with IDM under such challenging situations. It showed that prior analysis of the external sources in combination with the wind direction is important to detect sites where measurements are likely to fail (like BGP-4 with insufficient localisation of grazing cattle, wind edge). After selecting a site, a careful analysis of trade-offs regarding placing measurement devices must be done. Often, a compromise is required between extending the distance toward the source to have the turbulence re-established and limiting it for obtaining sufficient difference between the upwind and downwind concentrations. For the measuring campaign itself, sufficient time should be planned for, especially where only one general wind direction for measurements is possible. In this study, we showed a procedure for treatment of external sources. Additionally, an approach was introduced for more accurate emission calculations for sources of greater complexity. For this approach, the individual sources within a source complex were specified

and the total emission was calculated according to these relative weights. We showed that such an approach is necessary for large sources like WWTPs. This approach can be refined with additional available measurement data from individual sources. The future use of source apportionment will provide further experience and by this, increase the accuracy of measurements with IDM under complex situations; this also allies for treatment of external sources.

Acknowledgements

The funding for the project regarding wastewater treatment plants by the Swiss Federal Office for the Environment (Contract number: 06.0091.PZ/R281-0748) is gratefully acknowledged. In the framework of the project 'Evaluation and reduction of methane emissions from different European biogas plant concepts' (EvEmBi), this work was supported by the Swiss Federal Office of Energy SFOE (contract number SI/501679-01) and the Swiss Federal Office for the Environment (contract number 17.0083.PJ/R035-0703). We thank Ökostrom Schweiz for the valuable inputs and discussions regarding biogas plants. We thank the operators of the wastewater treatment plants, biogas plants and the farmers of the land in the surrounding areas. We are grateful to the support and assistance during the measurements of Martin Häberli-Wyss (School of Agricultural, Forest and Food Sciences, Zollikofen) and the highly valuable support of Albrecht Neftel (Neftel Research Expertise, Wohlen bei Bern).

A. Annex

Here the derivation on how to combine multiple sources is given.

A. Combining multiple sources

We have calculated D_i (h m^{-1}) values that are a function of the micrometeorological parameters and the source-sensor geometry for N sources. We intend to combine all N sources into one source with an average emission of Q_{tot}. The emission of a sources Q_i (with unit kg h^{-1}) is defined as:

$$Q_i = E_i \cdot A_i \qquad \text{Eq. A1}$$

Whereas E is the emission density (kg m^{-2} h^{-1}) and A (m^2) the area of the source.

Each source Q_i contributes to the total emission Q_{tot}

$$Q_{tot} = \sum_{i=1}^{N} Q_i \qquad \text{Eq. A2}$$

Assumption: The relative emission strengths w_i to a reference source Q_{ref}, which is a source within the source complex, are known:

$$Q_i = Q_{ref} \cdot w_i \qquad \text{Eq. A3}$$

Expanding Eq. A3 gives

$$Q_i = E_{ref} \cdot A_{ref} \cdot w_i \qquad \text{Eq. A4}$$

Combining Eq. A1-A4 results in

$$Q_{tot} = E_{ref} \cdot A_{ref} \cdot \sum_{i=1}^{N} w_i \qquad \text{Eq. A5}$$

The bLS model simulates the dispersion factor D_i between each individual source E_i and its partial concentration effect ΔC_i:

$$\Delta C_i = D_i \cdot E_i \qquad \text{Eq. A6}$$

The measured concentration difference is a sum (superposition) of the individual concentration effects of all sources:

$$\Delta C_{tot} = \sum_{i=1}^{N} \Delta C_i \qquad \text{Eq. A7}$$

Combining Eq. A3, A4, A6 and A7

$$\Delta C_{tot} = E_{ref} \cdot A_{ref} \cdot \sum_{i=1}^{N} \left(\frac{w_i \cdot D_i}{A_i} \right) \quad \text{Eq. A8}$$

Solving for E_{ref}

$$E_{ref} = \frac{\Delta C_{tot}}{A_{ref} \cdot \sum_{i=1}^{N} \left(\frac{w_i \cdot D_i}{A_i} \right)} \quad \text{Eq. A9}$$

Once E_{ref} is known, the emission of the total source complex can be calculated.

$$Q_{tot} = \frac{\Delta C_{tot}}{\sum_{i=1}^{N} \left(\frac{w_i \cdot D_i}{A_i} \right)} \cdot \sum_{i=1}^{N} w_i \quad \text{Eq. A10}$$

Note, as the weights w_i are defined in relation to Q_i, they are different for the EHD and EWS approach. In Table 4 the w_i for the two approaches are given.

As for the EHD approach the w_i are reduced to the ratio of the areas, Eq. A10 can be reduced to:

$$Q_{tot} = \frac{\Delta C_{tot}}{\sum_{i=1}^{N} D_i} \cdot \sum_{i=1}^{N} A_i \quad \text{Eq. A11}$$

6. Publication bibliography

Bakkaloglu, Semra; Lowry, Dave; Fisher, Rebecca E.; France, James L.; Brunner, Dominik; Chen, Huilin; Nisbet, Euan G. (2021): Quantification of methane emissions from UK biogas plants. In *Waste management (New York, N.Y.)* 124, pp. 82–93. DOI: 10.1016/j.wasman.2021.01.011.

Baldé, Hambaliou; VanderZaag, Andrew C.; Burtt, Stephen; Evans, Leigh; Wagner-Riddle, Claudia; Desjardins, Raymond L.; MacDonald, J. Douglas (2016): Measured versus modeled methane emissions from separated liquid dairy manure show large model underestimates. In *Agric. Ecosyst. Environ.* 230, pp. 261–270. DOI: 10.1016/j.agee.2016.06.016.

Bühler, Marcel; Häni, Christoph; Ammann, Christof; Mohn, Joachim; Neftel, Albrecht; Schrade, Sabine et al. (2021): Assessment of the inverse dispersion method for the determination of methane emissions from a dairy housing. In *Agric. For. Meteorol.* 307, p. 108501. DOI: 10.1016/j.agrformet.2021.108501.

Daelman, M. R. J.; van Voorthuizen, E. M.; van Dongen, L. G. J. M.; Volcke, E. I. P.; van Loosdrecht, M. C. M. (2013): Methane and nitrous oxide emissions from municipal wastewater treatment - results from a long-term study. In *Water science and technology : a journal of the International Association on Water Pollution Research* 67 (10), pp. 2350–2355. DOI: 10.2166/wst.2013.109.

Daelman, Matthijs R. J.; van Voorthuizen, Ellen M.; van Dongen, Udo G. J. M.; Volcke, Eveline I. P.; van Loosdrecht, Mark C. M. (2012): Methane emission during municipal wastewater treatment. In *Water research* 46 (11), pp. 3657–3670. DOI: 10.1016/j.watres.2012.04.024.

Delre, Antonio; Mønster, Jacob; Scheutz, Charlotte (2017): Greenhouse gas emission quantification from wastewater treatment plants, using a tracer gas dispersion method. In *The Science of the total environment* 605-606, pp. 258–268. DOI: 10.1016/j.scitotenv.2017.06.177.

Eijo-Río, Elena; Petit-Boix, Anna; Villalba, Gara; Suárez-Ojeda, María Eugenia; Marin, Desirée; Amores, Maria José et al. (2015): Municipal sewer networks as sources of nitrous oxide, methane and hydrogen sulphide emissions: A review and case studies. In *Journal of Environmental Chemical Engineering* 3 (3), pp. 2084–2094. DOI: 10.1016/j.jece.2015.07.006.

Flesch, T. K.; Vergé, X. P. C.; Desjardins, R. L.; Worth, D. (2013): Methane emissions from a swine manure tank in western Canada. In *Canadian Journal of Animal Science* 93 (1), pp. 159–169. DOI: 10.4141/cjas2012-072.

Flesch, T. K.; Wilson, J. D.; Harper, L. A.; Crenna, B. P. (2005): Estimating gas emissions from a farm with an inverse-dispersion technique. In *Atmospheric Environment* 39 (27), pp. 4863–4874. DOI: 10.1016/j.atmosenv.2005.04.032.

Flesch, T. K.; Wilson, J. D.; Harper, L. A.; Crenna, B. P.; Sharpe, R. R. (2004): Deducing ground-to-air emissions from observed trace gas concentrations: A field trial. In *Journal of Applied Meteorology* 43 (3), pp. 487–502. DOI: 10.1175/1520-0450(2004)043<0487:DGEFOT>2.0.CO;2.

Flesch, Thomas K.; Desjardins, Raymond L.; Worth, Devon (2011): Fugitive methane emissions from an agricultural biodigester. In *Biomass and Bioenergy* 35 (9), pp. 3927–3935. DOI: 10.1016/j.biombioe.2011.06.009.

FOEN (2021a): Emissionen von Treibhausgasen nach CO_2-Gesetz und Kyoto-Protokoll, 2. Verpflichtungsperiode (2013-2020). Federal Office for the Environment FOEN. Bern. Available online at https://www.bafu.admin.ch/dam/bafu/de/dokumente/klima/fachinfo-daten/CO2_Statistik.pdf.download.pdf/CO2_Publikation_de_2021-07.pdf, checked on 8/3/2021.

FOEN (2021b): Switzerland's Greenhouse Gas Inventory 1990-2019, National Inventory Report. Including reporting elements under the Kyoto Protocol. Submission of April 2021 under the United Nations Framework Convention on Climate Change and under the Kyoto Protocol. With assistance of R. Röthlisberger, AA. Bass, S. Schenker, C. Stettler, D. Bretscher, A. Schellenberger et al. Federal Office for the Environment FOEN. Bern. Available online at https://www.bafu.admin.ch/dam/bafu/en/dokumente/klima/klima-climatereporting/National_Inventory_Report_CHE.pdf.download.pdf/National_Inventory_Report_CHE_2021.pdf, checked on 8/5/2021.

Gill Instruments (2016): Technical key note: Software bug affecting 'w' wind component of the WindMaster family. Gill Instruments. Lymington, UK. Available online at http://gillinstruments.com/data/manuals/KN1509_WindMaster_WBug_info.pdf.

Groth, Angela; Maurer, Claudia; Reiser, Martin; Kranert, Martin (2015): Determination of methane emission rates on a biogas plant using data from laser absorption spectrometry. In *Bioresour. Technol.* 178, pp. 359–361. DOI: 10.1016/j.biortech.2014.09.112.

Guisasola, Albert; Haas, David de; Keller, Jurg; Yuan, Zhiguo (2008): Methane formation in sewer systems. In *Wat. Res.* 42 (6-7), pp. 1421–1430. DOI: 10.1016/j.watres.2007.10.014.

Gujer, Willi (2007): Siedlungswasserwirtschaft. 3. bearbeitete Auflage: Springer-Verlag Berlin Heidelberg.

Häni, C.; Flechard, C.; Neftel, A.; Sintermann, J.; Kupper, T. (2018): Accounting for field-scale dry deposition in backward Lagrangian stochastic dispersion modelling of NH_3 emissions. In *Atmosphere* 9 (4), p. 146. DOI: 10.3390/atmos9040146.

Häni, Christoph; Bühler, Marcel; Neftel, Albrecht; Ammann, Christof; Kupper, Thomas (2021): Performance of open-path GasFinder3 devices for CH_4 concentration measurements close to ambient levels. In *Atmospheric Measurement Techniques* 14 (2), pp. 1733–1741. DOI: 10.5194/amt-14-1733-2021.

Harper, L. A.; Denmead, O. T.; Flesch, T. K. (2011): Micrometeorological techniques for measurement of enteric greenhouse gas emissions. In *Animal Feed Science and Technology* 166-167, pp. 227–239. DOI: 10.1016/j.anifeedsci.2011.04.013.

Hrad, Marlies; Piringer, Martin; Huber-Humer, Marion (2015): Determining methane emissions from biogas plants--Operational and meteorological aspects. In *Bioresour. Technol.* 191, pp. 234–243. DOI: 10.1016/j.biortech.2015.05.016.

Kaharabata, S. K.; Schuepp, P. H.; Desjardins, R. L. (1998): Methane emissions from above ground open manure slurry tanks. In *Global Biogeochem. Cycles* 12 (3), pp. 545–554. DOI: 10.1029/98GB01866.

Kilgour, Robert J. (2012): In pursuit of "normal": A review of the behaviour of cattle at pasture. In *Applied Animal Behaviour Science* 138 (1-2), pp. 1–11. DOI: 10.1016/j.applanim.2011.12.002.

Kupper, Thomas; Häni, Christoph; Neftel, Albrecht; Kincaid, Chris; Bühler, Marcel; Amon, Barbara; VanderZaag, Andrew (2020): Ammonia and greenhouse gas emissions from slurry storage - A review. In *Agriculture, Ecosystems & Environment* 300, p. 106963. DOI: 10.1016/j.agee.2020.106963.

Liebetrau, J.; Reinelt, T.; Clemens, J.; Hafermann, C.; Friehe, J.; Weiland, P. (2013): Analysis of greenhouse gas emissions from 10 biogas plants within the agricultural sector. In *Water science and technology : a journal of the International Association on Water Pollution Research* 67 (6), pp. 1370–1379. DOI: 10.2166/wst.2013.005.

Mannina, Giorgio; Butler, David; Benedetti, Lorenzo; Deletic, Ana; Fowdar, Harsha; Fu, Guangtao et al. (2018): Greenhouse gas emissions from integrated urban drainage systems: Where do we stand? In *Journal of Hydrology* 559, pp. 307–314. DOI: 10.1016/j.jhydrol.2018.02.058.

Nisbet, E. G.; Fisher, R. E.; Lowry, D.; France, J. L.; Allen, G.; Bakkaloglu, S. et al. (2020): Methane Mitigation: Methods to Reduce Emissions, on the Path to the Paris Agreement. In *Rev. Geophys.* 58 (1). DOI: 10.1029/2019RG000675.

Reinelt, Torsten; Delre, Antonio; Westerkamp, Tanja; Holmgren, Magnus A.; Liebetrau, Jan; Scheutz, Charlotte (2017): Comparative use of different emission measurement approaches to determine methane emissions from a biogas plant. In *Waste management (New York, N.Y.)* 68, pp. 173–185. DOI: 10.1016/j.wasman.2017.05.053.

Samuelsson, J.; Delre, A.; Tumlin, S.; Hadi, S.; Offerle, B.; Scheutz, C. (2018): Optical technologies applied alongside on-site and remote approaches for climate gas emission quantification at a wastewater treatment plant. In *Water research* 131, pp. 299–309. DOI: 10.1016/j.watres.2017.12.018.

Scheutz, Charlotte; Fredenslund, Anders M. (2019): Total methane emission rates and losses from 23 biogas plants. In *Waste management (New York, N.Y.)* 97, pp. 38–46. DOI: 10.1016/j.wasman.2019.07.029.

Stocker, T. F.; Qin, D.; Plattner, G.-K.; Alexander, L. V.; Allen, S. K.; Bindoff, N.L et al. (2013): Technical Summary. In: Climate Change 2013: The Physical Science Basis. Contribution of Working Group I to the Fifth Assessment Report of the Intergovernmental Panel on Climate Change. Edited by T. F. Stocker, D. Qin, G.-K. Plattner, M. Tignor, S. K. Allen, J. Boschung et al. Cambridge, United Kingdom and New York, NY, USA.

STOWA (2010): Emissies van broeikasgassen van RWZI's. Amersfoort, the Netherlands.

VanderZaag, A. C.; Flesch, T. K.; Desjardins, R. L.; Baldé, H.; Wright, T. (2014): Measuring methane emissions from two dairy farms. Seasonal and manure-management effects. In *Agricultural and Forest Meteorology* 194, pp. 259–267. DOI: 10.1016/j.agrformet.2014.02.003.

VanderZaag, Andrew C.; Baldé, Hambaliou; Crolla, Anna; Gordon, Robert J.; Ngwabie, N. Martin; Wagner-Riddle, Claudia et al. (2018): Potential methane emission reductions for two manure treatment technologies. In *Environmental technology* 39 (7), pp. 851–858.

Yoshida, Hiroko; Mønster, Jacob; Scheutz, Charlotte (2014): Plant-integrated measurement of greenhouse gas emissions from a municipal wastewater treatment plant. In *Water research* 61, pp. 108–118. DOI: 10.1016/j.watres.2014.05.014.

Supporting Information 1

For the publication from Bühler et al. entitled "Determination of methane emissions from complex source configurations with the inverse dispersion method"

1. Description of WWTPs

Wastewater treatment plant 1 (WWTP-1) consists of a conventional activated sludge treatment with complete nitrification and denitrification. The primary sludge passes a thickener from where it enters the digesters with a dry matter content of 4%. The anaerobic digestion is operated at mesophilic conditions (average temperature during measurement campaign: 37.8°C). The biogas is fed to a combined heat and power (CHP) unit for electrical power production. The heat is used for heating the digester. The excess heat is fed to a district heating network. The gas torch was never operated during the measurement campaign. After a residence time of approximately 20 days the sludge is again dewatered to 8% of dry matter after addition of a flocculant by means of a rotary screen and then transferred to open sludge storage tanks (total volume: 1,960 m^3). The sludge is regularly evacuated and transported to a larger WWTP for further treatment and disposal. Before the transport, the tanks are stirred to achieve pumpability of the sludge.
The water line at the WWTP-2 (Fig2b) consists of a screen, a grit chamber, primary clarification basins and a sequencing batch reactor where the pre-treated sewage undergoes three cycles of 8 h each: (1) filling of one of the three reactors, (2) aeration, (3) sedimentation of the secondary sludge and extraction of excess sludge and discharge of the treated water into the retention basin from where it is regularly discharged into the receiving water.
The primary sludge passes a pre-thickener and is then directed to a belt thickener and enters the digesters with a dry matter content of 2 to 3%. The anaerobic digestion is operated at mesophilic conditions (average temperature in 2020: 37.6°C for digester 1 and 34.4°C for digester 2). After a residence time of approximately 20 days the sludge is again dewatered to 5% of dry matter after addition of a flocculant by means of a rotary screen and then transferred to one of the two open sludge storage tanks (volume: 400 m^3). The biogas is fed to a CHP for electrical power production. The heat is used for regulating the temperature in the digester. The sludge is regularly evacuated and transported to a larger WWTP for further treatment and disposal. The tank for sludge storage is regularly stirred in the morning. The supernatants are removed from the surface in the afternoon and filled into the storage tank for sludge water. The gas torch is rarely used, i.e. mainly to evacuate condensation water in the gas pipe system.

Table S1 Characteristics of the wastewater inflow at WWTP-1 and WWTP-2: annual values of 2019 and/or 2020 and recorded during measurement campaigns; C: concentration, COD: Chemical Oxygen Demand, NH4-N: ammonium given as nitrogen, F: flow, MC: Measuring campaign.

	Inflow [m^3 d^{-1}]	C-COD [g L^{-1}]	C-NH_4-N [g L^{-1}]	F- COD [kg d^{-1}]	F-NH_4-N [kg d^{-1}]
WWTP-1					
Average 2019	12268	293	33	3483	376
Median 2019	10248	307	36	3377	368
Minimum 2019	7829	156	11	1866	230
Maximum 2019	30660	424	48	6133	1034
Average during MC	11168	299	36	2862	336
Median during MC	9380	310	311	2933	341
WWTP-2					
Average 2019	4458	240	34	1010	138
Median 2019	3710	233	36	995	139
Minimum 2019	2321	113	14	566	95
Maximum 2019	12967	373	51	1757	168
Average 2020 (01.01-30.06)	4606	259	33	1126	137
Median 2020 (01.01-30.06)	3798	248	35	1009	139
Minimum 2020 (01.01-30.06)	2417	134	9	631	69
Maximum 2020 (01.01-30.06)	11829	577	50	2388	164
Average during MC	4005	270	37	1076	140
Median during MC	3469	279	39	994	139

In Table S2 the a priori emission used for the source combination are given. The emissions for the sludge storage tanks were estimated based on emission rate 1.8 g CH_4 m^{-2} h^{-1} derived from data for pig slurry from Kupper et al. (2020) (i.e. baseline emissions for tank, temperate season, Supplementary data 5), a correction factor which takes into account the lower methanisation potential by 35% for anaerobically digested slurry (VanderZaag et al. 2018) and the sludge volume from Table 1. Emission estimates for the CHP are based on emission factor of 1.74% of the utilised CH_4 (Liebetrau et al. 2013) and the gas production from Table 1, CH_4 content in biogas: 65% (Kvist and Aryal 2019); conversion factor of m^3 CH_4 to kilograms CH_4: 0.671 (IPCC 2006).

Table S2 Data used for source the combination of the individual sources within the WWTPs. PE = Population equivalent. The given literature data was used to define the a priori emissions. Given are the emissions per area.

Source	Literature data	Scaling	Area [m^2]		Emission [g CH_4 m^{-2} d^{-1}]	
			WWTP-1	WWTP-2	WWTP-1	WWTP-2
Inlet	Ren et al. 2013	PE	NA	123	NA	0.3
Sand trap	Czepiel et al. 1993; Liu et al. 2014; Ren et al. 2013; Samuelsson et al. 2018; STOWA 2010	PE	163	41	30.8	39.3
Primary clarifier	Ren et al. 2013	Area	808	156	3.4	3.4
Activated sludge tanks	eawag 3/24/2020	PE	2258	171	0.7	3.2
Secondary clarifier	Ren et al. 2013; Samuelsson et al. 2018; Tumendelger et al. 2019; Wang et al. 2011	PE	1501	NA	0.4	NA
SBR	eawag 3/24/2020; Ren et al. 2013; Samuelsson et al. 2018; Tumendelger et al. 2019; Wang et al. 2011	PE	NA	1017	NA	0.4
Thickener for primary sludge	Ren et al. 2013	PE	92	246	21.8	2.6
Overflow sludge	Ren et al. 2013; Samuelsson et al. 2018; Tumendelger et al. 2019; Wang et al. 2011	PE/Area	320	NA	0.1	NA
Digester	Own assumptions	other	236	NA	4.2	NA
Digester + CHP unit	own assumptions, IPCC 2006; Liebetrau et al. 2013	other	NA	274	NA	22.2
Sludge storage tanks	Kupper et al. 2020; VanderZaag et al. 2018	Area	336	69	28.1	28.1
Supernatants	Ren et al. 2013	Area	226	69	3.4	15.4
Balloon for biogas storage	Own assumptions	other	120	151	2.5	2.0
CHP unit	IPCC 2006; Liebetrau et al. 2013	other	44	NA	216.9	NA

1.1 Meteorological conditions

Figure S1 shows the meteorological condition during the measurement campaign in 2019 at WWTP-1. The conditions were normal for autumn and winter although the temperatures were periodically at the upper range for the season and periods with high wind speeds occurred.

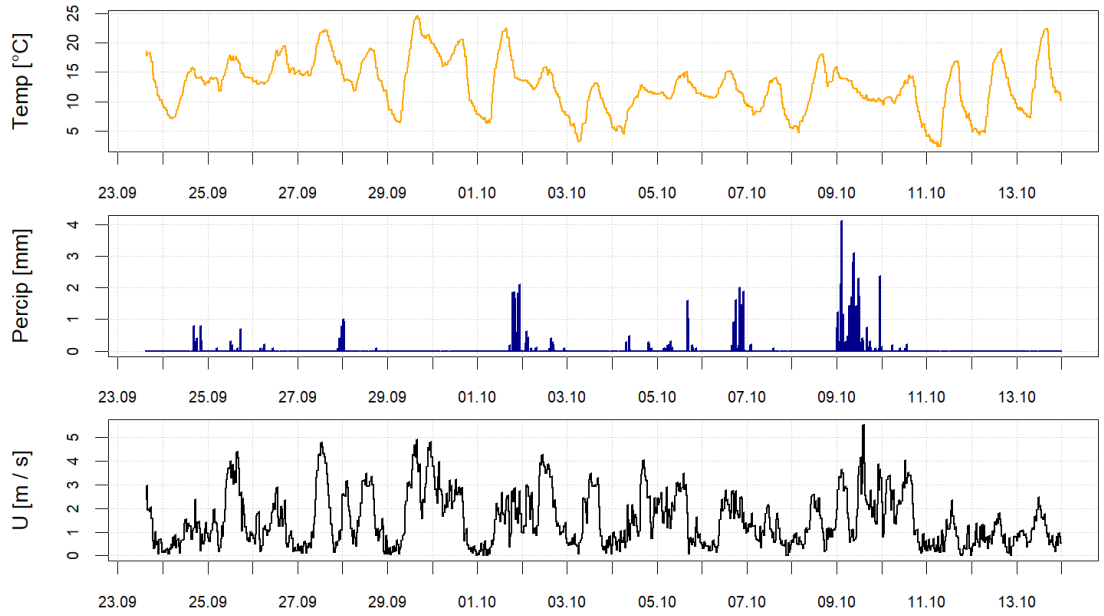

Figure S1: Overview on the temperature, precipitation and wind speed from our own weather station during the measurements conducted at WWTP-1.

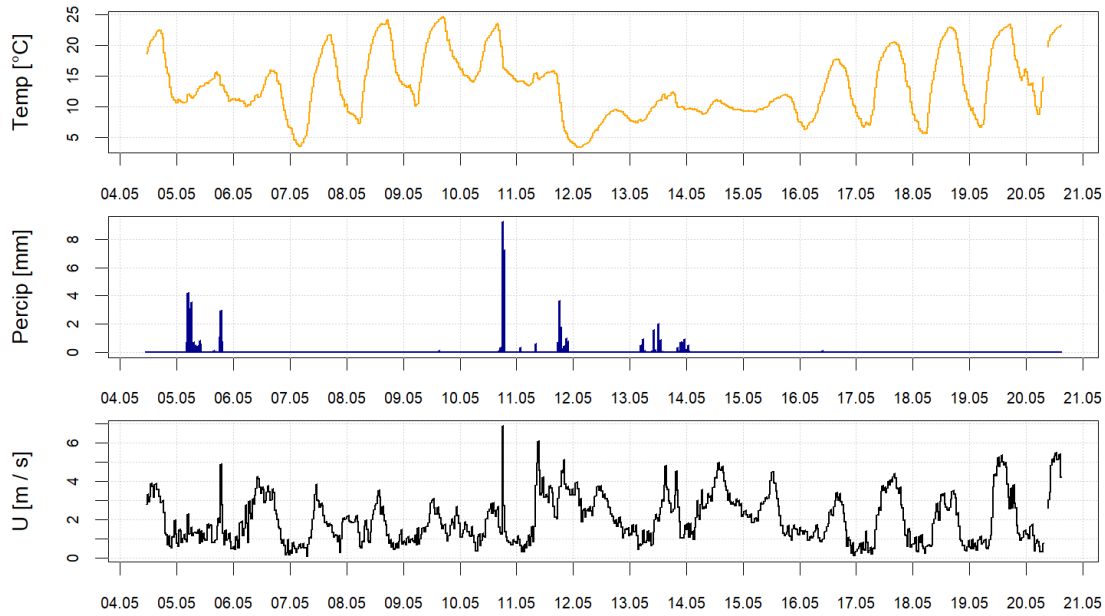

Figure S2: Overview on temperature, precipitation, and wind speed from our own weather station during the measurements conducted at WWTP-2.

The meteorological conditions during the measuring campaign in May 2020 at the WWTP-2 were normal for late spring (Figure S2).

2. Data filtering

In Table S3 the applied data filtering for each site is given.

Table S3 Quality filter criteria that were applied at the different sites. It shows what kind of data was kept. N_TD = Number of touchdowns within the source. z_{canopy} = canopy height, A = Area of the source.

		filter criteria									
Site	**N of trajectories**	u^*	σ_u/u^*	σ_v/u^*	$C0$	$\lvert L\rvert$	z_0	N_TD	D/A	ΔC	WD
WWTP-1	250000	> 0.06	< 7	< 7	-	< 2	< 0.1	-	-	-	yes
WWTP-2	250000	> 0.05	< 6	< 6	< 10	< 2	< 0.1	-	> 6.00E-05	-	yes
BGP-1.1	50000	> 0.05	< 8	< 8	< 10	< 2	$z_0 > \frac{z_{canopy}}{100}$ & $z_0 < \frac{z_{canopy}}{3}$	> 8.00E+04	> 8.20E-05	> -0.08	yes
BGP-1.2	50000	> 0.06	< 8	< 8	< 10	< 2	$z_0 > \frac{z_{canopy}}{100}$ & $z_0 < \frac{z_{canopy}}{3}$	> 8.00E+04	> 8.20E-05	> -0.08	yes
BGP-2.1	50000	> 0.05	< 8	< 8	< 10	< 2	$z_0 > \frac{z_{canopy}}{100}$ & $z_0 < \frac{z_{canopy}}{3}$	> 2.70E+05	> 8.20E-05	> -0.08	yes
BGP-2.2	50000	> 0.06	< 8	< 8	< 10	< 2	$z_0 > \frac{z_{canopy}}{100}$ & $z_0 < \frac{z_{canopy}}{3}$	> 2.70E+05	> 8.20E-05	> -0.08	yes
BGP-3	250000	> 0.10	< 8	< 8	< 10	< 2	$z_0 > \frac{z_{canopy}}{100}$ & $z_0 < \frac{z_{canopy}}{3}$	> 4.20E+05	> 1.00E-04	> -0.08	yes

3. GasFinder

3.1 Intercomparison of GasFinder devices

An intercomparison of the GasFinder was conducted after each WWTP campaign. This was necessary because of the offset and span between the GasFinder sensors (Häni et al. 2021). The concentrations were corrected for span and offset. As reference device the GasFinder used as background concentration (at both sites the same sensor) was used. A concentration during the campaign with wind sectors where all used GasFinders were exposed to the same background concentration was for the WWTP campaigns not possible.
For BGP-1 the concentrations were corrected with wind sectors for which all GasFinders were exposed to background concentration. For BGP-1.2, additionally a correction from an intercomparison was applied that was conducted some weeks prior to the campaign. For BGP-2.1 wind sectors were used and for BGP-2.2 an intercomparison that was conducted after the measurements. For BGP-3 the intercomparison conducted at WWTP-1 was used.

3.2 Fixation of GasFinders

Running the GasFinders out in the field can lead to a misalignment of the laser beam with the retroreflector. This often happens due to soil movement (wetting, drying, freezing, unfreezing) or wind gusts. If no automatic realignment system is available, even a daily realignment could be necessary. However, we run the devices for days without supervision and a car drive every day of several hours to the devices was not possible. Fixing the tripods with a clamp set to the ground really helped to reduce the data loss. The tripods of the retroreflectors were also fixed with a clamp set.

4. Comparison of WWTP emissions with literature data

Samuelsson et al. (2018) report an average CH_4 emission of a Swedish WWTP of 337 g PE^{-1} y^{-1}. Delre et al. (2017) conducted measurements at five different WWTPs with average emissions between 153 g PE^{-1} y^{-1} and 919 g PE^{-1} y^{-1} and Yoshida et al. (2014) report CH_4 emission of 1339 g PE^{-1} y^{-1} from a WWTP in Denmark. Scheutz and Fredenslund (2019) measured emissions from several WWTPs and BGPs which were between 257 g PE^{-1} y^{-1} and 747 g PE^{-1} y^{-1} (data from four WWTPs that are not already included in Delre et al. (2017), Samuelsson et al. (2018) and Yoshida et al. (2014). Daelman et al. (2012) and Daelman et al. (2013) reported CH_4 emissions of a WWTP in the Netherlands of 306 g PE^{-1} y^{-1} and 390 g PE^{-1} y^{-1}, respectively. STOWA (2010) measured emissions of three different WWTPs in the Netherlands between 140 and 310 g PE^{-1} y^{-1}. Detailed information on the individual WWTPs is given in Table S4

The average of the 16 WWTPs reported above is 458 g PE^{-1} y^{-1} (median: 324 g PE^{-1} y^{-1}). Scaled to COD in the influent, the average emissions were 0.9% with a range of 0.3%-1.7%. The 16 WWTPs have a size between 40,000 and 805,000 PE and the sewage was mostly of domestic origin.

The CH_4 emissions of 177 g PE^{-1} y^{-1} and 420 g PE^{-1} y^{-1} for WWTP-1 and WWTP-2, respectively, lay within the range of the reported literature data of 140 – 1339 g PE^{-1} y^{-1}. Compared to the literature data the emissions of WWTP-1 are on the lower end. In terms of COD in the influent the emissions of 0.7% and 1.5% lie also within the range of the reported literature. Overall, the measured emission observed in our study are in line with investigations conducted previously.

Table S4: Methane emissions per day and scaled to Population Equivalent (PE) and in percent of Chemical Oxygen Demand (COD) from the present study in from the literature

WWTP	PE	kg CH_4 h^{-1}	g CH_4 PE^{-1} y^{-1}	% of COD	Source
Moossee-Urtenenbach	43,534	0.82	166	0.7%	This study
Gürbetal	14,071	0.61	381	1.4%	This study
Göteborg	805,000	31.0	337	0.6%	Samuelsson et al. (2018)
Holbæk	60,000	2.6	380	1.0%	Delre et al. (2017)
Växjö	95,000	10.0	919	1.7%	Delre et al. (2017)
Källby	120,000	8.6	628	1.3%	Delre et al. (2017)
Lundtofte	150,000	2.6	153	0.3%	Delre et al. (2017)
Lynetten	750,000	14.2	165	0.3%	Delre et al. (2017)
Avedøre	265,000	40.5	1,339	NA	Yoshida et al. (2014)
Avedøre	265,000	13.5	446	NA	Scheutz, Fredenslund (2019)
NA	420,000	12.3	257	NA	Scheutz, Fredenslund (2019)
NA	95,000	8.1	747	NA	Scheutz, Fredenslund (2019)
NA	125,000	10.0	701	NA	Scheutz, Fredenslund (2019)
Kralingseveer	360,000	12.6	306	1.3%	Daelman et al. (2012)
Papendrecht	40,000	1.2	266	0.9%	STOWA (2010)
Kortenoord	100,000	1.6	140	0.5%	STOWA (2010)
Kralingseveer	360,000	12.8	310	1.2%	STOWA (2010)
Kralingseveer	360,000	9.5	230	0.8%	STOWA (2010)

5. Measurement data

The processed data from all sites is given in the Supporting information 2.

6. Publication bibliography

Czepiel, Peter M.; Crill, Patrick M.; Harriss, Robert C. (1993): Methane emissions from municipal wastewater treatment processes. In *Environ. Sci. Technol.* 27 (12), pp. 2472–2477. DOI: 10.1021/es00048a025.

Daelman, M. R. J.; van Voorthuizen, E. M.; van Dongen, L. G. J. M.; Volcke, E. I. P.; van Loosdrecht, M. C. M. (2013): Methane and nitrous oxide emissions from municipal wastewater treatment - results from a long-term study. In *Water science and technology : a journal of the International Association on Water Pollution Research* 67 (10), pp. 2350–2355. DOI: 10.2166/wst.2013.109.

Daelman, Matthijs R. J.; van Voorthuizen, Ellen M.; van Dongen, Udo G. J. M.; Volcke, Eveline I. P.; van Loosdrecht, Mark C. M. (2012): Methane emission during municipal wastewater treatment. In *Water research* 46 (11), pp. 3657–3670. DOI: 10.1016/j.watres.2012.04.024.

Delre, Antonio; Mønster, Jacob; Scheutz, Charlotte (2017): Greenhouse gas emission quantification from wastewater treatment plants, using a tracer gas dispersion method. In *The Science of the total environment* 605-606, pp. 258–268. DOI: 10.1016/j.scitotenv.2017.06.177.

eawag (2020): CH4 emissions from the activated sludge tanks conducted with chamber measurements. written to M. Bühler, 3/24/2020.

Häni, Christoph; Bühler, Marcel; Neftel, Albrecht; Ammann, Christof; Kupper, Thomas (2021): Performance of open-path GasFinder3 devices for CH_4 concentration measurements close to ambient levels. In *Atmospheric Measurement Techniques* 14 (2), pp. 1733–1741. DOI: 10.5194/amt-14-1733-2021.

IPCC (2006): 2006 IPCC Guidelines for National Greenhouse Gas Inventories. Volume 4, Agriculture, Forestry and Other Land Use. Edited by H. S. Eggleston, L. Buendia, K. Miwa, T. Ngara, K. Tanabe.

Kupper, Thomas; Häni, Christoph; Neftel, Albrecht; Kincaid, Chris; Bühler, Marcel; Amon, Barbara; VanderZaag, Andrew (2020): Ammonia and greenhouse gas emissions from slurry storage - A review. In *Agriculture, Ecosystems & Environment* 300, p. 106963. DOI: 10.1016/j.agee.2020.106963.

Kvist, Torben; Aryal, Nabin (2019): Methane loss from commercially operating biogas upgrading plants. In *Waste management (New York, N.Y.)* 87, pp. 295–300. DOI: 10.1016/j.wasman.2019.02.023.

Liebetrau, J.; Reinelt, T.; Clemens, J.; Hafermann, C.; Friehe, J.; Weiland, P. (2013): Analysis of greenhouse gas emissions from 10 biogas plants within the agricultural sector. In *Water science and technology : a journal of the International Association on Water Pollution Research* 67 (6), pp. 1370–1379. DOI: 10.2166/wst.2013.005.

Liu, Yan; Cheng, Xiang; Lun, Xiaoxiu; Sun, Dezhi (2014): CH4 emission and conversion from A2O and SBR processes in full-scale wastewater treatment plants. In *Journal of Environmental Sciences* 26 (1), pp. 224–230. DOI: 10.1016/S1001-0742(13)60401-5.

Ren, Y. G.; Wang, J. H.; Li, H. F.; Zhang, J.; Qi, P. Y.; Hu, Z. (2013): Nitrous oxide and methane emissions from different treatment processes in full-scale municipal wastewater treatment plants. In *Environmental technology* 34 (21-24), pp. 2917–2927. DOI: 10.1080/09593330.2012.696717.

Samuelsson, J.; Delre, A.; Tumlin, S.; Hadi, S.; Offerle, B.; Scheutz, C. (2018): Optical technologies applied alongside on-site and remote approaches for climate gas emission quantification at a wastewater treatment plant. In *Water research* 131, pp. 299–309. DOI: 10.1016/j.watres.2017.12.018.

Scheutz, Charlotte; Fredenslund, Anders M. (2019): Total methane emission rates and losses from 23 biogas plants. In *Waste management (New York, N.Y.)* 97, pp. 38–46. DOI: 10.1016/j.wasman.2019.07.029.

STOWA (2010): Emissies van broeikasgassen van RWZI's. Amersfoort, the Netherlands.

Tumendelger, Azzaya; Alshboul, Zeyad; Lorke, Andreas (2019): Methane and nitrous oxide emission from different treatment units of municipal wastewater treatment plants in Southwest Germany. In *PloS one* 14 (1), e0209763. DOI: 10.1371/journal.pone.0209763.

VanderZaag, Andrew C.; Baldé, Hambaliou; Crolla, Anna; Gordon, Robert J.; Ngwabie, N. Martin; Wagner-Riddle, Claudia et al. (2018): Potential methane emission reductions for two manure treatment technologies. In *Environmental technology* 39 (7), pp. 851–858.

Wang, Jinhe; Zhang, Jian; Xie, Huijun; Qi, Pengyu; Ren, Yangang; Hu, Zhen (2011): Methane emissions from a full-scale A/A/O wastewater treatment plant. In *Bioresour. Technol.* 102 (9), pp. 5479–5485. DOI: 10.1016/j.biortech.2010.10.090.

Yoshida, Hiroko; Mønster, Jacob; Scheutz, Charlotte (2014): Plant-integrated measurement of greenhouse gas emissions from a municipal wastewater treatment plant. In *Water research* 61, pp. 108–118. DOI: 10.1016/j.watres.2014.05.014.

Chapter 5

Conclusions and outlook

The main objective of this thesis was to validate the application of the IDM method under real-world conditions. CH_4 emissions from a release experiment inside a barn, a dairy housing, two WWTPs, and four agricultural BGPs were measured with the IDM. The first two studies were used to assess the accuracy of the IDM. The release experiment inside a barn yielded recovery rates lower than 1 that could not be sufficiently explained. In the second study, the difference in emissions between the IDM and iTRM for simultaneous emission intervals was small and within the uncertainty of either of the two methods. The measurements in the third study were conducted to assess the handling of complex source configurations with the IDM and determine emission factors for BGPs and WWTPs. The measurements at the WWTPs allowed to introduce approaches for measurements of complex source configurations. The emissions determined at the WWTPs and the BGPs agree with the data from the literature.

An advantage of the IDM is that long-term measurements are possible. This is of high interest as emissions might have short- and long-term fluctuations. The IDM has its strength to determine mean emissions over a long time period (e.g., weeks or longer). However, it is also possible to detect diurnal cycles, but for this purpose, the expected variation in concentration at the sensor location over the course of a day should be higher than the precision of the concentration measurement device. If a diurnal cycle in the emission of a source is expected, it is important to have sufficient data over the course of a day. Due to lower wind speeds during the night, the data loss in the night is usually higher compared to the day. To counteract the large data loss of the IDM compared to other measurement methods (e.g., TRM), it is advised to measure for at least 10 consecutive days.

Based on all the measurements conducted during this thesis, the following points should be considered for a successful campaign:

- It is of great importance to select the measurement sites according to the requirements of the IDM.
- The turbulence parameters derived from sonic measurements should best reflect the turbulence acting on the dispersion of the emission plume between the source and the downwind concentration measurements.

- The entire plume should be located within the measurement path. Otherwise, the wind direction has a strong influence on the estimated emissions and small deviations between the modelled plume and the real plume will potentially lead to larger biases in the emission data.
- The GasFinders showed a precision about 10 times lower than stated by the manufacturer and, in addition, arbitrary drifts and step changes occurred.
- The GasFinders were usually placed about 100 m downwind of the source location. At this distance the plume is already considerably diluted. To measure a detectable concentration enhancement between the up- and downwind measurements, the source emission should be sufficiently high. It is advised to execute the bLS model in advance and to verify if a concentration enhancement can be detected with the expected level of source emission.
- The quality filtering of the emission data assures that only emission intervals are used that do not substantially deviate from the MOST assumptions. However, the standard quality filter criteria would have led to large data losses. A combination of different filter criteria was introduced that increased the data retention but still excluded obvious erroneous emission measurements.

To further optimise the IDM application, it is suggested to continue with release experiments as done in this thesis.

- A qualitative analysis of the plume is recommended during at least part of the release time to detect unexpected deviations between the modelled and the real plume and for improving the interpretation of the recovery rate. A coarse plume mapping could be done with a drone or a hand-held high-precision measurement device. Such measurements are also of interest for any other measurement campaign.
- Longer path lengths of the GasFinders are advisable in order to be less sensitive to wind direction fluctuations, but this could induce a too low concentration enhancement if the emission level of the source is not high enough.
- Another possible variant of a release experiment is a simultaneous application of GasFinder and sonic measurements at various heights up to 5 m above ground at a fixed distance from the barn (e.g., at 10 times the barn height), to investigate the extent of differences in the recovery rate. However, for such an experiment, two towers are needed to attach the GasFinders and sonics making the experiment cost and labour intensive.
- Additionally, simultaneous measurements with a TRM for various sources are of high interest.

At present, one of the limiting factors of the IDM for CH_4 emission determination are the concentration measurements. To my knowledge, there is only one other open-path device commercially available, which includes variable path lengths of up to several hundred meters. However, the ORION® CH4 (MIRICO, Didcot, UK) is difficult to handle due to its weight and is more expensive compared to a GasFinder. A newer approach for the IDM is using a closed-path measurement device (e.g., Picarro G2509) connected to a sampling line with multiple inlets that simulates an open-path

device as investigated by the Department of Biological and Chemical Engineering at Aarhus University, Denmark*.

To summarise, the IDM can be considered as a reliable measurement method that can be used for emission measurements of various source types with a small emitting surface like slurry stores or large sources like WWTPs. The IDM has the potential to improve knowledge on complex emission sources, and thus, contribute to the improvement of national emission inventories. Moreover, it enables investigation of effects due to mitigation measures and thus might contribute to the reduction of GHG emissions.

*e.g., Lemes, Y., Häni, C., Kamp J.N., Nyord, T., Feilberg, A.: Evaluation of open and closed path sampling for flux estimates with inverse dispersion modelling by controlled ammonia and methane release, in preparation.

Annex

Ammonia and greenhouse gas emissions from slurry storage – A review

Thomas Kupper[1], Christoph Häni[1], Albrecht Neftel[2], Chris Kincaid[3], Marcel Bühler[1,4,5], Barbara Amon[6,7], Andrew VanderZaag[3]

[1]Bern University of Applied Sciences School of Agricultural, Forest and Food Sciences, Switzerland
[2]Neftel Research Expertise, Switzerland
[3]Agriculture and Agri-Food Canada, Canada
[4]Oeschger Centre for Climate Change Research, University of Bern, Switzerland
[5]Institute of Geography, University of Bern, Switzerland
[6]Leibniz Institute for Agricultural Engineering and Bioeconomy (ATB), Germany
[7]University of Zielona Góra, Faculty of Civil Engineering, Architecture and Environmental Engineering, Poland

Agriculture, Ecosystems and Environment, Vol. 300, 106963, 2020

Abstract. Storage of slurry is an important emission source for ammonia (NH_3), nitrous oxide (N_2O), methane (CH_4), carbon dioxide (CO_2) and hydrogen sulfide (H_2S) from livestock production. Therefore, this study collected published emission data from stored cattle and pig slurry to determine baseline emission values and emission changes due to slurry treatment and coverage of stores. Emission data were collected from 120 papers yielding 711 records of measurements conducted at farm-, pilot- and laboratory-scale. The emission data reported in a multitude of units were standardized and compiled in a database. Descriptive statistics of the data from untreated slurry stored uncovered revealed a large variability in emissions for all gases. To determine baseline emissions, average values based on a weighting of the emission data according to the season and the duration of the emission measurements were constructed using the data from farm-scale and pilot-scale studies. Baseline emissions for cattle and pig slurry stored uncovered were calculated. When possible, it was further

distinguished between storage in tanks without slurry treatment and storage in lagoons which implies solid-liquid separation and biological treatment. The baseline emissions on an area or volume basis are: for NH_3: 0.12 g m^{-2} h^{-1} and 0.15 g m^{-2} h^{-1} for cattle and pig slurry stored in lagoons, and 0.08 g m^{-2} h^{-1} and 0.24 g m^{-2} h^{-1} for cattle and pig slurry stored in tanks; for N_2O: 0.0003 g m^{-2} h^{-1} for cattle slurry stored in lagoons, and 0.002 g m^{-2} h^{-1} for both slurry types stored in tanks; for CH_4: 0.95 g m^{-3} h^{-1} and 3.5 g m^{-3} h^{-1} for cattle and pig slurry stored in lagoons, and 0.58 g m^{-3} h^{-1} and 0.68 g m^{-3} h^{-1} for cattle and pig slurry stored in tanks; for CO_2: 6.6 g m^{-2} h^{-1} and 0.3 g m^{-2} h^{-1} for cattle and pig slurry stored in lagoons, and 8.0 g m^{-2} h^{-1} for both slurry types stored in tanks; for H_2S: 0.04 g m^{-2} h^{-1} and 0.01 g m^{-2} h^{-1} for cattle and pig slurry stored in lagoons. Related to total ammoniacal nitrogen (TAN), baseline emissions for tanks are 16 % and 15 % of TAN for cattle and pig slurry, respectively. Emissions of N_2O and CH_4 relative to nitrogen (N) and volatile solids (VS) are 0.13 % of N and 0.10 % of N and 2.9 % of VS and 4.7 % of VS for cattle and pig slurry, respectively. Total greenhouse gas emissions from slurry stores are dominated by CH_4. The records on slurry treatment using acidification show a reduction of NH_3 and CH_4 emissions during storage while an increase occurs for N_2O and a minor change for CO_2 as compared to untreated slurry. Solid-liquid separation causes higher losses for NH_3 and a reduction in CH_4, N_2O and CO_2 emissions. Anaerobically digested slurry shows higher emissions during storage for NH3 while losses tend to be lower for CH_4 and little changes occur for N_2O and CO_2 compared to untreated slurry. All cover types are found to be efficient for emission mitigation of NH_3 from stores. The N_2O emissions increase in many cases due to coverage. Lower CH_4 emissions occur for impermeable covers as compared to uncovered slurry storage while for permeable covers the effect is unclear or emissions tend to increase. Limited and inconsistent data regarding emission changes with covering stores are available for CO_2 and H_2S. The compiled data provide a basis for improving emission inventories and highlight the need for further research to reduce uncertainty and fill data gaps regarding emissions from slurry storage.

Agriculture, Ecosystems and Environment 300 (2020) 106963

Contents lists available at ScienceDirect

Agriculture, Ecosystems and Environment

journal homepage: www.elsevier.com/locate/agee

Ammonia and greenhouse gas emissions from slurry storage - A review

Thomas Kupper[a,*], Christoph Häni[a], Albrecht Neftel[b], Chris Kincaid[c], Marcel Bühler[a,d,e], Barbara Amon[f,g], Andrew VanderZaag[c]

[a] Bern University of Applied Sciences School of Agricultural, Forest and Food Sciences, Laenggasse 85, 3052 Zollikofen, Switzerland
[b] Neftel Research Expertise, 3033, Wohlen b Bern, Switzerland
[c] Agriculture and Agri-Food Canada, 960 Carling Avenue, Ottawa, Ontario, K1A0C6, Canada
[d] Oeschger Centre for Climate Change Research, University of Bern, Hochschulstrasse 4, 3012 Bern, Switzerland
[e] Institute of Geography, University of Bern, Hallerstrasse 12, 3012 Bern, Switzerland
[f] Leibniz Institute for Agricultural Engineering and Bioeconomy (ATB), Max-Eyth-Allee 100, 14469 Potsdam, Germany
[g] University of Zielona Góra, Faculty of Civil Engineering, Architecture and Environmental Engineering, ul. Licealna 9, 65–762 Zielona Góra, Poland

ARTICLE INFO

Keywords:
Store
Cover
Treatment
Emission reduction
Baseline emission
Lagoon

ABSTRACT

Storage of slurry is an important emission source for ammonia (NH_3), nitrous oxide (N_2O), methane (CH_4), carbon dioxide (CO_2) and hydrogen sulfide (H_2S) from livestock production. Therefore, this study collected published emission data from stored cattle and pig slurry to determine baseline emission values and emission changes due to slurry treatment and coverage of stores. Emission data were collected from 120 papers yielding 711 records of measurements conducted at farm-, pilot- and laboratory-scale. The emission data reported in a multitude of units were standardized and compiled in a database. Descriptive statistics of the data from untreated slurry stored uncovered revealed a large variability in emissions for all gases. To determine baseline emissions, average values based on a weighting of the emission data according to the season and the duration of the emission measurements were constructed using the data from farm-scale and pilot-scale studies. Baseline emissions for cattle and pig slurry stored uncovered were calculated. When possible, it was further distinguished between storage in tanks without slurry treatment and storage in lagoons which implies solid-liquid separation and biological treatment. The baseline emissions on an area or volume basis are: for NH_3: 0.12 g m^{-2} h^{-1} and 0.15 g m^{-2} h^{-1} for cattle and pig slurry stored in lagoons, and 0.08 g m^{-2} h^{-1} and 0.24 g m^{-2} h^{-1} for cattle and pig slurry stored in tanks; for N_2O: 0.0003 g m^{-2} h^{-1} for cattle slurry stored in lagoons, and 0.002 g m^{-2} h^{-1} for both slurry types stored in tanks; for CH_4: 0.95 g m^{-3} h^{-1} and 3.5 g m^{-3} h^{-1} for cattle and pig slurry stored in lagoons, and 0.58 g m^{-3} h^{-1} and 0.68 g m^{-3} h^{-1} for cattle and pig slurry stored in tanks; for CO_2: 6.6 g m^{-2} h^{-1} and 0.3 g m^{-2} h^{-1} for cattle and pig slurry stored in lagoons, and 8.0 g m^{-2} h^{-1} for both slurry types stored in tanks; for H_2S: 0.04 g m^{-2} h^{-1} and 0.01 g m^{-2} h^{-1} for cattle and pig slurry stored in lagoons. Related to total ammoniacal nitrogen (TAN), baseline emissions for tanks are 16% and 15% of TAN for cattle and pig slurry, respectively. Emissions of N_2O and CH_4 relative to nitrogen (N) and volatile solids (VS) are 0.13% of N and 0.10% of N and 2.9% of VS and 4.7% of VS for cattle and pig slurry, respectively. Total greenhouse gas emissions from slurry stores are dominated by CH_4. The records on slurry treatment using acidification show a reduction of NH_3 and CH_4 emissions during storage while an increase occurs for N_2O and a minor change for CO_2 as compared to untreated slurry. Solid-liquid separation causes higher losses for NH_3 and a reduction in CH_4, N_2O and CO_2 emissions. Anaerobically digested slurry shows higher emissions during storage for NH_3 while losses tend to be lower for CH_4 and little changes occur for N_2O and CO_2 compared to untreated slurry. All cover types are found to be efficient for emission mitigation of NH_3 from stores. The N_2O emissions increase in many cases due to coverage. Lower CH_4 emissions occur for impermeable covers as compared to uncovered slurry storage while for permeable covers the effect is unclear or emissions tend to increase. Limited and inconsistent data regarding emission changes with covering stores are available for CO_2 and H_2S. The compiled data provide a basis for improving emission inventories and highlight the need for further research to reduce uncertainty and fill data gaps regarding emissions from slurry storage.

* Corresponding author.
E-mail addresses: thomas.kupper@bfh.ch, thomaskupper@sunrise.ch (T. Kupper).

https://doi.org/10.1016/j.agee.2020.106963
Received 17 October 2019; Received in revised form 7 April 2020; Accepted 10 April 2020

1. Introduction

Livestock production systems around the world generate slurry—a mixture of feces and urine from housed livestock, mixed with bedding material and cleaning water (Pain and Menzi, 2011). Storage of slurry is required to enable the spreading in the field at appropriate time to supply nutrients to crops. Thus, a major part of the slurry is transferred from housings to outdoor stores such as tanks (at or above ground level) or earthen lagoons. Stores have variable forms and dimensions (e.g. up to several hectares for lagoons) according to the required storage volume. They have been identified as important emission sources for ammonia (NH_3), hydrogen sulfide (H_2S) and greenhouse gases (GHGs) including nitrous oxide (N_2O), methane (CH_4) and carbon dioxide (CO_2) from livestock production. Slurry stores are complex systems which influence emissions in many ways (Sommer et al., 2006; VanderZaag et al., 2008; Sommer et al., 2013).

A thorough description on principal mechanisms influencing the release of NH_3, GHGs and H_2S from slurry stores can be obtained from several studies (Olesen and Sommer, 1993; Ni, 1999; Sommer et al., 2006; VanderZaag et al., 2008; Sommer et al., 2013). Some important basic principles are summarized here. Slurry stores have a defined area where the gas exchange with the atmosphere takes place. It is a diffusive process and is quantified by emission rate values with the unit mass per area and time. Dissolved species of the gases are produced through microbial breakdown of nitrogen or organic compounds in the bulk slurry. Depending on prevailing chemical equilibria (e.g. NH_3/NH_4^+ which shifts to NH_4^+ at a low pH-value) and absence of microbial consumption, the gases move towards the emitting surface driven by diffusion (i.e. movement due to concentration gradients) and convection where parcels of air or liquid induce a movement of the compounds in the slurry (Sommer et al., 2013). At the slurry-air interface, the compounds pass gas- and liquid-phase resistances and diffuse into the air where they are transported to the atmosphere by convection. Transport within the liquid phase is temperature dependent and the gas-phase transfer is dependent on both temperature and turbulence (VanderZaag et al., 2015). Depending on the dry matter content of the slurry or more precisely, the amount of particles in the slurry which is influenced by the slurry type, animal species, animal diets, the thickness of the slurry bulk layer in the stores and meteorological conditions (Smith et al., 2007), a natural crust at the slurry surface can develop. It constitutes a barrier to the gas molecules between the liquid and the air. NH_3 and CH_4 may be consumed due to microbial activity in the crust leading to an emission reduction (Petersen and Ambus, 2006; Nielsen et al., 2010) while N_2O production may be enhanced (VanderZaag et al., 2009).

Ammonia has a large variety of negative environmental impacts which encompass the quality of air, soil and water, ecosystems and biodiversity. Moreover, it contributes to the formation of particulate matter which impairs human health (Sutton et al., 2011). N_2O and CH_4 are strong GHGs (Myhre et al., 2013). H_2S is often related to odor nuisances and can be lethal to animals and humans at high exposure levels (Sommer et al., 2013). NH_3 and GHG emissions have been regulated by the 1999 Gothenburg Protocol to Abate Acidification, Eutrophication and Ground-level Ozone (UNECE, 1999) and by the Kyoto protocol arising from the UN Framework Convention on climatic change (UN, 1997), respectively. Member countries of these protocols are obliged to calculate and report their national emissions annually, to track changes and compare to national emission ceilings where applicable. The methods for emission reporting are defined in EEA (2016) for NH_3 and in IPCC (2006) for N_2O and CH_4.

EEA (2016); IPCC (2006) and UNECE (2014) provide emission factors for slurry storage or numbers for emission reduction related to mitigation techniques which are used for emission reporting in emission inventories. However, a considerable number of recent studies on emissions from slurry storage provide updated information. The present review paper aims therefore to collect the data on NH_3, GHGs (CH_4, N_2O, CO_2) and H_2S emissions from these recent but also from previous studies and to provide a comprehensive overview on emissions from cattle or pig slurry stored uncovered and emission changes due to slurry treatment and coverage of slurry stores. This information can be used for the purpose of guide values, e.g. for the evaluation of emission data, and for improving emission inventories (greater accuracy, reduced uncertainty), e.g. for the determination of baseline emissions or emission reductions due to slurry treatment or coverage of slurry stores. The compiled data is entirely provided in the Supplementary data 2 for tracking the present or conducting future analyses.

2. Material and methods

2.1. Data search and data selection

A literature research was carried out with Web of Science [5.3] using the following search terms: “storage”, “slurry”, “emission”; “lagoon”, “slurry”, “emission”. These searches were done on January 10, 2018 and yielded 601 papers in total. In a first screening, 290 papers were eliminated because they did not encompass livestock slurry. The remaining 311 articles were retained. In addition, 58 papers were found in the reference list of the screened articles. Therefore, in total, 369 articles were retained for further screening according to the following criteria:

(i) The investigated slurry was produced in an animal operation and consisted of urine and feces excreted from the animals onto a floor of a barn, a hardstanding or a milking parlor. The slurry might contain solids like bedding material or feed residues and be diluted with water. The investigated slurry was untreated or submitted to a treatment such as solid-liquid separation, anaerobic digestion, addition of an acid (acidification), additives or co-substrates. The treatment occurred under real-world conditions or after slurry sampling in the laboratory. Studies based on synthetic slurry, e.g. urine and feces collected separately from animals and subsequently combined in the laboratory, were excluded since fresh animal excretions substantially differ in chemical composition from stored slurry (Table 6). Moreover, urine and feces deposited onto a floor can rapidly undergo processes leading to gaseous losses. Hence, synthetic slurries might induce different emission levels as compared to slurries submitted to real-world conditions.

(ii) The untreated or treated slurry was transferred from the animal operation to a storage tank or a lagoon outside of animal housings and then submitted to measurements under real-world conditions or the slurry as characterized under point (i) was collected from a floor, an underfloor pit or an outside store and subsequently transferred to an experimental vessel where emissions were measured at pilot- or laboratory-scale. Studies encompassing e.g. emissions from a pit below an animal confinement were excluded since such facilities provide an environment which substantially differs from outside stores (e.g. exposure to outdoor climate, disturbance of the slurry surface due to continuous addition of animal excretions over almost the whole area of a pit).

(iii) The reported emission data are based on experimental determination of emission rates as defined by VanderZaag et al. (2008). Studies providing gas concentrations only were excluded.

(iv) The article provides numerical data encompassing emission data or percent differences in emissions between a slurry submitted to a treatment or slurry stored with covering and a reference system with untreated slurry or uncovered storage, respectively.

After evaluation, 120 papers complied with criteria (i) to (iv). 93 papers did not provide numerical data or comply with these criteria but included substantial information on emissions from slurry storage, e.g. basic mechanisms driving emissions. The remaining 156 papers were excluded because they were out of topic or did not provide substantial

information. An overview on the screened papers is in Supplementary data 1.

2.2. Data extraction

Data from the 120 papers were extracted. The parameters as shown in Table 1 were transformed, standardized or aggregated where necessary and then compiled in a database. Overall, 711 records were available for the analysis where one record is defined as an ensemble of entries listed in Table 1 (i.e. multiple records may be created from a single paper). Each record may differ in completeness according to the information provided in a paper.

2.3. Standardization of emission data

Emissions were reported in the papers using numerous units involving the gas molecule (i.e. NH_3, N_2O, CH_4, CO_2 and H_2S) or N, C or S included therein and various units for weight, time and surface or volume. Also, cumulative emissions were given over the entire experimental period. Overall, 36, 22, 31, 13 and 3 different ways for emission reporting were found for NH_3, N_2O, CH_4, CO_2 and H_2S, respectively. Standardization was performed in the present study to obtain comparable values over all records. For all emission rates, the unit g of molecules was used according to UNECE, (2015) and IPCC (2006). An emission on an area basis was applied for NH_3, N_2O, CO_2 and H_2S. For CH_4, the emission relative to the bulk volume was employed. Due to the availability of numerous additional records, data relative to the area were also provided for CH_4. For the area and the volume, the unit m^2

Table 1
Parameters extracted from the papers after transformation or standardization and transferred into the database. Explanations are given for parameters marked with symbols in the table footnote. The complete extracted data are provided in the Supplementary data 2.

Parameter	Explanation
Year	Date the study was published
Country	Location where the study was done
Slurry type	Cattle or pig
Slurry treatment	Untreated, solid-liquid separation, anaerobic digestion, acidification, aeration, addition of additives, dilution with water, addition of co-substrates (also denoted off-farm materials; mostly organic residues from e.g. food industry or energy crops) and combinations of treatments (e.g. solid-liquid separation and anaerobic digestion)
Slurry characteristics	Chemical analysis of the slurry: dry matter (DM), volatile solids (VS), total nitrogen (N_{tot}), ammonium (NH_4^+; TAN (total ammoniacal nitrogen) is often used instead of NH_4^+), total carbon (C), total sulfur (S) in g L^{-1}, pH
Type of study*	Farm-scale, pilot-scale, laboratory-scale
Type of store	For farm-scale studies: tank, lagoon according to Pain and Menzi (2011)**
Replicates	Number of replicates of real-world stores or experimental vessels
Store characteristics	Investigated store surface (m^2), depth (m), and volume (m^3); agitation of slurry (number of agitation events); other producer events or meteorological conditions; slurry temperature (°C)
Experimental conditions	Duration of storage of investigated slurry (days); duration of the study (days); number of measurement periods and total duration of the measurement (hours); season of measurements: cold, temperate, warm; for the determination of the season, the meteorological winter, spring or fall and summer were considered
Meteorological conditions	Air temperature during measurements (°C); air speed over the emitting surface during measurements (m s^{-1}); rainfall (cumulative amount during measurements in mm)
Measurement methods applied	Measurement method for the gases: dispersion modeling based on a backward Lagrangian stochastic (bLS) dispersion model or UK-ADMS atmospheric dispersion model, flux chamber method, flux gradient method, micrometeorological mass balance method (e.g. integrated horizontal flux, IHF; vertical radial plume mapping, VRPM), sampling at exhaust chimney, tracer gas method, method not further defined; instrument used for the concentration measurements of the gases
Cover type	Storage uncovered or covered; For covered storage: cover type according to VanderZaag et al. (2015): impermeable structural covers: lid (wood or concrete), tent covering; impermeable floating covers: plastic film; permeable synthetic floating covers: plastic fabrics, expanded clay, other materials such as expanded polystyrene, plastic tiles; permeable natural floating covers: peat, straw, vegetable oil, other organic materials (wood chips, sawdust etc.), other cover types such as storage bag
Occurrence of a natural crust at the store's surface	Formation of natural crust: yes or no, crust thickness (cm), time for natural crust formation (days)***
Measurement data****	NH_3 (g NH_3 m^{-2} h^{-1}, g NH_3 m^{-3} h^{-1}, g NH_3 AU^{-1} h^{-1}), NH_3-N in % TAN and in % N, N_2O (g N_2O m^{-2} h^{-1}, g N_2O m^{-3} h^{-1}, g N_2O AU^{-1} h^{-1}), N_2O-N in % TAN and % N, CH_4 (g CH_4 m^{-2} h^{-1}, g CH_4 m^{-3} h^{-1}, g CH_4 AU^{-1} h^{-1}), CH_4-C % VS, CO_2 (g CO_2 m^{-2} h^{-1}, g CO_2 m^{-3} h^{-1}, g CO_2 AU^{-1} h^{-1}), CO_2-C in % VS, CO_2eq (g CO_2eq m^{-2} h^{-1}, g CO_2eq m^{-3} h^{-1}, g CO_2eq AU^{-1} h^{-1}), H_2S (g H_2S m^{-2} h^{-1}, g H_2S m^{-3} h^{-1}, g H_2S AU^{-1} h^{-1}); Difference between untreated and treated slurry or between slurry stored uncovered and stored covered in percent for NH_3, N_2O, CH_4, CO_2, CO_2eq, H_2S

* Type of study: Farm-scale: measurements carried out at real-world storage facilities at a farm site. This information could be obtained from the description of the experimental setup given in the papers. Pilot-scale and laboratory-scale: measurements conducted under controlled conditions in experimental vessels. Due to a lack of definition for these study types, a discrimination according to the following characteristics was employed: Pilot-scale: volume of slurry investigated: ≥ 500 L with experimental vessels situated outdoors, with or without a shelter and submitted to ambient meteorological conditions. Laboratory-scale: volume of slurry investigated: < 500 L. Most of the studies defined as laboratory-scale studies were conducted indoors in a temperature-controlled room. Three studies deviated from the conditions regarding study situation or temperature control and for four studies, this information was not available (Supplementary data 2). Despite these gaps in information, the studies were retained.

** A tank is a large, normally open-top, in most cases circular vessel made from pre-fabricated vitreous enameled steel, concrete or wood panels charged from a reception pit and emptied using a pump. It is a facility constructed at or below ground level and may extend above ground with a depth of several meters. Earthen storage basins not designed for biological treatment of slurry are considered as stores equivalent to tanks. Like earthen storage basins, a lagoon is a large rectangular or square shaped structure with sloping earth bank walls and may be lined with water impermeable material. Lagoons are designed for both storage and biological treatment (Pain and Menzi, 2011). They are not emptied below a specific depth necessary for slurry treatment except for maintenance (Hamilton et al., 2001).

*** We did not consider a natural crust as a mitigation technique equivalent to covering of slurry stores. The significance of crusting and considerations regarding distinction between crusting and storage covering are specifically addressed in Section 4.2.4.

**** For units: see Section 2.3. Acronyms: AU: animal unit = animal with a live weight of 500 kg; CO_2eq: carbon dioxide equivalent. CO_2eq is a standardized unit for different greenhouse gases. The numbers reported rest on data provided by the authors of the papers which were mostly based on IPCC (2007); TAN: total ammoniacal nitrogen; N: nitrogen; VS: volatile solids.

and m^3 was used, respectively. For all gases, the time unit hour was applied (reasons are given in section 4.1). Where useful for inventories, the time unit year was additionally provided for emissions. In this paper, the emission data standardized as explained above are denoted emission on an area or volume basis.

Since emission inventories do usually not apply emissions on an area or volume basis but emission factors which express emissions as a proportion of a compound present in the slurry store, data were additionally scaled as follows: percent of TAN for ammonia (EEA, 2016), percent of N for N_2O (IPCC, 2006) and percent of VS for CH_4 (IPCC, 2006) and CO_2. To be consistent with the notion "emission on an area or volume basis" regarding terminology, we used the term flow-based emission. Flow-based emissions were either taken from the papers or determined based on the emission rate, the N, TAN or VS content of the slurry, the volume of the store and the duration of the experiment. Dividing the cumulative emission which was derived from the emission rate and the duration of the study by the amount of the compounds present in the store at the beginning of the experiment (derived from the slurry content of N, TAN or VS and the slurry volume) yielded the flow-based emission. It was only calculated if no slurry addition or discharge occurred during the experiment.

2.4. Data analysis

2.4.1. Descriptive statistics of the emission data

In a first step, descriptive statistics (number of records, minimum, 1 st quantile, median, average, 3rd quantile, maximum, standard deviation) were calculated over all records encompassing slurry stored uncovered. There were eight categories for data reporting resulting from the combination of two slurry types (cattle and pig) with four study types (farm-scale lagoon comprising solid-liquid separation and biological treatment of slurry; farm-scale tank, pilot-scale and laboratory-scale which include untreated slurry).

2.4.2. Baseline emissions

2.4.2.1. Definition. We define the term baseline emission as the average emission occurring with slurry storage according to the reference technology without emission control similar to VanderZaag et al. (2015). This implies uncovered storage in the following types of store: i) tanks or earthen stores without slurry treatment; ii) lagoons with solid-liquid separation and biological treatment occurring during storage (Hamilton et al., 2001). The baseline emission is considered as representative for average emissions over the whole course of a year. According to EEA (2016), baseline emissions are given separately for cattle and pig slurry. We further distinguished between storage in tanks (or earthen stores) and lagoons. Baseline emissions were calculated from uncovered slurry stores regardless of the occurrence of a natural crust because its formation can be only partially controlled and thus varies widely between stores (Smith et al., 2007). Moreover, there was insufficient information about the presence of crusts in the data impeding a distinction between crusted and non-crusted store's surfaces.

2.4.2.2. Determination. Baseline emissions were calculated using farm-scale and pilot-scale studies published in peer-review papers. For the calculation of representative emissions, important influencing factors should be considered such as the meteorological conditions (mainly air temperature, wind speed, precipitation) and operations at storage facilities (Sommer et al., 2013). Among these factors, we were able to include air temperature since the season used for emission measurements which can be used as surrogate for the temperature was available for more than 90% of the records. Records were dropped where conditions prevailed which are not representative for slurry storage in practice over a longer period, e.g. if daily agitation of slurry occurred. More detailed information on meteorological conditions and operations at storage facilities was not available and could not be included in the evaluation of emissions (e.g. only approx. 60% of records provided numerical air temperature data). Information on wind speed, precipitation and crust formation was available for less than half of the records.

We hypothesized that for generating emission data which are representative over the whole course of a year, emission values generated during the cold, the warm and the temperate season (spring, fall) should be equally covered. To achieve this, a weighting of the emission data for season was done. Values were aggregated according to the categorization "Season code" ("c": cold season = winter, "t": temperate season = spring or fall, "w": warm season = summer, "c,t": cold and temperate season, "c,w": cold and warm season, "t,w": temperate and warm season, "c,t,w": cold, temperate and warm season), "Slurry type" (cattle, pig), "Type of study" (farm-scale, pilot-scale) and "Type of store" (for farm-scale studies: lagoon, tank). For some papers, emission values for each individual season "c", "t", and "w" were provided and also the average value over the year, i.e. the "c,t,w" value. In these cases, the "c,t,w" value is denoted as redundant in the database (Supplementary data 2). It was used for the further calculations and not the values of the individual seasons. The aggregated values were averaged afterwards in the following manner:

i) Study duration varied considerably, i.e. individual experiments ranged from less than one day up to several months. The individual records were thus weighted according to measurement durations of records within each "Season code" category. The individual records were aggregated to four classes of measurement durations: a) ≥1 month, b) ≥1 week to < 1 month, c) ≥1 day to < 1 week, d) < 1 day. Weighting was done based on the square-root of the median of the measurement duration for each class to avoid over-emphasis of long-term measurements. The median values of the measurement duration for the 4 classes a, b, c and d were 146.5 days, 16.9 days, 4.5 days and 0.34 days, respectively. This implied the following respective weights 12.1, 4.1, 2.1 and 0.6. Therefore, a record based on a measurement of more than one month received a weighting 20.8 times higher than a record based on a measurement over less than a day.
ii) Average values for each season "c", "t" and "w" were calculated from all available values within one category (based on "Slurry type", "Type of study" and "Type of store"). Averaging was done in a way that values spanning over more than one season were attributed to the respective seasons, i.e. a value for "c,t" was attributed half to "c" and half to "t", a value of "c,t,w" was counted one fourth to seasons "c" and "w" and one half to season "t". For example, to average a "c" value based on a 2 weeks measurement (c_{2weeks}), a "c" value based on a 2 days measurement (c_{2days}) and a "c,w" value that based on a 2 months measurement ($cw_{2months}$) led to the following average "c" value: $"c_{avg}" = (c_{2weeks}*weight_{2weeks} + c_{2days}*weight_{2days} + cw_{2months}*0.5*weight_{2months})/(weight_{2weeks} + weight_{2days} + 0.5*weight_{2months})$.
iii) These average values were further averaged to annual emission rates "c,t,w" by weighting the value for season code "t" twice as high as the seasons "c" and "w" (i.e. $"c,t,w_{avg}" = ¼*"c" + ½*"t" + ¼*"w"$) since the temperate season code "t" includes two seasons (spring and fall). These final averaged values are listed in column "Avg" in Tables 8, 9 and Supplementary data 4.

Numbers for baseline emissions are reported as average emission values if at least one record for each of the season "c", "t" and "w" was available. Included can be a record from an individual season (i.e. "c", "t" or "w"), or any kind of seasons combination (i.e. "c,t" "c,w" "t,w" or "c,t,w"). The lower and upper 95% confidence bounds (l95, u95) for baseline emissions were determined using bias-corrected and accelerated bootstrap intervals (Efron, 1987) if at least three individual records for each of the season "c", "t" and "w" were available. Again, this can be in the form of an individual season or any kind of seasons

combination as for the calculation of the average. The bootstrapping was done as non-parametric bootstrapping with sampling stratified by season. To test whether there are significant ($p < 0.05$) differences in these baseline emission values, 95% confidence intervals were obtained from bootstrapping the differences between each combination of values. If a confidence interval of a difference did not include 0, the difference was marked as statistically significant.

The data resulting from this procedure related to emissions on an area or volume basis were aggregated according to the slurry type (cattle and pig) and the study types farm-scale tank and pilot-scale and for the two study types combined which were denoted as baseline emissions tank. The baseline emissions for lagoons are based on measurements carried out at farm-scale for lagoons. Baseline emissions expressed as flow-based emissions were given separately for cattle and pig slurry for tanks only due to a lack of appropriate data for lagoons. The calculation procedure is additionally illustrated based on an example in the Supplementary data 9.

2.4.3. Emissions and emission changes due to slurry treatment and covering of slurry stores

We determined the emission changes due to slurry treatment techniques and covering of slurry stores using records with a treatment or a cover and a reference system (uncovered storage with untreated slurry) to compare the emissions on an area or volume basis from both. Due to the limited number of available records, the restriction to peer review papers and exclusion of laboratory-scale studies was not applied. For storage covering, all records with less than 20 cm of slurry depth were excluded from the data analysis since it is likely that such conditions differ too much from the real-world and even more evident if the thickness of the cover material is similar to that of the bulk slurry layer. Studies where slurry depth was not provided were excluded.

Although a natural crust is often listed as abatement measure together with slurry store covers (Bittman et al., 2014) we did not consider it as a mitigation technique equivalent to covering of slurry stores. In contrast to coverings such as impermeable floating covers, it is not applicable for all stores since it does not form at each slurry type. Crusting was neither considered for the analysis on emission changes due to slurry treatment and covering of slurry stores because of insufficient information about the presence of crusts in the experimental data. The significance of crusting is specifically addressed in Section 4.2.4.

The numbers from different studies were aggregated without a weighting for season or measurement duration due to the limited number of records. We tested whether the differences between treatments or covers and the reference system (untreated slurry or uncovered storage) were significantly different from zero by a two-sided t-test.

3. Results

3.1. Characterization of the database

3.1.1. General characteristics

The literature review yielded a total of 711 records. Among them, 13% were from before 2000. The period between 2000 and 2010 contributed 43%, and 44% were published after 2010 (Table 2). US and CA generated 28% and 19%, respectively, of the records while 11 European countries provided 48%. Two countries from Asia and Oceania contributed 3% and 2% of the records. Ammonia was studied in 38% of the records, while 59% were on GHGs, and 3% on H_2S. Among GHGs, CH_4 was most often investigated with a share of 30% of all records. 47% of the records included one gas and 53% several gases.

Table 3 shows the types of studies. A share of 46% of the records are based on studies conducted at farm-scale. Pilot-scale studies contributed 31% and laboratory-scale 23% of the records. Records from pilot-scale studies are similarly represented over all three periods before 2000, between 2000 and 2010 and after 2010. In contrast, data from farm-scale studies and conducted in the laboratory occur more frequently from 2000 onwards.

An overview of the investigated slurry types is shown in Table 4. Cattle and pig slurry each account for about 50% of the investigated slurries. Cattle slurry mostly originated from dairy cows while for pig slurry fattening pigs and breeding pigs or a mixture of both was studied. Other types of slurry were included in measurements as well, but these occur much less. The proportion of untreated slurries is 65% and 87% for cattle slurry and pig slurry, respectively. Solid-liquid separation occurs for 16% (cattle slurry) and 3.7% (pig slurry) of the records. Anaerobic digestion of unseparated slurry applies for 7.2% (cattle slurry) and 3.7% (pig slurry) of the records while for anaerobically digested and separated slurry, the numbers are 8.1% for cattle slurry and 0.6% for pig slurry, respectively. Other treatments encompass acidification, aeration, supplementation with additives or dilution of slurry, but these treatments occur less.

Approximately 140 records compare the emissions between covered and uncovered storage. More than 80% of these data are from pilot and laboratory studies. Straw covers and other natural materials such as wood chips or maize stalks were most often investigated (51 in total). Also, cover types such as a lid, plastic film and fabrics were frequently addressed resulting in approximately 15 records for each.

Measurement methods employed in the experiments are shown in Table 5. Roughly, two thirds of all measurements were carried out using a flux chamber method. While this is almost the only option for pilot- and laboratory-scale studies, this system was also used for approximately 30% of the measurements conducted at farm sites. Methods like dispersion modeling or micrometeorological mass balance method make up about 60% of the records from farm-scale studies. Other methods e.g. using a tracer gas were rarely applied.

Slurry analyses are shown in Table 6. Not all studies provided analytical data of the slurry (e.g., only 84% of NH_3 studies presented TAN values). While most laboratory studies analyzed TAN, only 67% of the studies carried out at farm sites reported this parameter. Pilot-scale studies lie in between with 92% of records reporting TAN data. The availability of analytical data is similar for other parameters (e.g. DM) as for TAN but with somewhat lower numbers. The composition of the mixture of urine and feces as excreted by animals published by ASAE (2005) and Richner et al. (2017) is added at the bottom of Table 6. They provide numbers for cattle on DM, VS and TAN in the range of 80 to 90 g L^{-1}, 53 to 70 g L^{-1} and 1.4 to 2.1 g L^{-1}, respectively. For pigs, the values for DM, VS and TAN are in the range of 50 to 90 g L^{-1}, 36 g L^{-1} and 3.4 to 5.0 g L^{-1}. The slurry analyses given in the records show substantially lower numbers for DM and VS contents for untreated slurries which is most likely due to dilution with water from farm operation and rainfall at the farms (Table 6). Studies at farm-scale based on tanks, at pilot-scale and at laboratory-scale exhibit DM contents which are in a similar range within cattle and pig slurry. Numbers for DM are lower for pig slurries compared to cattle slurry except for laboratory scale studies. Pig slurry exhibits higher N_{tot} and TAN contents than cattle slurry. Within farm-scale studies, the numbers for all analytes strongly differ between slurry from tanks and from lagoons. Values for DM, VS, N_{tot} and TAN are lower for lagoons by a factor of approximately two to eight as compared to slurry stored in tanks. Slurries from lagoons compare better with slurries after solid-liquid separation (Table 6) than with untreated slurries.

3.1.2. Descriptive statistics of emission data from cattle and pig slurry stored uncovered

Descriptive statistics are shown in Table 7 for NH_3, N_2O, CH_4, CO_2 and H_2S over all records encompassing untreated cattle and pig slurry stored uncovered from studies conducted at farm-, pilot- and laboratory-scale (farm-scale studies with lagoons include biologically treated and separated slurry; see section 2.4.2.1). Data from measurements conducted during warm, temperate and cold seasons are unevenly

Table 2
Number of records listed by country and year of publication and share of total records by country.

Country	Before 2000		2000 to 2010		After 2010		total			Share of total
	Cattle	Pig	Cattle	Pig	Cattle	Pig	Cattle	Pig	Cattle and pig	
AT	0	0	15	6	0	0	15	6	21	3%
AU	0	0	0	0	0	4	0	4	4	1%
CA	1	1	47	10	72	5	120	16	136	19%
CN	0	0	0	0	0	17	0	17	17	2%
DE	8	9	4	2	0	0	12	11	23	3%
DK	20	17	0	0	6*	14	22	35	57	8%
ES	0	0	0	0	1	0	1	0	1	0.1%
FR	0	0	2	33	0	6	2	39	41	6%
IT	0	0	23	32	12	12	35	44	79	11%
JP	0	0	0	0	3	0	3	0	3	0.4%
LT	0	0	0	0	0	21	0	21	21	3%
NL	13	11	4	4	0	0	17	15	32	5%
NZ	6	0	1	1	2	0	9	1	10	1%
PT	0	0	4	0	4	8	8	8	16	2%
SE	0	0	1	0	6	3	7	3	10	1%
UK	1	3	13	2	6	13	20	18	38	5%
US	1	3	13	86	74	25	88	114	202	28%
Total	50	44	127	176	182	132	359	352	711	100%
Share of total	13%		43%		44%		100%			

* Cattle slurry with addition of other types of manure and feedstock materials.

Table 3
Number of records classified by type of study (farm-scale, pilot-scale, laboratory-scale) and time periods of publication and in percent of the total.

Type of study	Before 2000	2000 - 2010	After 2010	Total	Share of study types
Farm-scale	27	157	141	325	46%
Pilot-scale	54	75	90	219	31%
Laboratory-scale	13	77	77	167	23%
Total	94	309	308	711	100%
Publication of study types over time (in percent of total)					
Farm-scale	8%	48%	43%	100%	
Pilot-scale	25%	34%	41%	100%	
Laboratory-scale	8%	46%	46%	100%	

Table 4
Overview on investigated slurry types stored uncovered or covered: number of records listed by slurry treatments, slurry types and share of the total records in percent.

Slurry treatment	Cattle n	Pig	Other*	Cattle Percent of total	Pig	Other*
Untreated	233	302	–	65%	87%	–
Solid-liquid separation	57	13	–	16%	3.7%	–
Anaerobic digestion	26	13	–	7.2%	3.7%	–
Anaerobic digestion, solid-liquid separation	29	2	4	8.1%	0.6%	100%
Acidification	5	3	–	1.4%	0.9%	–
Acidification, anaerobic digestion	–	2	–	–	0.6%	–
Acidification, anaerobic digestion, solid-liquid separation	–	1	–	–	0.3%	–
Acidification, solid-liquid separation	–	1	–	–	0.3%	–
Dilution	5	2	–	1.4%	0.6%	–
Addition of additives	3	3	–	0.8%	0.9%	–
Aeration	1	4	–	0.3%	1.1%	–
Aerobic treatment	–	2	–	–	0.6%	–
Total	359	348	4	100%	100%	100%

* Cattle slurry with addition of other types of manure and feedstock materials.

Table 5
Number of records classified by the measuring method and by the type of study.

Measuring method	Farm-scale	Pilot-scale	Laboratory-scale	Total	
Dispersion modeling based on bLS* or ADMS**	107	2		109	15%
Dispersion modeling based on bLS* and VRPM***	8			8	1.1%
Flux chamber method	98	213	167	478	67%
Flux gradient method	4			4	0.8%
Micrometeorological mass balance method	92			92	13%
Sampling at exhaust chimney	4			4	0.6%
Tracer gas method	7			7	1.0%
Method not defined	5	4		9	1.3%
Total	325	219	167	711	100%

* backward Lagrangian stochastic (bLS) dispersion model.
** UK-ADMS atmospheric dispersion model (Hill et al., 2008).
*** Vertical Radial Plume Mapping.

distributed over all records (Supplementary data 3). The minimum and maximum emission values differ by one to several orders of magnitude for all gases. The average often exceeds the median by a factor of two or more which is most pronounced for N_2O. This indicates a distribution of data being right skewed by high values. The variability of data and the occurrence of high maximum values is most pronounced for laboratory-scale studies. Striking high values exceeding the median by at least one order of magnitude for NH_3, CH_4 and CO_2 are reported in the laboratory-scale study of Guarino et al. (2006). For N_2O, high values were found from three studies conducted at farm- and pilot-scale (Clemens et al., 2006; Amon et al., 2007; Leytem et al., 2011) (Supplementary data 2,8,11). For H_2S, one figure from a laboratory-scale study stands out which exceeds all other values by two orders of magnitude (Hobbs et al., 1999).

Table 6
Number of records of a slurry type (cattle, pig), type of study (f: farm-scale; p: pilot-scale; l: laboratory-scale), type of store for farm-scale studies, and slurry treatment (untreated, sol-liq sep: solid-liquid separation) in the database. Number of records (n) with analytical data on DM, VS, N_{tot}, TAN and average contents of DM, VS, N_{tot}, TAN in g L^{-1} for untreated slurry.

Slurry type	Type of study*	Type of store	Slurry treatment**	Total number of records	DM	VS	N_{tot}	TAN	DM	VS	N_{tot}	TAN
				n	n				g L^{-1}			
Cattle	f	lagoon	untreated	73	19	7	13	14	17	3.7	1.2	0.2
Cattle	f	tank	untreated	39	21	9	19	25	67	48	3.1	1.5
Cattle	p		untreated	106	97	36	93	97	62	53	3.2	1.6
Cattle	l		untreated	35	31	24	29	31	57	43	3.0	1.3
Pig	f	lagoon	untreated	109	19	23	50	76	9.7	4.5	0.8	0.6
Pig	f	tank	untreated	55	35	9	33	35	42	37	3.3	1.9
Pig	p		untreated	63	56	30	56	54	50	33	4.6	3.2
Pig	l		untreated	68	68	43	64	64	59	56	4.7	2.9
Cattle	f tank, p, l		sol-liq sep	23	19	10	17	17	39	29	2.4	1.2
Pig	f tank, p, l		sol-liq sep	14	10	5	8	12	29	23	3.8	2.3
Cattle	Contents of mixture of urine and feces obtained from ASAE (2005)								*80*	*53*	*3.0*	*1.4*
Pig									*61-90*	*n.a.*	*4.7-7.0*	*3.4-5.0*
Cattle	Contents of mixture of urine and feces obtained from Richner et al. (2017)								*90*	*70*	*3.9*	*2.1*
Pig									*50*	*36*	*6.5*	*4.6*

n.a.: not available.
* f: farm-scale; p: pilot-scale; l: laboratory-scale.
** sol-liq sep: solid-liquid separation.

Table 7
Emissions from cattle and pig slurry stored uncovered in tanks at farm-scale, pilot-scale and laboratory-scale without slurry treatment and in lagoons with solid-liquid separation and biological treatment; descriptive statistics for NH_3, N_2O, CH_4, CO_2 and H_2S in g m^{-2} h^{-1} or g m^{-3} h^{-1}. n: number of records; Min: minimum; 1 st Qu: first quartile; 3 st Qu: third quartile; Max: maximum; Std: standard deviation. Additional information is provided in Supplementary data 3.

Slurry type	Study type		n	Min	1 st Qu	Median	Average	3rd Qu	Max	Std
				NH_3 g m^{-2} h^{-1}						
Cattle	Farm-scale	lagoon	35	< 0.01	0.03	0.10	0.13	0.21	0.36	0.11
Cattle	Farm-scale	tank	20	0.02	0.04	0.06	0.13	0.16	0.68	0.15
Cattle	Pilot-scale		53	< 0.01	0.03	0.07	0.09	0.11	0.44	0.08
Cattle	Laboratory-scale		19	< 0.01	0.02	0.04	0.26	0.33	1.4	0.43
Pig	Farm-scale	lagoon	74	< 0.01	0.04	0.08	0.15	0.18	0.68	0.18
Pig	Farm-scale	tank	23	0.03	0.06	0.10	0.22	0.27	1.0	0.26
Pig	Pilot-scale		22	0.01	0.06	0.20	0.24	0.26	0.92	0.23
Pig	Laboratory-scale		20	< 0.01	0.03	0.23	0.69	0.71	4.5	1.16
				N_2O g m^{-2} h^{-1}						
Cattle	Farm-scale	lagoon	13	< 0.001	< 0.001	< 0.001	0.002	0.001	0.02	0.006
Cattle	Farm-scale	tank	3	< 0.001	0.001	0.002	0.002	0.003	0.003	0.002
Cattle	Pilot-scale		46	< 0.001	< 0.001	0.001	0.003	0.004	0.04	0.007
Cattle	Laboratory-scale		6	< 0.001	< 0.001	< 0.001	0.005	0.001	0.03	0.01
Pig	Farm-scale	lagoon	6	< 0.001	< 0.001	< 0.001	0.003	0.002	0.01	0.005
Pig	Farm-scale	tank	5	Not detected						
Pig	Pilot-scale		17	< 0.001	< 0.001	< 0.001	0.01	0.001	0.06	0.02
Pig	Laboratory-scale		4	< 0.001	< 0.001	< 0.001	0.003	0.003	0.01	0.006
				CH_4 g m^{-3} h^{-1}						
Cattle	Farm-scale	lagoon	3	0.27	0.29	0.30	0.77	1.0	1.7	0.83
Cattle	Farm-scale	tank	7	< 0.01	0.26	0.75	0.83	1.3	1.9	0.71
Cattle	Pilot-scale		46	0.01	0.07	0.42	0.56	0.75	3.6	0.69
Cattle	Laboratory-scale		15	< 0.01	0.15	0.64	10	16	51	16
Pig	Farm-scale	lagoon	2	< 0.01	0.88	1.8	1.8	2.6	3.5	2.5
Pig	Farm-scale	tank	10	0.02	0.25	0.55	1.6	3.1	5.0	1.8
Pig	Pilot-scale		21	0.01	0.13	0.18	0.77	1.0	3.4	1.1
Pig	Laboratory-scale		18	0.02	1.3	2.9	7.4	6.6	33	10
				CO_2 g m^{-2} h^{-1}						
Cattle	Farm-scale	lagoon	18	0.27	1.9	2.3	4.7	5.3	27	6.4
Cattle	Farm-scale	tank	3	11	11	11	16	18	25	8.1
Cattle	Pilot-scale		15	0.17	2.8	4.3	5.6	6.3	21	5.2
Cattle	Laboratory-scale		14	0.45	2.4	8.0	86	189	332	120
Pig	Farm-scale	lagoon	7	< 0.01	< 0.01	0.03	0.89	0.74	4.7	1.8
Pig	Farm-scale	tank	1	5.7	5.7	5.7	5.7	5.7	5.7	–
Pig	Pilot-scale		7	3.2	3.6	4.4	6.6	9.0	13	4.1
Pig	Laboratory-scale		14	1.0	6.3	9.1	52	80	217	75
				H_2S g m^{-2} h^{-1}						
Cattle	Farm-scale	lagoon	3	0.02	0.04	0.06	0.05	0.07	0.07	0.03
Cattle	Laboratory-scale		3	< 0.01	< 0.01	0.01	0.01	0.01	0.02	0.01
Pig	Farm-scale	lagoon	14	< 0.01	< 0.01	< 0.01	0.01	0.03	0.08	0.02
Pig	Laboratory-scale		6	< 0.01	< 0.01	< 0.01	0.47	0.02	2.8	1.1

Table 8
Emissions on an area or volume basis from cattle and pig slurry stored uncovered in tanks at pilot-scale and at farm-scale without slurry treatment and in lagoons with solid-liquid separation and biological treatment. Baseline emissions for storage in tanks and lagoons given in g m^{-2} h^{-1} / kg m^{-2} y^{-1} for NH_3, N_2O and CO_2 and in g CH_4 m^{-3} h^{-1} / kg CH_4 m^{-3} y^{-1}. n: number of records after aggregation; Avg: average; l95, u95: lower and upper 95% confidence bounds; cells denoted with "-": value is not available; #: values denoted with different letters are significantly different ($p < 0.05$). Detailed information is provided in Supplementary data 4.

Slurry type	Study type/baseline emissions		n	Avg	l95	u95	#	Avg yearly amount
				NH_3 g m^{-2} h^{-1}				NH_3 kg m^{-2} y^{-1}
Cattle	Pilot-scale studies		34	0.08	0.07	0.09	a	–
Cattle	Farm-scale studies	tank	11	0.09	0.05	0.13	ab	–
Cattle	**Baseline emissions***	**lagoon**	**28**	**0.12**	0.10	0.15	**bc**	**1.1**
Cattle	**Baseline emissions****	**tank**	**45**	**0.08**	0.07	0.09	**a**	**0.67**
Pig	Pilot-scale studies		15	0.24	0.15	0.38	def	–
Pig	Farm-scale studies	tank	8	0.23	0.13	0.37	cdef	–
Pig	**Baseline emissions***	**lagoon**	**40**	**0.15**	0.12	0.19	**ce**	**1.3**
Pig	**Baseline emissions****	**tank**	**23**	**0.24**	0.17	0.34	**f**	**2.1**
				N_2O g m^{-2} h^{-1}				N_2O kg m^{-2} y^{-1}
Cattle	Pilot-scale studies		33	0.002	0.001	0.002	a	–
Cattle	Farm-scale studies	tank	–	–	–	–	–	–
Cattle	**Baseline emissions***	**lagoon**	**11**	**< 0.001**	–	–	–	**< 0.01**
Cattle	**Baseline emissions****	**tank**	**35**	**0.002**	**0.001**	**0.002**	**a**	**0.02**
Pig	Pilot-scale studies		12	0.002	< 0.001	0.005	a	–
Pig	Farm-scale studies	tank	2	< 0.001	–	–	–	–
Pig	**Baseline emissions***	**lagoon**	–	–	–	–	–	–
Pig	**Baseline emissions****	**tank**	**14**	**0.002**	**< 0.001**	**0.005**	**a**	**0.01**
				CH_4 g m^{-3} h^{-1}				CH_4 kg m^{-3} y^{-1}
Cattle	Pilot-scale studies		35	0.49	0.38	0.70	a	–
Cattle	Farm-scale studies	tank	6	1.2	0.88	1.5	b	–
Cattle	**Baseline emissions***	**lagoon**	**3**	**0.95**	**0.40**	**1.5**	ab	**8.3**
Cattle	**Baseline emissions****	**tank**	**41**	**0.58**	**0.46**	**0.76**	a	**5.1**
Pig	Pilot-scale studies		16	0.67	0.38	1.1	a	–
Pig	Farm-scale studies	tank	3	0.76	–	–	–	–
Pig	**Baseline emissions***	**lagoon**	**1**	**3.5**	–	–	–	**31**
Pig	**Baseline emissions****	**tank**	**19**	**0.68**	**0.41**	**1.1**	a	**6.0**
				CO_2 g m^{-2} h^{-1}				CO_2 kg m^{-2} y^{-1}
Cattle	Pilot-scale studies		6	7.0	–	–	–	–
Cattle	Farm-scale studies	tank	–	–	–	–	–	–
Cattle	**Baseline emissions***	**lagoon**	**14**	**6.6**	**2.6**	**17**	–	**58**
Cattle	**Baseline emissions****	**tank**	**8**	**8.0**	–	–	–	**70**
Pig	Pilot-scale studies		4	8.8	–	–	–	–
Pig	Farm-scale studies	tank	1	5.7	–	–	–	–
Pig	**Baseline emissions***	**lagoon**	**3**	**0.30**	–	–	–	**2.7**
Pig	**Baseline emissions****	**tank**	**5**	**8.0**	–	–	–	**70**

Cells denoted with "-": value is not available.
* Baseline emissions lagoon are entirely based on values from farm-scale studies lagoon.
** Based on the average from studies at farm-scale tank and pilot-scale.

3.2. Baseline emissions

3.2.1. Emissions on an area or volume basis

Table 8 shows emissions on an area or volume basis from cattle and pig slurry stored uncovered in tanks at farm-scale and at pilot-scale without slurry treatment and in lagoons with solid-liquid separation and biological treatment for NH_3, N_2O, CH_4 and CO_2. Average NH_3 emissions from farm-scale studies conducted at lagoons are higher than those from tanks for cattle slurry but lower for pig slurry. Pilot-scale studies exhibit similar emissions as farm-scale studies conducted at tanks, but they differ when compared to measurements from lagoons. The range between the lower and upper 95% confidence bounds is relatively small for cattle slurry but large for pig slurry with the greatest range for farm-scale studies from tanks (0.13 to 0.37 g NH_3 m^{-2} h^{-1}). The baseline emission for lagoons is 0.12 g NH_3 m^{-2} h^{-1} and 0.15 g NH_3 m^{-2} h^{-1} for cattle and pig slurry, and for tanks 0.08 g NH_3 m^{-2} h^{-1} and 0.24 g NH_3 m^{-2} h^{-1} for cattle and pig slurry, respectively. Baseline emissions given as a yearly average emitted amount for lagoons are 1.1 kg NH_3 m^{-2} y^{-1} and 1.3 kg NH_3 m^{-2} y^{-1} for cattle and pig slurry, and for tanks 0.67 kg NH_3 m^{-2} y^{-1} and 2.1 kg NH_3 m^{-2} y^{-1} for cattle and pig slurry, respectively. The differences between baseline emissions for cattle slurry and pig slurry, and the difference between lagoons and tanks are both statistically significant ($p < 0.05$).

Values for N_2O emissions mostly originate from pilot-scale studies. The data from the three studies which exhibit high values mentioned in section 3.1.2 were excluded for the calculation of baseline emissions. The N_2O losses shown in Table 8 are very low and often close to the limit of detection. Negative fluxes are reported e.g. in VanderZaag et al. (2009) or values lower than the limit of detection in Misselbrook et al. (2016). Pig slurry exhibits a large range between the lower and upper 95% confidence bounds (< 0.001-0.005 g N_2O m^{-2} h^{-1}). Baseline emissions are 0.002 g N_2O m^{-2} h^{-1} for cattle and pig slurry stored in tanks. Storage in lagoons for cattle slurry is 0.0003 g N_2O m^{-2} h^{-1} while for pig slurry no baseline value is available. Statistically significant differences were not found for N_2O.

Farm-scale studies exhibit higher CH_4 emissions than pilot-scale studies (Table 8). For both study types, pig slurry has a higher emission level as compared to cattle slurry. The baseline emission values for lagoons are 0.95 g CH_4 m^{-3} h^{-1} (cattle slurry) and 3.5 g CH_4 m^{-3} h^{-1} (pig slurry), and for tanks 0.58 g CH_4 m^{-3} h^{-1} (cattle slurry) and 0.68 g CH_4 m^{-3} h^{-1} (pig slurry), respectively. The baseline emission for lagoon storage of pig slurry is based on one record only. But its distinctly higher emission level as compared to the baseline for tank storage and relative to the baseline emissions of cattle slurry stored in lagoons and tanks is confirmed by the area based CH_4 emissions where the data basis is much larger and statistically significant differences ($p < 0.05$) were found (Supplementary data 4).

For CO_2, the number of observations is relatively small. Some studies exhibit high values for cattle slurry which are greater than 20 g CO_2 m^{-2} h^{-1} (Leytem et al., 2011; Minato et al., 2013; Misselbrook

Table 9
Flow based baseline emissions for tanks from untreated cattle and pig slurry stored uncovered for NH_3 given in percent of total ammoniacal nitrogen (TAN), N_2O in percent of nitrogen (N), CH_4 and CO_2 in percent of volatile solids (VS). The average (Avg) and the lower and upper 95% confidence bounds (l95, u95) are shown. The numbers are mainly based on pilot-scale studies. Cells denoted with "-": value is not available; #: values denoted with different letters are significantly different ($p < 0.05$). Detailed information is provided in Supplementary data 4.

	n	Avg	l95	u95	#
		NH_3% TAN			
Cattle	31	16%	14%	19%	a
Pig	17	15%	9.2%	23%	a
		N_2O% N			
Cattle	16	0.13%	0.08%	0.18%	a
Pig	8	0.10%	0.01%	0.18%	a
		CH_4% VS			
Cattle	27	2.9%	2.3%	3.7%	a
Pig	14	4.7%	2.1%	10%	a
		CO_2% VS			
Cattle	4	11%	–	–	–
Pig	3	9.2%	–	–	–

Cells denoted with "-": value is not available.

et al., 2016). The baseline emissions for lagoon storage are 6.6 g CO_2 m^{-2} h^{-1} and 0.30 g CO_2 m^{-2} h^{-1} for cattle and pig slurry, respectively, and for tank storage, 8.0 g CO_2 m^{-2} h^{-1} for both slurry types. Data on H_2S emission are sparse and a calculation of baseline emissions is only feasible for lagoon storage which are 0.04 g H_2S m^{-2} h^{-1} for cattle slurry and 0.01 g H_2S m^{-2} h^{-1} for pig slurry (Supplementary data 4).

3.2.2. Flow-based emissions

Flow-based emissions, i.e. emissions given in percent of TAN, N or VS present in the store are shown for NH_3, N_2O, CH_4 and CO_2 in Table 9. Almost all data originate from pilot-scale studies (Supplementary data 4) which can be used for baseline emissions for tanks but not for lagoons. Baseline emission values for NH_3 are 16% of TAN for cattle slurry and 15% of TAN for pig slurry, respectively. N_2O emissions are 0.13% of N for cattle slurry and 0.10% of N for pig slurry. Baseline emissions for CH_4 are 2.9% of VS for cattle slurry and 4.7% of VS for pig slurry. Emissions for CO_2 reach 11% of VS and 9.2% of VS for cattle and pig slurry, respectively, but the data basis is limited. The ranges between the lower and upper 95% confidence bounds are large in most cases and are partially skewed to high values, especially for N_2O and CH_4 from pig slurry. There were no statistically significant differences.

3.3. Emission changes due to slurry treatments

Acidification clearly reduces NH_3 emissions by ca. 70% during storage compared to untreated cattle and pig slurry (Table 10). The effect is even higher for CH_4 (61%–96%) but lower for CO_2. For NH_3 and CH_4, the differences are statistically significant ($p < 0.05$). An emission reduction also occurs for digested slurries and slurries after solid-liquid separation combined with acidification for all gases except for N_2O (Supplementary data 6). In contrast, the emissions are enhanced for N_2O emissions compared to untreated cattle and pig slurry although limited data are available and the differences not statistically significant. Data on H_2S emissions are sparse. Fangueiro et al. (2015) state in their review that H_2S emissions were either unaffected or decreased following acidification.

The number of studies on emission changes due to anaerobic digestion is limited. Where more than one observation is available, both an increase and a decrease in emissions occur for storage after anaerobic digestion as compared to untreated slurry (Supplementary data 6). NH_3 and N_2O exhibit on average greater emissions from anaerobically digested slurry. Most studies comparing anaerobically digested and untreated slurry exhibit lower emissions of CH_4 for the former. An emission increase is observed for N_2O and CO_2 for pig slurry, although this is based on only one observation for both gases. Statistically significant differences do not occur for anaerobic digestion.

Average NH_3 emissions during storage from the liquid fraction are significantly ($p < 0.05$) higher as compared to untreated cattle slurry (Table 10). But for pig slurry, only a slight effect of solid-liquid separation on NH_3 release can be observed which is statistically insignificant. CH_4 and CO_2 exhibit lower emissions from the liquid fraction as compared to untreated slurry with a statistically significant difference for CH_4. A statistically significant reduction ($p < 0.05$) in N_2O emissions occurs for cattle slurry. But the release of N_2O is greater for pig slurry compared to untreated slurry where the difference is statistically not significant.

Five studies examined the effect of slurry dilution with water and found an average reduction of all investigated gases in the range of approximately 30–50%. Statistically significant effects occurred for cattle slurry for NH_3 and N_2O. Maximum abatement effects of 88% and 86% were found for N_2O and CH_4, respectively (Supplementary data 6).

3.4. Emission changes due to covering of slurry stores

The average NH_3 emission percent reduction due to covers ranges between approximately 50% up to ca. 90% for most cover types (Table 11). However, the variability of values is large. Minimum values can be around 15% and maximums higher than 95% (Supplementary data 7). The emission mitigation does not systematically differ between cattle and pig slurry on a percentage basis. Emission reductions lie in a similar range for structural covers, impermeable floating covers, permeable floating covers and the other cover materials. The differences are statistically significant ($p < 0.05$) for the following covers and

Table 10
Percentage emission change (i.e. % change of emissions on an area or volume basis) during storage due to acidification, anaerobic digestion, solid-liquid separation and dilution of cattle and pig slurry for NH_3, N_2O, CH_4 and CO_2 relative to untreated slurry. Positive figures indicate a decline, negative numbers an increase in emissions. n: number of records, Avg: average emission change; Std: standard deviation; cells denoted with "-": value is not available. Detailed information is provided in Supplementary data 6.

		NH_3			N_2O			CH_4			CO_2		
		n	Avg	Std	n	Avg	Std	n	Avg	Std	n	Avg	Std
Acidification	Cattle	5	71%*	17%	1	−4%	–	5	61%*	36%	5	7%	23%
	Pig	3	77%*	22%	1	−39%	–	3	96%*	3%	1	67%	–
Anaerobic digestion	Cattle	3	−59%	64%	3	−16%	29%	5	−2%	129%	1	53%	–
	Pig	1	45%	–	1	−363%	–	1	99%	–	1	−22%	–
Solid-liquid separation	Cattle	12	−23%*	21%	6	43%*	36%	10	32%*	27%	7	18%	24%
	Pig	7	−1%	18%	1	−258%	–	7	39%*	39%	5	13%	12%
Dilution	Cattle	5	48%*	29%	5	57%*	38%	5	39%	33%	–	–	–
	Pig	–	–	–	–	–	–	2	47%	15%	2	30%	11%

Cells denoted with "-": value is not available.
* Numbers with an asterisk indicate a statistically significant difference ($p < 0.05$) between the treated and the untreated slurry.

Table 11
Percentage emission change (i.e. % change of emissions on an area or volume basis) from storage of cattle and pig slurry due to different types of covers relative to uncovered storage for NH_3, N_2O, CH_4, CO_2 and H_2S. Positive figures indicate a decline, negative numbers an increase in emissions. n: number of records, Avg: average emission change; Std: standard deviation; cells denoted with "-": value is not available. Detailed information is provided in Supplementary data 7.

		Slurry type	NH_3			N_2O			CH_4			CO_2			H_2S		
			n	Avg	Std	n	Avg	Std	n	Avg	Std	n	Avg	Std	n	Avg	Std
Impermeable structural covers	Lid (wood or concrete)	Cattle	6	73%*	29%	2	−4%	23%	2	15%	2%	–	–	–	–	–	–
		Pig	7	64%*	35%	4	31%	56%	4	45%*	17%	–	–	–	–	–	–
	Tent covering	Cattle	2	77%	9%	–	–	–	–	–	–	–	–	–	–	–	–
		Pig	2	89%	7%	–	–	–	–	–	–	–	–	–	–	–	–
Impermeable synthetic floating covers	Plastic film	Cattle	4	66%*	22%	–	–	–	–	–	–	–	–	–	–	–	–
		Pig	6	88%*	18%	2	100%	0%	2	62%	54%	–	–	–	–	–	–
Permeable synthetic floating covers	Plastic fabrics	Cattle	1	89%	–	1	68%	–	1	−2%	–	1	15%	–	–	–	–
		Pig	5	39%*	15%	–	–	–	3	−17%	18%	–	–	–	4	50%*	20%
	Expanded clay	Cattle	4	59%	39%	–	–	–	2	11%	7%	2	0.1%	1%	–	–	–
		Pig	12	74%*	20%	1	−8%	–	6	8%	17%	5	29%*	8%	–	–	–
	Expanded polystyrene	Cattle	2	79%	2%	–	–	–	–	–	–	–	–	–	–	–	–
		Pig	4	64%*	32%	–	–	–	2	−26%	41%	2	26%	35%	–	–	–
	Plastic tiles	Cattle	–	–	–	–	–	–	–	–	–	–	–	–	–	–	–
		P	2	88%	11%	1	−7%	–	1	25%	–	–	–	–	–	–	–
Permeable natural floating covers	Peat	Cattle	2	90%	13%	–	–	–	–	–	–	–	–	–	–	–	–
		Pig	3	59%	31%	–	–	–	1	−33%	–	1	−31%	–	–	–	–
	Straw cover	Cattle	8	71%*	19%	2	−79%	30%	4	3%	30%	4	−6%	10%	–	–	–
		Pig	8	73%*	22%	–	–	–	7	0.2%	36%	2	13%	9%	–	–	–
	Other organic material#	Cattle	4	51%*	32%	–	–	–	4	−13%	37%	4	−46%	71%	–	–	–
		Pig	4	45%	44%	–	–	–	4	−9%	37%	4	20%	17%	–	–	–
	Vegetable oil	Cattle	4	71%*	16%	–	–	–	2	39%	6%	2	27%	9%	–	–	–
		Pig	4	94%*	10%	–	–	–	2	11%	2%	–	–	–	–	–	–

Cells denoted with "-": value is not available; # materials like maize stalks or wood chips; cells denoted with "-": value is not available.
* Numbers with an asterisk indicate a statistically significant difference ($p < 0.05$) between storage with a cover and uncovered storage.

both slurry types: lid, plastic film, straw cover, vegetable oil; other organic materials for cattle slurry; plastic fabrics, expanded clay, expanded polystyrene for pig slurry.

For N_2O, an increase in emissions is observed in many cases. But reduced emissions occur as well (Supplementary data 7). However, the number of records providing emission changes from slurry storage due to store covers is sparse and the effects are statistically insignificant. CH_4 emissions being lower by approximately 10% to 60% occur for impermeable covers (lid and plastic film), plastic tiles and vegetable oil compared to uncovered storage (Table 11). For plastic fabrics, expanded polystyrene and peat, the emissions are higher by 2% to 33%. The other cover types (expanded clay, straw and organic materials such as corn stalks or wood chips) show both increases and reductions in CH_4 emission (Supplementary data 7). On average, CH_4 emissions from slurry stores covered with permeable materials moderately differ in emission levels as compared to uncovered storage. The differences in CH_4 emissions are statistically not significant ($p < 0.05$) except for pig slurry covered with a lid. Stores covered with plastic fabrics, expanded clay and expanded polystyrene emit less CO_2 while higher emissions are observed for peat and straw covers than for the uncovered controls, but the differences are statistically not significant. Plastic fabrics induce a significant ($p < 0.05$) emission reduction for pig slurry by 50% for H_2S. Data on both CO_2 and H_2S emissions are sparse.

4. Discussion

4.1. Variability in emissions

The high variability of emission levels as shown by descriptive statistics (Table 7) may be due to different meteorological conditions, disturbance of the slurry surface induced by operations at the stores and slurry characteristics. The enhanced variability in laboratory-scale studies compared to the other study types is striking. In laboratory-scale studies, the environment is expected to be largely uniform since the experiments were mostly conducted in a temperature-controlled room with ambient temperatures lying in a narrow range and the slurry being undisturbed. As most of the laboratory-scale studies aimed at a comparison of different techniques or systems, the representativeness of the resulting emission rates for real-world conditions was not the primary focus and discrepancies between different approaches are very likely present. A thorough evaluation of potential biases of the laboratory studies is not possible due to missing information on the measuring systems and is beyond the scope of this paper (see Liu et al. (2020) and the related discussion). Also, for other study types, the occurrence of methodological biases cannot be ruled out which may lead to implausible results. Detection of striking values might be hampered due to the multitude in units used in the papers. Therefore, a standardization as used here and providing guide values are important issues. For this, a favorable option is the unit g m^{-2} h^{-1} or g m^{-3} h^{-1} of a molecule. It is equally suitable to illustrate an emission pattern within one day, also in combination with important influencing factors such as temperature or wind speed which can change over short time periods and to compare them with e.g. average emissions over one year. If a yearly amount of a gas release is required, data can be obtained from Table 8. Alternatively, the unit mol m^{-2} h^{-1} could be used to facilitate the comparability between different molecules, even if to date, it is generally not used in the context of emission inventories.

4.2. Important factors influencing emissions

The relevance of important influencing factors on emissions from slurry stores is discussed in this section in order to support interpretation and understanding of the data used to determine baseline emissions and emission changes due to slurry treatment and coverage of slurry stores. It should be noted that a part of these influencing factors could not be included in the data processing such as the weighting or the statistical analysis of emission data due to insufficient information in the records. This data limitation applied for operations at stores, the meteorological parameters rain and wind speed and the natural crust.

4.2.1. Type of slurry

Records from the same study where both cattle and pig slurry have been investigated using the same approach were compared. Eight studies (De Bode, 1991; Sommer et al., 1993; Husted, 1994; Kaharabata

et al., 1998; Balsari et al., 2007; Dinuccio et al., 2008; Mosquera et al., 2010; Misselbrook et al., 2016; Baral et al., 2018) with a total of 14, 2, 8 and 3 pairs of records on NH_3, N_2O, CH_4 and CO_2 emissions, respectively, were available. For NH_3, 85% of data pairs, exhibited higher emissions for pig slurry than for cattle slurry. Similar for N_2O, CH_4 and CO_2, pig slurry exceeds emissions of cattle slurry in most cases. These findings agree with the data reported in Table 8 (except for CO_2) and with data previously published by Sommer et al. (2006) and VanderZaag et al. (2015).

4.2.2. Operations at stores

Operations at the storage tank, such as agitation, filling and removing of slurry are necessarily related to real-world storage systems. Their effects are usually reflected in farm-scale measurements using non-intrusive methods but rarely included in pilot studies or farm-scale studies using chamber systems. A series of studies specifically investigated such processes (see Supplementary data 10). They showed consistent results and provided evidence that disturbance of the manure surface due to slurry agitation, filling and discharging of the stores induces large episodic emissions for NH_3, CH_4, CO_2 but not for N_2O. While emissions of CH_4 and CO_2 rapidly decline after cessation of the operations and can even drop to levels below the previously undisturbed stores, increased emission levels persist for NH_3. Due to the relatively short time duration of agitation over the year and the subsequent drop below average levels for CH_4, this operation per se does not substantially contribute to annual NH_3 and GHG emissions from slurry (VanderZaag et al., 2009). A more detailed overview on emissions during and following operations at stores is given in the Supplementary data 10.

4.2.3. Meteorological conditions

Increasing air temperature and wind speed enhance the emissions since they directly affect diffusion and convection of gases near the emitting surfaces (Sommer et al., 2013). The relationship between the temperature as represented by the season of measurements and the emission level could be demonstrated in the present study (Supplementary data 5). It must be considered however, that the air temperature is a simplistic surrogate for the slurry temperature which is a determinant factor for GHG emissions. Rennie et al. (2018) demonstrated that slurry store design and operations (i.e. filling level, agitation) influence the slurry temperature and the emission level of gases such as CH_4. In 25 studies, slurry temperatures during different seasons are available. Slurry temperatures increase as expected in the order cold < temperate < warm for 94% of the cases. The effects of temperature and wind speed are not discussed further in the present study because this topic has been previously covered by e.g. Ni (1999) or Sommer et al. (2006). In contrast, emission changes related to the influence of rain events and thawing of the slurry surface are summarized here since they have been less frequently addressed in the literature. Petersen et al. (2013) found lower NH_3 emission from uncovered storage of pig slurry with precipitation than from the treatment without rain although the differences are not statistically significant. It was shown that ammonia emissions can decline towards zero during rain events after slurry spreading (Hafner et al., 2019) due to sorption of NH_3 onto wet surfaces. Moreover, the TAN-concentration at the emitting surface may decrease with precipitation due to dilution or transport of TAN from a crusted slurry surface into the bulk liquid. Overall, it can thus be assumed that NH_3 emissions from slurry storage during rain events are low. In contrast, an increase in emissions of CH_4 has been observed. Balde et al. (2016b) reported average emissions of 1.8 g CH_4 m^{-2} h^{-1} for digested slurry while peak emissions during rain events reached 10 g CH_4 m^{-2} h^{-1}. This was likely due to bursting of bubbles at or near the surface. Elevated emissions were also observed by Balde et al. (2016a) from storage of the liquid fraction of cattle slurry which confirms earlier findings from Kaharabata et al. (1998) and Minato et al. (2013) on slurry stored in open tanks or lagoons. Kaharabata et al. (1998) suggested that the emission increase is due to more disturbance at the slurry surface induced by rain and thus enhancement of the CH_4 exchange through the liquid surface area and of incidental outburst of gas bubbles (ebullition). Petersen et al. (2013) found a drop of N_2O emissions to zero as a result of rewetting of the crust after rainfall inducing a shift towards anaerobic conditions. Grant and Boehm (2015) did not find a relationship between H_2S emissions and rain events.

VanderZaag et al. (2011) observed important bubble flux events in late winter/early spring that coincided with surface thawing which were probably due to a release of previously produced CH_4 that was trapped under the frozen slurry surface. In the study of VanderZaag et al. (2010a) which encompassed winter and spring, N_2O release was only recorded during spring thaw. A moderate increase in CH_4 emissions was observed during the same period at slurry temperatures above 0 °C while NH_3 and CO_2 flows were unaffected by spring thaw. Elevated CH_4 emissions due to thawing of the manure store were also reported by Leytem et al. (2017).

4.2.4. Natural crust

There is agreement that crusting impacts the gas release in many ways: enhanced resistance to mass transfer (Olesen and Sommer, 1993), oxidation of NH_3 (Nielsen et al., 2010) and CH_4 (Petersen et al., 2005) and formation of N_2O related to nitrification and denitrification occurring in liquid–air interfaces near air-filled pores present in crusts (Petersen and Miller, 2006). Several studies investigated the effect of a natural crust on the emission level (Sommer et al., 1993; Misselbrook et al., 2005; Aguerre et al., 2012; Wood et al., 2012). All studies showed that a natural crust provided an efficient barrier leading to an emission reduction for NH_3. Baldé et al. (2018) confirmed these findings by measurements conducted under farm conditions at tanks and earthen basins containing slurries with differing ability to form natural crusts (i.e. raw cattle slurry, the liquid fraction of cattle slurry produced by solid-liquid separation, digested slurry with and without solid-liquid separation). They confirmed that slurry stored with a thick surface had lower NH_3 losses. Grant and Boehm (2015) found that crusting of a lagoon surface containing dairy cow slurry reduced NH_3 but not H_2S emissions. Nielsen et al. (2010) showed that NH_3-oxidizing bacteria may contribute to a significant reduction of NH_3 emissions if a natural crust is present on a slurry store. Grant and Boehm (2018) found emissions from a tank containing pig slurry to be greater by 10% when the surface was covered with a crust than without crusting (difference not statistically significant). They explained their findings by the higher TAN content of the crusted slurry surface as compared to a non-crusted one. Sommer et al. (2000) and Husted (1994) found higher emissions of CH_4 from slurry without than from slurry with a natural surface crust. Wood et al. (2012) investigated the emissions from dairy slurry with varying DM contents and thus natural crusts with different thicknesses and coverage of the storage surfaces. They were not able to relate the CH_4 fluxes to the presence of a natural crust. N_2O production was found to be enhanced after build-up of a natural crust (VanderZaag et al., 2009).

In the literature (e.g. Vanderzaag et al., 2015), a natural crust is often classified as abatement measure for NH_3 similar as slurry store covers. However, crust formation can only be controlled to a limited extent. Crusts are of variable thickness, coverage of the store and durability. Their effectiveness for emission abatement has therefore be considered as inconsistent (Vanderzaag et al., 2015). Crusts only develop for slurry types with a high content of fibrous material (Bittman et al., 2014). This applies mainly for cattle slurry (Smith et al., 2007) and less for pig slurry (Sommer et al., 2006). Crusting is likely to occur at a slurry DM content of more than 20 g L^{-1} (Sommer et al., 2006; Wood et al., 2012) which mostly does not apply for slurry stored in lagoons (Table 6). Consequently, they have much less ability to form a natural crust as shown by e.g. Balde et al. (2018).

We therefore did not consider crusting as an emission mitigation technique equivalent to slurry store covers but rather as a parameter

influencing emissions from stored slurry and thus excluded it from the analysis of emission changes due to covering of stores. But we stress that if a natural crust is present, it is likely to significantly contribute to an emission reduction and, therefore, should be preserved by e.g. reducing slurry agitation and addition of manure below the surface.

The limited information in the data impedes our ability to clearly distinguish between crusted and non-crusted stores. This may be relevant for (i) the calculation of baseline emissions and (ii) emissions changes due to slurry treatments and covering of stores: (i) baseline emissions determined here may include stores with variable occurrence of a natural crust. For lagoons, information on crusting was available for 45% (cattle slurry) and 19% (pig slurry) of the records, respectively. Among these, 62% of the lagoons containing cattle slurry were fully or partly covered by a crust during the emission measurements. For pig slurry, this applies for 21% only. Among records used for the determination of baseline emissions for tanks, 78% and 50% included information regarding crusting for cattle and pig slurry, respectively. Of these, 83% (cattle slurry) and 48% (pig slurry) had a fully or partly crusted surface. This complies with findings that crusting occurs less on lagoon surfaces and stores containing pig slurry. The proportion of crust occurrence for cattle slurry stored in tanks is in line with earlier findings (Smith et al., 2007). We thus suggest that the baseline emissions determined here are based on studies which appropriately reflect the range of store surface crusts occurring at farms. (ii) A natural crust may occur in combination with a storage cover and thereby be enhanced (Chadwick et al., 2011) since the slurry surface is less exposed to wind turbulence. In experiments comparing uncovered and covered storage, it is thus difficult to stringently distinguish between the effect of covering and of crusting. Moreover, this information is not always available: only 60% of the records used to determine the emission change due to covering included information on crusting. From these, about half had crusted surfaces and the other half not. This might partly explain the variability of emission changes due to covering found here. These considerations should be taken into account for the discussion in the Sections 4.4 and 4.6.

4.3. Study types to be included for baseline emissions

Data should only be included for the calculation of baseline emissions if they can be considered as representative or typical for gas flows occurring at farm conditions. In principle, this applies for farm-scale studies. Pilot-scale studies imply some aspects of farm-scale studies due to measurements conducted in outdoor facilities and a slurry volume in the order of several cubic meters. But there are concerns extrapolating data from pilot-scale studies to real-world systems. VanderZaag et al. (2009, 2010a, 2010b) who performed pilot-scale studies state that although measured fluxes were reported, emission trends and treatment differences or temporal trends were the focus of their analysis. Moreover, almost all pilot-scale studies are based on flux chambers. VanderZaag et al. (2010b) argued that steady-state chambers alter the enclosed environment and concluded that absolute fluxes measured might deviate from emissions that would occur without chambers. Nevertheless, several studies conducted in pilot-scale facilities similar to that of VanderZaag et al. (2009, 2010a, 2010b) quantified emissions of NH_3 and GHGs and derived emission factors for slurry storage (e.g. Amon et al., 2006, 2007; Rodhe et al., 2012). Petersen et al. (2009) presented a pilot-scale facility and suggested to use the obtained results for better documentation of emission data for GHG and ammonia inventories. Pilot-scale studies have occasionally been conducted with simulation of real-world conditions by including mixing of the slurry or filling of tanks during the experiment (VanderZaag et al., 2009; Rodhe et al., 2012).

Emission peaks for CH_4 were observed in several studies (VanderZaag et al., 2011; Balde et al., 2016a) due to ebullition. They may remain unrecorded (Rodhe et al., 2012) unless the gas measurements are continuous with a high temporal resolution. This shortcoming may apply for pilot-scale studies where e.g. a flow chamber is used which is moved between several experimental tanks (e.g. Amon et al., 2006). Intermittent gas sampling can hamper measurements at a farm-scale as well. Grant et al. (2015) assumed differences in emission levels between two locations due to under-sampling of ebullition events given the short measurement periods. Sampling large storage areas using chambers might be hampered if the sampled surface areas are not representative for the entire store. Balde et al. (2016b) found average emissions of CH_4 measured at an earthen storage containing liquid digestate with a floating chamber which were about four-fold greater than measured at the same time with a non-intrusive bLS technique. The authors explained this by the limited area covered by the chamber and by disturbances induced by the chamber causing bubble formation and bursting thereby increasing emissions.

To summarize, it can be hypothesized that farm-scale measurements using non-intrusive methods are a preferential option. Still, data from such studies are limited at present time. Therefore, inclusion of records from pilot-scale and farm-scale studies appears to be the best opportunity for the determination of baseline emissions. This approach provides a larger data basis as if only farm-scale studies were included. Moreover, Table 8 shows that emissions from pilot-scale studies comply with farm-scale studies tank for NH_3 but less for CH_4. On the other hand, we excluded laboratory-scale studies for the determination of baseline emissions. They are mostly not designed for generating emission rates. Their experimental conditions strongly deviate from an environment that occurs under practical conditions. The enhanced variability found in emissions level from laboratory-scale studies (section 3.1.2) points to severe methodological shortcomings which might bias baseline values.

4.4. Baseline emissions

4.4.1. Emissions on an area or volume basis

NH_3 emissions from pig slurry are higher as expected due to its higher TAN content and its lower ability to form a natural crust compared to cattle slurry. Sommer et al. (2006) and VanderZaag et al. (2015) suggested lower emissions on an area basis from pig slurry stored in lagoons than from storage in tanks. This complies with the results of this study (Table 8). Lagoons are the prevailing system for slurry storage in the US (Sorensen et al., 2013). They usually have a greater surface area than tanks which would imply more exposure to the ambient air turbulence suggesting a higher emission potential. Slurries from lagoons have on average a lower dry matter and TAN content as compared to tanks. This might be due to a stronger dilution with water: e.g. five out of six lagoons investigated by Leytem et al. (2017) collected parlor wash water and not slurry from a pit of a livestock housing. We assume that solid-liquid-separation was applied at the farms studied which have lagoons although this was not always clearly defined in the papers. This is supported by the low contents in DM and TAN in slurry from lagoons as shown in Table 6. The lower solids content would enhance the emission potential due to less ability for formation of a natural crust at the slurry surface (Wood et al., 2012). But the lower TAN content induces the opposite effect on NH_3 emissions (Sommer et al., 2006). The overall impact of these effects combined on the emission level is difficult to assess. The present data suggest higher emissions from lagoons than from tanks containing cattle slurry but the opposite for pig slurry.

The baseline emissions (lagoons: 0.12 g NH_3 m^{-2} h^{-1} and 0.15 g NH_3 m^{-2} h^{-1} for cattle and pig slurry, tanks: 0.08 g NH_3 m^{-2} h^{-1} and 0.24 g NH_3 m^{-2} h^{-1} for cattle and pig slurry, respectively), are mostly lower than numbers given by VanderZaag et al. (2015), Sommer et al. (2006) and Bittman et al. (2014). VanderZaag et al. (2015) suggested emissions for crusted and non-crusted cattle slurry of 0.11 and 0.19 g NH_3 m^{-2} h^{-1}, respectively, from tanks or lagoons. For pig slurry stored in a lagoon, they give 0.12 g NH_3 m^{-2} h^{-1}, and stored in a tank, 0.40 g NH_3 m^{-2} h^{-1}. Sommer et al. (2006) provided similar values. Bittman

et al. (2014) gave baseline emissions between 0.19 and 0.40 g NH_3 m^{-2} h^{-1}. They attributed the lower value to slurry which is frozen in the store for several months, and the higher value applies to warm countries. For N_2O, most studies exhibit emissions clearly below 0.01 g N_2O m^{-2} h^{-1} (Supplementary data 8). In contrast, three papers reach values from 0.02 to 0.06 g N_2O m^{-2} h^{-1} and N_2O losses ranging between 25% and 160% of the NH_3 emissions determined concomitantly (Clemens et al., 2006; Amon et al., 2007; Leytem et al., 2011). Unless at very low levels of NH_3 emissions, flows of both NH_3 and N_2O in the same order of magnitude do not occur in other records and have not been reported in the livestock sector (e.g. EEA, 2016). Therefore, the data from the three studies were excluded for the calculation of baseline emissions. If they were kept, the baseline emissions for N_2O would be higher by a factor of two and three for cattle and pig slurry stored in tanks, respectively. Chadwick et al. (2011) stated in their review that N_2O emission from slurry stores without a surface cover are negligible which supports the baseline emissions shown in Table 8.

For CH_4, higher emissions occur for farm-scale studies than for pilot-scale studies (Table 8; statistically significant differences for emissions on an area basis; $p < 0.05$; Supplementary data 4). This could be due to the temperature dependency of methanogenesis (Elsgaard et al., 2016). Pilot-scale studies exhibit lower slurry volumes as compared to farm-scale stores which suggests faster cooling of the slurry and therefore a lower methane conversion rate. Another reason could be the batch-filling of vessels used for pilot-scale studies which differs from continuous filling and incomplete removal of slurry at farm-scale stores. Under such conditions, aged slurry may act as inoculum which was shown to enhance emissions of CH_4 (Wood et al., 2014). Overall, the lower emission level for CH_4 measured at pilot-scale included for the determination of baseline emissions tank could lead to an underestimation thereof.

The review of Owen and Silver (2015) reported CH_4 emission data from lagoons and tanks of dairy systems being 2.3 and 2.7 g CH_4 m^{-2} h^{-1}, respectively. This is higher than data from farm-scale studies reported here which are 1.2 and 1.3 g CH_4 m^{-2} h^{-1} for cattle slurry stored in lagoons and tanks, respectively (Supplementary data 4). However, the data basis of Owen and Silver (2015) is smaller and measurements carried out in the warm season tend to be overrepresented. The higher CH_4 emissions from pig slurry as compared to cattle slurry are expected due to the higher methane production potential of pig slurry (Triolo et al., 2011). Both cattle and pig slurry exhibit lower losses from tanks than from lagoons. Moreover, lagoon storage produces a solid fraction which includes a large proportion of the slurry VS generating additional emissions. According to VanderZaag et al. (2010b), a CO_2-C:CH_4-C ratio of 50:50 is expected from stores. Looking at records which include emission data of both CH_4 and CO_2, a large variation occurs. The average CO_2-C:CH_4-C ratio is approximately 65:35 which also differs from the CH_4 to CO_2 relationship expected from anaerobic digestion of livestock slurries (ca. 55%–70% CH_4 content of dry biogas; Triolo et al., 2011). This could be due to a tendency for greater CO_2-C:CH_4-C ratios in pilot-scale studies which increases the average CO_2-C:CH_4-C ratio of all records included. The greater ratios were also linked to studies with low CH_4 fluxes. This is likely because pilot-scale studies had less ability to provide appropriate conditions for CH_4 production as mentioned above. On the other hand, CO_2 seems to be emitted more consistently in all studies.

As the aim of all studies considered for the calculation of baseline values in the present paper was the determination of emission rates we think that the baseline emissions are robust and reflect the current state of knowledge. But the confidence intervals shown in Table 8 may be substantial. This suggests an inherent variability in the systems which can be due to differing conditions regarding meteorological conditions, operations at stores and occurrence of a natural crust. Baseline values must be considered as average numbers. In a specific situation and e.g. for representative regional values, deviations from the presented baseline values can occur. Moreover, methodological biases cannot be ruled out and different experimental approaches might entail systematic differences in results (e.g. possibly CH_4 emissions from pilot-scale studies). Such effects have been observed for experimental data on NH_3 emissions from slurry application (Hafner et al., 2018).

4.4.2. Flow-based emissions

The determined baseline emission values for NH_3 of 16% of TAN and 15% of TAN for cattle and pig slurry, respectively, which are mostly based on pilot-scale studies exhibit similar values as the emission factors of EEA (2016) which give 20% of TAN and 14% of TAN as Tier 2 default values for cattle and pig slurry. Data from farm-scale studies have comparable numbers for storage in tanks for cattle slurry: 16% of TAN (Baldé et al., 2018) and 13% of TAN (McGinn et al., 2008) but lower emissions for pig slurry (Dinuccio et al., 2012) with 2% and 5% of TAN. Flow-based emissions are not available for lagoons. IPCC (2006) and EEA (2016) suggest an N_2O emission factor being zero for slurry storage without a natural crust. For a crusted store, IPCC (2006) and EEA (2016) give EFs of 0.5% of N and 1% of TAN entering the store, respectively. These values are higher than the values determined in this study which are 0.13% of N and 0.10% of N for cattle and pig slurry, respectively (Table 9). The eight highest values for flow-based N_2O emissions originate from records that include slurry stores with a crust which supports the occurrence of N_2O emissions with crusted store surfaces. This complies with Sommer et al. (2000) who suggest that N_2O is produced in drying of natural crusts where aerobic and anaerobic zones exist. Drying enhances convection of liquid upward through the cover, where dissolved ammonium can be oxidized by nitrifying bacteria in an aerobic environment and under such conditions, molecules produced from nitrification can be denitrified. During ammonium oxidation and denitrification, N_2O is released as an intermediate or final product. At limited oxygen availability, formation of N_2O is enhanced.

For CH_4, a direct comparison between the suggested baseline emissions with default emission factors used in models for emission inventories is not possible. A simplified application of the approach of Mangino et al. (2001) and IPCC (2006) using the methane conversion factor (MCF) for slurry in a cool climate with an annual average temperature of 14 °C results in a CH_4 emission of ca. 4.0% of VS and 7.5% of VS for cattle slurry and pig slurry, respectively. These figures are somewhat higher than the baseline emissions suggested (Table 9) which are 2.9% of VS and 4.7% of VS for cattle and pig slurry, respectively. It should be noted that emission values for CH_4 derived from such model approaches can strongly deviate from measured values as shown by several studies (e.g. Kariyapperuma et al., 2018).

For the determination of flow-based emissions, analytical data of the slurry, the flow volume of slurry into storage and its residence time in the store must be known. Determining these three parameters is not straightforward which might explain the high degree of absence regarding flow-based emissions in farm-scale studies. This particularly applies for lagoons where extended slurry residence times, accumulation of solids over long time periods and repeated recycling of liquids used for flushing or recharging pits of livestock housings represent additional challenges. Generally, lagoons have a greater surface to volume ratio and longer slurry residence times as compared to tanks. These two factors will lead to higher flow-based emissions for lagoons as compared to tanks if identical emissions on an area basis are assumed for both storage systems.

For inventory purposes, emission factors could be calculated using the baseline emissions on an area or volume basis and an assumption of the surface or volume of the storage system, the average values for the residence time of the slurry in the store and the slurry contents of TAN, N or VS. These values are specific for different countries and production systems. A further assessment thereof is outside the scope of this paper. The calculation of flow-based emissions (and emission factors) is subject to additional uncertainties as compared to emissions on an area basis due to the requirement of further parameters.

4.5. Emission changes due to slurry treatments

The pH value has a strong effect on gaseous emissions from slurry stores (Sommer et al., 2013). This is appropriately reflected by the data on emission changes due to slurry acidification through addition of inorganic acids shown in Table 10. The variability in the achieved reduction is likely related to the degree of acidification and the different pH values in slurry (Dai and Blanes-Vidal, 2013). The emission reductions found for NH_3 and CH_4 are in line with the review of Fangueiro et al. (2015). Similarly, Petersen et al. (2012) observed significant reduction effects for NH_3 and CH_4 due to acidification. The data point at an increase in N_2O emission but this is based on limited data. Bastami et al. (2016) concluded that self-acidification of slurry induced by addition of substrates rich in carbon may be a promising alternative to slurry acidification using concentrated acids for abatement of CH_4 emissions. Additives other than acids to reduce gaseous emissions or odor nuisance from manure storage have been investigated in some studies (Martinez et al., 2003; Sun et al., 2014; Owusu-Twum et al., 2017). A clear emission reduction due to other additives did not occur. Similarly, Van der Stelt et al. (2007); Wheeler et al. (2011) and Holly and Larson (2017a) found little evidence that manure additives other than acids have a clear influence on the release of ammonia and GHGs. Still, individual investigations have shown an emission reduction potential for certain additives (Bastami et al., 2016).

The number of studies allowing a direct comparison of emissions from storage of untreated slurry and anaerobically digested slurry is limited since biogas plants are mostly fed with manure and off-farm organic feedstock material which hampers a direct comparison with unamended untreated slurry. The increase of NH_3 emissions due to anaerobic digestion complies with studies which include anaerobic digestion with addition of organic feedstock material. Baldé et al. (2018) measured NH_3 emissions from two stores at different farms containing untreated livestock slurry and liquid digestate obtained from livestock slurry and organic feedstock materials under farm conditions. Emissions from the untreated slurry were lower. Koirala et al. (2013) suggested that anaerobic digestion of dairy slurry significantly increased the NH_3 volatilization potential. The most important factor was the enhanced ammonium dissociation. Anaerobic digestion seems to reduce CH_4 emissions during slurry storage. Maldaner et al. (2018) found lower CH_4 losses from the liquid fraction of anaerobically digested slurry amended with organic feedstock material compared to unamended raw slurry from the same farm before the installation of anaerobic digestion. This is likely due to the reduction of the VS load after digestion but also a consequence of solids removal with solid-liquid separation of the major part of the digestate. Furthermore, Maldaner et al. (2018) suggested that VS remaining in the digestate was less degradable which leads to a reduced CH_4 production. VanderZaag et al. (2018) showed the CH_4 emission potential (B_0) from digestate was 35% lower than the B_0 of untreated manure. In contrast, Sommer et al. (2000) and Rodhe et al. (2015) measured higher emissions from anaerobically digested slurry as compared to untreated cattle slurry. They explained this by the presence of a larger and more active microbial community in digested slurry. However, most storage tanks are never completely empty. Residual aged slurry may act as inoculum and enhance the production of CH_4 (Sommer et al., 2007; Ngwabie et al., 2016). Although, the microbial population in aged slurry may be less efficient for methane production as compared to microbes present in anaerobically digested slurry, the higher amount of degradable organic carbon available in untreated slurry might compensate this. It can therefore be hypothesized that untreated slurries as occurring in real-world stores imply a higher potential for CH_4 emissions than anaerobically digested slurry.

Solid-liquid separation reduces the solids content of the slurry and thus the potential to develop a natural crust. This enhances NH_3 emissions during storage which complies with the increasing emissions of cattle slurry due to solid-liquid separation. Pig slurry exhibits a lower ability to form a natural crust which could explain why almost no effect of solid-liquid separation on NH_3 emissions can be observed (Table 10). Baldé et al. (2018) investigated the NH_3 emissions from two stores situated at different dairy farms containing untreated slurry and separated liquids under farm conditions. They measured higher emissions from the liquid fraction than from the untreated slurry and reported similar findings for the separated liquids from digestate derived from livestock slurry and organic feedstock materials. In contrast, Hjorth et al. (2009) found significantly higher NH_3 emissions from raw and digested slurries than from the corresponding liquid fractions. They explained their findings by the higher ammonium and N contents of the unseparated raw and pre-digested slurries compared with the liquid fractions, which increased the potential for NH_3 volatilization. The lower N_2O storage emissions of the liquid fraction for cattle slurry as compared to raw slurry is in line with the conclusions of the review paper published by Chadwick et al. (2011). The reduced emissions of CH_4 due to solid-liquid separation results from the reduction of the total solids content in the slurry which can be considered as a surrogate for the available VS pool. This leads to a lower amount of organic matter which can be degraded to CH_4 and CO_2 (Wood et al., 2012). However, yearly average CH_4 emissions of 1.4 g CH m^{-3} h^{-1} and 2.2 g CH m^{-3} h^{-1} for the first and second year of measurements were reported for dairy slurry from a farm-scale study conducted at a tank (Balde et al., 2016a). These numbers exceed the baseline emission and emissions from farm-scale studies from tanks for cattle slurry given in Table 8. Balde et al. (2016a) explained the elevated emission levels by the high biodegradability of the liquid fraction and the limited crust development. VanderZaag et al. (2018) showed that the speed of CH_4 production was much higher for the separated liquid fraction, compared to untreated slurry. Grant et al. (2015) found CH_4 emissions on an area basis from the liquid fraction of cattle slurry stored in a lagoon which are similar to the baseline emission for cattle slurry (Supplementary data 4). The discrepancy between the emission changes given in Table 10 and the high emissions found in these two studies is difficult to explain.

Dilution of slurry with water changes its DM content. DM of slurry can be considered as an indicator for the N/TAN- and VS-content which influences the potential production of NH_3, N_2O, CH_4 and CO_2, respectively (Wood et al., 2012). However, DM affects the formation of a natural crust as well (section 4.2.4). Overall, dilution leads to a reduction of all investigated gases which complies with the findings of Ni et al. (2010) for NH_3 and CO_2 and of Habetwold et al. (2017) for CH_4. But this conclusion is based on pilot-scale studies where the slurry volume is identical for the diluted and untreated slurry. Under practical conditions, addition of water leads to a higher amount of slurry. If the area of manure stores is thereby increased due to requiring larger storage capacities, the reduction might be overcompensated due to a rise in emitting surface (Ni et al., 2010).

Aeration of slurry is a technique which is used to remove excess N from slurries. It induces nitrification and denitrification that converts TAN in the slurry to nitrite/nitrate with the aim of a complete denitrification to N_2. If the process is not properly controlled aeration can produce substantial amounts of NH_3 and N_2O (Loyon et al., 2007). The effect of aeration was investigated in several laboratory- and pilot-scale studies. Amon et al. (2006) found a strong increase of NH_3 emissions by up to a factor of five. Molodovskaya et al. (2008) reported NH_3 emissions of up to 50% of total slurry N. Losses were increased at greater aeration rates. Many studies found a strong increase in emissions for N_2O with aeration (Beline et al., 1999; Beline and Martinez, 2002; Amon et al., 2006; Loyon et al., 2007). Low emissions for both NH_3 and N_2O were achieved from low flow phased oxic/anoxic treatment (Molodovskaya et al., 2008). A reduction of CH_4 by ca. 50% to almost 100% emissions was observed by Martinez et al. (2003) and Amon et al. (2006) if slurry aeration was applied. Concomitantly, CO_2 emissions were reduced (Martinez et al., 2003).

An increase in emissions of a specific gas during slurry storage due to a treatment technique does not necessarily indicate a conflict related

to emission mitigation. Enhanced losses during storage can be reduced by e.g. storage covering and might be overcompensated by reduced emissions during subsequent field application. The overarching goal of manure management is the reduction of gaseous losses between the excretion by livestock and uptake by arable and fodder crops. Therefore, the discussion on effects of slurry treatments on emissions from slurry storage must consider the context of good management practices along the whole manure management chain (Sajeev et al., 2018).

4.6. Emission changes due to coverage of slurry stores

Almost all types of covers induce a substantial emission reduction for NH_3 which complies with the review of VanderZaag et al. (2008). Emission reductions lie in a similar range for all categories of covers and for both cattle and pig slurry. This contrasts to Bittman et al. (2014) who give distinct values for the different cover types and lower values for "Low technology" floating covers such as permeable natural floating covers. VanderZaag et al. (2015) give an emission reduction of 80% for impermeable structural covers and for impermeable synthetic floating covers which is in the range of the values given in Table 11. A larger layer thickness of natural floating covers leads to a higher emission reduction (Guarino et al., 2006; VanderZaag et al., 2009). This is probably due to a more efficient barrier for the gas transport between the slurry and the ambient air (VanderZaag et al., 2009). Other cover types not included in the data analysis according to section 2.4.3 also efficiently reduce NH_3 emissions. Organic materials such as steam-treated wood or biochar were shown to exhibit similar effects as floating covers consisting of straw or peat (Holly and Larson, 2017b). Minerals like perlite or zeolite were also found to be efficient in NH_3 emission reduction (Hörnig et al., 1999; Portejoie et al., 2003).

The increase in emissions observed for N_2O in many cases agrees with the previously published literature (VanderZaag et al., 2008; Chadwick et al., 2011). Petersen et al. (2013) observed lower N_2O flows with a straw cover exposed to precipitation as compared to straw covers where wetting by precipitation was excluded. Sommer et al. (2000) suggested that N_2O is only produced in periods with drying surface layers. Storage covers can influence the formation of a natural crust (Chadwick et al., 2011). A natural surface crust on slurry can provide sites with aerobic conditions where nitrification occurs which produces N_2O (Sommer et al., 2000). Therefore, the variability in emission changes due to slurry storage covering could be driven by differing moisture contents of the manure surfaces and differing formation of a natural crust due to covering. However, the number of records related to emission changes for N_2O due to store covers is sparse and these findings can be uncertain.

The observed increase in CH_4 emissions for plastic fabrics, expanded polystyrene and peat complies with the review of VanderZaag et al. (2008). Straw covers provide additional carbon but might reduce ebullition and increase aerobic microbial activity at the upper storage layer (VanderZaag et al., 2009). This induces contrasting effects on CH_4 net emissions. VanderZaag et al. (2009) suggested that the reduction of CH_4 emissions due to a straw cover is related to areas in a crust where microbial breakdown of CH_4 might occur. It can be assumed that the enhanced CH_4 consumption overcompensates the increased potential for CH_4 production due to the additional carbon supply with straw. An opposite effect can occur if straw is incorporated into the bulk slurry during storage due to e.g. agitation. Petersen et al. (2013) found that an elevated CH_4 concentration in the gas phase above the slurry surface is required for a significant stimulation of methane oxidation. This would support the preponderant emission reduction found for impermeable covers. For other cover types, the CH_4 concentration above the emitting surface might have been inconsistent in the experiments which could explain the contrasting emission changes for CH_4 due to storage covering. Similar to NH_3, a larger layer thickness of straw covers leads to a higher emission reduction for CH_4 although the differences of the emissions are low (Guarino et al., 2006; VanderZaag et al., 2009).

The contribution of the different gases to the total of GHG emissions is largest for CH_4 with a proportion of ca. 80% (VanderZaag et al., 2009; Petersen et al., 2013). Therefore, the changes of GHG equivalents due to effects of covers is moderate with a slight trend towards lower total GHG emissions.

VanderZaag et al. (2010b) have shown that a permeable synthetic floating cover was more efficient regarding emission reduction of NH_3 and CH_4 when slurry is agitated as compared to undisturbed slurry. VanderZaag et al. (2009) found that agitation increased NH_3 losses from straw covered tanks less than from the uncovered reference. CH_4 emissions from covered and control tanks were similarly changed.

Although found efficient in emission reduction, low cost floating covers such as straw covers are probably not efficient for emission mitigation in practice since they may be destroyed when the slurry surface is disturbed due to strong winds or operations at a store. Therefore, we consider impermeable structural covers or synthetic floating covers as most reliable for emission mitigation.

4.7. Recommendations for further research

The emission data provided in records from different studies range over several orders of magnitude even for the same slurry type, the same type of study and identical seasons of measurement. This may be partly due to varying conditions related to manure management and meteorological conditions occurring during the measurements. In addition, different study designs and measuring methods are likely to contribute to the variability in emissions. An important issue in future research should thus focus to identify and quantify potential experimental biases. This aspect requires the simultaneous use of independent approaches to determine emissions.

Farm-scale studies using non-intrusive methods such as micrometeorological mass balance (Wagner-Riddle et al., 2006) or dispersion modeling (Flesch et al., 2009) are likely to be a preferential option. Such approaches avoid interactions with emitting processes and determined emission rates best reflect the emissions occurring under conditions at farm-scale. They have the ability to cover large area sources (Gao et al., 2008) and can thus integrate the large inhomogeneity of emissions over space and time. For dispersion modeling, the limiting factor is the requirement of a simple topography allowing for representative turbulence measurements. Most of the micrometeorological methods require a minimum wind speed. Many sensors, e.g. for NH_3, have a minimum detection limit which may be higher than gas concentrations occurring under conditions with low emissions (Balde et al., 2019). Consequently, farm-scale studies using non-intrusive methods have a risk to overestimate the true average emissions (Baldé et al., 2018). This risk can be minimized by using recently developed sensors such as DOAS systems (Volten et al., 2012; Bell et al., 2017). Moreover, it would be important to quantify such potential biases by an assessment of gap filling procedures used for missing data due to e.g. non-detection at low concentration levels as done by Voglmeier et al. (2018). For reliable results from farm-scale studies, extended measurement periods are required covering all seasons of a year. Moreover, recent research has demonstrated that the history of the storage may play an important role for CH_4 emissions (Kariyapperuma et al., 2018) pointing at the necessity of measurement campaigns over several years for an adequate determination of representative emission rates. This implies a large effort in labor and costs. In addition, thorough recording of the operations at the storage facilities (agitation, filling, discharging of the stores by using e.g. a webcam, continuous measuring of the slurry volume stored), of crusting at the stores surface (thickness, structure, coverage of the surface), of slurry temperature at several depths, of meteorological conditions as well as slurry sampling and analyses are required. A few studies comply with these requirements (e.g. Baldé et al., 2018; Kariyapperuma et al., 2018). Still, collection of such data can be challenging or even hardly

feasible (e.g. representative slurry sampling at large lagoons). Also, operations at stores can largely differ between individual farms and consequently, it is difficult to select an experimental site at farm-scale which is appropriate to generate baseline emissions. Therefore, several measurement campaigns that consider the variety of different conditions occurring at slurry stores are required.

Pilot-scale studies are indispensable for studying principal mechanisms and influencing factors driving emissions or to evaluate the effectiveness of emission mitigation techniques. Facilities allowing for continuous measurements e.g. as presented by Petersen et al. (2009) are probably the best option. Further advantages of pilot-scale studies are the possibility to conduct experiments in replicates and a better control of the experimental conditions. There is also a potential to generate bases for modeling which could be used to complement data from farm-scale studies. Further progress for the quantification of emissions from slurry storage could be achieved by an analysis of individual measurement intervals from several experiments and model construction on this basis as e.g. done for slurry application by Hafner et al. (2019). The measurement intervals should include the relevant information regarding influencing factors. For this, we recommend that the researchers provide the emission data along with parameters as given in the Supplementary data 2. For indistinct parameters such as crusting, we suggest the elaboration of a standardized procedure to achieve a definition which reliably reflects its influence on the emission level.

5. Conclusions

The present article provides a comprehensive overview on published emission data from slurry storage which serves as a basis to determine guide values and baseline emissions for NH_3, GHGs and H_2S. Standardization of the emission data is an important issue in the present study due to the use of a large variety of units in the studies. Accompanying parameters (e.g. data on slurry analyses) were only partly available in the papers and could thus not be used for a more advanced data analysis. However, the season of the experimental period which served as a surrogate for the temperature was provided in most studies. Descriptive statistics of the emission data revealed a large variability for all gases. Data generated during warm, temperate and cold seasons are unevenly distributed over all records. Therefore, the calculation of an average annual value completed with a confidence range based on a weighting of the emission data according to the season and measurements duration was done. The baseline emissions on an area or volume basis determined for cattle and pig slurry stored in lagoons and tanks (Table 8) are mostly lower than existing reference values. NH_3 baseline emissions for tanks related to TAN are 16% of TAN (range: 14%–19% of TAN) and 15% TAN (range: 9.2%–23% of TAN) for cattle slurry and for pig slurry, respectively, and thus similar to emission factors used in emission inventory models. The flow-based baseline emissions for N_2O and CH_4 are lower than current emission factors. Total GHG emissions from slurry stores based on the global warming potential using a 100-year time horizon are dominated by CH_4.

Techniques for slurry treatment exhibit contrasting effects on emission levels during storage. Acidification was found to be efficient in reducing the emissions of NH_3 and CH_4 but less for CO_2 while the release of N_2O was enhanced in few studies. Solid-liquid separation causes higher losses for NH_3 and a reduction in CH_4, N_2O and CO_2 emissions. Anaerobic digestion promoted NH_3 emissions in most studies. In contrast, emission changes during slurry storage were less explicit for CH_4, although there is evidence toward an emission reduction. The effect of anaerobic digestion on N_2O and CO_2 emissions is unclear. It is essential to consider the context of good management practices along the whole manure management chain when the effect of slurry treatments on emissions from slurry storage is assessed.

All storage cover types reduce emissions of NH_3 while the effect is small for CH_4 and CO_2 with a trend toward a reduction. Permeable covers increase emissions of N_2O. Total GHG emissions tend to be lower with coverage of slurry stores. Overall, coverage of slurry is efficient to abate NH_3 emissions involving a minimum risk of pollution swapping.

The present study provides a robust data basis for the determination of baseline emissions except for flow-based baseline emissions for lagoons which could not be calculated. The emission data in the records from different studies may vary over several orders of magnitude even for the same slurry type, the same type of study and identical seasons of measurement. For future research, appropriate study designs are required to generate baseline emissions appropriate to improve emission inventories. For this, farm-scale studies using non-intrusive methods are likely to be a preferential option. Pilot-scale studies are important to complement results from farm-scale studies.

Declaration of Competing Interest

The authors declare that they have no known competing financial interests or personal relationships that could have appeared to influence the work reported in this paper.

Acknowledgements

This review was conducted out upon request of the Expert Panel on Mitigating Agricultural Nitrogen under the UNECE Task Force on Reactive Nitrogen. Funding by the Swiss Federal Office for the Environment (Contract 00.5100.P2 / R102-0866) is gratefully acknowledged. We thank Cor van Bruggen for crosschecking data and Tony van der Weerden for revision of the manuscript. The members of the EAGER group (www.eager.ch) are acknowledged for useful discussions and critical comments regarding this review.

Appendix A. Supplementary data

Supplementary material related to this article can be found, in the online version, at doi:https://doi.org/10.1016/j.agee.2020.106963.

References

Aguerre, M.J., Wattiaux, M.A., Powell, J.M., 2012. Emissions of ammonia, nitrous oxide, methane, and carbon dioxide during storage of dairy cow manure as affected by dietary forage-to-concentrate ratio and crust formation. J. Dairy Sci. 95, 7409–7416.

Amon, B., Kryvoruchko, V., Amon, T., Zechmeister-Boltenstern, S., 2006. Methane, nitrous oxide and ammonia emissions during storage and after application of dairy cattle slurry and influence of slurry treatment. Agric. Ecosyst. Environ. 112, 153–162.

Amon, B., Kryvoruchko, V., Frohlich, M., Amon, T., Pollinger, A., Mosenbacher, I., Hausleitner, A., 2007. Ammonia and greenhouse gas emissions from a straw flow system for fattening pigs: housing and manure storage. Livest. Sci. 112, 199–207.

ASAE, 2005. ASAE Standard D384.2: Manure Production and Characteristics. ASAE Standards. American Society of Agricultural Engineering, St. Joseph, MI.

Balde, H., VanderZaag, A., Smith, W., Desjardins, R.L., 2019. Ammonia emissions measured using two different GasFinder open-path lasers. Atmosphere 10.

Balde, H., VanderZaag, A.C., Burtt, S., Evans, L., Wagner-Riddle, C., Desjardins, R.L., MacDonald, J.D., 2016a. Measured versus modeled methane emissions from separated liquid dairy manure show large model underestimates. Agric. Ecosyst. Environ. 230, 261–270.

Balde, H., VanderZaag, A.C., Burtt, S.D., Wagner-Riddle, C., Crolla, A., Desjardins, R.L., MacDonald, D.J., 2016b. Methane emissions from digestate at an agricultural biogas plant. Bioresour. Technol. Rep. 216, 914–922.

Baldé, H., VanderZaag, A.C., Burtt, S.D., Wagner-Riddle, C., Evans, L., Gordon, R., Desjardins, R.L., MacDonald, J.D., 2018. Ammonia emissions from liquid manure storages are affected by anaerobic digestion and solid-liquid separation. Agric. Forest Meteorol. 258, 80–88.

Balsari, P., Airoldi, G., Dinuccio, E., Gioelli, F., 2007. Emissions from farmyard manure heaps and slurry stores - effect of environmental conditions and measuring methods. Biosys. Eng. 97, 456–463.

Baral, K.R., Jego, G., Amon, B., Bol, R., Chantigny, M.H., Olesen, J.E., Petersen, S.O., 2018. Greenhouse gas emissions during storage of manure and digestates: key role of methane for prediction and mitigation. J. Agric. Food Syst. Community Dev. 166, 26–35.

Bastami, M.S.B., Jones, D.L., Chadwick, D.R., 2016. Reduction of methane emission during slurry storage by the addition of effective microorganisms and excessive carbon source from brewing sugar. J. Environ. Qual. 45, 2016–2022.

Beline, F., Martinez, J., 2002. Nitrogen transformations during biological aerobic treatment of pig slurry: effect of intermittent aeration on nitrous oxide emissions. Bioresour. Technol. Rep. 83, 225–228.

Beline, F., Martinez, J., Chadwick, D., Guiziou, F., Coste, C.M., 1999. Factors affecting nitrogen transformations and related nitrous oxide emissions from aerobically treated piggery slurry. J. Agr. Eng. Res. 73, 235–243.

Bell, M., Flechard, C., Fauvel, Y., Häni, C., Sintermann, J., Jocher, M., Menzi, H., Hensen, A., Neftel, A., 2017. Ammonia emissions from a grazed field estimated by miniDOAS measurements and inverse dispersion modelling. Atmos. Meas. Tech. 10, 1875–1892.

Bittman, S., Dedina, M., Oenema, O., Sutton, M.A., 2014. Options for Ammonia Mitigation: Guidance from the UNECE Task Force on Reactive Nitrogen. Centre for Ecology and Hydrology, Edinburgh, UK.

Chadwick, D., Sommer, S., Thorman, R., Fangueiro, D., Cardenas, L., Amon, B., Misselbrook, T., 2011. Manure management: implications for greenhouse gas emissions. Anim. Feed Sci. Tech. 166–167, 514–531.

Clemens, J., Trimborn, M., Weiland, P., Amon, B., 2006. Mitigation of greenhouse gas emissions by anaerobic digestion of cattle slurry. Agric. Ecosyst. Environ. 112, 171–177.

Dai, X.R., Blanes-Vidal, V., 2013. Emissions of ammonia, carbon dioxide, and hydrogen sulfide from swine wastewater during and after acidification treatment: effect of pH, mixing and aeration. J. Environ. Manage. 115, 147–154.

De Bode, M.J.C., 1991. Odour and ammonia emissions from manure storage. In: Nielsen, V.C., Voorburg, J.H., L'Hermite, P. (Eds.), Odour and Ammonia Emissions from Livestock Farming. Elsevier Applied Science, London, England, pp. 69–76.

Dinuccio, E., Berg, W., Balsari, P., 2008. Gaseous emissions from the storage of untreated slurries and the fractions obtained after mechanical separation. Atmos. Environ. 42, 2448–2459.

Dinuccio, E., Gioelli, F., Balsari, P., Dorno, N., 2012. Ammonia losses from the storage and application of raw and chemo-mechanically separated slurry. Agric. Ecosyst. Environ. 153, 16–23.

EEA, 2016. EMEP/EEA Air Pollutant Emission Inventory Guidebook 2016. Technical Guidance to Prepare National Emission Inventories. European Environment Agency, Luxembourg.

Efron, B., 1987. Better bootstrap confidence-intervals. J. Am. Stat. Assoc. 82, 171–185.

Elsgaard, L., Olsen, A.B., Petersen, S.O., 2016. Temperature response of methane production in liquid manures and co-digestates. Sci. Total Environ. 539, 78–84.

Fangueiro, D., Hjorth, M., Gioelli, F., 2015. Acidification of animal slurry– a review. J. Environ. Manage. 149, 46–56.

Flesch, T.K., Harper, L.A., Powell, J.M., Wilson, J.D., 2009. Inverse-dispersion calculation of ammonia emissions from Wisconsin dairy farms. Trans. ASABE 52, 253–265.

Gao, Z.L., Desjardins, R.L., van Haarlem, R.P., Flesch, T.K., 2008. Estimating gas emissions from multiple sources using a backward Lagrangian stochastic model. J. Air Waste Manage. Assoc. 58, 1415–1421.

Grant, R.H., Boehm, M.T., 2015. Manure ammonia and hydrogen sulfide emissions from a Western dairy storage basin. J. Environ. Qual. 44, 127–136.

Grant, R.H., Boehm, M.T., 2018. Ammonia emissions from an in-ground finisher hog manure tank. Atmos. Environ. 190, 43–52.

Grant, R.H., Boehm, M.T., Bogan, B.W., 2015. Methane and carbon dioxide emissions from manure storage facilities at two free-stall dairies. Agric. Forest Meteorol. 213, 102–113.

Guarino, M., Fabbri, C., Brambilla, M., Valli, L., Navarotto, P., 2006. Evaluation of simplified covering systems to reduce gaseous emissions from livestock manure storage. Trans. ASABE 49, 737–747.

Habetwold, J., Gordon, R.J., Wood, J.D., Wagner-Riddle, C., VanderZaag, A.C., Dunfield, K.E., 2017. Dairy manure total solid levels impact CH4 flux and abundance of methanogenic archaeal communities. J. Environ. Qual. 46, 232–236.

Hafner, S.D., Pacholski, A., Bittman, S., Burchill, W., Bussink, W., Chantigny, M., Carozzi, M., Genermont, S., Häni, C., Hansen, M.N., Huijsmans, J., Hunt, D., Kupper, T., Lanigan, G., Loubet, B., Misselbrook, T., Meisinger, J.J., Neftel, A., Nyord, T., Pedersen, S.V., Rochette, P., Sintermann, J., Vermeulen, B., Vestergaard, A., Voylokov, P., Williams, J.R., Sommer, S.G., 2018. The ALFAM2 database on ammonia emission from field-applied manure: description and illustrative analysis. Agric. Forest Meteorol. 258, 66–78.

Hafner, S.D., Pacholski, A., Bittman, S., Carozzi, M., Chantigny, M., Genermont, S., Häni, C., Hansen, M.N., Huijsmans, J., Kupper, T., Misselbrook, T., Neftel, A., Nyord, T., Sommer, S.G., 2019. A flexible semi-empirical model for estimating ammonia volatilization from field-applied slurry. Atmos. Environ. 199, 474–484.

Hamilton, D.W., Fulhage, C.D., Clarkson, W., Lalman, J., 2001. Treatment lagoons for animal agriculture. In: J.M, Rice, Humenik, F.J. (Eds.), Animal Agriculture and the Environment: National Center for Manure and Animal Waste Management White Papers. American Society of Agricultural and Biological Engineers, St. Joseph, Michigan, USA, pp. 547–574.

Hill, R.A., Smith, K., Russell, K., Misselbrook, T., Brookman, S., 2008. Emissions of ammonia from weeping wall stores and earth-banked lagoons determined using passive sampling and atmospheric dispersion modelling. J. Atmos. Chem. 59, 83–98.

Hjorth, M., Nielsen, A.M., Nyord, T., Hansen, M.N., Nissen, P., Sommer, S.G., 2009. Nutrient value, odour emission and energy production of manure as influenced by anaerobic digestion and separation. Agron. Sustain. Dev. 29, 329–338.

Hobbs, P.J., Misselbrook, T.H., Cumby, T.R., 1999. Production and emission of odours and gases from ageing pig waste. J. Agr. Eng. Res. 72, 291–298.

Holly, M.A., Larson, R.A., 2017a. Effects of manure storage additives on manure composition and greenhouse gas and ammonia emissions. Trans. ASABE 60, 449–456.

Holly, M.A., Larson, R.A., 2017b. Thermochemical conversion of biomass storage covers to reduce ammonia emissions from dairy manure. Water Air Soil Pollut. Focus. 228.

Hörnig, G., Turk, M., Wanka, U., 1999. Slurry covers to reduce ammonia emission and odour nuisance. J. Agr. Eng. Res. 73, 151–157.

Husted, S., 1994. Seasonal-variation in methane emission from stored slurry and solid manures. J. Environ. Qual. 23, 585–592.

IPCC, 2006. In: Eggleston, H.S., Buendia, L., Miwa, K., Ngara, T., Tanabe, K. (Eds.), 2006 IPCC Guidelines for National Greenhouse Gas Inventories, Prepared by the National Greenhouse Gas Inventories Programme. IGES, Japan.

IPCC, 2007. In: Solomon, S., Qin, D., Manning, M., Chen, Z., Marquis, M., Averyt, K.B., Tignor, M., Miller, H.L. (Eds.), Climate Change 2007: The Physical Science Basis. Contribution of Working Group I to the Fourth Assessment Report of the Intergovernmental Panel on Climate Change. Cambridge University Press, Cambridge, United Kingdom and New York, NY, USA.

Kaharabata, S.K., Schuepp, P.H., Desjardins, R.L., 1998. Methane emissions from aboveground open manure slurry tanks. Global Biogeochem. Cy. 12, 545–554.

Kariyapperuma, K.A., Johannesson, G., Maldaner, L., VanderZaag, A., Gordon, R., Wagner-Riddle, C., 2018. Year-round methane emissions from liquid dairy manure in a cold climate reveal hysteretic pattern. Agric. Forest Meteorol. 258, 56–65.

Koirala, K., Ndegwa, P.M., Joo, H.S., Frear, C., Stockle, C.O., Harrison, J.H., 2013. Impact of anaerobic digestion of liquid dairy manure on ammonia volatilization process. Trans. ASABE 56, 1959–1966.

Leytem, A.B., Bjorneberg, D.L., Koehn, A.C., Moraes, L.E., Kebreab, E., Dungan, R.S., 2017. Methane emissions from dairy lagoons in the western United States. J. Dairy Sci. 100, 6785–6803.

Leytem, A.B., Dungan, R.S., Bjorneberg, D.L., Koehn, A.C., 2011. Emissions of ammonia, methane, carbon dioxide, and nitrous oxide from dairy cattle housing and manure management systems. J. Environ. Qual. 40, 1383–1394.

Liu, D., Rong, L., Kamp, J., Kong, X., Adamsen, A.P.S., Chowdhury, A., Feilberg, A., 2020. Photoacoustic measurement with infrared band-pass filters significantly overestimates NH3 emissions from cattle houses due to volatile organic compound (VOC) interferences. Atmos. Meas. Tech. 13, 259–272.

Loyon, L., Guiziou, F., Beline, E., Peu, P., 2007. Gaseous emissions (NH_3, N_2O, CH_4 and CO_2) from the aerobic treatment of piggery slurry - comparison with a conventional storage system. Biosys. Eng. 97, 472–480.

Maldaner, L., Wagner-Riddle, C., VanderZaag, A.C., Gordon, R., Duke, C., 2018. Methane emissions from storage of digestate at a dairy manure biogas facility. Agric. Forest Meteorol. 258, 96–107.

Mangino, J., Bartram, D., Brazy, A., 2001. Development of a Methane Conversion Factor to Estimate Emissions from Animal Waste Lagoons. Technical Report. pp. 14. (Accessed 30 January 2020). https://www.epa.gov/ttn/chief/conference/ei11/ammonia/mangino.pdf2001.

Martinez, J., Guiziou, F., Peu, P., Gueutier, V., 2003. Influence of treatment techniques for pig slurry on methane emissions during subsequent storage. Biosys. Eng. 85, 347–354.

McGinn, S.M., Coates, T., Flesch, T.K., Crenna, B., 2008. Ammonia emission from dairy cow manure stored in a lagoon over summer. Can. J. Soil Sci. 88, 611–615.

Minato, K., Kouda, Y., Yamakawa, M., Hara, S., Tamura, T., Osada, T., 2013. Determination of GHG and ammonia emissions from stored dairy cattle slurry by using a floating dynamic chamber. Anim. Sci. J. 84, 165–177.

Misselbrook, T., Hunt, J., Perazzolo, F., Provolo, G., 2016. Greenhouse gas and ammonia emissions from slurry storage: impacts of temperature and potential mitigation through covering (pig slurry) or acidification (cattle slurry). J. Environ. Qual. 45, 1520–1530.

Misselbrook, T.H., Brookman, S.K.E., Smith, K.A., Cumby, T., Williams, A.G., McCrory, D.F., 2005. Crusting of stored dairy slurry to abate ammonia emissions: pilot-scale studies. J. Environ. Qual. 34, 411–419.

Molodovskaya, M., Singurindy, O., Richards, B.K., Steenhuis, T.S., 2008. Nitrous oxide from aerated dairy manure slurries: effects of aeration rates and oxic/anoxic phasing. Bioresour. Technol. Rep. 99, 8643–8648.

Mosquera, J., Schils, R.L.M., Groenestein, C.M., Hoeksma, P., Velthof, G., Hummelink, E., 2010. Emissions of Nitrous Oxide, Methane and Ammonia From Manure After Separation. Rapport 427, Lelystad..RApport 387 (in Dutch). Livestock Research, Wageningen UR, Wageningen, The Netherlands.

Myhre, G., Shindell, D., Bréon, F.-M., Collins, W., Fuglestvedt, J., Huang, J., Koch, D., Lamarque, J.-F., Lee, D., Mendoza, B., 2013. Anthropogenic and natural radiative forcing. In: Stocker, T.F., Qin, D., Plattner, G.-K., Tignor, M., Allen, S.K., Boschung, J., Nauels, A., Xia, Y., Midgley, P.M. (Eds.), Climate Change 2013: The Physical Science Basis. Contribution of Working Group I to the Fifth Assessment Report of the Intergovernmental Panel on Climate Change. Cambridge University Press, Cambridge, United Kingdom and New York, NY, USA, pp. 659–740.

Ngwabie, N.M., Gordon, R.J., VanderZaag, A., Dunfield, K., Sissoko, A., Wagner-Riddle, C., 2016. The extent of manure removal from storages and its impact on gaseous emissions. J. Environ. Qual. 45, 2023–2029.

Ni, J.Q., 1999. Mechanistic models of ammonia release from liquid manure: a review. J. Agr. Eng. Res. 72, 1–17.

Ni, J.Q., Heber, A.J., Sutton, A.L., Kelly, D.T., Patterson, J.A., Kim, S.T., 2010. Effect of swine manure dilution on ammonia, hydrogen sulfide, carbon dioxide, and sulfur dioxide releases. Sci. Total Environ. 408, 5917–5923.

Nielsen, D.A., Nielsen, L.P., Schramm, A., Revsbech, N.P., 2010. Oxygen distribution and potential ammonia oxidation in floating, liquid manure crusts. J. Environ. Qual. 39, 1813–1820.

Olesen, J.E., Sommer, S.G., 1993. Modelling effects of wind speed and surface cover on ammonia volatilization from stored pig slurry. Atmos. Environ. Part A Gen. Topics 27A, 2567–2574.

Owen, J.J., Silver, W.L., 2015. Greenhouse gas emissions from dairy manure management: a review of field-based studies. Glob. Change Biol. Bioenergy 21, 550–565.

Owusu-Twum, M.Y., Polastre, A., Subedi, R., Santos, A.S., Ferreira, L.M.M., Coutinho, J., Trindade, H., 2017. Gaseous emissions and modification of slurry composition during storage and after field application: effect of slurry additives and mechanical separation. J. Environ. Manage. 200, 416–422.

Pain, B., Menzi, H., 2011. Glossary of Terms on Livestock and Manure Management, second edition. Ramiran, pp. 80.

Petersen, S.O., Ambus, P., 2006. Methane oxidation in pig and cattle slurry storages, and effects of surface crust moisture and methane availability. Nutr. Cycl. Agroecosys. 74, 1–11.
Petersen, S.O., Amon, B., Gattinger, A., 2005. Methane oxidation in slurry storage surface crusts. J. Environ. Qual. 34, 455–461.
Petersen, S.O., Andersen, A.J., Eriksen, J., 2012. Effects of cattle slurry acidification on ammonia and methane evolution during storage. J. Environ. Qual. 41, 88–94.
Petersen, S.O., Dorno, N., Lindholst, S., Feilberg, A., Eriksen, J., 2013. Emissions of CH4, N2O, NH3 and odorants from pig slurry during winter and summer storage. Nutr. Cycl. Agroecosys. 95, 103–113.
Petersen, S.O., Miller, D.N., 2006. Greenhouse gas mitigation by covers on livestock slurry tanks and lagoons? J. Environ. Sci. Health B 86, 1407–1411.
Petersen, S.O., Skov, M., Droscher, P., Adamsen, A.P.S., 2009. Pilot scale facility to determine gaseous emissions from livestock slurry during storage. J. Environ. Qual. 38, 1560–1568.
Portejoie, S., Martinez, J., Guiziou, F., Coste, C.M., 2003. Effect of covering pig slurry stores on the ammonia emission processes. Bioresour. Technol. Rep. 87, 199–207.
Rennie, T.J., Gordon, R.J., Smith, W.N., VanderZaag, A.C., 2018. Liquid manure storage temperature is affected by storage design and management practices-A modelling assessment. Agric. Ecosyst. Environ. 260, 47–57.
Richner, W., Flisch, R., Mayer, J., Schlegel, P., Zähner, M., Menzi, H., 2017. 4/ Eigenschaften und Anwendung von Düngern. In: Richner, W., Sinaj, S. (Eds.), Grundlagen für die Düngung landwirtschaftlicher Kulturen in der Schweiz / GRUD 2017. Agrarforschung Schweiz, Spezialpublikation 8, 4/1-4/23.
Rodhe, L.K.K., Abubaker, J., Ascue, J., Pell, M., Nordberg, A., 2012. Greenhouse gas emissions from pig slurry during storage and after field application in northern European conditions. Biosys. Eng. 113, 379–394.
Rodhe, L.K.K., Ascue, J., Willén, A., Persson, B.V., Nordberg, Å, 2015. Greenhouse gas emissions from storage and field application of anaerobically digested and non-digested cattle slurry. Agric. Ecosyst. Environ. 199, 358–368.
Sajeev, E.P.M., Winiwarter, W., Amon, B., 2018. Greenhouse gas and Ammonia emissions from different stages of liquid manure management chains: abatement options and emission interactions. J. Environ. Qual. 47, 30–41.
Smith, K., Cumby, T., Lapworth, J., Misselbrook, T., Williams, A., 2007. Natural crusting of slurry storage as an abatement measure for ammonia emissions on dairy farms. Biosys. Eng. 97, 464–471.
Sommer, S.G., Christensen, B.T., Nielsen, N.E., Schjorring, J.K., 1993. Ammonia volatilization during storage of cattle and pig slurry - effect of surface cover. J. Agr. Sci. 121, 63–71.
Sommer, S.G., Christensen, M.L., Schmidt, T., Jensen, L.S., 2013. Animal Manure Recycling: Treatment and Management. John Wiley Sons Ltd, West Sussex, UK.
Sommer, S.G., Petersen, S.O., Sogaard, H.T., 2000. Greenhouse gas emission from stored livestock slurry. J. Environ. Qual. 29, 744–751.
Sommer, S.G., Petersen, S.O., Sorensen, P., Poulsen, H.D., Moller, H.B., 2007. Methane and carbon dioxide emissions and nitrogen turnover during liquid manure storage. Nutr. Cycl. Agroecosys. 78, 27–36.
Sommer, S.G., Zhang, G.Q., Bannink, A., Chadwick, D., Misselbrook, T., Harrison, R., Hutchings, N.J., Menzi, H., Monteny, G.J., Ni, J.Q., Oenema, O., Webb, J., 2006. Algorithms determining ammonia emission from buildings housing cattle and pigs and from manure stores. Adv. Agron. 89, 261–335.
Sorensen, C.A.G., Sommer, S.G., Bochtis, D., Rotz, A., 2013. Technologies and logistics for handling, transport and distribution of animal manures. In: Sommer, S.G., Christensen, M.L., Schmidt, T., Jensen, L.S. (Eds.), Animal Manure Recycling: Treatment and Management. John Wiley Sons Ltd, West Sussex, UK, pp. 211–236.
Sun, F., Harrison, J.H., Ndegwa, P.M., Johnson, K., 2014. Effect of manure treatment on ammonia emission during storage under ambient environment. Water Air Soil Pollut. Focus. 225.
Sutton, M.A., Oenema, O., Erisman, J.W., Leip, A., van Grinsven, H., Winiwarter, W., 2011. Too much of a good thing. Nature 472, 159–161.
Triolo, J.M., Sommer, S.G., Moller, H.B., Weisbjerg, M.R., Jiang, X.Y., 2011. A new algorithm to characterize biodegradability of biomass during anaerobic digestion: influence of lignin concentration on methane production potential. Bioresour. Technol. Rep. 102, 9395–9402.
UN, 1997. Kyoto Protocol to the United Nations Framework Convention on Climate Change. New York NY. .
UNECE, 2015. Guidelines for reporting emissions and projections data under the Convention on Long-range Transboundary Air Pollution. Paper ECE/EB.AIR/128. United Nations Economic Commission for Europe (UNECE), Geneva, Switzerland.
UNECE, 1999. Protocol to Abate Acidification, Eutrophication and Ground-level Ozone to the Convention on Long-range Transboundary Air Pollution. (Accessed 30 January 2020). http://www.unece.org/env/ lrtap/multi_h1.html.
UNECE, 2014. Guidance Document for Preventing and Abating Ammonia Emissions from Agricultural Sources. Paper ECE/EB.AIR/120, February 7, 2014. United Nations Economic Commission for Europe (UNECE), Geneva, Switzerland.
Van der Stelt, B., Temminghoff, E.J.M., Van Vliet, P.C.J., Van Riemsdijk, W.H., 2007. Volatilization of ammonia from manure as affected by manure additives, temperature and mixing. Bioresour. Technol. Rep. 98, 3449–3455.
VanderZaag, A., Amon, B., Bittman, S., Kuczynski, T., 2015. Ammonia abatement with manure storage and processing techniques. In: Reis, S., Howard, C., Sutton, M.A. (Eds.), Costs of Ammonia Abatement and the Climate Co-Benefits. Springer, Netherlands, pp. 75–112.
VanderZaag, A.C., Baldé, H., Crolla, A., Gordon, R.J., Ngwabie, N.M., Wagner-Riddle, C., Desjardins, R., MacDonald, J.D., 2018. Potential methane emission reductions for two manure treatment technologies. Environ. Technol. 39, 851–858.
VanderZaag, A.C., Gordon, R.J., Glass, V.M., Jamieson, R.C., 2008. Floating covers to reduce gas emissions from liquid manure storages: a review. Appl. Eng. Agric. 24, 657–671.
VanderZaag, A.C., Gordon, R.J., Jamieson, R.C., Burton, D.L., Stratton, G.W., 2009. Gas emissions from straw covered liquid dairy manure during summer storage and autumn agitation. Trans. ASABE 52, 599–608.
VanderZaag, A.C., Gordon, R.J., Jamieson, R.C., Burton, D.L., Stratton, G.W., 2010a. Effects of winter storage conditions and subsequent agitation on gaseous emissions from liquid dairy manure. Can. J. Soil Sci. 90, 229–239.
VanderZaag, A.C., Gordon, R.J., Jamieson, R.C., Burton, D.L., Stratton, G.W., 2010b. Permeable synthetic covers for controlling emissions from liquid dairy manure. Appl. Eng. Agric. 26, 287–297.
VanderZaag, A.C., Wagner-Riddle, C., Park, K.H., Gordon, R.J., 2011. Methane emissions from stored liquid dairy manure in a cold climate. Anim. Feed Sci. Tech. 166-67, 581–589.
Voglmeier, K., Jocher, M., Häni, C., Ammann, C., 2018. Ammonia emission measurements of an intensively grazed pasture. Biogeosciences 15, 4593–4608.
Volten, H., Bergwerff, J.B., Haaima, M., Lolkema, D.E., Berkhout, A.J.C., van der Hoff, G.R., Potma, C.J.M., Kruit, R.J.W., van Pul, W.A.J., Swart, D.P.J., 2012. Two instruments based on differential optical absorption spectroscopy (DOAS) to measure accurate ammonia concentrations in the atmosphere. Atmos. Meas. Tech. 5, 413–427.
Wagner-Riddle, C., Park, K.H., Thurtell, G.W., 2006. A micrometeorological mass balance approach for greenhouse gas flux measurements from stored animal manure. Agric. Forest Meteorol. 136, 175–187.
Wheeler, E.F., Adviento-Borbe, A.A., Brandt, R.C., Topper, P.A., Topper, D.A., Elliott, H.A., Graves, R.E., Hristov, A.N., Ishler, V.A., Bruns, M.V., 2011. Amendments for mitigation of dairy manure ammonia and greenhouse gas emissions: preliminary screening. Agric. Eng. Int. CIGR J. 13, 1–14.
Wood, J.D., Gordon, R.J., Wagner-Riddle, C., Dunfield, K.E., Madani, A., 2012. Relationships between dairy slurry total solids, gas emissions, and surface crusts. J. Environ. Qual. 41, 694–704.
Wood, J.D., VanderZaag, A.C., Wagner-Riddle, C., Smith, E.L., Gordon, R.J., 2014. Gas emissions from liquid dairy manure: complete versus partial storage emptying. Nutr Cycl Agroecosys 99, 95–105.

Acknowledgements

Science thrives on the constant exchange of ideas in lively discussions. Thus, this work would never have been possible without the contribution of the people I had the great pleasure to work with throughout my graduate career. In particular, I would like to thank

Prof. Dr. Stefan Brönnimann, my supervisor from the University of Bern, for giving me the opportunity to write this thesis as an external PhD student in his group. I learnt a lot from his inputs on manuscripts and presentations. It was always a joy to be a part of his group.

Dr. Christof Ammann, my co-supervisor from the Climate and Agriculture Group at Agroscope, for his great support during my PhD and his expert knowledge on micrometeorology. I learnt a lot from his countless inputs, and long discussions if I was stuck with the data analysis or writing a manuscript.

Dr. Andrew VanderZaag, Agriculture and Agri-Food Canada, for his agreement to function as external referee.

I am highly grateful to the Swiss Federal Office for the Environment (Contract 00.5082.PZ/BECDD68E6, 00.5082.P2I R254-0652, 06.0091.PZ/R281-0748, 17.0083.PJ/R035-0703) and the Swiss Federal Office for Energy (Contract SI/501679-01) that funded this work.

Many thanks go to all the people at the School of Agriculture, Forest and Food Sciences HAFL of the Bern University of Applied Sciences. I had my office at the HAFL and was a member of the group Gaseous Emissions from Agriculture. I would like to thank in particular

Thomas Kupper, my group leader at the HAFL, to whom my biggest gratitude belongs. I am deeply grateful that you offered me a position in your group in 2016 and gave me later the opportunity to write a PhD thesis. In the 3.5 years of my PhD and the preceding 2 years, I truly appreciated working with you. This thesis would not have been possible without you. Thank you, Thomas.

Christoph Häni, my office mate, for introducing me to the inverse dispersion method with the bLS model and helping me setting up some of the field experiments. I am especially grateful for all the help and support I got with data handling in R and the numerous R scripts he provided.

Dr. Albrecht Neftel, for his expert knowledge on emission measurements, his inputs to manuscripts in all those fruitful discussions and, for his support in the last days of my thesis.

Simon Bowald, for his great support in the planning and construction of the CH_4 source and for drawing most of Figure 3 and 4 in this thesis.

Patrice Bühler, for his great support in the planning and construction of the CH_4 source and for spending almost 24 hours with me in the field in freezing conditions during the CH_4 release experiment.

Martin Häberli-Wyss for offering me a hand during the setup and dismount of most field campaigns.

I thank the colleagues from Agroscope and the staff of the experimental dairy housing in Aadorf for their support and very fruitful collaboration. I highly acknowledge the operators of the wastewater treatment plants Moossee-Urtenenbach and Gürbetal, the operators of the biogas plants, the owner of the barn in the Grand Marais and the farmers who provided their agricultural fields in the surrounding areas of the measuring sites for their support and the very helpful cooperation.

Additionally, I would like to thank

my brother Mario, for proofreading this thesis.

all my friends and family members that supported me in the non-scientific life all these years.

Michael aka Soak, my very dear friend, for proofreading this thesis. I am especially grateful for all the discussions we had about life, music, and science either in person or later by videocall. Alerta!

Declaration of consent

on the basis of Article 18 of the PromR Phil.-nat. 19

Name/First Name: Bühler Marcel

Registration Number: 08-104-200

Study program: PhD in Climate Sciences

Bachelor ☐ Master ☐ Dissertation ☑

Title of the thesis: Measurement of methane emissions from confined sources using the inverse dispersion method

Supervisor: Prof. Dr. Stefan Brönnimann

I declare herewith that this thesis is my own work and that I have not used any sources other than those stated. I have indicated the adoption of quotations as well as thoughts taken from other authors as such in the thesis. I am aware that the Senate pursuant to Article 36 paragraph 1 litera r of the University Act of September 5th, 1996 and Article 69 of the University Statute of June 7th, 2011 is authorized to revoke the doctoral degree awarded on the basis of this thesis.
For the purposes of evaluation and verification of compliance with the declaration of originality and the regulations governing plagiarism, I hereby grant the University of Bern the right to process my personal data and to perform the acts of use this requires, in particular, to reproduce the written thesis and to store it permanently in a database, and to use said database, or to make said database available, to enable comparison with theses submitted by others.

Bern, 10.01.2022

Place/Date

Signature

Curriculum Vitae

Personal

Marcel Bühler
Born June 3rd, 1988, in Erlenbach im Simmental, Switzerland
ma.buehler@gmx.net

Education

since 2018 — PhD student in Climate Sciences
Oeschger Centre for Climate Change Research
University of Bern, Bern, Switzerland
in collaboration with
School of Agriculture, Forest and Food Sciences HAFL
Bern University of Applied Sciences, Zollikofen, Switzerland
Thesis: *Measurement of methane emissions from confined sources using the inverse dispersion method*

2012 - 2016 — Master of Science in Climate Sciences with special qualification in Atmospheric Sciences
Oeschger Centre for Climate Change Research
University of Bern, Bern, Switzerland
Thesis: *Testing and application of an AirCore device for vertical air profiling*

2008 - 2012 — Bachelor of Science in Geography with Minor Biology
University of Bern, Bern, Switzerland

Student Exchange

2011 - 2012 — Erasmus exchange semester
University of Exeter, Exeter, United Kingdom

Professional Experience

2017 - 2018 — Scientist at the
School of Agricultural, Forest and Food Sciences HAFL
Bern University of Applied Sciences, Zollikofen, Switzerland

2016 — Internship at the
School of Agricultural, Forest and Food Sciences HAFL
Bern University of Applied Sciences, Zollikofen, Switzerland

Journal Publications

Bühler, M., Häni, C., Ammann, C., Brönnimann, S., and Kupper T. Determination of methane emissions from complex source configurations with inverse dispersion method, Atmos. Environ. X, in revision.

Bühler, M., Häni, C., Ammann, C., Mohn, J., Neftel, A., Schrade, S., Zähner, M., Zeyer, K., Brönnimann, S., and Kupper, T. (2021) Assessment of the inverse dispersion method for the determination of methane emissions from a dairy housing. Agricultural and Forest Meteorology. 307, 108501, doi: 10.1016/j.agrformet.2021.108501.

Häni, C., **Bühler, M.**, Neftel, A., Ammann, C., and Kupper, T. (2021) Performance of open-path GasFinder3 devices for CH4 concentration measurements close to ambient levels, Atmospheric Measurement Techniques, 14, 1733–1741, doi: 10.5194/amt-14-1733-2021.

Brönnimann, S., **Bühler, M.**, and Brugnara, Y. (2020) The Series from Geneva, 1799–1863. In: Brönnimann, S. (Ed.) Swiss Early Instrumental Meteorological Series. Geographica Bernensia G96, p. 47– 59, doi: 10.4480/GB2020.G96.04.

Kupper, T., Häni, C., Neftel, A., Kincaid, C., **Bühler, M.**, Amon, B., and VanderZaag, A. (2020). Ammonia and greenhouse gas emissions from slurry storage - A review. Agriculture, Ecosystems & Environment, 300, 106963. doi: 10.1016/j.agee.2020.106963.

Auchmann, R., Brönnimann, S., Breda, L., **Bühler, M.**, Spadin, R., and Stickler, A. (2012) Extreme climate, not extreme weather: the summer of 1816 in Geneva, Switzerland. Climate of the Past, 8, 325-335, doi:10.5194/cp-8-325-2012.

Conference Talks

Bühler M., Häni C., Ammann C., Mohn J., Neftel A., Schrade S., Zähner M., Zeyer K., Brönnimann S., Kupper T., Assessment of the inverse dispersion method for the determination of methane emissions from a dairy housing, Cost and LivAGE, Final Conference, 9-10 September, Gent, ILVO, Belgium / Hybrid format, 2021.

Bühler M., Häni C., Kupper T., Ammann C. Brönnimann S., Quantification of methane emissions from a wastewater treatment plant in Switzerland. 18th Swiss Geoscience Meeting, Zürich, November 17-18, 2020.

Bühler M., Häni C., Kupper T., Ammann C. Brönnimann S., Quantification of methane emissions from waste water treatment plants. In: EGU General Assembly 2020: Sharing Geoscience Online. Vienna: EGU, 4-8 May 2020. 10.5194/egusphere-egu2020-13389, 2020.

Bühler M., Häni C., Kupper T., Schrade S., Zähner M., Wyss S., Mohn J., Ammann C. Brönnimann S., Assessment of methane emissions from a dairy farm using an inverse dispersion technique. 17th Swiss Geoscience Meeting, Fribourg, November 22-23, 2019.

Bühler M., Kupper T., 2017. Agricultural emission factors of particulate matter and non-methane volatile organic compounds for Switzerland. Emissions of Gas and Dust from Livestock – Saint-Malo, France – May 21-24, 2017.

Conference Posters

Bühler M., Häni C., Kupper T., Schrade S., Zähner M., Wyss S., Mohn J., Ammann C. Brönnimann S., Assessment of methane emissions from a dairy farm using an inverse dispersion technique. In: EGU General Assembly 2019. Vienna: EGU, 7-12 April, 2019.

Bühler M., Häni C., Kupper T., Ammann C. Brönnimann S., Assessment of methane emissions from animal and waste processing operations using an inverse dispersion technique. 16th Swiss Geoscience Meeting, Bern, November 30 – December 01, 2018.